OIL PRODUCTION FORECASTING USING HIGHER ORDER NEURAL NETWORKS AND RESERVOIR HISTORY MATCHING WITH THE APPLICATION OF ADAPTIVE GENETIC ALGORITHM

By

N C CHITHRA CHAKRA

COLLEGE OF ENGINEERING STUDIES

Under the Guidance of

Dr D N SARAF

Submitted

In Partial Fulfillment for the Requirement of the Degree of

DOCTOR OF PHILOSOPHY

To

UNIVERSITY OF PETROLEUM AND ENERGY STUDIES
DEHRADUN-248007

December, 2013

ACKNOWLEDGEMENTS

Foremost, I wish to express my heartfelt gratitude to my supervisor, Professor D N Saraf, without whose guidance, patience and support, would not have made me to overcome the obstacles that I faced through the journey of my PhD work. He is the best supervisor one could ever have. His valuable knowledge, continuous assistance and comments have inspired me to shape my research ideas and interests. I am grateful for his persistent encouragement that has made me to purse my studies at difficult times. I had a good learning exercise with him, which will be with me throughout my life. I also extend my gratitude to his wife, Puspha Saraf, for care and consideration during my visit to their home.

I would like to extend my special thanks to Professor B P Pandey, for his valuable advice, encouragement and sharing his vast knowledge about the reservoir engineering and simulation and spiritual concepts as well. Dr S J Chopra, a cheerful and knowledgeable person, whose advice and support has always enlightened for the success of this work.

I take this occasion to thank the management of University of Petroleum and Energy Studies, for providing me this golden opportunity and the financial support during my research work. I am particularly grateful to Dr Parag Diwan, Vice Chancellor of the University for his support throughout my stay at UPES and extra financial assistance towards the end of my work. My special thanks to Suraj Anand, who have showed me the entrance to the University of Petroleum and Energy Studies for my research work, his great advice have supported me a lot through this 4 years journey. Special thanks to Dr Shrihari, Dr S K Gupta, Dr Pushpa Sharma, and Dr S K Nanda, for their valuable comments and suggestions provided during my abstract presentation. I also thank Dr Sanket Goel for the support provided during my studies.

I am indebted to my another advisor, Professor Madan M Gupta, for his valuable knowledge, encouragement and financial support provided during my stay at Canada. I would also express my thanks to his wife Suman Gupta for her love and care. Very special thanks to Dr Ki-Young Song, more than a co-guide, he is my best friend whose instructions, critiques and thoughts have highly influenced in my working approach

and my life's attitude. My special thanks to his better-half, Manica Song and his family for providing a pleasant stay at Saskatoon. The financial support from the Canadian Commonwealth Scholarship is greatly acknowledged, which provided me an opportunity to do my partial research work at University of Saskatchewan, Canada.

I also would like to thank Prof Sirish Shah, Dr Saneej Balakrishna Pillai, and Dr Japan Trivedi for their valuable time and support during my stay at University of Alberta. I also like to express my sincere gratitude to Prof Sirish Shah, for providing me an opportunity to visit University of Alberta.

My deepest gratitude to Institute of Reservoir Studies (IRS), ONGC, Ahmedabad for the valuable materials provided for this research work. Sincere thanks to Dr R V Marathe, for providing me a chance at IRS to learn about petroleum reservoir. I am thankful to Shri O N Gyani, for his valuable recommendations, support and encouragement towards this research work. Sincere appreciation to Mr Ramachandran, of IRS his care, consideration and valuable time spend to teach me reservoir modeling and simulation during his busy schedule are greatly acknowledged.

I am grateful to my dear friends from graduation, Saskatoon and Silver Heights; especially Bibhas Karmakar, Geo Jose Frenandez and towards the family of Mr Ravindra Yatagiri and Mr Manikandan, whose constant affection and support provided me a platform towards successful completion of my work. I also thank my colleagues from UPES for their support.

Words are too short to express my gratitude towards my parents and brother, for their endless prayers, blessings and encouragement. I also thank for the love, care and support provided by my in-laws which helped in successful completion of my thesis. Finally, to my beloved husband, Sanoop Sivadasan, your unconditional love, and care have always been a great strength in me. The patience and sacrifices you held during my studies had helped me most to complete my PhD thesis.

Above all, I am thankful to Almighty God, my trust and faith says his power dwells behind any success.

This thesis is dedicated to everlasting love of my life:

My husband— Sanoop Sivadasan

and

My Parents— N V Chakrapani and Money Chakrapani

DECLARATION

I, **N C Chithra Chakra** hereby declare that the work presented in this thesis **"OIL PRODUCTION FORECASTING USING HIGHER ORDER NEURAL NETWORKS AND RESERVOIR HISTORY MATCHING WITH THE APPLICATION OF ADAPTIVE GENETIC ALGORITHM"**, to the best of my knowledge and belief, is original and my own work carried out at **UNIVERSITY OF PETROLEUM AND ENERGY STUDIES**, and has not been submitted elsewhere for a degree, also it contains no material previously published or written by another person except where due acknowledgment has been made in the text.

N C Chithra Chakra
Doctoral Research Fellow
College of Engineering
University of Petroleum & Energy Studies
Dehradun-248007

THESIS COMPLETION CERTIFICATE

This is to certify that the thesis entitled **"OIL PRODUCTION FORECASTING USING HIGHER ORDER NEURAL NETWORKS AND RESERVOIR HISTORY MATCHING WITH THE APPLICATION OF ADAPTIVE GENETIC ALGORITHM"** by Ms. N C Chithra Chakra in Partial completion of the requirements for the award of the Degree of Doctor of Philosophy in Engineering is an original work carried out by her under my supervision and guidance.

It is certified that the content of the thesis, in full or parts have not been submitted to any other Institute or University for the award of any other degree or diploma.

Internal Guide

Dr D N Saraf

Research Advisor

University of Petroleum and Energy Studies

Dehradun- 248007, India

EXECUTIVE SUMMARY

Ever increasing input material cost coupled with environmental concerns has put pressure on profits of oil industry. There is a serious concern to plan, develop and exploit the oil and gas reserves in an efficient and optimal way. Production forecasting and reservoir modeling can provide vital inputs to efficient management of this hugely important energy source. Building reliable numerical reservoir models that incorporate all the geological, geophysical, geochemical, and petrophysical data of the reservoir available through petroleum exploration process, can help mitigate this problem. Since the reservoirs are highly heterogeneous and nonlinear in nature, it is often difficult to obtain accurate estimates of the spatial distribution of rock properties representing the reservoir and corresponding production profiles. Petroleum engineers always seek to construct reservoir models which are capable of consistent production forecasts such that further reservoir development in terms of locating new wells, recovery strategies (primary, secondary and tertiary), and surface facilities can be optimally designed.

Once a geological model of a reservoir is constructed with spatial distribution of rock properties like porosity and permeability, a flow model is required which can estimate multi-phase flow of oil, water and gas through the flow channels into the well. Here dynamic rock and fluid properties such as relative permeabilities, fluid saturations etc., become important in addition to initial and boundary conditions of the reservoir. Several numerical flow models are commercially available such as CMG® (Computational Modeling Group, Calgary, Canada), ECLIPSE (Schlumberger), JewelSuite™ (Baker Hughes, Houston, Texas) etc., which can predict the oil, gas and water production rates along with bottom hole flowing pressure in each well provided all the required inputs are available. However, the static rock properties such as permeability and porosity are only available at well locations (exploratory or production) and there is no reasonable way to find how these vary between the wells and in the rest of the reservoir. Wells may occupy no more than a few percent of the total area and we have no clue about these properties over most of the reservoir. The available reservoir models cannot, therefore, be used directly. To overcome this

difficulty, an inverse problem is usually defined where one searches for porosity and permeability distribution maps, relative permeabilities etc., which, when used as input to the reservoir simulator, will yield the same production history as has been actually recorded in the field. Needless to say this is a tedious exercise and the solution is never unique since any number of distributions can be found which will result in similar production history. This process is called history matching and was traditionally carried out manually which is a very time consuming process. Although some reservoir engineers still use it, more often, optimization based automated history matching has now become popular.

In the present study two different techniques, both relatively new, were applied for forecasting oil production. The first approach is artificial neural networks (ANN) based modeling and the second is genetic algorithm (GA) based optimization. A higher-order neural network (HONN) – has been applied for oil production forecast from a real field reservoir. The method was first applied for oil production forecasting from a single well and then cumulative oil production forecasting from the entire reservoir. Neural network approach is simple to use but requires large amount of fairly accurate data for training the network which is difficult to get. Forecasting cumulative oil production required only individual well production data and that being available; a one-step-ahead predictor was designed using HONN to make predictions. It being an empirical or black-box model approach, one cannot use it except for prediction in immediate future which limits its usefulness. In principle, it is possible to develop another ANN/HONN model which could possibly predict porosity and permeability distributions; however this will require a lot of geological, petrophysical, seismic and a variety of log data as input which was not available in the present study.

Towards the automatic history matching problem through reservoir characterization, a global optimization method called genetic algorithm (GA) has been employed. The methodology was tested and validated by implementing it on a known 2D synthetic black-oil reservoir. Subsequently it was applied to a real reservoir situated in Cambay Basin, Gujarat, India.

Higher Order Neural Network (HONN) Modeling

In conventional NN, there exists a linear correlation between the neural inputs and synaptic weights. Higher-order neural network embeds higher-order synaptic operations (HOSO) (n^{th} order) that nonlinearly correlate the neural inputs with the synaptic weights. In present study, the HONN with HOSO architecture embeds the linear (conventional) (LSO), quadratic (QSO) and cubic synaptic operations (CSO) for cumulative oil production forecasts. Reduced network size, faster training and smaller forecasting errors are some of the advantages achieved for HONN over the conventional NN. In a pre-processing step the input field production data were treated with a low-pass filter which helped reduce noise. Also auto-correlation (ACF) and cross-correlation functions (CCF) were employed for choosing optimal neural inputs. The HONN model performance was validated using the statistical methods; root mean square error (RMSE) and mean absolute percentage error (MAPE).

The efficacy of HONN procedure was tested for oil production forecasting from a single well of the reservoir with input data for: i) only oil production and ii) oil, gas and water productions (Chakra, et al., 2013.b). Monthly production data for 94 months were available, from which the last 16 months' data were used for validation keeping remaining data for training and testing the HONN model. After careful experimentation one hidden layer was used with different number of neurons (1 ~ 5). Hyperbolic tangent and linear mapping functions were selected for hidden and output layers respectively. The initial learning rate was set to 0.01 which got dynamically updated by multiplying with 1.05 for decreasing error and with 0.7 for increasing error for each HONN model.

The simulation results from HONN employing only oil production data as neural input shows that the HONN with LSO having 5 neurons in the hidden layer with single lag resulted in mean absolute percent error (MAPE)of 13.86 %. The best model using oil, gas and water as the neural inputs was HONN with QSO having 4 neurons in the hidden layer with MAPE=15.13% which is more than single input case. While additional inputs are expected to improve model performance, the inherent noise present in the field data overshadowed the advantage.

The study was subsequently extended to cumulative oil production forecasts from multiple wells from the same reservoir (Chakra, et al., 2013.a). Again, two sets of inputs were used a before: i) oil production from five wells and ii) oil, gas and water production from five wells. The structure of HONN for cumulative oil production included one hidden layer with different number of neurons (1~10) using the same somatic function as before. Proceeding with the pre-processing step, 34 data were chose for training, 17 for testing and remaining 10 for validating the HONN model. Using only oil production data from all the 5 wells as input, the model with CSO having four neurons in the hidden layer resulted in the best performance with a MAPE of 3.46%. For the HONN model with oil, gas and water productions as input, HONN with CSO having 3 neurons in the hidden layer performed the best with MAPE=3.99%.

Once again, the lack of improvement in the accuracy of prediction with additional inputs can be attributed to noisy data. It may be noted that while cumulative oil prediction from all the wells had an error of about 4%, the single well case had a much higher error of about 15%. This is because of interference of neighboring wells in case of a single well model not being accounted for.

History Matching Using Genetic Algorithm

Automated history matching through reservoir characterization has been attempted by employing a global stochastic evolutionary optimization algorithm called genetic algorithm (GA). The algorithm starts with an initial population of potential candidates in the search space. This population evolves to improved solutions with every generation which consists of three operations; selection, reproduction (crossover) and mutation. The power of genetic algorithm comes from the crossover and mutation operators. The rate at which the chromosomes experience the crossover and mutation are decided by crossover probability (P_c) and mutation probability (P_m). It is often a difficult task to assign these control parameters to reach optimum solutions at a fast pace. This limitation of simple GA was overcome by an adaptive version of GA, called AGA, where these parameters are dynamically adjusted according to the fitness of the population during each generation. The GA code for history matching was

developed in MATLAB environment that interfaces with the MATLAB geostatistical toolbox "mGstat" and CMG®–IMEX™ reservoir simulator.

The 2D synthetic reservoir from the 10th SPE Comparison Solution Project (Christie and Blunt, 2001) has been chosen for validating the SGA and AGA code and for history matching methodology. The reservoir has grid dimensions of 100 x 1 x 20 in x, y and z directions forming a total of 2000 grid blocks. The model consists of 2 production wells on either side of the reservoir with 1 injection well at the center. Two core holes are assumed to be drilled between the production and the injection wells. The reservoir grid blocks are populated with known values of permeability and are assumed to be true and resulting production profile from forward simulations from the true case is considered as historical field observations. Grid block values represented by the well locations are unaltered during GA operations. The objective of the study is to estimate the grid block permeability distributions that are conditioned to the field observations. The tournament selection operator, uniform k-point crossover operator with $P_c = 0.5$ and uniform mutation operator with $\mathrm{P_m} = (0.001, 0.005)$ have been used as parameters for SGA in this study.

The objective function (Q) for history matching problem minimizes the square of difference between the past field production history and corresponding simulator output over time. A set of 40 initial realizations was generated using GSLIB's VSIM geostatistical software packages via 'mGstat' interface of MATLAB. The generated initial realization has the fitness function (Q) values ranging between 1.77 ~ 68.13 and average objective function value (Q_{avg}) of 12.01. SGA with crossover probability; $P_c = 0.5$ and mutation probability; $P_m = 0.001$and 0.005 were the two sets of computations carried out and the results compared after 400 iterations. The set with $P_m = 0.005$ performed better resulting in converged Q values ranging between 0.69 ~ 17.42 and $Q_{avg} = 6.13$. At this stage the best solution from SGA resulted in a satisfactory match of simulator output with production history. Both oil and gas production rates over the entire period, matched reasonably well with the field production history. In case of AGA, optimization was carried out with initial crossover probability, $P_c^0 = 0.5$ and mutation probability; $P_m^0 = 0.001$ and 0.005 . Both sets resulted in nearly the same optimization with the set with $P_m^0 = 0.005$ performing slightly better. The best permeability realization was achieved at 172th

iteration with objective function value, $Q_{min} = 0.502$, $Q_{max} = 12.23$ and $Q_{avg} = 4.41$. Both SGA and AGA algorithms were able to generate satisfactory history matched models which resulted in permeability maps close to the true permeability distribution that was hidden from the algorithm. A comparison between the performance of SGA and AGA shows that the AGA was able to converge to optimal reservoir realizations much faster than the SGA with fewer iterations.

The 3D real field reservoir model was divided into 50 x 60 x 3 grid blocks in x, y and z directions for the purpose of computations. The reservoir consists of three oil bearing sands with top layer known to be essentially homogenous with uniform permeability. The permeabilities of the second and third layers were taken to be variable. The reservoir has 6 producing wells having 8 years production history. The reservoir has a strong water drive provided by two aquifers and surrounded by non-communicating faults on the remaining boundaries. In present study, field permeability distribution is considered as the most sensitive parameter and hence the objective of the present study was set to estimate the grid block permeabilities which are conditioned to oil production rates, water cut, gas/oil ratio (GOR) and flowing bottom hole pressure (BHP). The objective function included oil production rate, GOR, water cut and BHP from all 6 producing wells over a period of 6 years of production history (2000 ~ 2005). The initial permeability realizations for a population of 30 chromosomes were generated using MATLAB's 'mGstat' interface to GSLIB's SGeMS, geostatistical software package, assuming suitable variogram model. The initial realizations are conditioned to the permeability values at the grid blocks that represent the well locations and these values do not undergo GA operations. The minimum and maximum fitness function values of initial realizations ranged between 24.58 ~ 68.19 with average objective function value, $Q_{avg} = 35.096$. The tournament selection operator, uniform k-point crossover and mutation operators with $P_c = 0.5$ and $P_m = 0.005$ were selected parameters for SGA. At 240th iteration the range of minimum and maximum objective function shrank to 19.98 ~ 54.34 and Q_{avg} to 25.673. AGA with initial values of $P_c^0 = 0.5$ and $P_m^0 = 0.005$ converged in 120 iterations with the objective function values $Q_{min} = 19.61, Q_{max} = 40.18$ and $Q_{avg} = 21.515$. The optimized permeability maps resulting from SGA and AGA

when used with the simulator provided perfect history match for oil production rates, and satisfactory match for water cut, GOR, and for BHP.

The AGA outperformed SGA by its faster convergence to reach optimum solutions in lesser iterations. The best model obtained from the GA optimization was then, used for forecasting productions for next two years (2006 ~ 2008) from the entire field. Since historical data were available for these 2 years also (not used in model development), a comparison of model predicted results with field data showed a good match thus validating the reservoir simulation. The individual well production forecasts were also found to be in agreement with measurements. Two new wells were drilled in the year 2009 which did not exist earlier and hence not accounted for in the model development. Only scant measurements are available for these two wells but whatever is available is in agreement with predictions. Thus further validating the model resulting from the history matching exercise using genetic algorithm.

To conclude Higher-Order Neural Network modeling, which was tried for the first time for production forecasting, was able to predict cumulative oil production with mean absolute error less than 5%. Careful selection of input parameters and preprocessing raw field data to reduce noise were crucial to the success of this new technique. Genetic algorithm was successfully used as an optimization tool for history matching. Adaptive GA was found to be superior to simple GA by reducing the computation load with better convergence characteristics. Genetic algorithm provides global solution since GA starts with a large number of initial feasible solutions and while these evolve to optimum solution with each generation, the population is kept diversified at all times thus exploring entire search space at the same time. Successful match of historic production of oil, water and gas and satisfactory future predictions from existing and new wells established the efficacy of the technique. While only permeability was included in the present study, the technique can easily be extended to include other parameters in the search vector to make it a general tool for more complex reservoirs.

CONTENTS

LISIT OF FIGURES

LIST OF TABLES

NOMENCLATURE

ACF	Autocorrelation function	
BHP	Bottom hole flowing pressure	psia, kg/cm^2
CCF	Cross-correlation function	
DWOC	Depth of water-oil contact	ft, m
GOR	Gas-oil ratio	v/v
MAPE	Mean Absolute Percentage Error	%
MSE	Mean Square Error	
WC	water cut	%
A	Cross sectional area normal to flow	ft^2, m^2
B	Formation volume factor	v/v
C_f	Fluid compressibility	psi^{-1}, kPa^{-1}
C_1 and C_2	Parent chromosomes	
d^O	Observed fluid production data	
d^S	Predicted output	
e	Error	
E	Overall performance error	
$f_{avg}, f_{min}, f_{max}$	Average, Minimum and Maximum fitness of the population	
i	Number of generations	
h	Hydraulic pressure head	psia, kg/cm^2
k	Time lag	darcy, mD
k	Permeability	
k_r	Relative permeability	
K_c, K_m	Number of locations in the chromosome for crossover and mutation	
L	Length of porous domain	ft, m
L_c	Length of the chromosome	
n	Number of sample points.	
n_t	Total number of months/quarters for which fluid data are used	
n_p	Number of fluid phases produced	
n_w	Number of wells	
N_1 and N_2	New chromosomes	
P	Pressure	psia, kg/cm^2
P^0	Initial pressure	psia, kg/cm^2
P_b	Bubble point pressure	psia, kg/cm^2
P_c	Crossover probability	
P_{cgo}, P_{cwo}	Gas/oil , oil/water capillary pressure	psia, kg/cm^2
P_c^0,P_m^0	Initial crossover and mutation probability	
P_m	Mutation probability	
P_{nw}	Pressure in nonwetting phase	
P_w	Pressure in wetting phase	psia, kg/cm^2
q	Sink or source	
q_x	Flow rate in x direction	m^3/day, RB/day
Q	Objective function	

$r_{(k)}$	Autocorrelation coefficient	
$r_{xy(k)}$	Cross-correlation coefficient	
R	Random number (chapter-5 & 6)	
R_{so}	Solution gas oil ratio	m^3/m^3, SCF/STB
S	Fluid saturation	fraction
S_o, S_g, S_w	Fractional saturation of oil, gas and water	fraction
t	Time step	
v	Output of synaptic operation	
V	Volume	ft^3, m^3
V_b	Bulk volume	ft^3, m^3
w_a	Synaptic weight	
x_a	Neural input	
X	Spatial variables ($x, y,$ & z directions)	
Δt	Time step size	days, months
ΔP	Pressure gradient	psia, kg/cm^2
Δx	Spatial step size	ft, m
α	Learning rate (chapter-3)	
β_1	Functions of PVT terms	
β_2	Production terms	m^3/day, RB/day
φ	Porosity	fraction
μ	Fluid viscosity	cp
λ	Mobility of fluid phase	m d/Kg, D/lbm
λ_T	Total mobility of oil, gas and water	m d/Kg, D/lbm
ρ	Density of fluid	lb/ft^3, gm/c^3
ζ	Activation function	
$\emptyset$	Fluid potential	kg/ (md^2),lbm/ftD^3
Ω	Solution domain	ft^3, m^3
Γ	Boundary of Ω	ft^2, m^2
$A_x, A_y and\ A_z$	Cross sectional areas normal to $x, y\ and\ z$ directions	
$g_{\alpha,1}, g_{\alpha,2}, g_{\alpha,3}$	Boundary Data	
a, b, c, d, e, f, g, h	Experimental coefficients (chapter-4)	
ξ , ω and η	Experiment Coefficients for calculating P_c and P_m (Chapter-5, & 6)	
Subscripts		
α	Phase index	
o, g,w	Oil, Gas, and water phase	
T	Reservoir temperature	

Note: The units used in thesis are a mix of British Metric and SI systems which is same that generally being used in petroleum industry. The commercial simulation software also uses the mixed units system, and no attempt was, therefore made to convert everything to SI units.

CHAPTER-1

INTRODUCTION

Petroleum – a natural energy source from the subsurface, occupies a prominent position in the world's present day energy basket and this is likely to continue since renewable energy contribution is not expanding rapidly enough. Oil and gas industries invest huge amount of money, time and technology for efficient exploration and exploitation of petroleum reserves. Reservoir production forecasting, modeling and simulation play a vital role in efficient field development, its management and strategies under various operating and maintenance scenarios. Reservoir flow simulation aims to construct a consistent numerical model that resembles the real physics of flow of fluids in the actual reservoir in terms of its geological, petrophysical, and geochemical properties. Building a consistent geological reservoir model that replicates all the geological realism available through petroleum exploration process is not an easy task because of its heterogeneous and nonlinear nature. The geological and petrophysical data available from the exploration and production wells represent only a minuscule area, when compared to the total reservoir. Moreover, these rock properties (porosity and permeability) vary in an unpredictable way with space, and it is often difficult to gain accurate estimates of these spatial properties. Challenging fact is that there is no clue how these spatial properties are distributed in the region between the wells or the region that does not have any production or injection wells.

Inspite of all these factors, reservoir engineers always try to construct models that resemble geological realism and reproduce historical field observations when simulated. A reliable reservoir model assures confidence in production forecast and can be used to better understand the present and future reservoir behavior under various operating scenarios such as workover, well completion and artificial lift strategies etc., Thorough understanding of reservoir behavior is essential for efficient and optimal future field development plans such as optimizing the well location, surface facilities, and recovery strategies (primary, secondary and tertiary).

To understand and, therefore, reliably predict the future performance of a reservoir, it is clear that we need to construct a geological model with all rock and fluid properties well established. However, one wonders if without going through an elaborate exercise of modeling and simulation which is expensive and time consuming, is it possible to predict production of oil by any other means. Can artificial intelligence which is making a paradigm shift in almost all spheres of human activity not help us? More specifically, artificial neural networks (ANN) appear to be promising tool for such an attempt.

1.1 PRODUCTION FORECASTING EMPLOYING HONN

Artificial neural networks (ANN) based modeling is simple and does not require either detailed reservoir characterization or complex flow equations to be solved numerically. One simply provides available production data as input and trains a network of neurons to give future production of oil. Design of network architecture is part of model development. A modified version of ANN called higher order neural networks (HONN) may be more suited for this complex problems as HONN models may require simpler architecture since these use nonlinear relation between neural input and synaptic weights.

Higher order neural network embeds higher order synaptic operations (HOSO), which nonlinearly correlate the neural inputs with the past knowledge (synaptic weights), whereas, for conventional NN, there exists a linear correlation between the neural input and the synaptic weights. HONN outperforms conventional NN in terms of fast network training, reduced network size, and smaller forecasting errors. First order HONN reduces to the linear or conventional ANN. Second order (QSO) and third order (CSO) HONN have been used by researchers in other fields. If the neural input data are noisy, and field measurements are always noisy, a pre-processing step such as use of a low pass moving average filter can help noise reduction. For evaluating the patterns in time series production data at different time steps (lag), auto-correlation (ACF) and across-correlation functions (CCF) are commonly applied. Moreover, the ACF and CCF functions help to identify the optimal inputs for HONN training, as the performance of the network also depends on the choice of optimal neural inputs. The statistical measures such as root mean square error (RMSE) and mean absolute

percentage error (MAPE) provide quantitative tools for comparing and validating the performance of HONN models.

However, there are limitations to ANN or HONN models which result from the fact that such models do not embed any physics of the process being modeled. While such models can be trained to act as one-step-ahead predictors, one cannot expect such models to be valid for oil field development. Use of production data as input to HONN from a single or multiple wells are likely to predict production in near future after training but since rock and fluid flow properties are neither used nor generated one simply cannot expect such models to be useful for planning better recovery methods or even long term production forecasting reliability.

1.2 RSERVOIR MODELING THROUGH HISTORY MATCHING

The numerical reservoir models comprise of highly nonlinear partial differential equations (PDE) with both space and time as independent variables. The solution of these equations require initial and boundary conditions which are usually quite complex in petroleum reservoirs. These PDEs describe the mass transfer process and hydrodynamical fluid flow within the reservoir system, expressed as a function of spatially varying rock properties (porosity and permeability etc.,), fluid properties (PVT properties, viscosities etc.,), and rock-fluid interaction properties (relative permeabilities, connate water saturation, fluid saturations etc.,). Several numerical simulators are commercially available for this purpose, which divide the entire reservoir in thousands of three dimensional grid blocks and numerically integrate the flow equations to find the solution.

However, most of these properties, particularly the rock properties are not available except at well locations. Unlike correlations being available for estimating relative permeabilities, there is no way to estimate rock properties between wells and rest of the reservoir. Reservoir simulation therefore, cannot be used directly to find field production profile in absence of requite information.

History matching is one technique to salvage this situation where one aims to find all missing information such that when used with the simulator, the output will match with the field observations which are typically production of oil, gas and water and

bottom hole flowing pressure. The early efforts in this direction were made by manually adjusting these parameters and then checking if the predictions matched with field observations. This manual trial and error procedure although extremely tedious and time consuming, was the only way to find the critical properties such as porosity and permeability. The reservoirs being highly heterogeneous, these properties were assigned grid block wise and adjusted until a satisfactory match was obtained. If two persons attempt to history match the same reservoir independently, they came up with very different permeability maps yet claimed equally good match. Clearly history matching is an ill-defined problem and does not have a unique solution although modeling and simulation do provide a unique solution. The inverse problem as history matching is usually referred to, can have infinitely many valid solutions.

1.3 AUTOMATIC HISTORY MATCHING

During last few decades, several approaches for automatic history matching have been developed based on: gradient methods; stochastic-global optimization methods; and data assimilation methods. Automatic history matching can be viewed as a minimization problem where one aims to minimize the objective function that embraces sum of the squared differences between the model predictions and observed data. Many gradient-based algorithms are available such as Steepest Decent and Gauss-Newton, Singular Value Decomposition and Adjoint method etc which have been applied to the ill-posed history matching problems.

1.3.1 History Matching Using Genetic Algorithm

Genetic algorithm (GA) is a relatively new optimization technique which is evolutionary in nature. GA as a stochastic optimization tool outperforms other gradient based methods (steepest descent, Gauss- Newton method, conjugate gradient etc.,) towards reaching a global optimum solution escaping the local optima.

Genetic algorithm grounds on the principle of Darwin's theory of "survival of the fittest". The method belongs to the class of evolutionary algorithms that mimics the natural selection and genetics of organisms. The algorithm initializes with an ensemble of feasible initial solutions called initial population. The initial solutions in the population undergo operations like selection, recombination (crossover) and

mutation to generate new chromosomes. The crossover results in exchange of genetic materials between chromosomes and mutation operation maintains genetic diversity in the solutions. The fitness of newly generated chromosomes are evaluated using a fitness function which characterizes the performance of chromosomes in the defined search space. This process continues until the algorithm converges to best set of chromosomes, which are considered as the potential solutions to the problem. The fitness function represents the individual chromosome fitness and is expressed by the objective function. The best member of this population is taken to represent the optimal solution. Although GA finds only near optimal solutions, for all practical purposes these are accepted as optimal.

The performance of GA is largely controlled by the genetic operators; crossover operation and mutation operation. The crossover and mutation probabilities (P_c and P_m) are the deciding factors whether the selected chromosome (or individual) should go through crossover and mutation process. The GA performance is highly sensitive to these parameters. Selecting the optimal values for these parameters is usually a manual trial and error procedure. In case of simple GA, the values for P_c and P_m are pre-assigned by the user and will remain unchanged throughout the evolutions to reach optimal solutions. Hence the user has to try several times with different values for P_c and P_m to find optimal values. This drawback of SGA has been overcome by adaptive genetic algorithm (AGA) which seeks to adaptively update P_c and P_m according to the fitness function value of the population in subsequent generations. The adaptivity in the AGA code helps the algorithm to converge to feasible solutions at a faster rate (in fewer iterations) reducing the computational load compared to SGA.

1.4 RESEARCH OBJECTIVES

- To develop neural network based models which are capable of forecasting oil production based on available field observations for a single well and also cumulative production from all the wells.
- To improve overall performance of neural network by introducing higher-order neural network (HONN).

- To develop and validate history matching methodology using genetic algorithm as an optimization tool using a 2D synthetic reservoir with known permeability distribution map.
- To history match a real 3D reservoir and predict its performance in future

1.5 THESIS OUTLINE

There are 7 chapters in this thesis and their brief details are as follows:

Chapter-1 provides the importance of reservoir production forecasting and history matching problem towards efficient and optimal field development. A brief introduction is provided to the methodologies used for production forecasting and automating the history matching process.

Chapter-2 provides the literature review on neural network modeling and genetic algorithm optimization tools and their application to production forecasting and history matching of a reservoir.

Chapter-3 details the higher order neural network (HONN) methodology and preprocessing techniques used for oil production forecasting for single well and multiple wells in a real reservoir. The chapter also provides computational results obtained from HONN application, and discusses the limitations of this technique.

Chapter-4 discusses the numerical reservoir modeling and simulation approach used to compute the hydrodynamical fluid flow in the black-oil reservoir.

Chapter-5 discusses the details of genetic algorithm and its adaptive variant (GA) technique used as optimization tools to solve the history matching problem. This chapter also presents the application and validation of GA technique for 2D synthetic reservoir history matching.

Chapter-6 provides the application of SGA and AGA techniques towards a 3D real reservoir history matching. This chapter also discusses the potential of the developed technique in predicting reservoir performance in future.

Chapter-7 includes the conclusions and recommendations for future work in the area of history matching with genetic algorithm.

CHAPTER - 2

LITERATURE REVIEW

2.1 HONN APPLICATION TO OIL PRODUCTION FORECASTING

An important phase in the field of petroleum reservoir engineering is concerned with the forecasting of oil production from the reservoir. This estimation of reserves involves massive investment of money, time and technology under a wide range of operating and maintenance scenarios such as well operations and completion, artificial lift, workover, production, and injection operations. A fairly precise estimation of oil quantity in the reservoir is in demand; however, the rock and fluid properties of the reservoirs are highly nonlinear and heterogeneous in nature. Therefore, it is difficult to estimate an accurate upcoming oil production. The oil production from a reservoir depends on many static and dynamic parameters such as porosity and permeability of rocks (static parameters), and fluid saturation and pressure in the reservoir (dynamic parameters). When these static and dynamic parameters are available, the forecasting of oil production of a reservoir would be more accurate. However, all the parameter data are not always available. This limited data access from the oil fields lessens the accuracy of forecasting.

2.1.1 Literature Review on HONN

In the past, several forecasting methods have been developed from decline curve analysis to soft computing techniques (Tamhane, et al., 2000). Artificial intelligence tools such as neural computing, fuzzy inference systems and genetic algorithms have been extensively applied in petroleum industries because of their potential to handle the nonlinearities and time-varying situations (Mohaghegh, et al., 2001). Neural networks (NN) is one of the most attractive methods of artificial intelligence to cope with the nonlinearities in production forecasting (Weiss, et al., 2002) as well as in parameters estimation (Aminzadeh, et al., 2000) due to its ability to learn and adapt to new dynamic environments. Numerous researches have shown successful implementation of NN in the field of oil exploration and development such

as pattern recognition in well test analysis (Alkaabi and Lee, 1993), reservoir history matching (Maschio, et al., 2010), prediction of phase behavior (Habiballah, et al., 1996) prediction of natural gas production in the United States (Al-Fattah and Startzman, 2001) and reservoir characterization (Mohaghegh, et al., 2001) by mapping the complex nonlinear input-output relationship. In conventional NN model, each neural unit (neuron) performs linear synaptic operation of neural inputs and synaptic weights. Later, extensive researches on NN have been made by Gosh and Shin, (1992), Giles and Maxwell, (1987), Lee, et al., (1986), Rumelhart and McClelland, (1986), and Homma and Gupta, (2002) to capture the nonlinear synaptic operation of the input space.

As well, it has been reported that neural network models outperform any other conventional statistical model such as Autoregressive Integrated Moving Average (ARIMA), Autoregressive Moving Average (ARMA) and Autoregressive Conditioned Heteroskedasticity (ARCH). Castellano-Mendez, et al., (2004) reported multi-layer NN perform better for single step-off prediction than linear ARMA (Box and Jenkins, 1976) model. A superior performance of NN is reported by Donaldson, et al., (1993) when compared to specialized nonlinear finance models like ARCH. Donaldson, et al., (1993) found that ARCH could only partially remove the leptokurtosis and symmetric/asymmetric heteroskedasticity from the data used to evaluate the fat-tailed and heteroskedasticity nature of the stock return. Tiwari, et al., (2012) and Nayak, et al., (2004) also reported superiority of NN model over ARMA model in river flow forecasting of hydrological model.

Although the conventional time series models have several advantages and are widely applied for forecasting, but these models have their own limitations while attempting to solve highly nonlinear time series data and also not perform well at times (Tokar and Johnson, 1999) . More details on comparison between NN models and conventional statistical techniques for forecasting of time series data can be found in the research paper by Hill, et al., (1994).

In order to overcome the constraints of the conventional NN models, numerous methods of modification and improvement of NN model have been carried out. One innovative neural structure embeds higher-order synaptic operations (HOSO) and a

new NN model, named Higher-order neural network (HONN), was developed employing the HOSO architecture (Hou, et al., 2007; Gupta, et al., 2003). The exclusive feature of HONN is the expression of the correlation of neural inputs by computing products of the inputs. It has been found that HONN has significant advantages over conventional NN such as faster training, reduced network size, and smaller forecasting errors (Tiwari, et al., 2012, Gupta, et al., 2010; Redlapalli, 2004; Song, et al., 2009). The advantage of NN methods over conventional statistical techniques motivated us to employ HONN model for forecasting of highly nonlinear production data from petroleum reservoir.

HONN has been used to forecast cumulative oil production from an oil field reservoir with limited parameter data: i) oil production data and ii) oil, gas and water production data (no data on pressure and fluid saturation available). The case studies have been carried out to verify the potential of the proposed neural approach with limited available parameters from an oil field in Cambay basin, Gujarat, India. The prime case studies were carried out for forecasting the oil production data from single well using the oil, gas and water production data from the same well (Chakra, et al., 2013.b). Later, the cumulative oil production forecasting from 5 producing wells using the oil, gas and water production from 5 wells were also presented in this research work (Chakra, et al., 2013.a). The HONN for production forecasting was developed in MATLAB environment and the source code is presented in Appendix-A.

2.2 INTRODUCTION TO HISTORY MATCHING

The primary goal of history matching is to develop a valid reservoir simulation model that predicts reservoir performance under various operating scenarios; such that an appropriate reservoir field development and management could be achieved. The reservoir model as such created using any numerical flow simulator cannot be used directly for reservoir performance prediction unless the built model honors all the geological, geophysical and petrophysical properties of the reservoir. These properties are represented by several model parameters such as porosity and permeability which are spatially varying rock properties but otherwise static or time independent. The other model parameters include dynamic entities such as fluid saturations, pressure, relative permeabilities, location of oil/water interface etc along with the initial

condition of the reservoir. Reservoir simulation is the science of calculating the rate of production of various fluids given the model parameters. On the other hand history matching is the art of estimating model parameters given the production data as a function of time. From the above statements, history matching appears to be reverse of simulation but the solution is non-unique and to find a reasonable parameters set out of an infinity of possibilities, which is close to reality, is an art.

The reservoir flow models are set of highly nonlinear partial differential equations with space and time as independent variables together with appropriate initial and boundary conditions. These equations describe hydrodynamical flow of fluid and mass transfer process within the reservoir system, expressed as a function of spatially varying rock properties, fluid properties, and relative permeability characteristics of the reservoir. Solving these mathematical model equations analytically is too complex and therefore, numerical techniques are used to approximate the reservoir performance. For this purpose several simulators are commercially available. Once the output from the simulator model in terms of oil/gas production rates, gas-oil/ water-oil ratio, and pressure is obtained, the same has to be matched with the field history.

The process of adjusting the reservoir model parameters in the reservoir simulator until a reasonable match is achieved between the simulated production and pressure data with the observed data is referred to as History Matching. The history matching process is a time consuming phase of a reservoir simulation study, and it is an essential preface in crafting any sensible predictions with the simulator (Crichlow, 1977). Matching past history ensures that the model so constructed is a satisfactory approximation of the reservoir and is capable of predicting future performance which is a crucial step in managing the reservoir optimally. Indeed history matched models are necessary for analyzing the uncertainty in reservoir prediction and field development plans such as well placement, well type, well spacing, original oil in place, artificial lift strategies, enhanced oil recovery strategies (gas injection or water flooding), integration of subsurface and surface facilities (Hajizadeh, 2011).

During the process of history matching, several uncertain parameters, (refer to Section (2.3.2) for details) which influence production forecast, are altered to obtain a good match between the simulator output and the field history. These parameters are

varied either singly or collectively to lessen the difference between the observed data and those calculated by the simulator (Crichlow, 1977). History matching is, therefore, an iterative process where one gradually but systematically minimizes the difference between calculated and measured values by analyzing the changes made in the previous simulation run and incorporating the necessary change in the next simulation run.

This procedure of history matching can be done either manually or can be automated. Classical history matching technique in practice was manual, trial and error method, which is time consuming and cumbersome. Efforts have, however, been made to automate the process of history matching and there has been a significant progress in developing history matching algorithms which can continuously update the reservoir models by assimilating new data as it is obtained. These methods are iterative, in a general sense, and are usually coupled with some statistical analysis with optimization techniques to obtain the 'best' combination of sensitive parameters to attain a good history matched model.

2.3 OBJECTIVES OF HISTORY MATCH IN RESERVOIR MODELS

History matching aims to improve the reproducing capability of past hydrodynamical behavior of the initial reservoir model built by amalgamating the data obtained during field exploration and when the field was put on production. Hence the primary objective of history matching is to achieve a valid reservoir simulation model which is consistent with the available field history such as pressure, water- oil ratios, gas-oil ratios, water-gas ratios, fluid saturations and production rates. Additionally, history matching also aims to accomplish a better understanding of current status and description of reservoir and clarify the uncertainty related to the aquifer support, paths of fluid migration, communication barriers and depletion mechanisms (Ertekin, et al., 2001; Chidambaram and Ertekin, 2009; Odinukwe and Correia, 2010; Shahkarami, 2012).

History matched models are also used for verification and identification of the area of by-passed reserves and unusual operating conditions such as casing leaks and improper allocation of fluids to wells etc. (Mattax and Dalton, 1990). History matching process helps in improving the future field development plans and data

acquisition programs since the quality of the match better captures the production behavior of the reservoir. Moreover a higher degree of confidence in performance prediction of reservoir can be achieved with a history matched model (Ertekin, et al., 2001; Chen, 2007).

2.3.1 Key Performance Parameters To Be Matched

The reservoir engineer aims to determine the reservoir description that minimizes difference between the observed and the simulator performance during historical production period. There are several parameters available for establishing a good history match (Crichlow, 1977):

- Pressure
- Gas-oil ratios
- Flow rates
- Water-oil ratios

The above mentioned are the key parameters used as observed/ measured data that are monitored once the field is put on production. In fact the observed data are the time series data (hourly, daily, monthly, quarterly or yearly) that are observed at the production or injection well locations.

Flow rates of oil, gas and water productions and injection rates are normally treated as most accurate measurement data. Generally fluid production data at the well locations are functions of reservoir properties and their correlation to model descriptions are relatively complicated. Gas production rates from an old field may not be precise if the gas is flared. Generally, injection flow rates are considered to be less accurate in comparison to production rates, as there is a possibility of losing fluids at the casing or behind the pipe due to leakage. Moreover the production data are susceptible to well constraints and changes occur in the flow regimes and path with time (Oliver and Chen, 2011). However, inaccuracies associated with the production data for the above reasons mentioned can be determined and corrected.

Average reservoir pressure (shut- in pressure) or pressures at well locations are frequently available and are valuable for correcting pressures to bottomhole conditions. Bottomhole flowing pressure and shut-in bottomhole pressure are frequently available, but these are less reliable data than the average reservoir pressure (shut-in pressure) (Odinukwe and Correia, 2010).

2.3.2 Key Parameters Used For History Matching

Deciding and identifying of an uncertain parameter that is highly sensitive to observed reservoir performance is a difficult task in the history matching process. The prime idea of history matching is based on the concept of "hierarchy of uncertainty" (Fanchi, 2001) which represents the ranking of model input parameters according to its quality, that helps the engineer to decide which are the least and the most reliable parameters. There are numerous parameters that are modified individually or collectively to get a good match and are presented in Table 2.1 (adopted from Crichlow, 1977).

Table 2.1. Key reservoir parameters used for history matching problem.

Rock Modification Data	Fluid Modification Data	Relative Permeability Data	Individual Well Completion Data
♦Porosity at each grid block	♦Compressibilities	♦Shift in relative permeability curve	♦Skin effect
♦Vertical and horizontal permeabilities at each grid block	♦PVT	♦Shift in critical saturation data	♦Bottom hole pressure
♦Thickness ♦Fluid saturations	♦Viscosity		

Several researchers (Cosentino, 2001; Shahkarami, 2012) in 20th century reported that there are a few parameters in the above table, which have less uncertainty involved from the above mentioned table (Table 2.1). Those parameters are: PVT parameters, gross thickness, initial reservoir pressure, viscosity, pour point, temperature and initial water saturations. The most uncertain reservoir parameters which have significant impact on observed data are transmissibility, relative permeabilities and permeabilities at each grid location. Aquifer properties such as aquifer transmissibility, aquifer storage and strength are tuned to attain a good match if there is a presence of an aquifer in the reservoir.

The reservoir dynamic parameters such as: reservoir pressure, flow rates, gas-oil ratios, water-oil ratios are influenced by the three phase fluid saturations, since these

are directly related to the quantity of expansive energy within the porous rock. Inability to maintain a given production rate from an area and to maintain subsequent drop in pressure, saturations are most common cause observed during history matching. This is because of insufficient oil in place and influx in a given locality, which can be corrected by adjusting the pore volume and increasing the oil saturation. Rock compressibility is another reservoir parameter that can be adjusted to achieve drawdown pressure in the reservoir after considerable fluid withdrawal. An increase of water saturation in model without any influx or injection of water observed during history matching can be corrected by assigning low rock compressibility (Crichlow, 1977).

Relative permeability is an important complex reservoir parameter that directly influences the flow rate, gas-oil and water-oil ratios and reservoir pressure caused by fluid flow movement under pressure gradient. The uncertainty related to relative permeability is high since these data are obtained from flooding of core samples Fanchi, (2001), kept relative permeability at the top of his "hierarchy of uncertainty" list, because they are more frequently modified than other parameters. Changes in relative permeability can be incorporated by adjusting the imbibition and drainage curves within a considerable range.

2.4 MANUAL HISTORY MATCHING

Manual history matching is an art of science (Fanchi, 2001) where the reservoir engineer utilizes his years of experience, knowledge and personnel judgment to modify those parameters which he used as a measure of the reservoir system behavior that is sensitive to field observations (Crichlow, 1977). The parameter modifications are done, until the simulator produces a reasonable match between simulator responses and historical field observations. Manually matching reservoir history is an iterative and tedious process since the model parameters are sequentially adjusted by an ad hoc approach. The success of this methodogly depends on the quality and quantity of available data, characteristic of the reservoir under study and finally the engineer's knowledge about the reservoir model under study, and his experience on field operations (Gul, 2011; Shahkarami, 2012). Each of these principles consequently provides solutions that have non-uniqueness; hence there are no definite rules for

methodology of history matching processes. Several reports by Mattax and Dalton, (1990); Saleri and Toronyi, (1998); Williams, et al., (1998); Cosentino, (2001) and Ertekin, et al., (2001) presented detailed description of structured methodology for manual history matching process.

According to Saleri and Toronyi, (1998) and Williams, et al., (1998), manual history matching is performed in two phases. The first phase of the approach starts with an average reservoir pressure match by adjusting a few key parameters such as aquifer size, pore volume, aquifer transmissibility, permeability multipliers, rock compressibility factor and the ratio of vertical to horizontal permeability. A poor match of water-oil ratio and gas-oil ratio results in poor match of average reservoir pressure (Aziz and Settari, 1979). Once a substantial average reservoir pressure match is attained, one can adjust the individual well pressure and its nearby well properties across the well. Flow chart of pressure match crafted by Saleri and Toronyi, (1998), is presented by Figure 2.1.

The second phase of manual history matching process is about matching of fluid saturation in which the match in fluid saturations are attained by modifying the relative permeability curves and vertical transmissibility across the layers to control the water flow from lower to upper layer of the reservoir (Williams, et al., 1998). The key well histories such as production rates, gas-oil ratios, water cuts and breakthrough times are matched during this stage of history match. Figure 2.2 represents the flow diagram of the saturation match created by Saleri and Toronyi, (1998).

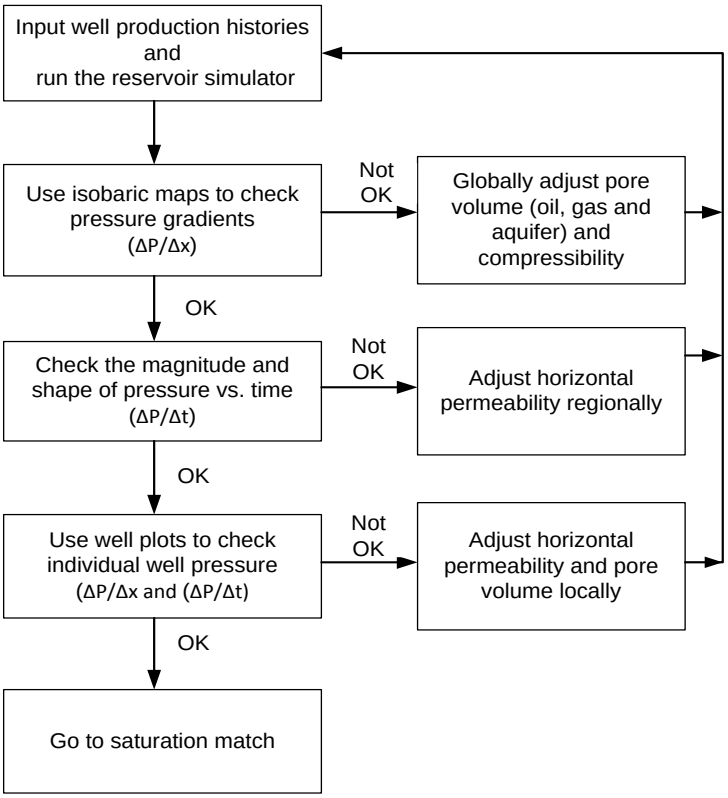

Figure 2.1. Pressure matching process by Saleri and Toronyi, (1998).

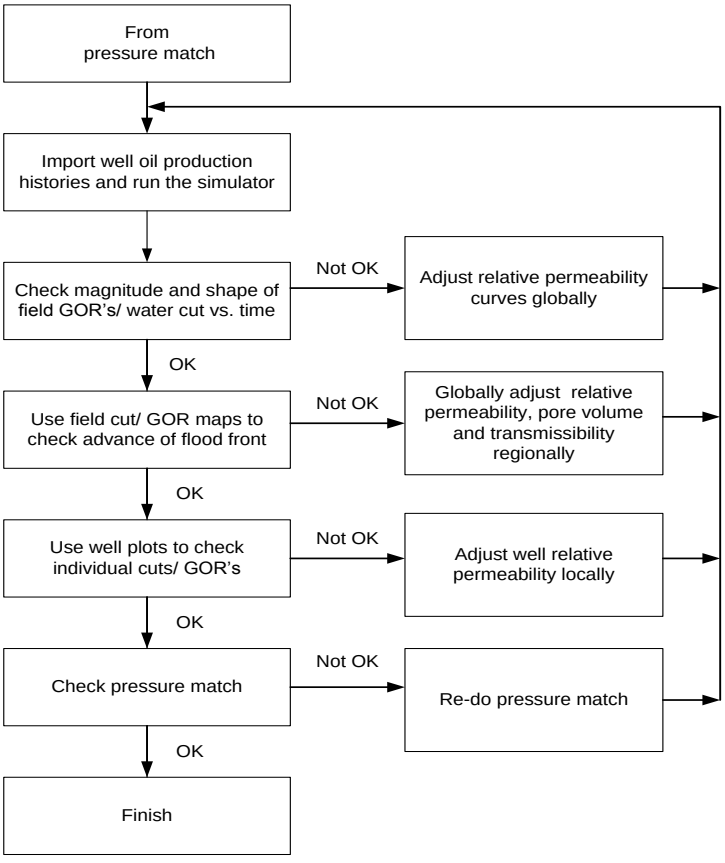

Figure 2.2 Saturation matching process by Saleri and Toronyi, (1998).

2.4.1 Challenges of Manual History Matching

The reservoirs are highly heterogeneous in nature and the manual history matching approach is a complex and time consuming task, with update at each simulation run being done on a single deterministic model. Although a good match on field performance and key well production histories can be achieved by an experienced reservoir engineer, but to attain a reasonable match on each well or completion basis (Oliver and Chen, 2011) will be complicated. Since non-matching regions are matched using regional multipliers, the history matched models may violet the geological constraint (Milliken, et al., 2001). This results in poor performance predictive capability of the history matched reservoir model. Furthermore, the manual history match does not address any uncertainties associated with performance predictions.

2.5 AUTOMATIC HISTORY MATCHING

As mentioned earlier, solving history matching problem manually is a tedious and complex job as it is an ill-posed and inverse problem with non-unique solutions. There have been numerous attempts since 1960's to automate the history matching process and thereby, to alleviate the burden of manual history matching. The approach is iterative in nature and couples some statistical analysis with optimization techniques to obtain the best parameter combination that matches a given reservoir history (Crichlow, 1977). Automatic history matching, in a general sense, utilizes the computer logic to modify those parameters that influence reservoir performance, consequently accomplishing a good reservoir history match. Moreover, automatic history matching also aims for multiple history matched reservoir models to increase the confidence in future reservoir production forecast and uncertainty quantification. Automatic history can be viewed as an optimization problem where the objective function minimizes the difference between observed reservoir history and reservoir simulator response during historical production period. General steps for automatic history matching are as follows:

1. Generate a representative set of simulation runs with known parameters selected randomly or otherwise.

2. Optimize the solution to get a best fit by using search-type methods over the uncertain parameters space.

It is essential to choose an efficient optimization algorithm for minimizing objective function for automatic history matching process. These methods are classified into two main categories: gradient-based methods and non-gradient methods.

2.5.1 Gradient Based Methods

Gradient based methods use traditional optimization approach opted from optimal control theory to compute single solution which is near local optimum to the initial guess (Landa, et al., 2005). The method calculates the gradients of the objective function and then determines the direction of the optimization search to solve the problem (Zhang and Reynolds, 2002). In history matching framework, the gradients (derivatives) of production responses with respect to changes in the reservoir parameters are calculated to determine the direction and the amount of changes required for the parameters (Hoffman, 2005). There are several optimization algorithms that calculate gradients of the objective function and some of them reported by Landa, (1997) and Liang, (2007) are:

- ♦Steepest descent
- ♦Levenberg- Marquardt
- ♦Singular value decomposition
- ♦Conjugate Gradient
- ♦Quasi-Newton
- ♦Gauss-Newton (GN)
- ♦Gradual deformation
- ♦Limited memory Broyden Fletcher- Goldfarb Shanno (LBFGS)

However, the nonlinear regression approach of these gradient methods needs both Jacobian (first derivative) or Jacobian and Hessian (second derivative) of the objective function with respect to static properties of the reservoir. These methods entail an estimation of sensitivity coefficient, which is a partial derivative of dynamic reservoir parameters such as saturation and pressure with respect to static reservoir parameters such as porosity, permeability and azimuth of geospatial variogram (Dadashpour, 2009). The partial derivative is normally attained through finite difference approximation.

The art of automating the history matching process was introduced by Kruger, (1961); by proposing a calculation procedure for determination of the areal permeability distribution of a 2D reservoir in case of flooding or cycling projects. In order to show the soundness of calculation procedure, he compared the results between the field measurements and calculated pressure distributions and concluded that the reservoir model should be conditioned to production data for a reliable performance prediction. Jacquard and Jains, (1965) introduced a method for computing sensitivity coefficients for history matching problem. They applied a modified steepest descent method for minimizing the difference between measured and simulated pressure to corresponding changes in the parameters for a 2D, single phase, transient flow reservoir model. They described their reservoir model in terms of an electrical analogue, where resistance, capacitance and inductance correspond to permeability, porosity and production rates of the reservoir model respectively. Although their application of history matching was conditional to the zonation of the permeability, a successful implementation on history matching problem was reported by the authors.

Jahns, (1966), used a nonlinear regression approach described by Jacquard and Jains, (1965), to match reservoir pressure obtained from interference test. In his approach, properties of each reservoir zone such as transmissibility and storage term (functions of pressure behavior) are varied using regression analysis to achieve a pressure match. He reported that while method can rigorously handle single phase flow, it is not suitable for multiphase flow if there is drastic change in fluid saturation. Coats, et al., (1970), introduced a gradient-based method which combines least square and linear programming to estimate a linear relationship between the error and the reservoir properties. They used the zonation approach as a parameterization method with upper and lower boundary constraints on reservoir descriptors such as permeability and porosity. They generated reservoir description within the constraints using a random generator from a number of runs via reservoir simulator. They tested their methodology on three 2D reservoirs experiencing single phase oil, single phase gas and two phase (gas and water) flows. Though their methodology produced a satisfactory match because of the constraints placed on the parameters, but their assumptions based on the linear relationship between pressure error and reservoir

properties may not be strongly valid. This drawback created limitations on the application of their methodology for further studies.

A gradient-based method as a search technique and linear programming was used by Slater and Durrer, (1971) to achieve a best history matched model. They modified the gradient method proposed by Jacquard and Jain with reduced computational time that finds the search direction and step size for correcting sensitivity coefficient, which is required to minimize the objective function. They reported that it was difficult to find the step size by gradient method in low permeability and porosity region due to high sensitivity and strong non-linear relationship between the objective function and the low permeability values. Thomas, et al., (1972) used a classical Gauss-Newton method as optimization tool for automatically varying the reservoir parameters to achieve better history matched reservoir models. Box-type constraints on the reservoir parameters (sensitivity coefficients) were implemented. They claimed that the method can handle non-linear cases better than the results reported by previous researches. Their methodology resulted in equivalent history match in fewer reservoir simulation runs when compared with the work of Coats, et al., (1970).

The calculation of gradients, based on sensitivity coefficient method was proposed by Carter, et al., (1974) and Hirasaki, (1975); in which the derivatives of all pressure and saturation with respect to model parameters; so-called sensitive coefficients are calculated. This is then used to calculate the Hessian matrix for second-order, gradient based optimization algorithms (Li, 2008). For reservoir history matching, Carter, et al., (1974), suggested two new iterative non-linear programming techniques for minimizing the objective function of a reservoir experiencing single phase, compressible flow. They utilized the Jacquard and Jain's method for sensitivity coefficient calculation using gradient method, but within predefined constraint intervals of reservoir parameter values. They reported that their method was equally effective in producing a good match between observed and calculated pressure in comparison with previous works, also with a guarantee to find reasonable reservoir parameter values in predefined constraint intervals. The drawback of this method is that, it is applicable only for single phase flow problems and requires additional computational time in sensitivity coefficient calculation and become less efficient near

the optimum solution. A semi-automatic history matching procedure suggested by Hirasaki, (1975), was useful for problems which required only matching oil production data, but the methodology was found to be inapplicable to complex reservoirs. He implemented the method to estimate the reservoir parameters by finding a relation between the derivative of cumulative oil production with respect to reservoir parameters (sensitivity coefficients) and dimensionless cumulative injection.

Chen, et al., (1974) and Chavent, et al., (1975), formulated the history matching problem as an optimal control problem, where the reservoir parameters: like permeability are considered as the forcing variables and observed data: pressure as the state variable. They used adjoint method to calculate the gradient of the objective function. Adjoint methods calculate the derivatives of an objective function which is the least squared error between observed and calculated production data. This is then subjected to first order gradient-based optimization algorithm to perform minimization process. Chen, et al., (1974), illustrated their work on a single phase synthetic reservoir and an actual single phase Saudi Arabian reservoir. Since history matching problem can be viewed as an optimal control problem they considered reservoir parameters as continuous function of space rather than limiting the parameters as uniform in the zones. The authors reported, that computation time required for optimization was less than the conventional constant-zone gradient optimization techniques. Chavent, et al., (1975), tested their methodology on a single phase semi-realistic reservoir model of dimension 9x19 grid with 10 producing wells having 5 years of historical pressure and production data. They applied steepest descent method to minimize a non-quadratic objective function and used adjoint method for calculating the gradients. They avoided the generation of unrealistic values of transmissivities occurring at any point during computation with the use of adjoints. The downside of the methodology was that it is only applicable to linear problems and requires numerous iterations for highly non-linear problems.

Watson, et al., (1980), successfully tested the method proposed by Chen, et al., (1974), and Chavent, et al., (1975), on a 2D, 2-phase reservoir model experiencing waterflooding. They used optimal control approach to estimate the spatially varying permeability, porosity and relative permeabilities. Yang and Watson, (1988), employed a constrained optimization technique called the variable-metric (or quasi-

Newton) method with optimal control theory for automatic history matching of reservoir models. They successfully applied two variable-metric methods such as the Broyden/ Fletcher/ Goldfarb/ Shanno (BFGS) method and a self-scaling variable-metric (SSVM) method, to test on two synthetic, two phase, 1D and 2D reservoir models. They claimed that the variable-metric methods; BFGS and SSVM are more attractive as compared to the steepest descent and conjugate-gradient methods, except when the permformance metrics is quadratic. The authors concluded that their methods were very efficient in handling the parameter inequalitlity constraints and improving the convergence rate which are necessary for the automatic history matching.

A probabilistic approach called the Bayesian framework for history matching as a substitute to zonation approach was introduced by Gavalas, et al., (1976), and Shah, et al., (1978). The methodology provides better estimates of true permeability and porosity distributions in the reservoir than the conventional zone-gradient optimization methods. The Bayesian framework was tested on a single phase, 1D synthetic reservoir. The Bayesian estimation uses prior statistical information (mean and co-variance) on the unknown parameters and incorporates geological information as a penalty term in the objective function to reduce statistical uncertainty in reservoir parameter estimation. Shah, et al., (1978), compared the results obtained using Bayesian estimation with those of reparameterization by zonation and sensitivity coefficient method, based on computation of the traces of a posterior co-variance matrix. Both groups, Gavalas, et al., (1976), and Shah, et al., (1978), reported that the correctness of the Bayesian estimates depends on the accuracy of the prior knowledge on the statistics and geological information.

de Marsily, et al., (1984), proposed a pilot point method in conjunction with the optimal control theory for parameterization of groundwater hydrology. The concept of the pilot point method was first adopted in petroleum engineering by Fasanino, et al., (1986), for single phase gas reservoir parameterization by perturbing reservoir parameter (such as permeability and porosity) values at selected locations of pilot points to match reservoir production history. The reservoir properties at the remaining locations are interpolated using kriging or conditional simulation with respect to the reservoir parameter values at the pilot points. Thus, pilot point technique

avoides gradient calculation in all grid blocks expect at the pilot points which, in turn, reduce unknown reservoir parameters that have to be estimated. This method provides only an approximate solution for the inverse problem like history matching, and also there is unceratinity about the number of pilot points to be specified and their locations to minimize the objective function. Further application of pilot point method and its extension in history matching can be found in works of Floris, (1996); Bissell, et al., (1997); Xue, et al., (1997); Landa and Horne, (1997); and Wen, et al., (1998). Bissell, et al., (1997), successfully applied the pilot point method on a synthetic reservoir to estimate the porosity values for history matching. They found optimal locations for pilot points using the sensitivity information computed from a direct method, which assumes that high sensitivity reservoir regions are influenced by the pilot point locations. Cuypers, et al., (1998), discussed how to choose number of pilot points and optimum location by combining the geological uncertainity and sensitivity to objective function. The pilot point technique suffers from a few drawbacks due it slow convergence to optimum solution, overshooting or undershooting of reservoir paramters at the pilot points, consequently resulting in fluctuations of objective functions as iterations proceed (Xue, et al., 1997, and Liu and Oliver, 2004).

Anterion, et al., (1989), extended the method, proposed by Carter, et al., (1974) and Chavent, et al., (1975), to multi-phase flow problem. The sensitivity coefficient calculation based on gradients are implemented on a fully implicit, synthetic, 3-phase, 3D reservoir. Their testing resulted in an improved accuracy of history matched models and reduced simulation runs and computer processing time as compared to other gradient methods. The authors concluded that the indulgence of experienced reservoir engineer on history matching problem cannot be automated/ substituted as computers do not have the ability to choose the parameters to be changed. Extensive studies and applications of gradient simulator to calculate sensitivity matrix have been reported by Bissell, (1994), Wu, et al., (1999), Wu and Datta-Gupta, (2002), Rodrigues, (2006), Cominelli, et al., (2007) and Oliver, et al., (2008). However, the experience of these authors shows that reservoir models with greater than a few thousands of grid blocks are to large and complex to be solved using direct methods due to limitations in memory and computation time. Although Killough, et al., (1995), tried speeding the iterative solver, but still 10% of forward simulation was required for

calculating the sensitivity coefficients. They introduced a multiple right hand side iterative linear equation solver (MRHS) for system of adjoint equations that considerably boost the gradient solver performance. The authors experimented their methodology on reservoir models having upto 10,000 grid blocks and showed a comparison between the MRHS iterative solver and standard red-black line successive overrelaxation (RBLSOR) and direct (D4) solvers.

Tan and Kalogerakis, (1992), applied a modified Guass-Newton method for history matching problem of a 3-phase, 3D synthetic reservoir to estimate the parameters such as permeability and porosity. They showed the successful execution of the methodology to automate completely the history matching procedure and resulted in achieving genuine permeability and porosity values from a wide range of intial guess. They also reported the capability of Guass-Newton method in reducing the number of sensitive coefficients to be calculated. This method was employed for hisotry matching problem of a single phase reservoir by Chu, et al., (1995). They tried to condition the well-test pressure data with the reservoir grid block permeability and porosity distributions with modified generlized pulse-spectrum technique (MGPST). They showed that the method achieved a reasonable estimate of the sensititvity related to the permeability distribution, but not with the porosity distribution. The authors also presented a technique for generating realizations of permeability and active well skin factors that are conditioned to the wellbore pressure. Reynolds, et al., (1996), used the Gauss-Newton methodology to construct a posteriori estimate of reservoir parameters and a reduced parameterization technique for history matching of multi-well pressure data. The authors applied a subspace method as parameterization technique to reduce the size of the Hessian matrix, that has to be solved during each Guass-Newton iteration. They reported, there was a significant reduction in computaion time required for generating realizations conditioned to prior geological and observed data. He, et al., (1997), applied the same approach used by Chu, et al., (1995), to generate sensititvity coefficients related to porosity fields for a single phase flow reservoir. They concluded that they did not achieve better estimates of sensitivity coefficeints related to porosity fileds, hence they extended the practice of Carter, et al., (1974), for estimating the sensitivity coefficients related to porosity and permeabiltiy fields. The methodology was further extended by Wu, et al., (1999), for 2D, 2-phase flow of oil

and water synthetic reservoir history matching problem. They achieved history matched model by adjusting the mean log-permeability of each layer rather than adjusting the individual grid block permeabilities. Li, et al., (2003), extended the methodology for a 3D, 3-phase reservoir history matching problem. The drawback reported by authors who applied Gauss-Newton method and its varients was its slow convergence for long time production data and undesirable match for the well-test pressure data in case of bad intial estimates.

Bi, et al., (2000), used Levenberg-Marquardt method, which is a version of Gauss-Newton method with modification in Hessian matrix to improve the convergence rate. They implemented the methodology to condition 3D stochastic channels to well-test pressure and well observation data, which is an extension of the work done by Landa and Horne, (1997) on conditioning 2D stochastic channels to pressure data. Zhang, et al., (2003), used the same methodology to condition 2D stochastic channels to pressure data and well observations by introducing a randomized maximum likelihood (RML) method for generating better initial guess for the Levenberg-Marquardt algorithm. The method was also applied by Vefring, et al., (2006) to estimate the reservoir properties by minimizing the difference between the measurements from the drilling process and corresponding reservoir simulation model states. However, the Levenberg-Marquardt algorithm resulted in slow convergence and also induced instability for models with large production data and parameters.

Conjugate gradient or quasi-Newton method, is believed to be more efficient and require less computation time to compute the sensitivity coefficients. This method requires only the gradients of the objective function and thus reduces the computational time needed for sensitivity coefficients to form Hessian matrix. Makhlouf, et al., (1993), employed this approach to estimate gridblock permeabilities of reservoir having 2-phase (oil and water) and 3-phase flows. The method used 6400 CPU seconds on a CRAYX-MP/48 for matching historical production data of the reservoir model with 450 gridblocks. They illustrated the effects of bi-cubic spline approximation against zonation and regularization techniques on history matching. Deschamps, et al., (1998), extended the work of Anterion, et al., (1989) on gradient optimizing algorithms, by examining six different gradient optimizers for 3-phase, 3D history matching problem. These include; Gauss-Newton/ steepest descent (ConReg),

quasi-Newton (QN), ConReg/QN hybrid, Dennis-Gay-Welsch (DGW) method, Double-Dog-Leg Strategy (DDLS) and the Al Baali-Fletcher (ABF) method. They concluded that the hybrid Gauss-Newton; ConReg and DDLS are more efficient than the quasi-Newton method except for larger reservoir models with gridblocks greater than 10,000 and 100's of parameters. A variant of quasi-Newton, called the limited memory BFGS (LBFGS) was utilized by Zhang and Reynolds, (2002), for complex history matching problems. LBFGS method needs only the gradient and objective function values from the previous iteration to construct the Hessian approximation, Zhang and Reynolds, presented extensive studies on various gradient optimizers such as: Levenberg-Marquardt, preconditioned conjugate gradient, BFGS and LBFGS for synthetic and real reservoirs. They stated that the LBFGS is a more efficient optimizer than the modified Levenberg-Marquardt and the Gauss-Newton minimizing algorithms for large scale reservoirs. A comparison between the simultaneous perturbation stochastic approximation (SPSA) and the LBFGS methods was presented by Gao and Reynolds, (2006). They concluded that SPSA provided slower convergence than the LBFGS algorithm, but was better than the steepest descent algorithm. They also suggested a line-search algorithm, data damping procedure and enforced constraints on model parameters for improving the efficiency of minimization algorithms. Liu and Oliver, (2004), tested the quasi-Newton method as minimizing algorithm and adjoint equation for gradient calculation on a 5-spot water injection problem with more than 73,000 model parameters. Dong and Oliver, (2005), used the same approach for automatic history matching problem of time-lapse seismic data, by minimizing the difference between measurement changes to that of reservoir simulator response. Eydinov, et al., (2009), reported the implementation of LBFGS algorithm for estimating the relative permeability curves and distribution of porosities and permeabilities for 3-phase synthetic reservoir.

A knowledge based system (KBS) was created by Parish, et al., (1993), in conjunction with Sequential Bayes method as a decision support tool for reservoir engineers. The knowledge based system assists the engineers to interact with the framework of automatic history matching. The KBS uses knowledge of the engineer about the field which is stored in a database and uses rule-based instructions such as IF… THEN, ELSE, statement to make suitable decisions on history matching.

An alternative to conventional gradient optimization method is the Gradual Deformation method which can be considered as a stochastic optimization method, since it does not require the calculations of gradients of objective functions to reach optimal solution. The method was proposed by Roggero and Hu, (1998) and Hu, (2000), for conditioning 3D stochastic reservoir models to the well-test and production data. The method is an efficient inverse algorithm that gradually deforms the Gaussian-related stochastic model whilst maintaining the statistical characteristics (spatial variability) of the reservoir models. The method is usually formulated as the linear combination of two Gaussian realizations with expected mean and covariance to generate new realizations, which better match the production data than the initial realizations. In this case, the history matching problem is transformed to 1D optimization problem, since the combinations are parameterized with a single parameter. The match obtained from newly generated realizations was further improved by combining with other equi-probable realization, this process continues until a satisfactory match is achieved by the newly generated reservoir model realizations. Hu, (2000), extended the work to multidimensional gradual deformation, local gradual deformation and deformation gradually with respect to structural parameters. Moreover the method is applicable for calibrating the non-Gaussian reservoir models by transforming the non-Gaussian framework to Gaussian framework (e.g. lognormal model, truncated Gaussian model).

Hu, et al., (2001), demonstrated the efficiency of this method for constraining reservoir facies model generated by sequential simulator to the production data. A prior constraint was included in the objective function by Ravalec-Dupin and Nœtinger, (2002), when they realized that the correct sampling of posterior probability density function was not granted using gradual deformation algorithm that has only data mismatch as the objective function. Caers, (2003), showed the application of gradual deformation method with multi-point geostatistics to generate initial realizations for a streamline simulation model that deforms the initial realization to match the observations at well locations. Liu and Oliver, (2004), concluded that the gradual deformation is better than Markov Chain Monte Carlo (MCMC) method when they compared the distribution of conditional realization obtained from both the methods. Further extension of application from pixel-based models to object based

model such as Boolean models was presented by Hu and Jenni, (2005). An application of local gradual deformation in history matching using real reservoir data was presented by Gervais, et al., (2007). They pointed out that an issue arises in defining the partition of the fine-scale geological model while applying local gradual deformation method.

The advantage of these type of gradients-based methods is that it converges fast to optimal solution. Even though these methods are very efficient and widely used, they suffer from drawbacks like converging to local optimum solution by escaping the global optimum solution and also calculation of first and second order derivatives of highly nonlinear objective function is a problem. These limitations of gradient based algorithms draws attention of researchers to come up with stochastic methods which are non-gradient based.

2.5.2 Non-Gradient Based Methods

Non-gradient methods are also known as stochastic algorithms, which perform better in approaching the global optimum and escaping local optimum solutions (Kathrada, 2009). Moreover, the non-gradient methods do not require any calculation of complex gradients to minimize the objective functions. On the other hand, stochastic algorithms usually require significant computation time and large number of simulation runs to converge to global optimum in comparison to gradient-based methods. However, stochastic algorithms are most suitable for non-unique history matching problems, as these methods do not require an initial guess close to the optimum. Instead, a number of equi-probable reservoir models are generated which evolve progressively with the help of certain operators until global optimum is reached (Liang, 2007). Over the past four decades there has been an enormous progress in developing the stochastic algorithms by several researchers. Some of the commonly used stochastic algorithms are:

- ♦Simulated Annealing
- ♦Scatter and Tabu searches
- ♦Neighborhood Algorithm
- ♦Particle swarm optimization
- ♦Ant colony optimization
- ♦Kalman filters
- ♦Genetic Algorithms
- ♦Simultaneous perturbation stochastic approximation

2.5.2.1. Simulated Annealing: Simulated annealing (SA) proposed by Kirkpatrick, et al., (1983) and Cerný, (1985) is a probabilistic heuristic method for finding global optimum solutions in a large discrete search space. SA was first introduced for reservoir characterization by Farmer, (1989). Extensive researches on SA for inverse modeling of reservoir have been accomplished by many researchers in early 90's. Ouenes, (1992), applied the methodology for simultaneously estimating and conditioning of the petrophysical properties of the reservoir. He confirmed the robustness of the methodology by making comparison with other gradients methods. Further, Ouenes, et al., (1992), employed SA for simultaneously estimating relative permeability curves and capillary pressure for gas/water laboratory core floods. Sultan, et al., (1993), used SA for automatic history matching of a black oil reservoir experiencing waterflooding. They reported, a good match with field production data was attained with the implementation of SA. Ouenes and Saad, (1993), proposed a new, fast, parallel SA algorithm to reduce computation time for minimizing the objective function of large scale reservoirs. They tested the parallel processing algorithm on a reservoir model with dimension 280 x 180 using a CRAY Y-MP with 4 processors. Panda and Lake, (1993), applied parallel SA algorithm using Intel's Hypercube processor iPSC 860 for estimating the permeability fields. Later, Ouenes, et al., (1994), applied SA algorithm for estimating the permeabilities, pore volume, reservoir wettability and wellbore properties of a fractured reservoir. Deutsch and Journel, (1994), applied the algorithm to construct a stochastic reservoir model that honors available geological and production data. Sagar, et al., (1995), used SA to minimize an objective function that included information on geometric average permeability along with the spatial statistics from well log/core data. Sen, et al., (1995), introduced a heat-bath algorithm for SA method instead of traditional Metropolis algorithm and applied it to a set of outcrops and tracer flow data for estimating permeability fields. The authors reported that for small simulation problems, SA based on metropolis performed well but for larger problems, heat-bath algorithm equaled and often outperformed metropolis algorithm. Abdassah, et al., (1996), reported that a better reservoir simulation can be achieved by incorporating acoustic impedance data to the conventional SA method. Portella and Frais, (1999), used SA method for solving automatic history matching problem by combining it with the pilot point method for reducing the number of adjusting parameters. Further, the

resultant history matched model was used to generate realizations by applying a geostatistical technique. Each of these realizations was subjected to flow simulations to ensure the desired confidence interval of reservoir performance predictions. Even though a satisfactory match was achieved with SA method, the slow convergence limited its application for further studies.

2.5.2.2. Scatter Search: Scatter search (SS) technique was proposed by Sousa, et al., (2006) for automatic history matching. SS starts with an initial set of solutions called reference set (RefSet), which have the best solutions acquired from the previous solution attempts. The idea behind this technique is to improve the quality of the RefSet by making a non-convex linear combination of the RefSet solutions, which gradually generate new sets of solutions. The newly created sets are ranked according to their fitness function, and then the fittest RefSet solutions are selected for the next iteration. Sousa, et al., (2006), tested their technique for history matching of homogeneous and heterogeneous synthetic reservoirs. They framed their history matching problem as a combinatorial optimization problem in which the uncertainty of the parameters had to be discretized. The reduction in the state space between the discretized parameter values enhances the accuracy of the results, consequently increases the number of possible solutions. Albeit, the implementation seems to be limited for small number of parameters, the SS technique reported to be quite efficient in generating the quality RefSet solutions that requires fewer simulation runs.

2.5.2.3. Neighbourhood Algorithm (NA): Neighbourhood algorithm is a global optimization, non-derivative search algorithm in a Bayesian framework used to sample the multidimensional parameter space. Similar to simulated annealing, NA generates ensembles of history matched models by first generating initial random sets of models, and then ranks each of them according to the degree of match with the data. The spatial properties of the geometrical construct, called the Voronoi cells, are used to create new models by uniform random walk from the previous best matched models. Sambridge, (1999), first introduced NA applications to petroleum engineering for highly non linear problems like waveform inversion of seismic data. He showed that the method was robust and efficient with reduction in the computation time and memory requirement depending on ensemble size and dimension of the parameter space. The author reported that the methodology was compatible with the distributed

systems. Subbey, et al., (2004) and Christie, et al., (2006), employed a Bayesian framework for quantification of uncertainty in flow through porous media by using NA algorithm to develop history matched models. Rotondi, et al., (2006), applied NA algorithm on an offshore gas field consisting of seven wells having 6 years of production history. The hydrocarbon forecasts and uncertainty quantification using Bayesian inference matched well with data when compared to other history matching algorithms. Erbaş and Christie, (2007), examined the efficacy of NA sampling algorithm for generating history matched models for a real field from North Sea reservoir. Their research was more inclined towards finding the inaccuracies associated with different sampling algorithms used for uncertainty quantification in reservoir performance predictions and parameter estimation. Suzuki, et al., (2008), combined neighbourhood algorithm with 'similarity distance' measure to accommodate large reservoir realizations.

2.5.2.4. Particle Swarm Optimization (PSO): Particle swarm optimization is a bio-inspired; population based stochastic optimization method for discrete and continuous optimization problems. PSO, an intelligent search technique, introduced by Kennedy and Eberhart, (1995), from the idea inspired by behavioral model of fish schooling or bird flocking. In particle swarm optimization, the possible solutions called the 'particles' are positioned in the search space and are moved through the search space. The position of the each particle represents each candidate solution for the optimization problem, where each particle searches for its best position according to the rule based on each particle's personal knowledge and swarm knowledge. Kathrada, (2009), introduced this methodology to reservoir engineering, when he tested PSO in conjunction with hierarchal clustering algorithm on a synthetic reservoir to generate history matched models. Fernández Martïnez, et al., (2009), applied PSO for seismic history matching by conditioning the subsurface facies model to match production history and time-lapse seismic data. They reported that PSO is as efficient as other global optimizer in terms of its convergence and in estimating the uncertainty of parameters of posterior models. Mohamed, et al., (2010), made a comparison between three stochastic algorithms: Hamiltonian Monte Carlo (HMC) algorithm, Neighbourhood Algorithm (NA), and the Particle Swarm Optimization (PSO) by generating multiple history matched models. They concluded that Hamiltonian Monte

Carlo and Particle Swarm Optimization are the potential techniques for uncertainity quantification of reservoir models. A combination of PSO with ANN-based soft-sensor and genetic algorithm was applied for optimzation of a real field by Ali Ahmadi, et al., (2012). Awotunde, (2012), improved the basic PSO method for generating multple history matched models of permeability distributions. Some of the applications of PSO in determininmg the optimal well locations can be found in the wok of Onwunalu and Durlofsky, (2010), Guojian, et al., (2012), and Nwankwor, et al., (2013).

2.5.2.5. Ant-colony Optimzation (ACO): Ant-colonoy optimzation is a population based stochatic optmization method that utilizes the swarm intelligence, developed from the social behavioral model of ants. ACO is a metaheuristic algortihm for combinatorial optimization problems, introduced by Dorigo, et al., (1996), from the stuides of communicative behavior among real ants in finding the shortest path between the food source and their nest. ACO is an evolutionary approach applicable to both disceret and continuous variable optimization problems, where many generations of artifical ants search for an optimal solution for the problem. Fatemeh and Farhang, (2008), proposed the application of ACO technique to estimate fluid injection rates, optimal well locations for production and injection, and well flow pressure. They coded the ACO algorithm in MATLAB environment and ilustrated its ability in providing fast convergence and accurate solutions. A mutidimensional, continuous, ACO was used by Rutkowski, et al., (2008), for estimating reservoir description of history matched models, and also for determining the number of optimum phase seperaters in oil industry. Li, et al., (2010), applied a hybrid particle swarm- ACO (PS- ACO) algorithm for recognizing oil-bearing zones of a reservoir. Hajizadeh, (2011), and Hajizadeh, et al., (2011), presented extensive studies on ACO, differential evolution (DE) algorithm for achieving multiple history matched reservoir models and quantification of uncertainity in ultimate oil recovery. They tested their methodologies on two reservoirs: a) simple Teal South Reservoir with eight reservoir parameters and a single well, b) PUNQ-3 complex reservoir. A comparison of ACO, DE algorithm with Neighbourhood Algorithm showed that the former provided an impoved quality of multiple history matched models and required lesser number of simulation runs to achieve quality match for PUNQ-3 complex reservoir. The same

methodology was found to be mariginal when applied to simple Teal South reservoir with sinlge well and univariate objective function. A comparison of ACO, DE algorithm with Neighbourhood Algorithm showed that the former provided an impoved quality of multiple history matched models and required lesser number of simulation runs to achieve quality match for PUNQ-3 complex reservoir. The same methodology was found to be mariginal when applied to simple Teal South reservoir with sinlge well and univariate objective function. Hajizadeh ans coworkers also extended the application of these methodologies for muti-objective history matching problems and reported that the DE-rand was a better option for such problems. The use of ACO with back- propagation algorithm (ACO- BP) proposed by, Irani and Nasimi, (2012), and Amir, et al., (2013), enhanced the evolution capability of the neural network and thereby, production forecasting of history matched models. They experimented the hybrid ACO-BP algorithm for estimating permability distributions from the well log data of Mansuri Bangestan reservoir of Iran. Their experimental results showed that, ACO-BP algorithm was more effcient in comparison with conventional BP algorithm for parameter estimation. Popa, et al., (2012), utilized ACO for waterflood analysis for an unconventional reservoir characterized with low permeability, high porosity and high oil saturation.

2.5.2.6. Ensemble Kalman Filters (EnKF) And Its Varients: Evensen, (1994), proposed a Monte Carlo type Kalman Filter called Ensemble Kalman filter (EnKF). EnKF incorporates prior knowledge of the parameter to be estimated with the knowledge about available observations to achieve an estimate that resembles the truth. For past two decades, there has been an enournous research and successful application of EnKF in reservoir engineering and inverse problem of history matching. The literature survey presented here on the application of EnKF in reservoir engineering showcases some of the impotant works done in past years.

Lorentz

en, et al., (2003), first introduced EnKF in petroleum engineering for tuning the parameters in a two phase flow model. First application of EnKF in history matching was presented by Nævdal, et al., (2002), for updating the static parameters in near-well reservoir modeling by tuning the permeability fields. Nævdal and co-workers extended the application of EnKF to update 2D, 3-phase, North Sea reservoir by continuously

adjusting permeability, saturations and pressure fields and simultaneously assimilating the new data as it arrive.

Gu and Oliver, (2005), used EnKF for continuous updating of porosity, permeability, pressure and saturation fields of 3D, PUNQ-S3 reservoir history matching problem. The authors reported the use of small ensemble size, which resulted in a fairly good history match and reduced computational cost incurred in generating 40 history matched models. They pointed out issues related to overshooting of permeability and porosity fields which required further investigations. Gao, et al., (2006), quantified the uncertainty for the PUNQ-S3 problem in a Bayesian setting with randomised maximum likelihood (RML) and showed the results were consistent with those obtained while using EnKF. Gu and Oliver, (2005), analysed the limitations of EnKF while working with non-Gaussian members in the state variables. Their investigation showed that non-physical values were generated during Kalman update when distribution of one of the state variables was far from normal. They also claimed that EnKF and linear inversion problem using Bayesian approach are the same.

Zafari and Reynolds, (2007), reported that EnKF failed to sample the posterior PDF for multi-model problems when the ensemble goes to infinity. However, they concluded that the RML method approximately sampled the correct posteriors. Reasonable results were obtained in case of a 2D synthetic reservoir which had less nonlinear problems. They also showed that for linear case, rerunning the time step proposed by Wen and Chen, (2005), to recompute time dependent parameters were inappropriate. Skjervheim, et al., (2007), used EnKF for continuous model updating by assimilating 4D seismic and production data which resulted in improved estimation of permeability field. The method was a combination of EnKF and Ensemble Kalman Filter Smoother when the seismic data were given as a difference between two surveys at the same location but at different times. They tested the methodology on a synthetic reservoir and a real North Sea reservoir. Good results were obtained in the case of synthetic reservoir, providing better permeability estimates when seismic data were added to the production data. But for the North Sea reservoir, very different permeability estimates were obtained with the addition of seismic data to production data, while retaining the production match. This means that interpretation of seismic

data in terms of permeability map may not be unique. Lodoen and Omre, (2008), illustrated how to account for an upscaling problem when using the filter, and quantified loss in accuracy and precision. The idea is to use coarse scale fluid flow simulation results to predict fine scale simulation results, and to assess the associated prediction uncertainty. The relationship between production properties from a coarse scale and a fine scale fluid flow simulator is estimated by the application of EnKF. Liu and Oliver, (2005), used EnKF to condition lithofacies realizations generated by pluri-Gaussian model. The authors, presented a comparison between the performance of EnKF and gradient-based minimization method for the problem of estimating the facies boundaries in history matching. For this purpose, distributions of reservoir model realizations from 20 independent ensembles were then compared with the distribution from 20 RML realizations for a 2D water flood model with 1 injector and 4 producers. The results showed that EnKF was effective for history matching the production data. Their investigations also showed computational effort to generate 20 independent realizations was similar for both the methods.

Wen and Chen, (2005), used EnKF with confirming option for continuously updating ensembles of permeability distriubution to match production history of real time reservoir model. They suggested, an ensemble size of 50 or 100 for EnKF, was too small to estimate the uncertainty in the model, whereas an ensemble size of 200 seemed to be sufficient. Arroyo-Negrete, et al., (2008), proposed a sensitivity-based covariance localization to overcome the limitations of traditional EnKF such as; instabilities, parameter over/undershooting and loss of geological realism. The robustness and practical ability of the approach were demonstrated using a synthetic example and Goldsmith field case. They showed a comparison of results obtained between standard EnKF and conditioned EnKF. They claimed, conditioned EnKF has the ability to retain the shape of the non-Gaussian nature of the histograms that leads to reasonable updated model. Haugen, et al., (2008), showed, how EnKF could be used for assisted history matching of a North Sea reservoir model by estimating the water-oil contact and gas-oil contact. Their investigations raised some issues related to EnKF which include the estimation of structural parameters and estimation of multi-model and non-Gaussian facies distributions. Jafarpour and McLaughlin, (2008), combined the Discrete Cosine Transforms (DCT) parameterization with EnKF to

estimate the unknown geological properties of large reservoirs. They examined the proposed method on two, 2-phase, 2D, synthetic reservoirs during waterflooding having different types of geological variability. The authors applied DCT parameterization to both state variables and model parameters which resulted in better history matched production data as compared with traditional EnKF. Chen, et al., (2008), proposed an ensemble based closed loop optimization method that combines a novel ensemble based optimization scheme (EnOpt) with EnKF and does not require any adjoints. Foss and Jensen, (2011), proposed an application in which they combined EnKF with Model Predictive Control (MPC) in a closed loop reservoir management scheme. This problem was solved using adjoint based optimization.

Agbalaka and Oliver, (2008), used EnKF to automate the history matching of facies distribution and production data. They demonstrated the use of sub-space methodology for problems of generating maximum posterior estimates and realizations of log-permeability and porosity fields conditioned to synthetic pressure data for single phase flow for both 2D and 3D cases. The method produced satisfactory results. Liang, et al., (2007), proposed a weighted EnKF, by modifying the assimilation equation with the addition of a weighting factor to each ensemble member. The method was applied to a complex reservoir having seventeen layers. They made a performance comparison between weighted EnKF and traditional EnKF. Chitralekha, et al., (2010), applied EnKF for characterization and history matching of an unconventional 3D steam assisted Gravity Drainage oil reservoir. Distance dependent covariance localization and globalization methods were used for updating grid block permeabilities by assimilating near-well measurement data. They assessed the quality of ensemble realizations in terms of their weighted mean square error (WMSE) and R-square values. Both the methods resulted in reasonable history match demonstrating the efficacy of the localization approach. However, their globalization method did not provide any significant improvement in the quality of production history match, but localized method yielded permeability values having low error when compared to truth case. Their 3D reservoir was synthetic with known permeability distribution which helped them to compare their EnKF predictions of permeabilities with actual values but lacked realism. They also observed that the RMSE in the estimated permeability of localized EnKF was consistently lower than

that of the global EnKF algorithm. Emerick and Reynolds, (2011), showed significant improvement in production data match and performance prediction with the use of half-iteration EnKF (HI-EnKF) with covariance localization for a field case, but the computational cost was high, as HI-EnKF required rerunning of ensemble from time zero at every data assimilation step. These authors compared the performance of HI-EnKF with covariance localization and that without covariance localization for a real field and reported that the former method avoided the propagation of spurious correlation and loss of variance by maintaining a better production match and performance prediction. Phale and Oliver, (2011), proposed constrained EnKF method (CEnKF), which takes into account the physical constraints on plausible values of the state variables during data assimilation. The problem such as, negative value for updated molar density of CO2 for some region encountered during history matching of 2D compositional model and highly heterogeneous 3-phase reservoir model, were avoided with the usage of CEnKF. They showed, CEnKF technique had the ability to enforce non-negativity constraints on molar densities and bound constraints on saturations and thus achieving a better estimation of reservoir properties.

When rock properties are modelled using Gaussian random field, there is a tendency to under estimate the uncertainty associated with geological structures. Zhang and Oliver, (2011), analysed uncertainty associated with regional trend as one important source of uncertainty, represented by stochastic trend coefficients. They proposed a method for representing and updating multiple scales of heterogeneity in EnKF, which was tested on deep water reservoir model having 2000,000 unknown parameters. Their analysis showed an unsatisfactory match for production history of a real field with traditional EnKF as it was difficult to match the water cut in the main producer. The results obtained with multi-scale parameterization showed an improved data and water cut match with the reduction in tendency to underestimate the uncertainty. The limitations of EnKF to quantify the uncertainties in data mismatch, sampling errors in posterior probability distributions and handling highly nonlinear problems, led to introduction of hybrid EnKF and its varients using stochastic algorithms. Kovalenko, et al., (2012), assessed the sampling error occuring at a single update step of EnKF. For this, they derived a distribution of Euclidean norm of the sampling error emering at a single step update, under assumptions of negligilbe observation error and

normality of forecast distributions. Several synthetic reservoir models were used for illustarting the error propagation at single step update. Emerick and Reynolds, (2013), compared the sampling performance of nine ensemble- based techniques with an adjoint method for a small, highly nonlinear reservoir, for which a MCMC sampling algorithm was used to generate reference posterior distribution of reservoir parameters. They conducted the performance analysis in terms of uncertainity quantification of history matched models and computaional cost incurred. Tavakoli, et al., (2013), introduced a parallel data assimilation framework for uncertainty quatification and reservoir characterization, where the multiple realizations were distributed among several computers for computations. The communication among these parallel systems were performed at data assimilation step. They tested the parallel ensemble-based framework on synthetic reservoir for EnKF and Ensemble Smoother (ES) method. They concluded that the parallel framework reduced the computation time as compared to the serial ones, a parallel efficiency of 35% was attained for EnKF and more than 50% for ES technique. Heidari, et al., (2013), used EnKF in conjunction with two second order parameterization methods such as; pilot points and gradual deformation to avoid deviation of constraint petrophysical properties from prior knowledge .

2.5.2.7. Genetic Algorithm (GA): Genetic algorithm is a direct search metaheuristic method that grounds on the evolutionary concept of natural selection and genetics. GA belongs to a class of evolutionary algorithms developed by Holland, (1975), based on Darwin's theory of "survival of the fitttest". This evolutionary process utilizes a population of individuals called chromosomes, are processed on the principles of natural selection, inheritance, recombination (crossover) and mutation, over generations using random search within the defined search space to reach potential solutions. The newly generated individuals of the population are evaluated using fitness function and the success of the reproduction varies with the fitness. GA have been widely applied in many engineering and real world problems such as protein structure prediction (Contreras-Moreira, et al., 2003), learning robotic behaviour (Birk, et al., 1998), computer automated system design (Li, et al., 2004), inverse problems in electromagnetics (Tanaka, et al., 1994), inverse modeling of coupled flow-mass trasportation (Mayer and Huang, 1999), optimal design of gas transmission

pipeline (Goldberg, 1987; Montoya-O, et al., 2000), design of optimal neural architecture for on-line soft-sensor development (Dam and Saraf, 2006) etc.

Genetic algorithm has proved to be an efficient and effective method for reservoir parameterization and ill-posed, inverse history matching problems. The application of genetic algorithm for reservoir modeling was first introduced by Sen, et al., (1995), for generating stochastic permeability distributions from a set of reservoir outcrops and tracer flow data, followed with uncertainty quantification of production forecasts. A string of binary coded chromosome that represents permeability values at each grid location with a population size of 200 was adopted in their stuides. The formulation of genetic algorithm used for their study was based on standard fitness-proportionate selection operator, k-point crossover operator, and bit-flip mutation operator. It was reported that they achieved global optimal solution with a crossover probability of 0.60, mutation probability of 0.01 and update probabiltiy of 0.90. The authors concluded that the peformance of GA was highly dependent on the choice of population size and crossover, mutation and update probabilities. A modified GA was proposed by Bush and Carter, (1996), for estimating parameters such as sand permeability, shale permeability and fault throw. Their modifed GA incorporated a non-standard binary encoding, modified breeding strategies and niching, and was tested on a vertical cross section of a synthetic PUNQ-S3 reservoir. They encoded the reservoir parameters in a variable length binary choromosome with 3 x 4 bit length to spot large scale structures. They transformed to 3 x 8 bit choromosome to identify small structures of reservoir after 10 iterations. Since the authors initially encountered difficulties with the ghost clusters, they employed inter-leaving procedure for chromosome construction rather than the concatenation procedure. It was reported that they used steady state GA with modified rank selection operator that includes elitism. In steady-state GA, the population size of offspring is equal as the parents population size after each iteration. They applied a random k-point crossover operator to generate two offspings followed by mutation operation. The authors reported that their modified GA outperformed the standard, GA. Another successful application of GA in identifying the hetrogeneous reservoir properties by matching the tracer breakthrough profiles using six reservoir parameters was demonstrated by Guerreiro, et al., (1998). They tested the proposed method on a hetrogeneous quarter of five-spot

synthetic reservoir, considering six parameters such as; the geometry of insertion and porosity inside and outside the insertion, for matching tracer breakthrough profile. The parameters were encoded in a 45 bit long binary chromosome, with a population size of 200, utilizing three crossover operators; single point, two point and uniform crossover operation with probabilities of 0.08, 0.48, 0.24 respectivey, and bilt-flip mutation with 0.02 mutation probability . They used a rank-based selection with elitism for selecting the best realization according to the individual's fitness value, which are the sum of the weighted absolute difference between the observed values and the candidate solutions. The authors concluded that they achieved a satisfactory optimal solution with their proposed work flow.

Huang, et al., (1998), developed a neural-genetic model for permeability estimation from well log data. They utilized genetic algotihm to optimize the connection weights for training the neural netwroks for permeability predictions. Their results showed that the performance error was consistenly reduced with the use of GA when compared with the results obtained for NN trained with backpropagation algorithm. However, they found that GA optimizer was limited due to its slower convergence. Later, Huang, et al., (2000), modified their work in neural-genetic modeling for fast convergence by integrating a fuzzy reasoning, which established a hybrid neural-fuzzy-genetic technique. In this technique the connection weights in GA are initialized by utilizing the weights trained by backpropagation algorithm. Soleng, (1999), applied steady state GA to condition the petrophysical properties of the reservoir to field observations. He examined the methodology on PUNQ S3 synthetic reservoir models of dimension 19 x 28 x 5. The grid block horizontal and vertical permeabilities and porosities are considered as the petrophysical parameters to be estimated, such that the reservior description is conditioned to field observations (bottom hole pressure, gas/oil ratio, and water cut). A population size of 50 was utilized and single point crossover, simple swap mutation and replacement operators were carried out for GA evolutions. The probability of swap mutation was considerd as zero at the grid block well locations. The author reported the method was fast in achieveing reasonable near-optimal solutions that are close to the realistic reservoir conditions. Soleng also analysed the uncertainity associated with total oil production from the field, using 10 history matched realizations resulting from independent GA

runs. He suggested that the disruptive effect of crossover can be eliminated with the use of 3D crosssover operation. The author tested his technique on a small reservoir considering only a few parameters for conditioning to field observations, but expressed his doubts about the efficiency of the method for large scale reservoir.

An extensive testing of the GA optimizer for reservoir history matching and a comparison with simulated annealing and GA with hill climbing were attempted by Romero and Carter, (2001). They tested on a coarse scale simulation model of synthetic PUNQ- S3 complex reservoir of dimension 12 x 44 x 10 having 11 producers and 6 injectors. 57 pilot points that included 17 well locations and 40 distributed pilot point locations in each of the nine layers (one inactive layer) were used for estimating the grid block permeabilities, porosities and shale volume. A sequential Guassian simulation was utilized for generating initial grid block parameters, which hornors paramaters at well locations and pilot points. They used seven sets of reservoir parameters such as permeability, porosity, V-shale, geostatistical parameters, well- skin factors, and relative permeability end points. Each set of parameters were allocated to a different chromosome, each chromosome being designed to allow any structure and were treated separately during crossover and mutation operations. A non-standard structure of the genome design for a population size of 20 was adopted for history matching. The permeability, porosity, and V-shale were encoded in a complex 3D chromosome structure with many extrons. The fault parameters were encoded as three real numbers with known upper and lower bounds and geostatistical parameters were encoded as four real numbers, with known upper and lower bounds. The skin factors were encoded as 17 real numbers and the relative permeability end-points were encoded as 36 real numbers, with all of the end-points for a particular layer grouped together in one part of the chromosome. All the parameters except the permeability, porosity, and V-shale were encoded in one dimensional chromosomes. They used k-point crossover operator for 1D chormosomes and bit-flip crossover operator for 3D choromosomes, subjected to three mutaion operators; jump mutation, creep mutation and shift mutation. Well skin factors were subjected to shift mutation, and all other reservoir parameters used jump and creep mutations. The authors concluded that the algorithm produced better optimal solutions than the results from simulated annealing and equalvent results with

manual history matching process. They showed the method to be inherently suitable for parallelization and reasonably insensitive to parameters settings used to control GA.

Williams, et al., (2004), proposed a novel concept called the top down reservoir modeling (TDRM) in history matching and uncertainty quantification. The TDRM approach is a trademarked technology of BP, which forms an important part of reservoir simulation as semi-automatic history matching tool. The approach utilizes genetic algorithm optimzer in conjunction with reservoir simulation model for TDRM workflow to find reasonable multiple history matched models, in depletion analysis and for uncertainty quantification. The authors reported that the tool had been successfully implemented in development, appraisal and mature stages of 18 oil and gas reservoirs. The authors claimed that the TDRM approach resulted in an increase of 20% in the estimated net present value (NPV) of the projects. Kromah, et al., (2005), succesfully applied the TDRM workflow proposed, in BP Trinidad and Tobago (bpTT) assets for finding optimal well locations in a mature oil field that had 30 years production history from 13 wells. It was reported they completed the history match and performance prediction within three weeks. In addition to TDRM, GA optimization has been utilized in commercial software called MEPO® by Scanpower Petroleum Technology, and ENABLE® by Energy Scitech, Roxar; for improving the quality of history matched models. A further utilization of MEPO® for automatic history matching, subsurface uncertainty quantification and infill well optimization was attempted by Choudhary, et al., (2007). They developed a structured workflow that used evolutionary strategy and genetic algorithm optimization methods for re-evaluation of multiple history matched models. Their approach was tested on two West African mature fields. Velez-Langs, (2005), presented a detailed review on the application of genetic algorithm to reservoir characterization and field development plans in petroleum engineering. Ballester and Carter, (2007), designed a new real-coded non-generational GA optimizer, to run on a cluster of 24 parallel computers (Sun Ultraspare5 workstations), for characterizing a real petroleum reservoir (Midge reservoir model) using available production data. The parallelization procedure reduced computation time required for several optimizations to achieve an ensemble of diverse and calibrated reservoir models. Further, they analyzed the optimized

ensembles generated by GA with a clustering algorithm in order to identify the number of distinct calibrated models that are consistent with the production data. They used real-coded crossover operator such as PNX and vSBX (for details refer Ballester and Carter, 2004) and a replacement operator with implicit elitism feature. A population size ranging from 10 – 150 allowing 10000 function evaluations was used. Their proposed methodology resulted in an improved quality and diversity of history matched models, in comparisons to previous studies on the same Midge reservoir model by BP. Their results also showed that it was possible to attain distinct reservoir models in spite of the use of regularization terms in the objective function.

It is often difficult to model a fractured reservoir with available field data. The characterization of multiphase flow properties of such fractured network having multiscale nature and its geological modeling imposes large computational cost. Lange, (2009), employed an inversion methodology based on GA optimization that was coupled with discrete fracture network (DFN) flow simulator to characterize the fractured reservoir models that are consistent with the well-test data. The coupling of GA with 3D DFN simulator enabled the execution of synchronized calibration of well-test data. The author examined the effectiveness of his methodology on a geologically realistic fractured model having 3 facies, 2 fracture sets, and 3 wells. He reported that the method was capable of characterizing consistent fractured properties such as mean conductivity, mean length, orientation dispersion factors, and fracture density. Other successful applications of genetic algorithm for optimzation of well locations in were reported by Jutila and Goodwin, (2006), Walker, et al., (2008), Litvak and Angert, (2009). Han, et al., (2011), presented multi-objective optimization using modified GA optimizer for history matching of waterflooding projects. The authors implemented GA that included non-dominated sorting and diversity preservation algorithms. The fitness of the population was sorted according to proximity and diversity was added by analyzing crowding distance as the approach to accomplish global optimum. The authors experimented on a 2D heterogeneous reservoir having 400 grid blocks, with 3 production wells and a single injection well. A reasonable estimate of the reservoir parameters, and improved prediction accuracy with small performance error for waterflooding project was reported with their method in comparison with conventional single objective history matching method. Monfared, et al., (2012), amalgamated

subsurface response modeling with genetic algorithm as an optimization tool for inverse history matching problem. The methodology was initialized by constructing proxy reservoir models based on the available measurements, which consitiute as the simulator response . A reservoir model was then built based on the minimized proxy model generated by GA, which required only a limited number of runs and a couple of seconds. They found, the evolution of proxy model using GA took shorter time at a low cost compared to other global optimization techniques. The authors reported that, they achieved high-quality proxy models from 79 forward simulation runs and a reduction in global objective function from 581.362 to 9.347 with the use GA. The authors tested their methodology on a field case study that had 41 years of production history and achieved history matched models which were consistent with the observed oil rate, shut-in pressure, repeated formation test pressure, and water cut. Murgante, et al., (2012), presented a comparison between genetic algoirthm and differential evolution for automatic history matching. They tested both the metholodgies on four case studies, each having varying number of parameters (2, 4, 9 and 16) to be estimated for the history matching inverse problem. A soft sensor was designed on the basis of a feed-forward neural network by Ali Ahmadi, et al., (2012), in order to estimate the reservoir permeabilities of a real field. They used a hybrid genetic algorithm and particle swarm optimization method for optimization of the neural network-based soft sensor. The optimal initial weighting of the reservoir parameters for the neural network was achieved using GA. They reported that there was a good agreement between the observed and predicted reservoir permeabilities with the use of hybrid optimization technique. A comparison between results obtained from the developed soft sensor and the conventional neural network was also demonstrated by the authors to show the efficiency of the proposed methodology.

Above literature review has amply brought out the importance of history matching for field development. A host of history matching methods have been tried with the aim of arriving at a method which is effeicient and accurate. However, the search is on even to this day for that elusive method and present study was motivated by the same desire. Genetic algorithm has been tried in the past but rarely on real reservoirs. Since of the present study was to first test the developed adaptive genetic algorithm on a simple synthetic reservoir and then use it for a real field case.

CHAPTER-3

HIGHER-ORDER NEURAL NETWORKS FOR CUMULATIVE OIL PRODUCTION FORECASTING OF PETROLEUM RESERVOIR

3.1 NEURAL NETWORKS (NN) AND ITS EXTENSION TO HIGHER-ORDER NEURAL NETWORKS (HONN)

Neural networks (NN) are composed of several layers of neural units (neurons): input layer, hidden layers and output layer. A neural unit is structured mainly with two operations: synaptic operation for weighting, and somatic operation for mapping. In a conventional neural unit, the weighting process is operated with linear correlation of neural inputs, $x_a = (x_0, x_1, x_2, \dots, x_n) \in R^{n+1}$ (x_0 is bias), and neural weights, $w_a = (w_0, w_1, w_2, \dots, w_n) \in R^{n+1}$ ($w_0 = 1$). The linear correlation can be expressed mathematically as

$$v = w_0 x_0 + \sum_{i=1}^{n} w_i x_i \tag{3.1}$$

However, in nature, the correlation of neural inputs and neural weights is not simply linear, but rather related nonlinearly. This observation introduced a nonlinear (higher-order) synaptic operation, and NN with the higher-order synaptic operation (HOSO) (see Figure 3.1) was developed and named as higher-order neural networks (HONN) (Song, et al., 2009; Gupta, et al., 2003). HOSO of HONN embraces the linear correlation (conventional synaptic operation) as well as the higher-order correlation of neural inputs with synaptic weights (up to nth-order correlation). An n^{th} order HOSO is defined as,

$$v = w_0 x_0 + \sum_{i_1=1}^{n} w_{i_1} x_{i_1} + \sum_{i_1=1}^{n} \sum_{i_2=i_1}^{n} w_{i_1 i_2} x_{i_1} x_{i_2} + \cdots + \sum_{i_1=1}^{n} \sum_{i_2=i_1}^{n} \cdots \sum_{i_N=i_{N-1}}^{n} w_{i_1 i_2 \ldots i_N} x_{i_1} x_{i_2} \ldots \ldots x_{i_N} \quad (3.2)$$

and the somatic operation, which yields the neural output, is defined as,

$$y = \zeta(v) \quad (3.3)$$

In this study, different HOSO have been applied up to third-order. The first-order (conventional linear correlation), the second-order and the third-order synaptic operations are called linear synaptic operation (LSO), quadratic synaptic operation (QSO) and cubic synaptic operation (CSO), respectively.

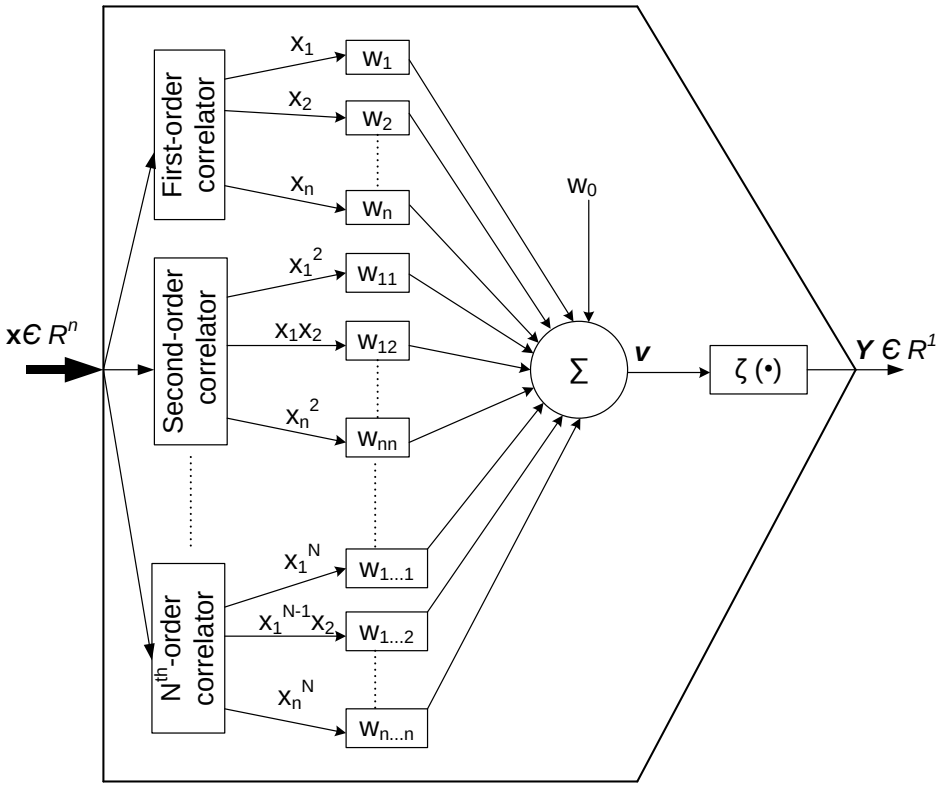

Figure 3.1. A neural unit (neuron) with higher-order synaptic operation (HOSO)

The higher-order neural network (HONN), illustrated in Figure 3.2, consists of multiple interconnected layers: input layer, hidden layers and output layer. The input layer conveys n number of input data to the first hidden layer. Each hidden layer includes different number of neurons, and the output layer contains m neurons, m

being the number of desired outputs. The number of the hidden layers and the number of neurons in each hidden layer can be assigned after careful investigation for different applications.

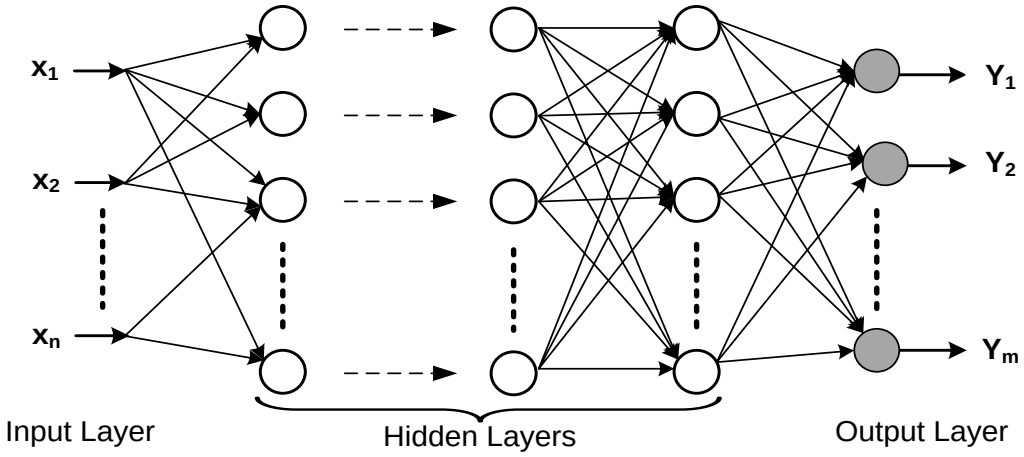

Figure 3.2. A schematic diagram of HONN with multilayer.

HONN is trained by an error based algorithm in which synaptic weights (connection strength) are adjusted to minimize the error between desired and neural outputs (Gupta, et al., 2010; Gupta, 2008; Gupta and Rao, 1994). Let $x(k) \in R^n$ be the neural input pattern at time step $k = 1,2 \ldots n$ corresponding to desired output $y_d(k) \in R^1$ and neural output $y(k)$. The error of a pattern can be calculated as,

$$e(k) = y(k) - y_d(k) \tag{3.4}$$

The overall error for an epoch $E(k)$ is defined as,

$$E(k) = \frac{1}{2} e^2(k) \tag{3.5}$$

The overall error (squared error) is minimized by updating the weight matrix w_a as,

$$w_a(k+1) = w_a(k) + \Delta w_a(k) \tag{3.6}$$

where the change in weight matrix is denoted by $\Delta w_a(k)$ which is proportional to the gradient of the error function $E(k)$ as,

$$\Delta w_a(k) = -\alpha \frac{\partial E(k)}{\partial w_a(k)} \tag{3.7}$$

where $\alpha > 0$ is the learning rate which effects the performance of the algorithm during the updating process. The details can be found in Gupta, et al., (2003).

3.1.1 Model Performance Evaluation Criteria

Several statistical methods have been used to evaluate the performance of neural networks in the literature. In these studies, the following performance measures are applied to substantiate the statistical accuracy of the performance of HONNs: mean square error (MSE), root mean square error (RMSE), and mean absolute percentage error (MAPE). These are the commonly used evaluation criteria in assessing a model performance for its ability to predict the values that deviate limits from the mean value. They indicate the deviation of prediction of applied HONN models, and are defined as

Mean Square Error (MSE):

$$MSE = \frac{1}{n}\sum_{i=1}^{n}(d_i^O - d_i^S)^2 \tag{3.8}$$

Root mean square error (RMSE):

$$RMSE = \sqrt{\frac{1}{n}\sum_{i=1}^{n}(d_i^O - d_i^S)^2} \tag{3.9}$$

Mean Absolute Percentage Error (MAPE) and Mean Absolute Error (MAE):

$$MAPE = \frac{100}{n}\sum_{i=1}^{n}\left|\frac{d_i^0 - d_i^S}{d_i^0}\right| \tag{3.10}$$

$$Mean\ Absolute\ Error\ (MAE) = \frac{MAPE}{100} \tag{3.11}$$

where d_i^0 is the observed data, d_i^S is the predicted data, and n is the number of data points. In order to illustrate the consistency in performance of HONN model towards forecasting the production data, we have used three performance measurement metrics. The results obtained using all three metrics are different in their calculated values, but the significance of each metrics is similar in performance evaluation of the HONN model. Since the raw production data may be scaled before using as input to HONN, it is preferable to use MAPE for estimating the relative error (Azadeh, et al., 2007).

3.1.2 Pre-Processing: Optimal Selection of Input Variables

Before performing a prediction by HONN, it is important and necessary to refine the available input parameter data by applying pre-processing because of two main reasons: i) noise reduction and ii) proper selection of input variables.

The measured oil production data from the field include noise. It is not advisable to use raw data for neural network training because in that case, NN requires extremely low learning rates. Thus, a preprocessing of the raw experimental production data was, therefore, incorporated in all cases. Moving average is a type of low pass filter that transforms the time series monthly production data into smooth trends. This filter does weighted averaging of past data points in the time series within the specified time span (window) to generate a smoothed estimate of a time series. The time span of moving average depends on the analytical objectives of the problem. For the present case studies, we used moving average filter with a time span of five-points since it is found to be optimal for reducing the random noise by retaining the sharpest step response associated with production data. Moving average filter is the simplest and perhaps optimal filter that can be used for time domain signals as reported by Smith, (1997).

After noise reduction process, cross-correlation analysis is carried out to find optimal input variables. Determining the significant input variables is an important task in the process of training HONN model for production forecasting. A thorough understanding of dynamics of petroleum reservoir is necessary to avoid missing key input variables and prevent introduction of spurious ones that create confusion in the training process. Currently, there are no defined rules for the selection of the input variables. Most of the heuristic methods for selecting the input variables are ad-hoc or have experimental basis. These statistical methods provide the correlation between different input variables by identifying potentially influencing variables at different time lags. The idea behind these statistical methods is to investigate the dependence between the input variables.

ACF is a set of auto-correlation coefficients arranged as a function of observations separated in time. It is a common tool for assessing the pattern in time series production data at numerous time lags. Consider the observations x_t and x_{t+k} ;

$t = 1,2,\dots,n$; then the autocorrelation coefficient $r_{(k)}$ at lagk can be calculated using Eq. 3.12

$$r_{(k)} = \frac{1}{n}\sum_{t=1}^{n-k}(x_t - \bar{x}) - (x_{t+k} - \bar{x})\,; \quad \bar{x} = \sum_{t=1}^{n} x_t \tag{3.12}$$

The CCF is a set of cross-correlation coefficients arranged as a function of observations of one or more time series data at different time steps (lag). Consider two time series x_t and y_t, $t = 1,2,\dots,n$; the time series y_t, may be related to the past lags of time series x_t and this can be calculated using Eq. 3.13. Here $r_{xy(k)}$ is the cross-correlation coefficient between x_t and y_t, and k is the lag. This means measurements in the variable y are lagging or leading those in x by k time steps.

$$r_{xy(k)} = \frac{n\sum(x_t - \bar{x})(y_{t-} \bar{y}) - \sum x_t \sum y_t}{\sqrt{n\sum x_t^2 - (\sum x_t)^2}\,\sqrt{n\sum y_t^2 - (\sum y_t)^2}} \tag{3.13}$$

In the present study only positive lags have been used. The presence of positive lagk between x_t and y_t indicates that the relationship between these time series will be most significant when the data in x at time t are related to data in y at time $t + k$.

3.2 HONN FOR PRODUCTION FORECASTING FROM A SINGLE WELL (CASE#1)

A novel neural approach was employed with HONN to forecast oil production from an oil field reservoir with limited input parameter data: i) oil production data and ii) oil, gas and water production data. Two case studies are carried out to verify the potential of the proposed neural approach with the limited available parameters from an oil field in Cambay basin, Gujarat, India. A pre-processing step is included for the preparation of neural inputs. The details are explained in the succeeding sections

In this study, forecasting of oil production from the oldest well of the field, Well-1, is considered. Two cases are studied for oil production forecasting using: i) only oil production data and ii) oil, water and gas production data. Table 3.1. (a) and (b) present the raw and smoothed monthly oil, gas and water productions ratios corresponding to each maximum production values of Well-1 from 2001 to 2009. For an efficient training for HONN, the monthly production ratios were calculated using

the maximum production of products (3000 m^3/month for oil, 150000 m^3/month for gas, and 1500 m^3/month for water) through the 9 years production history of Well-1. Data smoothing was carried out by using the five point moving average filter with each data point weighed equally.

Table 3.1. a. Ratio of monthly oil, gas and water production to corresponding maximum production value of nine years from Well-1.

Months	Oil	Gas	Water	Months	Oil	Gas	Water
1	0.982	0.982	0.096	48	0.240	0.164	0.920
2	0.930	0.930	0.135	49	0.241	0.163	0.965
3	0.950	0.950	0.245	50	0.198	0.140	0.625
4	0.907	0.907	0.244	51	0.192	0.150	0.670
5	0.862	0.862	0.144	52	0.200	0.160	0.653
6	0.704	0.704	0.074	53	0.174	0.131	0.603
7	0.922	0.922	0.060	54	0.157	0.110	0.699
8	0.972	0.972	0.076	55	0.147	0.102	0.686
9	0.874	0.884	0.057	56	0.101	0.073	0.810
10	0.927	0.914	0.052	57	0.097	0.073	0.785
11	0.818	0.806	0.287	58	0.150	0.108	0.602
12	0.764	0.753	0.326	59	0.091	0.065	0.386
13	0.884	0.872	0.152	60	0.123	0.088	0.557
14	0.862	0.849	0.134	61	0.205	0.148	0.666
15	0.813	0.801	0.111	62	0.207	0.149	0.622
16	0.624	0.618	0.180	63	0.205	0.145	0.664
17	0.393	0.387	0.542	64	0.133	0.096	0.516
18	0.507	0.500	0.410	65	0.102	0.071	0.635
19	0.517	0.386	0.366	66	0.114	0.076	0.701
20	0.536	0.401	0.375	67	0.107	0.073	0.686
21	0.490	0.368	0.420	68	0.110	0.073	0.688
22	0.486	0.364	0.537	69	0.127	0.089	0.626
23	0.478	0.359	0.552	70	0.059	0.040	0.224
24	0.396	0.297	0.688	71	0.124	0.093	0.612
25	0.462	0.346	0.369	72	0.118	0.089	0.644
26	0.454	0.341	0.529	73	0.050	0.038	0.784
27	0.474	0.356	0.498	74	0.127	0.098	0.645
28	0.451	0.338	0.735	75	0.117	0.090	0.473
29	0.460	0.242	0.665	76	0.109	0.083	0.489
30	0.440	0.264	0.712	77	0.129	0.099	0.572
31	0.352	0.211	0.636	78	0.160	0.122	0.590
32	0.350	0.210	0.643	79	0.142	0.108	0.556
33	0.315	0.189	0.671	80	0.147	0.114	0.555
34	0.326	0.196	0.690	81	0.165	0.130	0.490
35	0.336	0.245	0.651	82	0.141	0.111	0.547
36	0.248	0.170	0.904	83	0.162	0.126	0.507
37	0.351	0.235	0.725	84	0.095	0.073	0.570
38	0.344	0.230	0.692	85	0.090	0.067	0.546
39	0.165	0.078	0.434	86	0.141	0.107	0.478
40	0.166	0.117	0.432	87	0.104	0.080	0.579
41	0.146	0.109	0.398	88	0.092	0.079	0.551
42	0.163	0.121	0.439	89	0.076	0.047	0.539
43	0.158	0.109	0.420	90	0.081	0.055	0.583
44	0.173	0.119	0.419	91	0.078	0.050	0.663
45	0.267	0.183	0.812	92	0.087	0.059	0.599
46	0.207	0.142	0.616	93	0.009	0.006	0.159
47	0.281	0.193	0.886	94	0.418	0.284	0.270

Table 3.1. b. Ratio of smoothed monthly oil, gas and water production to corresponding maximum production value of nine years from Well-1.

Months	Oil	Gas	Water	Months	Oil	Gas	Water
1	0.982	0.917	0.096	48	0.233	0.149	0.802
2	0.954	0.890	0.159	49	0.230	0.151	0.813
3	0.926	0.865	0.173	50	0.214	0.145	0.767
4	0.871	0.813	0.168	51	0.201	0.139	0.703
5	0.869	0.811	0.153	52	0.184	0.129	0.650
6	0.873	0.815	0.120	53	0.174	0.122	0.662
7	0.867	0.811	0.082	54	0.156	0.107	0.690
8	0.880	0.821	0.064	55	0.135	0.091	0.717
9	0.903	0.840	0.106	56	0.130	0.087	0.716
10	0.871	0.808	0.160	57	0.117	0.079	0.654
11	0.853	0.789	0.175	58	0.112	0.077	0.628
12	0.851	0.783	0.190	59	0.133	0.091	0.599
13	0.828	0.762	0.202	60	0.155	0.105	0.567
14	0.789	0.727	0.181	61	0.166	0.112	0.579
15	0.715	0.658	0.224	62	0.175	0.117	0.605
16	0.640	0.589	0.275	63	0.170	0.114	0.621
17	0.571	0.503	0.322	64	0.152	0.100	0.628
18	0.515	0.428	0.375	65	0.132	0.086	0.640
19	0.489	0.381	0.423	66	0.113	0.073	0.645
20	0.507	0.377	0.422	67	0.112	0.071	0.667
21	0.501	0.351	0.450	68	0.103	0.066	0.585
22	0.477	0.334	0.514	69	0.105	0.069	0.567
23	0.462	0.324	0.513	70	0.108	0.072	0.559
24	0.455	0.319	0.535	71	0.096	0.065	0.578
25	0.453	0.317	0.527	72	0.096	0.067	0.582
26	0.447	0.313	0.564	73	0.107	0.076	0.632
27	0.460	0.303	0.559	74	0.104	0.074	0.607
28	0.456	0.288	0.628	75	0.106	0.076	0.593
29	0.435	0.263	0.649	76	0.128	0.092	0.554
30	0.411	0.236	0.678	77	0.131	0.094	0.536
31	0.383	0.208	0.665	78	0.137	0.098	0.552
32	0.357	0.200	0.670	79	0.149	0.107	0.553
33	0.336	0.196	0.658	80	0.151	0.109	0.548
34	0.315	0.189	0.712	81	0.151	0.110	0.531
35	0.315	0.193	0.728	82	0.142	0.103	0.534
36	0.321	0.201	0.732	83	0.131	0.095	0.532
37	0.289	0.179	0.681	84	0.126	0.090	0.530
38	0.255	0.155	0.637	85	0.118	0.084	0.536
39	0.234	0.143	0.536	86	0.104	0.076	0.545
40	0.197	0.122	0.479	87	0.101	0.071	0.539
41	0.160	0.100	0.425	88	0.099	0.069	0.546
42	0.161	0.107	0.422	89	0.086	0.058	0.583
43	0.181	0.120	0.498	90	0.083	0.054	0.587
44	0.194	0.126	0.541	91	0.066	0.040	0.509
45	0.217	0.139	0.631	92	0.135	0.085	0.455
46	0.234	0.149	0.731	93	0.171	0.109	0.343
47	0.247	0.158	0.840	94	0.418	0.265	0.270

3.2.1 Structure of HONN for Single Well Production Forecasting

A number of design factors for HONN were considered such as selection of neural structure (order of synaptic operation), numbers of neurons and hidden layers for this

study. Also, different mapping functions (somatic operation) were selected after careful investigation in each layer: a sigmoidal (hyperbolic tangent) function for hidden layers and a linear function for the output layer.

In this study, three synaptic operations were embedded in an HONN: linear synaptic operation (LSO), quadratic synaptic operation (QSO) and cubic synaptic operation (CSO). Only one hidden layer was used since it resulted in the best output for time sequence applications such as forecasting (Tiwari, et al., 2012) and different number of neurons (1~5) in the hidden layer were applied. Each HONN model was run with learning rate of 0.01 and different initial synaptic weights. The learning rate was dynamically updated by multiplying with 1.05 for decreasing error and with 0.7 for increasing error. The pre-processed data were divided into three segments for training, testing and validation. The number of data sets used for training and testing of HONN model for each case study changes; however, last 16 months (month 78~94) data are used to validate HONN models for case study. Each model was performed for 200 epochs for training and testing, and then, a validation was carried out.

The network was designed for prediction mode. If the input to the network was production data at time *t*, then the output is taken to at time *t+1*. During the network training, the network output was compared with the production data at time t+1 and the error was used to correct the synaptic weights. This means that the network is used as a one-step-ahead predictor. This is necessary for production forecasting.

3.2.2 Case#1.a

In this case study, the monthly oil production ratios from month 1 to month 94 were used for oil production forecasting as listed in Table 3.1.a and b. The graphical representation of original oil production data and smoothed data are shown in Figure 3.3. As seen in the figure, the high peaks of the data were smoothed. After the smoothing process, the auto-correlation of the oil production data was calculated by auto-correlation function (ACF). The ACF plot of oil production is presented in Figure 3.4. The ACF shows that the lags from lag0 to lag21 have some correlation within the 95% confidence level (above the region of marked line with scale 0.2, positive region). From the ACF plot, it was identified that lag1 and lag2 have the most significant correlation which means that the input variables in these lags are the

optimal to train HONN. In such condition, we had trained HONN to forecast oil production based on three scenarios:

1) using only lag1 (single lag1) for training,
2) using only lag2 (single lag2) for training
3) using lag1 and lag2 (accumulated lag2) for training.

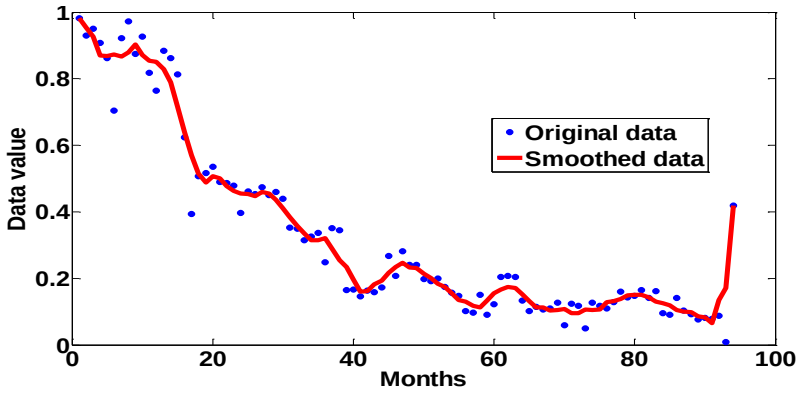

Figure 3.3. Oil production history of Well-1 from 2001~2009 before and after smoothing

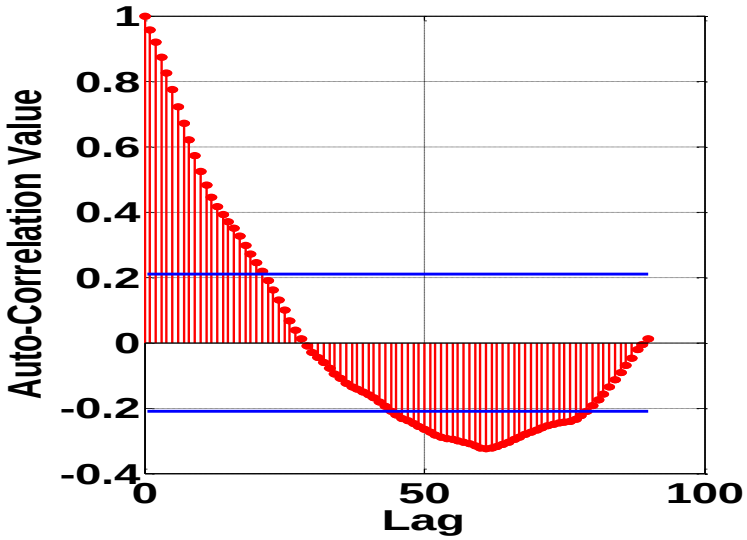

Figure 3.4. ACF of oil production after pre-processing. The blue line represents the confidential level of correlation (outside of the line represents 95% of confidence).

1) HONN using Single Lag1

In scenario 1, first 51 months data were used for training and next 26 months data for testing. The lag1 data presented to HONN after pre-processing is illustrated in Table

3.2. In Table 3.2, Input corresponds to oil productions rates of Well-1 and Target corresponds to the oil production data that has been advanced by one step.

During the simulation, the training process and validating process were studied by applying regression. The regression of the best HONN models with LSO, QSO and CSO for the validation set of data are presented in Figure 3.5 .(a), (b), (c); respectively.

Table 3.2. The train and test data used to train HONN model for scenario 1 (lag1)

Months	Input	Target	Months	Input	Target
1	0.982	0.954	40	0.197	0.160
2	0.954	0.926	41	0.160	0.161
3	0.926	0.871	42	0.161	0.181
4	0.871	0.869	43	0.181	0.194
5	0.869	0.873	44	0.194	0.217
6	0.873	0.867	45	0.217	0.234
7	0.867	0.880	46	0.234	0.247
8	0.880	0.903	47	0.247	0.233
9	0.903	0.871	48	0.233	0.230
10	0.871	0.853	49	0.230	0.214
11	0.853	0.851	50	0.214	0.201
12	0.851	0.828	51	0.201	0.184
13	0.828	0.789	52	0.184	0.174
14	0.789	0.715	53	0.174	0.156
15	0.715	0.640	54	0.156	0.135
16	0.640	0.571	55	0.135	0.130
17	0.571	0.515	56	0.130	0.117
18	0.515	0.489	57	0.117	0.112
19	0.489	0.507	58	0.112	0.133
20	0.507	0.501	59	0.133	0.155
21	0.501	0.477	60	0.155	0.166
22	0.477	0.462	61	0.166	0.175
23	0.462	0.455	62	0.175	0.170
24	0.455	0.453	63	0.170	0.152
25	0.453	0.447	64	0.152	0.132
26	0.447	0.460	65	0.132	0.113
27	0.460	0.456	66	0.113	0.112
28	0.456	0.435	67	0.112	0.103
29	0.435	0.411	68	0.103	0.105
30	0.411	0.383	69	0.105	0.108
31	0.383	0.357	70	0.108	0.096
32	0.357	0.336	71	0.096	0.096
33	0.336	0.315	72	0.096	0.107
34	0.315	0.315	73	0.107	0.104
35	0.315	0.321	74	0.104	0.106
36	0.321	0.289	75	0.106	0.128
37	0.289	0.255	76	0.128	0.131
38	0.255	0.234	77	0.131	0.137
39	0.234	0.197			

The simulation results from HONN model in terms of RMSE and MAPE are show in Table 3.3. The selection criteria for a better model are lower values of MAPE and RMSE.

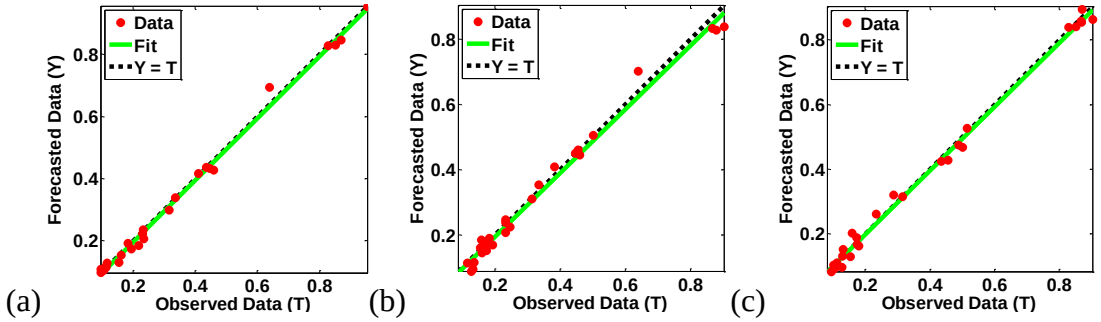

(a) (b) (c)

Figure 3.5 Regression of validation set of HONN with (a) LSO having 5 neurons in the hidden layer, (b) QSO having 5 neurons in the hidden layer (c) CSO having three neurons in the hidden layer.

From simulation results, the best model was HONN with LSO having five neurons in the hidden layers. The performance indices of best model shows HONN with LSO resulted in MAPE = 13.86% and RMSE=0.067. With CSO, MAPE =14.89% was achieved with three neural units in the hidden layer, and MAPE =15.98% was achieved with QSO having five neurons in the hidden layer.

Table 3.3. Performance measure of HONN with oil production ratio using single Lag1.

Synaptic Operation	Number of Hidden Layers	Number of Neurons	RMSE		MAPE	
			Mean	SD	Mean	SD
Linear Synaptic Operation	1	1	0.068	0.002	15.932	2.635
		2	0.067	0.001	15.680	2.195
		3	0.067	0.001	16.379	2.471
		4	0.068	0.001	14.500	1.660
		5	**0.067**	**0.001**	**13.863**	**0.442**
Quadratic Synaptic Operation	1	1	0.066	0.000	17.040	0.888
		2	0.067	0.001	18.370	2.575
		3	0.066	0.000	16.940	2.120
		4	0.067	0.001	16.554	0.840
		5	0.068	0.002	15.983	1.864
Cubic Synaptic Operation	1	1	0.066	0.000	15.647	1.081
		2	0.066	0.000	15.295	2.092
		3	0.066	0.000	14.890	1.689
		4	0.067	0.002	16.742	2.676
		5	0.066	0.001	16.375	1.264

1) HONN using Single Lag2

For scenario 2, first 50 months data for training and next 26 months data for testing were selected applying single lag2 after pre-processing and the data were arranged as listed in Table 3.4. In single lag2, the target data used for HONN has been advanced by 2 time steps.

Table 3.4. The train and test data used to train HONN model for scenario 2 (lag2)

Months	Input	Target	Months	Input	Target
1	0.982	0.926	39	0.234	0.160
2	0.954	0.871	40	0.197	0.161
3	0.926	0.869	41	0.160	0.181
4	0.871	0.873	42	0.161	0.194
5	0.869	0.867	43	0.181	0.217
6	0.873	0.880	44	0.194	0.234
7	0.867	0.903	45	0.217	0.247
8	0.880	0.871	46	0.234	0.233
9	0.903	0.853	47	0.247	0.230
10	0.871	0.851	48	0.233	0.214
11	0.853	0.828	49	0.230	0.201
12	0.851	0.789	50	0.214	0.184
13	0.828	0.715	51	0.201	0.174
14	0.789	0.640	52	0.184	0.156
15	0.715	0.571	53	0.174	0.135
16	0.640	0.515	54	0.156	0.130
17	0.571	0.489	55	0.135	0.117
18	0.515	0.507	56	0.130	0.112
19	0.489	0.501	57	0.117	0.133
20	0.507	0.477	58	0.112	0.155
21	0.501	0.462	59	0.133	0.166
22	0.477	0.455	60	0.155	0.175
23	0.462	0.453	61	0.166	0.170
24	0.455	0.447	62	0.175	0.152
25	0.453	0.460	63	0.170	0.132
26	0.447	0.456	64	0.152	0.113
27	0.460	0.435	65	0.132	0.112
28	0.456	0.411	66	0.113	0.103
29	0.435	0.383	67	0.112	0.105
30	0.411	0.357	68	0.103	0.108
31	0.383	0.336	69	0.105	0.096
32	0.357	0.315	70	0.108	0.096
33	0.336	0.315	71	0.096	0.107
34	0.315	0.321	72	0.096	0.104
35	0.315	0.289	73	0.107	0.106
36	0.321	0.255	74	0.104	0.128
37	0.289	0.234	75	0.106	0.131
38	0.255	0.197	76	0.128	0.137

Table 3.5 lists the simulation results using single lag2 from HONN models. The performance indices of the best HONN model with LSO resulted in MAPE = 18.6%

and RMSE=0.083. However, the HONNs with QSO and CSO did not result in acceptable outputs with single lag2. Parity plots are not included here for brevity.

Table 3.5 Performance measure of HONN with oil production ratio using single lag2.

Synaptic Operation	Number of Hidden Layers	Number of Neurons	RMSE		MAPE	
			Mean	SD	Mean	SD
Linear Synaptic Operation	1	1	0.082	0.003	19.182	1.392
		2	**0.083**	**0.002**	**18.599**	**0.818**
		3	0.083	0.002	18.985	1.224
		4	0.084	0.002	19.273	1.487
		5	0.080	0.004	21.345	1.785
Quadratic Synaptic Operation	1	1	0.076	0.001	25.953	2.882
		2	0.076	0.001	24.899	2.202
		3	0.077	0.001	23.824	2.189
		4	0.079	0.003	21.624	3.454
		5	0.076	0.000	24.146	0.930
Cubic Synaptic Operation	1	1	0.076	0.001	25.223	2.165
		2	0.078	0.001	21.822	1.798
		3	0.076	0.001	24.943	1.734
		4	0.076	0.000	25.745	0.716
		5	0.078	0.004	23.315	1.930

2) HONN using accumulated Lag2

In this scenario, after the pre-processing, the data were selected applying accumulated lag2 (lag1 and lag2), and the data were arranged for training and testing as shown in Table 3.6. The Input-1 and Input-2 in Table 3.6 corresponds to oil production from Well-1 at time lag1 and time lag-2. Both lag1 and lag2 are combined to form the training and validation data for accumulated lag2.

In this scenario, the accumulated lag2 were achieved by correlating the sum of observations of single lag1 and single lag2. The simulation studies presented that both HONN with LSO and CSO having two neurons in the hidden layer resulted in the best regression results with regression value for training = 0.997 and validation = 0.998.

The simulation results using accumulated lag2 from HONN models are presented in Table 3.7. From this table it is seen that HONN with LSO having two neurons in the hidden layer resulted in MAPE = 13.67% and RMSE=0.067. These results are comparable to those obtained in scenario (1) but the standard deviations are higher, meaning, thereby, that using lag2 in any form does not help the predictions.

Table 3.6 The train and test data used to train HONN model for scenario 3 accumulated lag2)

Months	Input-1	Input-2	Target	Months	Input-1	Input-2	Target
1	0.982	0.954	0.926	39	0.234	0.197	0.160
2	0.954	0.926	0.871	40	0.197	0.160	0.161
3	0.926	0.871	0.869	41	0.160	0.161	0.181
4	0.871	0.869	0.873	42	0.161	0.181	0.194
5	0.869	0.873	0.867	43	0.181	0.194	0.217
6	0.873	0.867	0.880	44	0.194	0.217	0.234
7	0.867	0.880	0.903	45	0.217	0.234	0.247
8	0.880	0.903	0.871	46	0.234	0.247	0.233
9	0.903	0.871	0.853	47	0.247	0.233	0.230
10	0.871	0.853	0.851	48	0.233	0.230	0.214
11	0.853	0.851	0.828	49	0.230	0.214	0.201
12	0.851	0.828	0.789	50	0.214	0.201	0.184
13	0.828	0.789	0.715	51	0.201	0.184	0.174
14	0.789	0.715	0.640	52	0.184	0.174	0.156
15	0.715	0.640	0.571	53	0.174	0.156	0.135
16	0.640	0.571	0.515	54	0.156	0.135	0.130
17	0.571	0.515	0.489	55	0.135	0.130	0.117
18	0.515	0.489	0.507	56	0.130	0.117	0.112
19	0.489	0.507	0.501	57	0.117	0.112	0.133
20	0.507	0.501	0.477	58	0.112	0.133	0.155
21	0.501	0.477	0.462	59	0.133	0.155	0.166
22	0.477	0.462	0.455	60	0.155	0.166	0.175
23	0.462	0.455	0.453	61	0.166	0.175	0.170
24	0.455	0.453	0.447	62	0.175	0.170	0.152
25	0.453	0.447	0.460	63	0.170	0.152	0.132
26	0.447	0.460	0.456	64	0.152	0.132	0.113
27	0.460	0.456	0.435	65	0.132	0.113	0.112
28	0.456	0.435	0.411	66	0.113	0.112	0.103
29	0.435	0.411	0.383	67	0.112	0.103	0.105
30	0.411	0.383	0.357	68	0.103	0.105	0.108
31	0.383	0.357	0.336	69	0.105	0.108	0.096
32	0.357	0.336	0.315	70	0.108	0.096	0.096
33	0.336	0.315	0.315	71	0.096	0.096	0.107
34	0.315	0.315	0.321	72	0.096	0.107	0.104
35	0.315	0.321	0.289	73	0.107	0.104	0.106
36	0.321	0.289	0.255	74	0.104	0.106	0.128
37	0.289	0.255	0.234	75	0.106	0.128	0.131
38	0.255	0.234	0.197	76	0.128	0.131	0.137

For case#1.a, the overall performance measure shows that HONN with LSO resulted in good performances by yielding a stable value between the range of, RMSE $=$ $0.066\sim0.084$ and $MAPE = 13\sim18\%$ with different configurations of neurons in the hidden layer.

Table 3.7 Performance measure of HONN with oil production ratio using accumulated lag2

Synaptic Operation	Number of Hidden Layer	Number of Neurons	RMSE		MAPE	
			Mean	SD	Mean	SD
Linear Synaptic Operation	1	1	0.071	0.005	15.153	1.598
		2	**0.067**	**0.003**	**13.671**	**1.068**
		3	0.072	0.004	14.714	1.170
		4	0.069	0.007	16.025	2.606
		5	0.069	0.002	14.575	1.000
Quadratic Synaptic Operation	1	1	0.064	0.002	16.651	1.670
		2	0.069	0.003	18.083	2.720
		3	0.069	0.002	17.302	1.777
		4	0.069	0.004	16.250	2.204
		5	0.065	0.004	16.229	3.492
Cubic Synaptic Operation	1	1	0.066	0.004	18.189	1.834
		2	0.071	0.004	15.315	0.964
		3	0.070	0.004	16.759	1.563
		4	0.070	0.009	17.034	1.780
		5	0.070	0.006	16.407	2.914

3.2.3 Case#1.b

For this simulation study, monthly oil, gas and water production rate of Well-1 from September 2001 to March 2009 were used for oil production forecasting. Table 3.1 (a) and (b) present the monthly oil, gas and water production data ratios for nine years (94 months) before and after smoothing.

This case study shows how additional input parameters (gas and water production) influence the performance of HONN model in forecasting oil production. The production data were preprocessed by applying smoothing process and cross-correlation. The smoothing process was carried out by a moving averaging filter with five sequence data points as discussed earlier. Oil, gas and water production ratios, before and after smoothing, are graphically presented in Figure 3.3 (for oil) and in Figure 3.6 (a), (b) for gas and water respectively. After that, and smoothed data were used to find cross-correlation function (CCF) between three production data as shown in Figure 3.7. The significant input variables were determined using CCF by identifying the correlation between oil and other components.

It is observed from the CCF plot that the correlations between oil and oil (auto-correlation), oil and gas, oil and water are significant at lag1, lag1 and lag2, and lag23,

respectively (Table 3.8). A total of 4 input vectors were identified for monthly oil production forecasting by HONN model. The smoothed data from Table 3.1 (b) were arranged applying the lags obtained from the CCF plot as presented in Table 3.8. Input1 represents the correlation of oil at lag1, input 2 and input 3 refers to the correlation of oil with gas production at lag1 and lag2, and input 4 represents the correlation of oil with water production at lag23 (see Table 3.9 for the input and output data for this case).

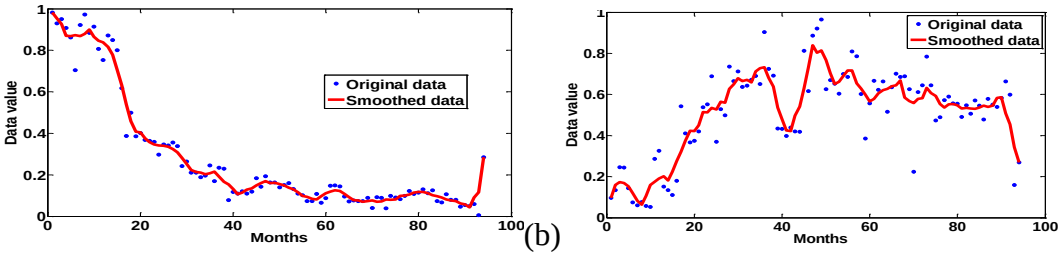

Figure 3.6. (a) Gas production data from Well-1 before and after smoothing (b) Water production from Well-1 before and after smoothing.

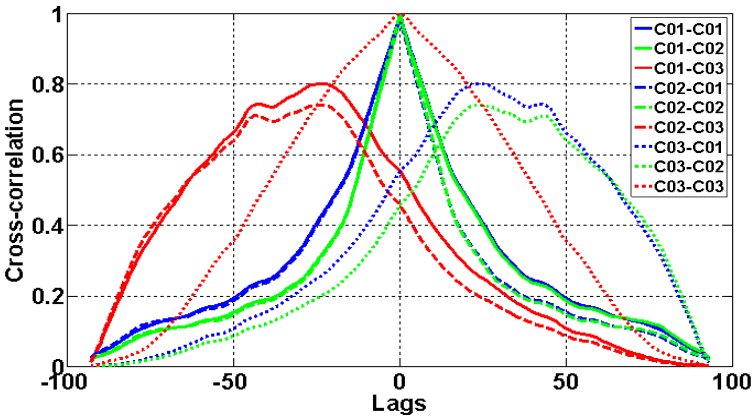

Figure 3.7. CCF of smoothed oil, gas and water production data. The legend represents the correlation between two parameters; notation inside the legend box C01, C02 and C03 represent oil, gas and water.

Table 3.8. Most significant input variable selected based on CCF of monthly production data

Cross-Correlation Variables	lags in significance
Oil-Oil	lag1
Oil-Gas	lag1 ,lag2
Oil-Water	lag23

Table 3.9 The train and test data sets used for training HONN model for case#1.b

Months	Input-1	Input-2	Input-3	Input-4	Target
1	0.462	0.347	0.358	0.096	0.455
2	0.455	0.341	0.347	0.159	0.453
3	0.453	0.34	0.341	0.173	0.447
4	0.447	0.336	0.34	0.168	0.46
5	0.46	0.325	0.336	0.153	0.456
6	0.456	0.308	0.325	0.12	0.435
7	0.435	0.282	0.308	0.082	0.411
8	0.411	0.253	0.282	0.064	0.383
9	0.383	0.223	0.253	0.106	0.357
10	0.357	0.214	0.223	0.16	0.336
11	0.336	0.21	0.214	0.175	0.315
12	0.315	0.202	0.21	0.19	0.315
13	0.315	0.207	0.202	0.202	0.321
14	0.321	0.215	0.207	0.181	0.289
15	0.289	0.192	0.215	0.224	0.255
16	0.255	0.166	0.192	0.275	0.234
17	0.234	0.154	0.166	0.322	0.197
18	0.197	0.131	0.154	0.375	0.16
19	0.16	0.107	0.131	0.423	0.161
20	0.161	0.115	0.107	0.422	0.181
21	0.181	0.128	0.115	0.45	0.194
22	0.194	0.135	0.128	0.514	0.217
23	0.217	0.149	0.135	0.513	0.234
24	0.234	0.16	0.149	0.535	0.247
25	0.247	0.169	0.16	0.527	0.233
26	0.233	0.16	0.169	0.564	0.23
27	0.23	0.162	0.16	0.559	0.214
28	0.214	0.155	0.162	0.628	0.201
29	0.201	0.149	0.155	0.649	0.184
30	0.184	0.138	0.149	0.678	0.174
31	0.174	0.131	0.138	0.665	0.156
32	0.156	0.115	0.131	0.67	0.135
33	0.135	0.098	0.115	0.658	0.13
34	0.13	0.093	0.098	0.712	0.117
35	0.117	0.084	0.093	0.728	0.112
36	0.112	0.081	0.084	0.732	0.133
37	0.133	0.096	0.081	0.681	0.155
38	0.155	0.112	0.096	0.637	0.166
39	0.166	0.119	0.112	0.536	0.175
40	0.175	0.125	0.119	0.479	0.17
41	0.17	0.122	0.125	0.425	0.152
42	0.152	0.107	0.122	0.422	0.132
43	0.132	0.092	0.107	0.498	0.113
44	0.113	0.078	0.092	0.541	0.112
45	0.112	0.076	0.078	0.631	0.103
46	0.103	0.07	0.076	0.731	0.105
47	0.105	0.074	0.07	0.84	0.108
48	0.108	0.077	0.074	0.802	0.096
49	0.096	0.07	0.077	0.813	0.096
50	0.096	0.072	0.07	0.767	0.107
51	0.107	0.082	0.072	0.703	0.104
52	0.104	0.08	0.082	0.65	0.106
53	0.106	0.082	0.08	0.662	0.128
54	0.128	0.098	0.082	0.69	0.131
55	0.131	0.1	0.098	0.717	0.137

Table 3.10 presents the results from HONN models with its performance measure in terms of RMSE and MAPE for different configurations of neurons in the hidden layer and synaptic operation. In this case study, the best model resulted in MAPE=15.13%, and RMSE=0.069 by HONN with QSO having four neurons in the hidden layer.

Table 3.10. Performance measure of HONN with oil, gas and water production ratio.

Synaptic Operation	Number of Hidden Layers	Number of Neurons	RMSE		MAPE	
			Mean	SD	Mean	SD
Linear Synaptic Operation (LSO)	1	1	0.068	0.005	17.896	3.547
		2	0.071	0.003	17.863	3.846
		3	0.076	0.004	17.951	1.533
		4	0.070	0.006	18.563	4.083
		5	0.068	0.005	20.223	1.955
Quadratic Synaptic Operation (QSO)	1	1	0.065	0.003	15.612	0.765
		2	0.061	0.010	15.853	1.541
		3	0.064	0.006	15.953	2.439
		4	**0.069**	**0.007**	**15.128**	**0.475**
		5	0.071	0.011	18.358	1.076
Cubic Synaptic Operation (CSO)	1	1	0.070	0.002	17.034	0.749
		2	0.076	0.007	16.073	1.684
		3	0.078	0.005	19.214	0.776
		4	0.074	0.002	16.363	0.774
		5	0.054	0.008	17.906	1.047

3.2.4 Discussions

From the case studies, the performance evaluation criteria indicates that the better oil production forecasting can be achieved using HONN with LSO with only one input parameter i.e. oil production data. In this study, the selection of lag time is an important factor that influences the forecasting results. Auto-correlation function (ACF) indicates that the most significant lag for oil production forecasting with only one parameter (oil production) is lag1, and HONN with LSO yields the best forecasting oil production in this case. Intuitively, it can be expected that QSO and CSO would result in better outcome than that of LSO. However, this case study comes up with opposite result. This can be explained by recalling that only one input parameter (oil production), used in case#1.a, does not generate complex correlation with target parameter (oil production to be predicted). Thus, in this case, linear combination of synaptic operations could result in better prediction. However, in case#1.b, the three input parameters, namely; oil, gas and water production rates may

generate nonlinearity and heterogeneity between input and target parameters. In this case, the higher-order synaptic operations, QSO and CSO, would be better suited to forecast the oil production.

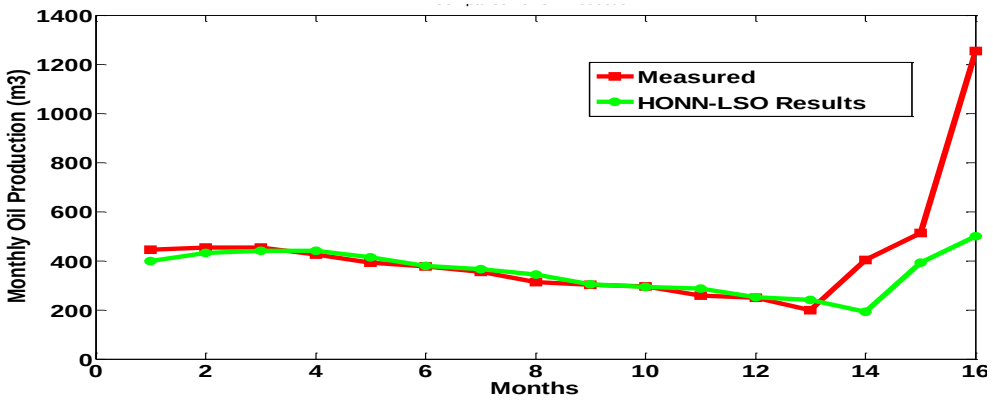

Figure 3.8 Comparison between the actual oil production and the forecasted results from HONN with LSO using single lag-1 from case#1.a.

Using the HONN, one-step-ahead production model, for Well-1 in the Tarapur block of Cambay Basin, predictions were made for 16 months (from February 2008 to September 2009 (i.e. month 77 ~ 94) beyond the date used for model development and its training. A comparison of the prediction by the best HONN model with LSO using single lag1 with the actual oil production is presented by Figure 3.8. As seen in this model, the match is satisfactory for the first 13 months.

It is observed that the performance of HONN with LSO in the case#1.a shows less MAPE than that in the case#1.b. One would expect that since gas and water production rates are intimately connected with oil production rate, case#1.b ought to have shown better match or lower MAPE. The contrary results may be attributed to the possibility that the noise in gas and water production measurements even after filtering may have overshadowed the advantage gained by added input information. Additionally, the number of input patterns in case#1.a is higher than that in the case#1.b. The reduction in the number of input patterns for training HONN in the case#1.b is caused by the number of lags. In the case#1.b, the highest number of lags is 23 which reduce the input pattern numbers as P – 23 where P is the number of initial input patterns. The patterns for oil, gas and water productions are selected based on cross-correlated pattern. Overall, it can be inferred that for the application of HONN

for forecasting, the number of input variables is one of the significant factors determining the order of synaptic operation.

Mean absolute percentage error (MAPE) is a measure of uncertainty in forecasting of oil production from a single well. A high value of 13 ~ 15% is indicative of lack of enough input information to the HONN model. One important information that is missing is clearly the well pressure (bottom hole pressure). Another one is the presence of other wells in its vicinity and their production pattern which, to some extent, could have been reflected by the well pressure. It may, therefore, be anticipated that if this procedure is used for all the five wells in this reservoir, MAPE will be reduced. The next section presents a study with five wells.

3.3 HONN FOR CUMULATIVE OIL PRODUCTION FORECASTING FROM MULTIPLE OIL PRODUCING WELLS (CASE#2)

HONN has been used for the first time to forecast cumulative oil production from an oil field reservoir with limited parameter data: i) oil production data and ii) oil, gas and water production data (no data on pressure and fluid saturation available). Again two case studies have been carried out to verify the potential of the proposed neural approach with limited available parameters from an oil field in Cambay basin, Gujarat, India. In case#2.a, data on only one dynamic parameter, oil production, from 5 producing wells, are used for forecasting, whereas in case#2.b, data on three dynamic parameters, oil, gas and water production from 5 producing wells, are used for forecasting. A pre-processing step is included for the preparation of neural inputs.

3.3.1 Structure of HONN for Five Wells Cumulative Oil Production Forecasting

In this study, a number of design factors for HONN were considered such as selection of neural structure (order of synaptic operation), numbers of neurons and hidden layers. Also, different mapping functions (somatic operation) were selected after careful investigation in each layer: a sigmoidal (hyperbolic tangent) function for hidden layers and a linear function for the output layer. In HONN, three synaptic operations were applied for HONN modeling: linear synaptic operation (LSO), quadratic synaptic operation (QSO) and cubic synaptic operation (CSO). It should be noted that LSO represents the synaptic operation of the conventional NN. Only one

hidden layer was used since it resulted in the best output for time sequence applications such as forecasting (Tiwari, et al., 2012) and different number of neurons (1~10 for case#2.a, and 1 ~ 5 for case#2.b) in the hidden layer were applied. Each HONN model was run with learning rate of 0.01 and different initial synaptic weights. The learning rate was dynamically updated by multiplying with 0.7 for increasing error and with 1.05 for reducing error. After pre-processing, the data were divided into three segments for training, test and validation. 35 data sets were used for training, 17 for testing and remaining 10 data for validation. Each model was trained and updated for 200 epochs for training test and before validation.

3.3.2 Case#2.a

In this case study, for training HONN, the monthly oil production ratios from month 1 to month 63 were used for cumulative oil production forecasting as shown in Table 3.11.a. The monthly production ratios were calculated using the maximum production of products (approximately 9500 m^3/month for oil) through the six year production history of Well-1, Well-2, Well-3, Well-4 and Well-5. For example, C1, the production ratio for Well-1, is calculated by dividing the first month's oil production from this well by 9500 and so on.

In the pre-processing stage, the oil production ratio data were smoothed using a five point moving average filter. Table 3.11.b. shows the smoothed oil production data for this case study. The graphical representation of original oil production verses smoothed production data for Well-1 to Well-5 is shown in Figure 3.9. As seen in this figure, the high peaks of the data were smoothed. After the smoothing process, the cross-correlations of the cumulative oil production data for the five wells were calculated by the cross-correlation function (CCF). The CCF plots of oil production after smoothing are presented in Figure 3.10. In Figure 3.10, C1 symbolizes the oil production ratio of Well-1 and so on and C6 symbolizes the cumulative oil production. C1-C6, in Figure 3.10, represents the cross-correlation between the oil production from Well-1 and cumulative oil production from all the wells. As shown, the highest correlation occurs at lag0. Since lag0 represents current time step (no step ahead), lag0 can be neglected for forecasting methods. From the CCF plot, it was identified that lag1 and lag2 have the most significant correlation which means that the input

variables in these lags are the optimal to train HONN. HONN was trained to forecast cumulative oil production based on three scenarios:

1) using only lag1 (single lag1) for training,

2) using only lag2 (single lag2) for training

3) using lag1 and lag2 (accumulated lag2) for training.

Table 3.11 a. Ratios of raw monthly oil production from Well-1, Well-2, Well-3, Well-4 and Well-5 and cumulative oil production.

Months	Well-1 (C1)	Well-2 (C2)	Well-3 (C3)	Well-4 (C4)	Well-5 (C5)	Cumulative Oil (C6)
1	0.111	0.072	0.309	0.09	0.237	0.82
2	0.111	0.073	0.307	0.088	0.237	0.815
3	0.099	0.06	0.292	0.075	0.226	0.752
4	0.103	0.061	0.29	0.081	0.209	0.744
5	0.106	0.057	0.298	0.072	0.211	0.744
6	0.078	0.091	0.313	0.058	0.197	0.737
7	0.111	0.049	0.326	0.084	0.212	0.781
8	0.109	0.048	0.32	0.07	0.208	0.755
9	0.052	0.049	0.337	0.088	0.18	0.706
10	0.053	0.049	0.332	0.089	0.18	0.702
11	0.046	0.043	0.303	0.079	0.196	0.668
12	0.051	0.029	0.337	0.097	0.193	0.707
13	0.05	0.028	0.327	0.051	0.187	0.643
14	0.055	0.031	0.359	0.01	0.205	0.659
15	0.084	0.031	0.286	0.11	0.163	0.674
16	0.065	0.02	0.228	0.094	0.093	0.5
17	0.089	0.027	0.276	0.131	0.12	0.644
18	0.076	0.023	0.306	0.102	0.155	0.662
19	0.076	0.023	0.307	0.064	0.155	0.626
20	0.062	0.02	0.28	0.066	0.142	0.571
21	0.061	0.022	0.316	0.045	0.164	0.607
22	0.063	0.023	0.348	0.047	0.176	0.657
23	0.055	0.02	0.308	0.081	0.153	0.617
24	0.05	0.031	0.496	0.062	0.114	0.753
25	0.046	0.029	0.479	0.058	0.107	0.72
26	0.032	0.02	0.419	0.063	0.093	0.626
27	0.031	0.018	0.401	0.061	0.086	0.597
28	0.047	0.021	0.391	0.041	0.1	0.601
29	0.043	0.032	0.322	0.034	0.084	0.515
30	0.039	0.043	0.252	0.026	0.068	0.429
31	0.065	0.04	0.45	0.077	0.083	0.714
32	0.065	0.05	0.463	0.078	0.073	0.729
33	0.065	0.048	0.443	0.077	0.07	0.702
34	0.042	0.029	0.357	0.033	0.069	0.531
35	0.032	0.035	0.508	0.046	0.079	0.701
36	0.036	0.039	0.693	0.053	0.089	0.909
37	0.034	0.037	0.647	0.049	0.083	0.849
38	0.035	0.016	0.665	0.05	0.095	0.86
39	0.04	0.019	0.609	0.04	0.092	0.8
40	0.018	0.013	0.218	0.013	0.054	0.317
41	0.039	0.018	0.601	0.039	0.089	0.786
42	0.037	0.017	0.579	0.037	0.086	0.757
43	0.016	0.019	0.632	0.038	0.059	0.763

Months	Well-1 (C1)	Well-2 (C2)	Well-3 (C3)	Well-4 (C4)	Well-5 (C5)	Cumulative Oil (C6)
44	0.04	0.035	0.564	0.04	0.046	0.725
45	0.037	0.033	0.576	0.044	0.057	0.748
46	0.034	0.03	0.579	0.041	0.053	0.737
47	0.041	0.028	0.543	0.038	0.001	0.651
48	0.051	0.024	0.584	0.041	0.001	0.699
49	0.045	0.014	0.567	0.048	0.054	0.728
50	0.046	0.013	0.577	0.046	0.056	0.739
51	0.052	0.06	0.563	0.055	0.033	0.764
52	0.044	0.128	0.592	0.058	0.031	0.853
53	0.051	0.123	0.596	0.044	0.03	0.844
54	0.03	0.12	0.593	0.039	0.017	0.798
55	0.028	0.124	0.655	0.046	0.025	0.878
56	0.045	0.124	0.572	0.041	0.032	0.814
57	0.033	0.218	0.514	0.029	0.033	0.827
58	0.029	0.193	0.44	0.028	0.031	0.722
59	0.024	0.176	0.426	0.027	0.018	0.671
60	0.026	0.188	0.457	0.029	0.019	0.718
61	0.025	0.167	0.346	0.021	0.015	0.574
62	0.027	0.183	0.364	0.027	0.001	0.602
63	0.003	0.14	0.339	0.031	0.204	0.717

Table 3.11.b Ratios of smoothed monthly oil production from Well-1, Well-2, Well-3, Well-4 and Well-5 and cumulative oil production.

Months	Well-1 (C1)	Well-2 (C2)	Well-3 (C3)	Well-4 (C4)	Well-5 (C5)	Cumulative Oil (C6)
1	0.111	0.072	0.309	0.09	0.237	0.82
2	0.107	0.068	0.303	0.084	0.233	0.796
3	0.106	0.065	0.299	0.081	0.224	0.775
4	0.099	0.068	0.3	0.075	0.216	0.758
5	0.099	0.064	0.304	0.074	0.211	0.752
6	0.101	0.061	0.309	0.073	0.207	0.752
7	0.091	0.059	0.319	0.074	0.202	0.745
8	0.081	0.057	0.326	0.078	0.195	0.736
9	0.074	0.048	0.324	0.082	0.195	0.722
10	0.062	0.044	0.326	0.085	0.191	0.708
11	0.05	0.04	0.327	0.081	0.187	0.685
12	0.051	0.036	0.332	0.065	0.192	0.676
13	0.057	0.032	0.322	0.069	0.189	0.67
14	0.061	0.028	0.307	0.072	0.168	0.637
15	0.069	0.027	0.295	0.079	0.154	0.624
16	0.074	0.026	0.291	0.089	0.147	0.628
17	0.078	0.025	0.281	0.1	0.137	0.621
18	0.074	0.023	0.279	0.091	0.133	0.601
19	0.073	0.023	0.297	0.082	0.147	0.622
20	0.068	0.022	0.311	0.065	0.158	0.625
21	0.063	0.022	0.312	0.061	0.158	0.616
22	0.058	0.023	0.35	0.06	0.15	0.641
23	0.055	0.025	0.389	0.059	0.143	0.671
24	0.049	0.025	0.41	0.062	0.129	0.675
25	0.043	0.024	0.421	0.065	0.111	0.663
26	0.041	0.024	0.437	0.057	0.1	0.659
27	0.04	0.024	0.402	0.051	0.094	0.612
28	0.038	0.027	0.357	0.045	0.086	0.554
29	0.045	0.031	0.363	0.048	0.084	0.571
30	0.052	0.037	0.376	0.051	0.082	0.598

Months	Well-1 (C1)	Well-2 (C2)	Well-3 (C3)	Well-4 (C4)	Well-5 (C5)	Cumulative Oil (C6)
32	0.055	0.042	0.393	0.058	0.073	0.621
33	0.054	0.04	0.444	0.062	0.075	0.675
34	0.048	0.04	0.493	0.057	0.076	0.714
35	0.042	0.038	0.53	0.052	0.078	0.738
36	0.036	0.031	0.574	0.046	0.083	0.77
37	0.035	0.029	0.624	0.048	0.088	0.824
38	0.033	0.025	0.566	0.041	0.083	0.747
39	0.033	0.021	0.548	0.038	0.083	0.722
40	0.034	0.017	0.534	0.036	0.083	0.704
41	0.03	0.017	0.528	0.033	0.076	0.685
42	0.03	0.02	0.519	0.033	0.067	0.67
43	0.034	0.024	0.59	0.04	0.067	0.756
44	0.033	0.027	0.586	0.04	0.06	0.746
45	0.034	0.029	0.579	0.04	0.043	0.725
46	0.041	0.03	0.569	0.041	0.031	0.712
47	0.042	0.026	0.57	0.042	0.033	0.713
48	0.043	0.022	0.57	0.043	0.033	0.711
49	0.047	0.028	0.567	0.046	0.029	0.716
50	0.048	0.048	0.577	0.05	0.035	0.757
51	0.048	0.068	0.579	0.05	0.041	0.786
52	0.045	0.089	0.584	0.048	0.033	0.8
53	0.041	0.111	0.6	0.048	0.027	0.827
54	0.04	0.124	0.602	0.046	0.027	0.837
55	0.037	0.142	0.586	0.04	0.027	0.832
56	0.033	0.156	0.555	0.037	0.028	0.808
57	0.032	0.167	0.521	0.034	0.028	0.782
58	0.031	0.18	0.482	0.031	0.027	0.75
59	0.027	0.188	0.437	0.027	0.023	0.702
60	0.026	0.181	0.407	0.026	0.017	0.657
61	0.021	0.171	0.386	0.027	0.051	0.656
62	0.018	0.163	0.35	0.026	0.073	0.631
63	0.003	0.14	0.339	0.031	0.204	0.717

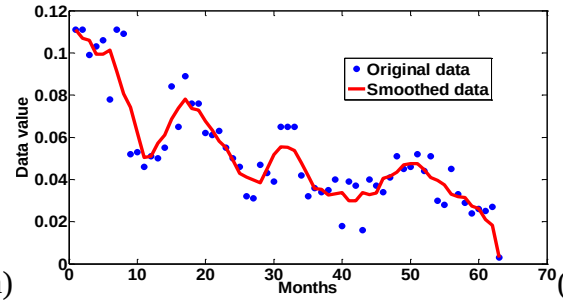

(a)

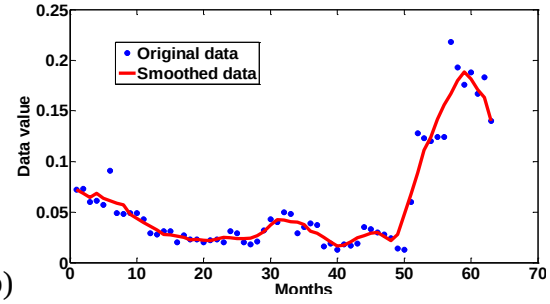

(b)

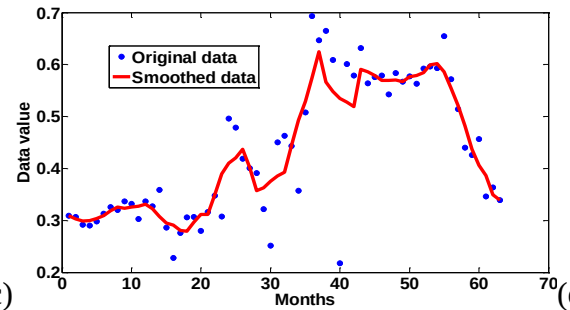

(c)

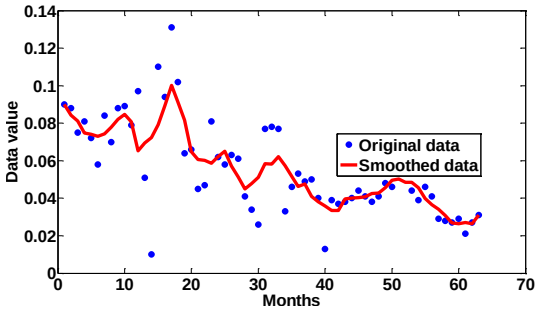

(d)

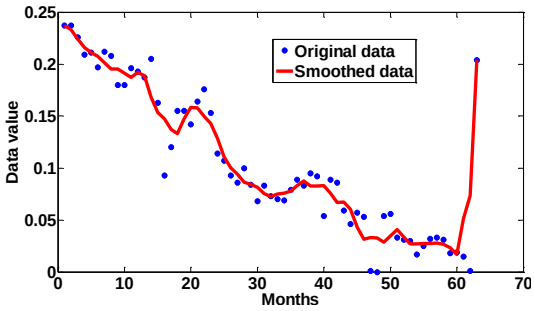

(e)

Figure 3.9. Oil production history from 2004~2009 before and after smoothing of (a) Well-1, (b) Well-2, (c) Well-3, (d) Well-4, (e) Well-5.

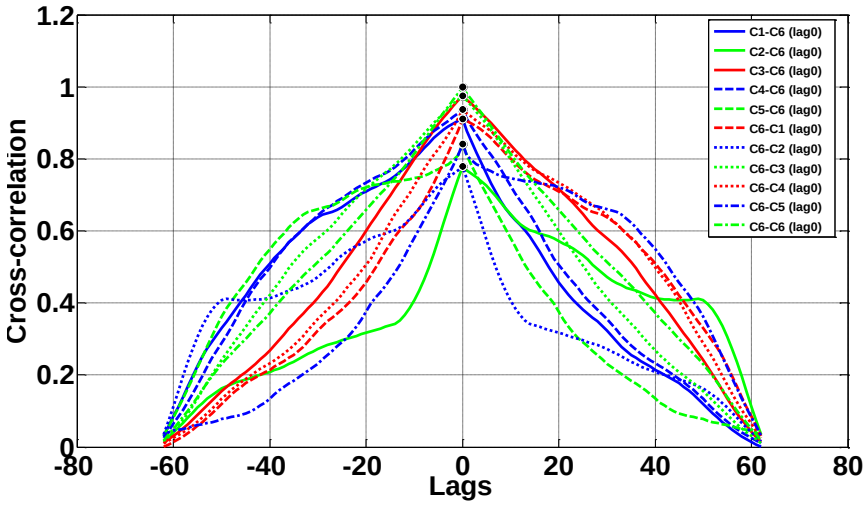

Figure 3.10 Cross-correlation of cumulative oil production to five wells. The legend represents the correlation between two parameters. The dark circles on the plot indicate the highest correlation between two parameters.

1) HONN using single Lag1

In scenario 1, first 35 months data were used for training and next 17 months data for testing the model. The data are shown in Table 3.12 wherein, Input-1, Input-2, Input-3, Input-4, Input-5 corresponds to oil productions rates from Well-1, Well-2, Well-3, Well-4 and Well-5 after smoothing. It may be noted that to account for this lag1, the cumulative oil production has been advanced by one time step.

Table 3.12 The training, test and target data used to train HONN models for scenario 1 (lag1).

Months	Input -1	Input -2	Input -3	Input -4	Input-5	Target
1	0.111	0.072	0.309	0.09	0.237	0.796
2	0.107	0.068	0.303	0.084	0.233	0.775
3	0.106	0.065	0.299	0.081	0.224	0.758
4	0.099	0.068	0.3	0.075	0.216	0.752
5	0.099	0.064	0.304	0.074	0.211	0.752
6	0.101	0.061	0.309	0.073	0.207	0.745
7	0.091	0.059	0.319	0.074	0.202	0.736
8	0.081	0.057	0.326	0.078	0.195	0.722
9	0.074	0.048	0.324	0.082	0.195	0.708
10	0.062	0.044	0.326	0.085	0.191	0.685
11	0.05	0.04	0.327	0.081	0.187	0.676
12	0.051	0.036	0.332	0.065	0.192	0.67
13	0.057	0.032	0.322	0.069	0.189	0.637
14	0.061	0.028	0.307	0.072	0.168	0.624
15	0.069	0.027	0.295	0.079	0.154	0.628
16	0.074	0.026	0.291	0.089	0.147	0.621
17	0.078	0.025	0.281	0.1	0.137	0.601
18	0.074	0.023	0.279	0.091	0.133	0.622
19	0.073	0.023	0.297	0.082	0.147	0.625
20	0.068	0.022	0.311	0.065	0.158	0.616
21	0.063	0.022	0.312	0.061	0.158	0.641
22	0.058	0.023	0.35	0.06	0.15	0.671
23	0.055	0.025	0.389	0.059	0.143	0.675
24	0.049	0.025	0.41	0.062	0.129	0.663
25	0.043	0.024	0.421	0.065	0.111	0.659
26	0.041	0.024	0.437	0.057	0.1	0.612
27	0.04	0.024	0.402	0.051	0.094	0.554
28	0.038	0.027	0.357	0.045	0.086	0.571
29	0.045	0.031	0.363	0.048	0.084	0.598
30	0.052	0.037	0.376	0.051	0.082	0.618
31	0.055	0.043	0.386	0.058	0.076	0.621
32	0.055	0.042	0.393	0.058	0.073	0.675
33	0.054	0.04	0.444	0.062	0.075	0.714
34	0.048	0.04	0.493	0.057	0.076	0.738
35	0.042	0.038	0.53	0.052	0.078	0.77
36	0.036	0.031	0.574	0.046	0.083	0.824
37	0.035	0.029	0.624	0.048	0.088	0.747
38	0.033	0.025	0.566	0.041	0.083	0.722
39	0.033	0.021	0.548	0.038	0.083	0.704
40	0.034	0.017	0.534	0.036	0.083	0.685
41	0.03	0.017	0.528	0.033	0.076	0.67
42	0.03	0.02	0.519	0.033	0.067	0.756
43	0.034	0.024	0.59	0.04	0.067	0.746
44	0.033	0.027	0.586	0.04	0.06	0.725
45	0.034	0.029	0.579	0.04	0.043	0.712
46	0.041	0.03	0.569	0.041	0.031	0.713
47	0.042	0.026	0.57	0.042	0.033	0.711
48	0.043	0.022	0.57	0.043	0.033	0.716
49	0.047	0.028	0.567	0.046	0.029	0.757
50	0.048	0.048	0.577	0.05	0.035	0.786
51	0.048	0.068	0.579	0.05	0.041	0.8
52	0.045	0.089	0.584	0.048	0.033	0.827

The simulation results from HONN model in terms of RMSE, MSE and MAPE is show in Table 3.13, comparing the performances with different number of neurons in the hidden layer. The selection criteria for a better model are lower values of MAPE, MSE and RMSE. From simulation results, the best model was HONN with CSO having four neurons in the hidden layer. The performance indices shows that the best model is the HONN with CSO resulted in MAPE = 3.459%, MSE = 0.001, and RMSE = 0.035. In case of HONN with LSO, MAPE = 4.055% was achieved having 10 neural units in the hidden layer, and MAPE = 3.89% was achieved by HONN with QSO having 9 neurons in the hidden layer.

Table 3.13. Performance measure of HONNs using single lag1.

Synaptic Operation	Number of Hidden Layers	Number of Neurons	MSE		RMSE		MAPE (%)	
			Mean	SD	Mean	SD	Mean	SD
Linear Synaptic Operation (LSO)	1	1	0.003	0.001	0.057	0.010	6.777	1.302
		2	0.003	0.001	0.054	0.011	5.954	1.181
		3	0.003	0.001	0.052	0.010	6.042	0.956
		4	0.002	0.000	0.047	0.004	5.425	0.489
		5	0.002	0.000	0.043	0.006	4.717	0.721
		6	0.002	0.000	0.044	0.004	5.041	0.599
		7	0.002	0.001	0.043	0.006	5.276	0.776
		8	0.002	0.001	0.049	0.006	5.979	0.799
		9	0.004	0.001	0.061	0.008	6.771	0.768
		10	0.002	0.000	0.041	0.004	4.055	0.620
Quadratic Synaptic Operation (QSO)	1	1	0.003	0.001	0.055	0.008	6.610	0.711
		2	0.001	0.000	0.038	0.003	3.943	0.383
		3	0.003	0.001	0.050	0.008	5.464	0.902
		4	0.001	0.000	0.038	0.005	4.355	0.852
		5	0.003	0.001	0.051	0.012	5.248	1.454
		6	0.001	0.000	0.038	0.004	4.081	0.781
		7	0.002	0.001	0.044	0.006	5.268	0.822
		8	0.001	0.000	0.036	0.006	4.131	0.831
		9	0.002	0.001	0.041	0.010	3.898	0.590
		10	0.003	0.001	0.052	0.010	5.663	1.127
Cubic Synaptic Operation (CSO)	1	1	0.003	0.001	0.056	0.005	6.517	0.481
		2	0.002	0.001	0.044	0.009	4.920	0.813
		3	0.002	0.001	0.047	0.006	5.368	0.981
		4	**0.001**	**0.001**	**0.035**	**0.010**	**3.459**	**0.452**
		5	0.003	0.001	0.050	0.007	5.758	1.001
		6	0.003	0.002	0.049	0.016	5.373	1.845
		7	0.002	0.000	0.041	0.003	4.044	0.741
		8	0.003	0.000	0.055	0.005	6.610	0.706
		9	0.001	0.001	0.033	0.009	3.634	0.930
		10	0.002	0.000	0.047	0.005	5.087	0.493

2) HONN using single Lag2

In scenario 2, first 34 months data were used for training and next 17 months data for testing were selected applying single lag2 after pre-processing and the data are listed in Table 3.14. Here again, the first number in C6 has been advanced by 2 time steps.

Table 3.14. The training, test and target data used to train HONN models for scenario 2 (lag2).

Months	Input 1	Input-2	Input -3	Input -4	Input-5	Target
1	0.111	0.072	0.309	0.09	0.237	0.775
2	0.107	0.068	0.303	0.084	0.233	0.758
3	0.106	0.065	0.299	0.081	0.224	0.752
4	0.099	0.068	0.3	0.075	0.216	0.752
5	0.099	0.064	0.304	0.074	0.211	0.745
6	0.101	0.061	0.309	0.073	0.207	0.736
7	0.091	0.059	0.319	0.074	0.202	0.722
8	0.081	0.057	0.326	0.078	0.195	0.708
9	0.074	0.048	0.324	0.082	0.195	0.685
10	0.062	0.044	0.326	0.085	0.191	0.676
11	0.05	0.04	0.327	0.081	0.187	0.67
12	0.051	0.036	0.332	0.065	0.192	0.637
13	0.057	0.032	0.322	0.069	0.189	0.624
14	0.061	0.028	0.307	0.072	0.168	0.628
15	0.069	0.027	0.295	0.079	0.154	0.621
16	0.074	0.026	0.291	0.089	0.147	0.601
17	0.078	0.025	0.281	0.1	0.137	0.622
18	0.074	0.023	0.279	0.091	0.133	0.625
19	0.073	0.023	0.297	0.082	0.147	0.616
20	0.068	0.022	0.311	0.065	0.158	0.641
21	0.063	0.022	0.312	0.061	0.158	0.671
22	0.058	0.023	0.35	0.06	0.15	0.675
23	0.055	0.025	0.389	0.059	0.143	0.663
24	0.049	0.025	0.41	0.062	0.129	0.659
25	0.043	0.024	0.421	0.065	0.111	0.612
26	0.041	0.024	0.437	0.057	0.1	0.554
27	0.04	0.024	0.402	0.051	0.094	0.571
28	0.038	0.027	0.357	0.045	0.086	0.598
29	0.045	0.031	0.363	0.048	0.084	0.618
30	0.052	0.037	0.376	0.051	0.082	0.621
31	0.055	0.043	0.386	0.058	0.076	0.675
32	0.055	0.042	0.393	0.058	0.073	0.714
33	0.054	0.04	0.444	0.062	0.075	0.738
34	0.048	0.04	0.493	0.057	0.076	0.77
35	0.042	0.038	0.53	0.052	0.078	0.824
36	0.036	0.031	0.574	0.046	0.083	0.747
37	0.035	0.029	0.624	0.048	0.088	0.722
38	0.033	0.025	0.566	0.041	0.083	0.704
39	0.033	0.021	0.548	0.038	0.083	0.685
40	0.034	0.017	0.534	0.036	0.083	0.67
41	0.03	0.017	0.528	0.033	0.076	0.756
42	0.03	0.02	0.519	0.033	0.067	0.746
43	0.034	0.024	0.59	0.04	0.067	0.725
44	0.033	0.027	0.586	0.04	0.06	0.712
45	0.034	0.029	0.579	0.04	0.043	0.713
46	0.041	0.03	0.569	0.041	0.031	0.711

Months	Input 1	Input-2	Input -3	Input -4	Input-5	Target
47	0.042	0.026	0.57	0.042	0.033	0.716
48	0.043	0.022	0.57	0.043	0.033	0.757
49	0.047	0.028	0.567	0.046	0.029	0.786
50	0.048	0.048	0.577	0.05	0.035	0.8
51	0.048	0.068	0.579	0.05	0.041	0.827

Table 3.15. lists the simulation results using single lag2 for HONN. The performance indices show that the best model is HONN with CSO resulting in MAPE = 4.882%, MSE = 0.002, and RMSE = 0.045 with two neurons in the hidden layer. HONN with QSO also resulted in low error having MAPE = 5.127, MSE = 0.002, RMSE = 0.043 with seven neurons in the hidden layer. However, the HONNs LSO resulted in higher errors compared to CSO and QSO with single lag2.

Table 3.15 Performance measure of HONNs using single lag2.

Synaptic Operation	Number of Hidden Layers	Number of Neurons	MSE		RMSE		MAPE (%)	
			Mean	SD	Mean	SD	Mean	SD
Linear Synaptic Operation (LSO)	1	1	0.004	0.001	0.065	0.010	7.562	0.831
		2	0.003	0.001	0.058	0.006	6.392	0.894
		3	0.003	0.001	0.055	0.006	6.169	0.793
		4	0.005	0.001	0.070	0.004	7.695	0.210
		5	0.002	0.001	0.049	0.006	5.925	0.821
		6	0.004	0.001	0.060	0.005	6.473	0.382
		7	0.003	0.001	0.054	0.007	6.110	0.722
		8	0.003	0.001	0.058	0.006	6.702	0.740
		9	0.004	0.000	0.060	0.004	6.884	0.667
		10	0.003	0.001	0.057	0.008	6.242	0.919
Quadratic Synaptic Operation (QSO)	1	1	0.003	0.001	0.057	0.007	6.220	0.699
		2	0.003	0.001	0.054	0.010	5.859	0.843
		3	0.002	0.001	0.047	0.011	5.216	1.057
		4	0.003	0.000	0.056	0.004	6.279	0.624
		5	0.003	0.001	0.051	0.008	5.358	1.124
		6	0.003	0.001	0.052	0.010	5.649	1.145
		7	0.002	0.000	0.043	0.004	5.127	0.694
		8	0.003	0.001	0.057	0.005	6.614	0.606
		9	0.002	0.001	0.049	0.008	5.445	1.431
		10	0.002	0.001	0.046	0.008	5.381	1.017
Cubic Synaptic Operation (CSO)	1	1	0.002	0.001	0.049	0.005	5.650	0.761
		2	**0.002**	**0.000**	**0.045**	**0.005**	**4.882**	**0.791**
		3	0.002	0.000	0.048	0.005	5.665	0.978
		4	0.003	0.001	0.052	0.006	5.818	0.862
		5	0.002	0.001	0.048	0.009	5.413	1.369
		6	0.003	0.000	0.055	0.003	6.222	0.577
		7	0.003	0.002	0.057	0.016	6.573	2.033
		8	0.002	0.001	0.049	0.007	5.276	0.614
		9	0.004	0.001	0.060	0.008	6.623	1.030
		10	0.008	0.005	0.083	0.030	9.662	2.979

1) HONN using accumulated Lag2

In this scenario, the data were selected applying accumulated lag2 (lag1 and lag2), as shown in Table 3.16. The Input-1 to Input-5 in Table 3.16 correspond to oil production from Well-1 to Well-5 at time step single lag1, and Input-6 to Input-10 in the table corresponds to oil production from Well-1 to Well-5 at time step single lag2 . Hence, both single lag1 and lag2 are combined to form the training data for accumulated lag2. The simulation results from HONN models are presented in Table 3.17 with their performance accuracy. The performance indices show that the best model is HONN with CSO having three neurons in the hidden layer which resulted in MAPE = 4.045%, MSE = 0.002, and RMSE = 0.039.

Table 3.16. The training, test and target data used to train HONN models for scenario 3 (accumulated lag2).

Months	Input -1	Input -2	Input -3	Input -4	Input -5	Input -6	Input -7	Input -8	Input -9	Input -10	Target
1	0.107	0.068	0.303	0.084	0.233	0.111	0.072	0.309	0.09	0.237	0.775
2	0.106	0.065	0.299	0.081	0.224	0.107	0.068	0.303	0.084	0.233	0.758
3	0.099	0.068	0.3	0.075	0.216	0.106	0.065	0.299	0.081	0.224	0.752
4	0.099	0.064	0.304	0.074	0.211	0.099	0.068	0.3	0.075	0.216	0.752
5	0.101	0.061	0.309	0.073	0.207	0.099	0.064	0.304	0.074	0.211	0.745
6	0.091	0.059	0.319	0.074	0.202	0.101	0.061	0.309	0.073	0.207	0.736
7	0.081	0.057	0.326	0.078	0.195	0.091	0.059	0.319	0.074	0.202	0.722
8	0.074	0.048	0.324	0.082	0.195	0.081	0.057	0.326	0.078	0.195	0.708
9	0.062	0.044	0.326	0.085	0.191	0.074	0.048	0.324	0.082	0.195	0.685
10	0.05	0.04	0.327	0.081	0.187	0.062	0.044	0.326	0.085	0.191	0.676
11	0.051	0.036	0.332	0.065	0.192	0.05	0.04	0.327	0.081	0.187	0.67
12	0.057	0.032	0.322	0.069	0.189	0.051	0.036	0.332	0.065	0.192	0.637
13	0.061	0.028	0.307	0.072	0.168	0.057	0.032	0.322	0.069	0.189	0.624
14	0.069	0.027	0.295	0.079	0.154	0.061	0.028	0.307	0.072	0.168	0.628
15	0.074	0.026	0.291	0.089	0.147	0.069	0.027	0.295	0.079	0.154	0.621
16	0.078	0.025	0.281	0.1	0.137	0.074	0.026	0.291	0.089	0.147	0.601
17	0.074	0.023	0.279	0.091	0.133	0.078	0.025	0.281	0.1	0.137	0.622
18	0.073	0.023	0.297	0.082	0.147	0.074	0.023	0.279	0.091	0.133	0.625
19	0.068	0.022	0.311	0.065	0.158	0.073	0.023	0.297	0.082	0.147	0.616
20	0.063	0.022	0.312	0.061	0.158	0.068	0.022	0.311	0.065	0.158	0.641
21	0.058	0.023	0.35	0.06	0.15	0.063	0.022	0.312	0.061	0.158	0.671
22	0.055	0.025	0.389	0.059	0.143	0.058	0.023	0.35	0.06	0.15	0.675
23	0.049	0.025	0.41	0.062	0.129	0.055	0.025	0.389	0.059	0.143	0.663
24	0.043	0.024	0.421	0.065	0.111	0.049	0.025	0.41	0.062	0.129	0.659
25	0.041	0.024	0.437	0.057	0.1	0.043	0.024	0.421	0.065	0.111	0.612
26	0.04	0.024	0.402	0.051	0.094	0.041	0.024	0.437	0.057	0.1	0.554
27	0.038	0.027	0.357	0.045	0.086	0.04	0.024	0.402	0.051	0.094	0.571
28	0.045	0.031	0.363	0.048	0.084	0.038	0.027	0.357	0.045	0.086	0.598
29	0.052	0.037	0.376	0.051	0.082	0.045	0.031	0.363	0.048	0.084	0.618
30	0.055	0.043	0.386	0.058	0.076	0.052	0.037	0.376	0.051	0.082	0.621
31	0.055	0.042	0.393	0.058	0.073	0.055	0.043	0.386	0.058	0.076	0.675
32	0.054	0.04	0.444	0.062	0.075	0.055	0.042	0.393	0.058	0.073	0.714
33	0.048	0.04	0.493	0.057	0.076	0.054	0.04	0.444	0.062	0.075	0.738
34	0.042	0.038	0.53	0.052	0.078	0.048	0.04	0.493	0.057	0.076	0.77

Months	Input -1	Input -2	Input -3	Input -4	Input -5	Input -6	Input -7	Input -8	Input -9	Input -10	Target
35	0.036	0.031	0.574	0.046	0.083	0.042	0.038	0.53	0.052	0.078	0.824
36	0.035	0.029	0.624	0.048	0.088	0.036	0.031	0.574	0.046	0.083	0.747
37	0.033	0.025	0.566	0.041	0.083	0.035	0.029	0.624	0.048	0.088	0.722
38	0.033	0.021	0.548	0.038	0.083	0.033	0.025	0.566	0.041	0.083	0.704
39	0.034	0.017	0.534	0.036	0.083	0.033	0.021	0.548	0.038	0.083	0.685
40	0.03	0.017	0.528	0.033	0.076	0.034	0.017	0.534	0.036	0.083	0.67
41	0.03	0.02	0.519	0.033	0.067	0.03	0.017	0.528	0.033	0.076	0.756
42	0.034	0.024	0.59	0.04	0.067	0.03	0.02	0.519	0.033	0.067	0.746
43	0.033	0.027	0.586	0.04	0.06	0.034	0.024	0.59	0.04	0.067	0.725
44	0.034	0.029	0.579	0.04	0.043	0.033	0.027	0.586	0.04	0.06	0.712
45	0.041	0.03	0.569	0.041	0.031	0.034	0.029	0.579	0.04	0.043	0.713
46	0.042	0.026	0.57	0.042	0.033	0.041	0.03	0.569	0.041	0.031	0.711
47	0.043	0.022	0.57	0.043	0.033	0.042	0.026	0.57	0.042	0.033	0.716
48	0.047	0.028	0.567	0.046	0.029	0.043	0.022	0.57	0.043	0.033	0.757
49	0.048	0.048	0.577	0.05	0.035	0.047	0.028	0.567	0.046	0.029	0.786
50	0.048	0.068	0.579	0.05	0.041	0.048	0.048	0.577	0.05	0.035	0.8
51	0.045	0.089	0.584	0.048	0.033	0.048	0.068	0.579	0.05	0.041	0.827

Table 3.17. Performance measure of HONNs using accumulated lag2.

Synaptic Operation	Number of Hidden Layers	Number of Neurons	MSE		RMSE		MAPE (%)	
			Mean	SD	Mean	SD	Mean	SD
Linear Synaptic Operation (LSO)	1	1	0.004	0.001	0.059	0.008	6.715	1.261
		2	0.004	0.001	0.063	0.008	7.134	0.563
		3	0.003	0.001	0.055	0.010	6.362	0.834
		4	0.004	0.001	0.059	0.010	6.670	1.081
		5	0.003	0.000	0.051	0.003	5.711	0.150
		6	0.003	0.000	0.054	0.004	6.266	0.565
		7	0.003	0.001	0.051	0.007	5.167	1.024
		8	0.002	0.000	0.042	0.003	4.748	0.802
		9	0.003	0.001	0.056	0.007	6.695	0.578
		10	0.002	0.001	0.047	0.005	5.134	0.671
Quadratic Synaptic Operation (QSO)	1	1	0.003	0.000	0.055	0.004	6.583	0.534
		2	0.002	0.000	0.041	0.003	4.465	0.547
		3	0.002	0.000	0.040	0.003	4.320	0.407
		4	0.003	0.001	0.051	0.011	5.438	1.413
		5	0.002	0.001	0.045	0.006	5.184	0.717
		6	0.002	0.001	0.045	0.010	5.289	1.534
		7	0.002	0.001	0.047	0.009	4.984	0.847
		8	0.003	0.001	0.055	0.005	5.525	0.576
		9	0.003	0.001	0.054	0.007	6.199	1.087
		10	0.005	0.002	0.070	0.015	7.320	1.138
Cubic Synaptic Operation (CSO)	1	1	0.003	0.000	0.056	0.003	6.456	0.516
		2	0.002	0.001	0.046	0.008	5.214	1.181
		3	**0.002**	**0.000**	**0.039**	**0.003**	**4.045**	**0.462**
		4	0.003	0.001	0.053	0.008	5.474	1.168
		5	0.003	0.001	0.058	0.009	6.141	1.016
		6	0.002	0.001	0.045	0.011	5.362	1.508
		7	0.004	0.001	0.063	0.007	7.013	0.853
		8	0.003	0.001	0.054	0.012	6.045	1.748
		9	0.004	0.001	0.063	0.008	7.293	0.901
		10	0.005	0.002	0.072	0.013	7.620	1.191

In case#2.a, overall, the performance measure of HONN models show that HONN with CSO is the best model for forecasting cumulative oil production by yielding a stable value between the range of MSE = 0.002 ~ 0.005, RMSE = 0.039 ~ 0.072 and MAPE = 4 ~ 7.6 % with few neurons in the hidden layer.

3.3.3 Case #2.b

For this simulation study, monthly oil, gas and water production ratios from Well-1,Well-2,Well-3,Well-4 and Well-5 for 63 months were used for forecasting of cumulative oil production. The production ratios used for this simulation were obtained by dividing the production of oil, gas and water with maximum cumulative productions (through 63 months) of oil, gas and water, approximately 9500 m^3, 275000 m^3, and 5200 m^3, respectively**.** Table 3.18 presents the smoothed monthly oil, gas and water production data ratios of 5 wells for 63 months.

This case study shows how additional input parameters (gas and water production) influence the efficiency of HONN model in forecasting cumulative oil production. The production data were preprocessed by applying smoothing process and cross-correlation.

Table 3.18. Ratios of smoothed monthly oil, gas and water production data for five wells.

Months	Well-1			Well-2		
	Oil (C1)	Gas (C2)	Water (C3)	Oil (C4)	Gas (C5)	Water (C6)
1	0.111	0.107	0.184	0.072	0.05	0.203
2	0.107	0.103	0.188	0.068	0.047	0.21
3	0.106	0.107	0.19	0.065	0.045	0.215
4	0.099	0.103	0.205	0.068	0.049	0.197
5	0.099	0.106	0.21	0.064	0.047	0.195
6	0.101	0.11	0.211	0.061	0.046	0.189
7	0.091	0.098	0.196	0.059	0.046	0.162
8	0.081	0.085	0.184	0.057	0.046	0.137
9	0.074	0.078	0.155	0.048	0.039	0.133
10	0.062	0.067	0.138	0.044	0.037	0.127
11	0.05	0.054	0.123	0.04	0.034	0.121
12	0.051	0.058	0.122	0.036	0.031	0.135
13	0.057	0.065	0.144	0.032	0.029	0.142
14	0.061	0.068	0.156	0.028	0.025	0.145
15	0.069	0.076	0.182	0.027	0.025	0.142
16	0.074	0.081	0.211	0.026	0.024	0.141
17	0.078	0.086	0.242	0.025	0.023	0.14
18	0.074	0.082	0.231	0.023	0.021	0.14
19	0.073	0.082	0.234	0.023	0.022	0.145
20	0.068	0.079	0.221	0.022	0.021	0.141
21	0.063	0.076	0.203	0.022	0.021	0.134

Months	Well-1			Well-2		
	Oil (C1)	Gas (C2)	Water (C3)	Oil	Gas	Water
22	0.058	0.07	0.187	0.023	0.023	0.125
23	0.055	0.067	0.191	0.025	0.024	0.122
24	0.049	0.059	0.199	0.025	0.023	0.112
25	0.043	0.05	0.207	0.024	0.022	0.101
26	0.041	0.047	0.207	0.024	0.022	0.088
27	0.04	0.046	0.2	0.024	0.023	0.074
28	0.038	0.045	0.193	0.027	0.026	0.058
29	0.045	0.052	0.184	0.031	0.029	0.065
30	0.052	0.06	0.175	0.037	0.035	0.069
31	0.055	0.064	0.178	0.043	0.04	0.078
32	0.055	0.064	0.175	0.042	0.039	0.086
33	0.054	0.062	0.179	0.04	0.038	0.084
34	0.048	0.055	0.181	0.04	0.037	0.067
35	0.042	0.047	0.185	0.038	0.034	0.054
36	0.036	0.04	0.186	0.031	0.028	0.049
37	0.035	0.039	0.192	0.029	0.026	0.057
38	0.033	0.036	0.169	0.025	0.022	0.065
39	0.033	0.038	0.163	0.021	0.019	0.084
40	0.034	0.039	0.161	0.017	0.016	0.104
41	0.03	0.036	0.167	0.017	0.017	0.116
42	0.03	0.037	0.168	0.02	0.02	0.096
43	0.034	0.042	0.182	0.024	0.024	0.093
44	0.033	0.041	0.175	0.027	0.027	0.08
45	0.034	0.041	0.171	0.029	0.029	0.065
46	0.041	0.05	0.16	0.03	0.03	0.049
47	0.042	0.051	0.154	0.026	0.026	0.05
48	0.043	0.053	0.159	0.022	0.022	0.039
49	0.047	0.058	0.159	0.028	0.028	0.03
50	0.048	0.059	0.158	0.048	0.049	0.019
51	0.048	0.06	0.153	0.068	0.069	0.012
52	0.045	0.056	0.154	0.089	0.091	0.005
53	0.041	0.051	0.154	0.111	0.112	0.01
54	0.04	0.049	0.153	0.124	0.124	0.013
55	0.037	0.046	0.155	0.142	0.142	0.022
56	0.033	0.041	0.157	0.156	0.16	0.033
57	0.032	0.039	0.156	0.167	0.165	0.04
58	0.031	0.038	0.158	0.18	0.174	0.043
59	0.027	0.032	0.168	0.188	0.177	0.049
60	0.026	0.029	0.169	0.181	0.166	0.048
61	0.021	0.022	0.147	0.171	0.147	0.045
62	0.018	0.019	0.137	0.163	0.142	0.049
63	0.003	0.003	0.046	0.14	0.13	0.054

Well-3			Well-4			Well-5			Cumulative oil
Oil (C7)	Gas (C8)	Water (C9)	Oil (C10)	Gas (C11)	Water (C12)	Oil (C13)	Gas (C14)	Water (C15)	
0.309	0.256	0.029	0.09	0.047	0.21	0.237	0.217	0.08	0.82
0.303	0.251	0.016	0.084	0.044	0.217	0.233	0.214	0.077	0.796
0.299	0.248	0.012	0.081	0.042	0.229	0.224	0.205	0.072	0.775
0.3	0.256	0.008	0.075	0.04	0.243	0.216	0.203	0.07	0.758
0.304	0.266	0.006	0.074	0.041	0.261	0.211	0.204	0.067	0.752
0.309	0.277	0.006	0.073	0.043	0.268	0.207	0.205	0.062	0.752
0.319	0.295	0.007	0.074	0.046	0.287	0.202	0.206	0.059	0.745
0.326	0.312	0.009	0.078	0.051	0.297	0.195	0.207	0.056	0.736
0.324	0.314	0.012	0.082	0.055	0.3	0.195	0.21	0.048	0.722

Well-3			Well-4			Well-5			Cumulative oil
Oil (C7)	Gas (C8)	Water (C9)	Oil (C10)	Gas (C11)	Water (C12)	Oil (C13)	Gas (C14)	Water (C15)	
0.326	0.323	0.015	0.085	0.056	0.302	0.191	0.21	0.041	0.708
0.327	0.327	0.018	0.081	0.058	0.287	0.187	0.208	0.035	0.685
0.332	0.33	0.015	0.065	0.048	0.222	0.192	0.215	0.026	0.676
0.322	0.32	0.02	0.069	0.058	0.161	0.189	0.211	0.023	0.67
0.307	0.302	0.022	0.072	0.067	0.106	0.168	0.187	0.049	0.637
0.295	0.286	0.025	0.079	0.082	0.047	0.154	0.17	0.088	0.624
0.291	0.281	0.033	0.089	0.093	0.041	0.147	0.163	0.121	0.628
0.281	0.271	0.048	0.1	0.104	0.062	0.137	0.151	0.16	0.621
0.279	0.271	0.053	0.091	0.095	0.082	0.133	0.147	0.189	0.601
0.297	0.296	0.053	0.082	0.086	0.106	0.147	0.168	0.19	0.622
0.311	0.321	0.048	0.065	0.07	0.128	0.158	0.187	0.178	0.625
0.312	0.327	0.041	0.061	0.068	0.155	0.158	0.19	0.172	0.616
0.35	0.366	0.039	0.06	0.067	0.162	0.15	0.182	0.188	0.641
0.389	0.404	0.045	0.059	0.065	0.167	0.143	0.173	0.208	0.671
0.41	0.42	0.049	0.062	0.069	0.163	0.129	0.154	0.238	0.675
0.421	0.426	0.053	0.065	0.071	0.158	0.111	0.129	0.269	0.663
0.437	0.44	0.057	0.057	0.062	0.13	0.1	0.115	0.287	0.659
0.402	0.408	0.056	0.051	0.056	0.127	0.094	0.109	0.285	0.612
0.357	0.366	0.053	0.045	0.05	0.119	0.086	0.101	0.289	0.554
0.363	0.372	0.046	0.048	0.053	0.117	0.084	0.099	0.293	0.571
0.376	0.382	0.045	0.051	0.056	0.114	0.082	0.095	0.294	0.598
0.386	0.391	0.048	0.058	0.064	0.107	0.076	0.088	0.31	0.618
0.393	0.398	0.04	0.058	0.063	0.102	0.073	0.084	0.306	0.621
0.444	0.446	0.029	0.062	0.067	0.108	0.075	0.086	0.299	0.675
0.493	0.484	0.033	0.057	0.061	0.114	0.076	0.086	0.288	0.714
0.53	0.506	0.04	0.052	0.054	0.123	0.078	0.087	0.28	0.738
0.574	0.533	0.042	0.046	0.048	0.129	0.083	0.092	0.261	0.77
0.624	0.572	0.054	0.048	0.049	0.138	0.088	0.098	0.267	0.824
0.566	0.515	0.059	0.041	0.042	0.121	0.083	0.093	0.241	0.747
0.548	0.505	0.078	0.038	0.04	0.12	0.083	0.096	0.234	0.722
0.534	0.504	0.101	0.036	0.039	0.121	0.083	0.099	0.232	0.704
0.528	0.516	0.11	0.033	0.038	0.119	0.076	0.093	0.222	0.685
0.519	0.517	0.111	0.033	0.038	0.119	0.067	0.084	0.206	0.67
0.59	0.589	0.116	0.04	0.046	0.14	0.067	0.086	0.223	0.756
0.586	0.587	0.106	0.04	0.046	0.143	0.06	0.077	0.218	0.746
0.579	0.581	0.084	0.04	0.046	0.141	0.043	0.066	0.209	0.725
0.569	0.569	0.079	0.041	0.047	0.139	0.031	0.066	0.213	0.712
0.57	0.569	0.078	0.042	0.048	0.132	0.033	0.068	0.212	0.713
0.57	0.57	0.082	0.043	0.049	0.124	0.033	0.068	0.206	0.711
0.567	0.57	0.086	0.046	0.053	0.114	0.029	0.063	0.206	0.716
0.577	0.584	0.087	0.05	0.058	0.106	0.035	0.059	0.207	0.757
0.579	0.59	0.078	0.05	0.059	0.107	0.041	0.053	0.207	0.786
0.584	0.596	0.062	0.048	0.057	0.108	0.033	0.043	0.21	0.8
0.6	0.607	0.042	0.048	0.057	0.112	0.027	0.035	0.21	0.827
0.602	0.604	0.033	0.046	0.053	0.118	0.027	0.034	0.193	0.837
0.586	0.586	0.049	0.04	0.046	0.125	0.027	0.034	0.182	0.832
0.555	0.563	0.076	0.037	0.043	0.127	0.028	0.035	0.176	0.808
0.521	0.514	0.116	0.034	0.039	0.133	0.028	0.035	0.172	0.782
0.482	0.467	0.166	0.031	0.034	0.138	0.027	0.033	0.172	0.75
0.437	0.411	0.191	0.027	0.029	0.146	0.023	0.028	0.18	0.702
0.407	0.372	0.192	0.026	0.028	0.147	0.017	0.02	0.145	0.657
0.386	0.333	0.188	0.027	0.027	0.142	0.051	0.057	0.112	0.656
0.35	0.304	0.163	0.026	0.026	0.14	0.073	0.082	0.063	0.631
0.339	0.301	0.159	0.031	0.031	0.11	0.204	0.23	0.011	0.717

The smoothing process was carried out by a moving averaging filter with five sequence data points to reduce noise. Oil, gas and water production ratios of 5 producing wells before and after smoothing are graphically represented in Figure 3.11. After that, the smoothed data were used to find correlation between the cumulative oil production and oil, gas, and water production from each well by cross-correlation function (CCF) as shown in Figure 3.12.

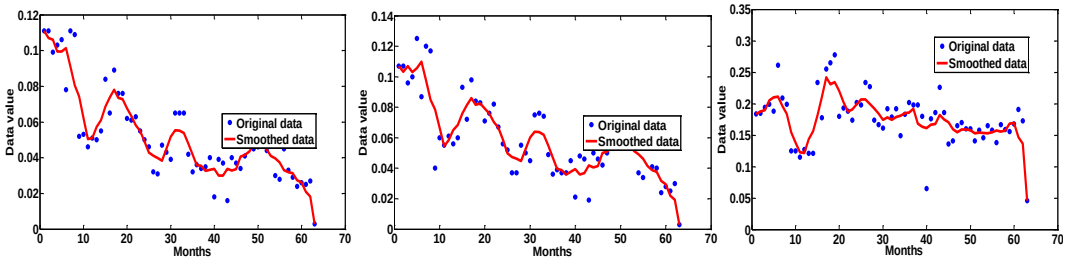

(1a) oil from well-1 (1b) water from well-1 (1c) gas from well-1

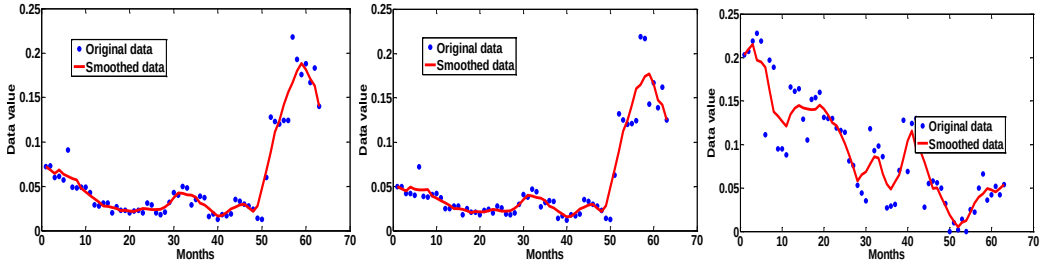

(2a) oil from well-2 (2b) water from well-2 (2c) gas from well-2

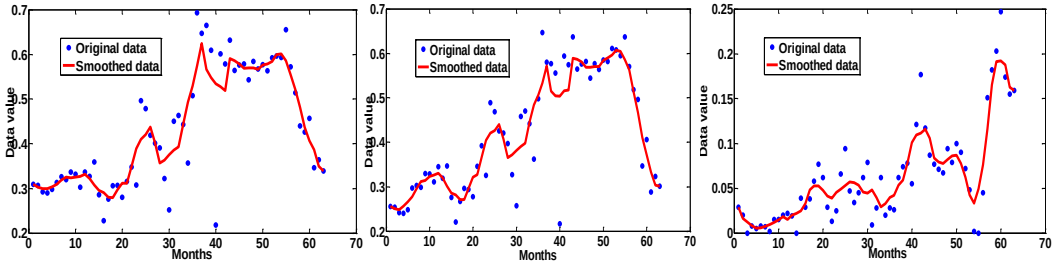

(3a) oil from well-3 (3b) water from well-3 (3c) gas from well-3

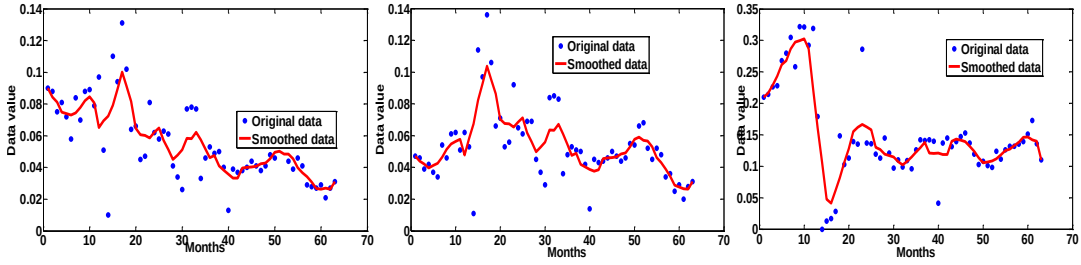

(4a) oil from well-4 (4b) water from well-4 (4c) gas from well-4

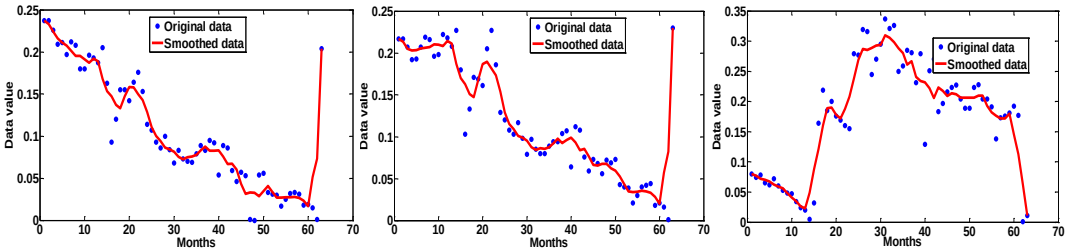

(5a) oil from well-5 (5b) water from well-5 (5c) gas from well-5

Figure 3.11. Before and after smoothing process of oil, gas and water productions from 5 wells.

The significant input variables were determined using the CCF plot. It is observed from the CCF plot (Figure 3.12) that the correlations between oil, gas, and water of 5 producing wells are the most significant at lag0. Since lag0 does not represent step ahead, lag1 was selected as the highest cross-correlation. Also, since the CCF for two parameters were calculated twice (i.e., Cx-C16 and C16-Cx, x=1, 2,…, 16), one of them was dropped. C16-C16 CCF was also dropped because it represented auto-correlation.

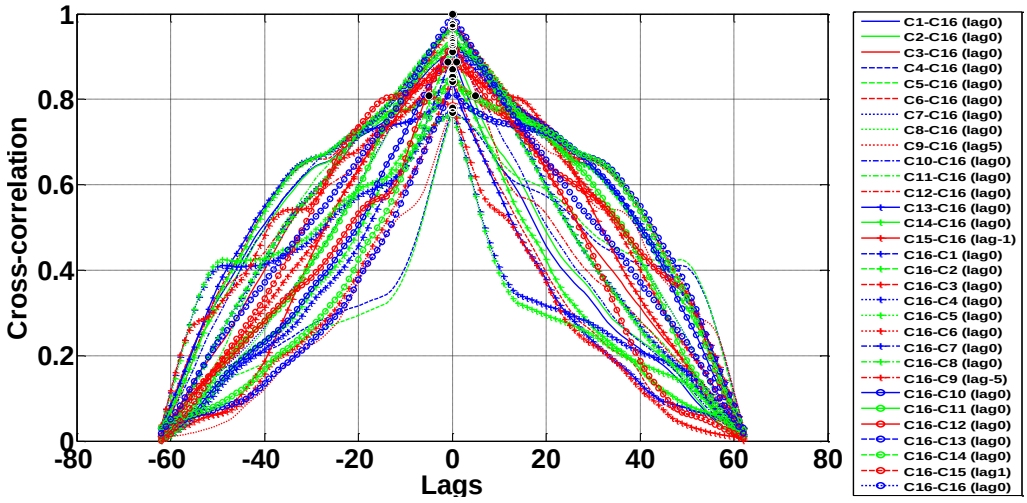

Figure 3.12. CCF of smoothed oil, gas and water production data. The dark circles on the plot indicate the highest correlation between two parameters.

A closer look at Figure 3.12 showed that the water production from Well-3 was negatively correlated with cumulative oil production and hence C9 was dropped from HONN inputs. Thus, overall 14 input vectors were rearranged for HONN models as listed in Table 3.19. Input1 to input 14 represents the correlation of oil, gas and water productions from each well at lag1 to the cumulative field oil production. First 35 months data were used for training and next 17 months data for validation

Table 3.19 The training, test and target data sets used for training HONN model for case#2.b.

Months	Input-1	Input-2	Input-3	Input-4	Input-5	Input-6	Input-7
1	0.111	0.107	0.184	0.072	0.05	0.203	0.309
2	0.107	0.103	0.188	0.068	0.047	0.21	0.303
3	0.106	0.107	0.19	0.065	0.045	0.215	0.299
4	0.099	0.103	0.205	0.068	0.049	0.197	0.3
5	0.099	0.106	0.21	0.064	0.047	0.195	0.304
6	0.101	0.11	0.211	0.061	0.046	0.189	0.309
7	0.091	0.098	0.196	0.059	0.046	0.162	0.319
8	0.081	0.085	0.184	0.057	0.046	0.137	0.326
9	0.074	0.078	0.155	0.048	0.039	0.133	0.324
10	0.062	0.067	0.138	0.044	0.037	0.127	0.326
11	0.05	0.054	0.123	0.04	0.034	0.121	0.327
12	0.051	0.058	0.122	0.036	0.031	0.135	0.332
13	0.057	0.065	0.144	0.032	0.029	0.142	0.322
14	0.061	0.068	0.156	0.028	0.025	0.145	0.307
15	0.069	0.076	0.182	0.027	0.025	0.142	0.295
16	0.074	0.081	0.211	0.026	0.024	0.141	0.291
17	0.078	0.086	0.242	0.025	0.023	0.14	0.281
18	0.074	0.082	0.231	0.023	0.021	0.14	0.279
19	0.073	0.082	0.234	0.023	0.022	0.145	0.297
20	0.068	0.079	0.221	0.022	0.021	0.141	0.311
21	0.063	0.076	0.203	0.022	0.021	0.134	0.312
22	0.058	0.07	0.187	0.023	0.023	0.125	0.35
23	0.055	0.067	0.191	0.025	0.024	0.122	0.389
24	0.049	0.059	0.199	0.025	0.023	0.112	0.41
25	0.043	0.05	0.207	0.024	0.022	0.101	0.421
26	0.041	0.047	0.207	0.024	0.022	0.088	0.437
27	0.04	0.046	0.2	0.024	0.023	0.074	0.402
28	0.038	0.045	0.193	0.027	0.026	0.058	0.357
29	0.045	0.052	0.184	0.031	0.029	0.065	0.363
30	0.052	0.06	0.175	0.037	0.035	0.069	0.376
31	0.055	0.064	0.178	0.043	0.04	0.078	0.386
32	0.055	0.064	0.175	0.042	0.039	0.086	0.393
33	0.054	0.062	0.179	0.04	0.038	0.084	0.444
34	0.048	0.055	0.181	0.04	0.037	0.067	0.493
35	0.042	0.047	0.185	0.038	0.034	0.054	0.53
36	0.036	0.04	0.186	0.031	0.028	0.049	0.574
37	0.035	0.039	0.192	0.029	0.026	0.057	0.624
38	0.033	0.036	0.169	0.025	0.022	0.065	0.566
39	0.033	0.038	0.163	0.021	0.019	0.084	0.548
40	0.034	0.039	0.161	0.017	0.016	0.104	0.534
41	0.03	0.036	0.167	0.017	0.017	0.116	0.528
42	0.03	0.037	0.168	0.02	0.02	0.096	0.519
43	0.034	0.042	0.182	0.024	0.024	0.093	0.59
44	0.033	0.041	0.175	0.027	0.027	0.08	0.586
45	0.034	0.041	0.171	0.029	0.029	0.065	0.579
46	0.041	0.05	0.16	0.03	0.03	0.049	0.569
47	0.042	0.051	0.154	0.026	0.026	0.05	0.57
48	0.043	0.053	0.159	0.022	0.022	0.039	0.57
49	0.047	0.058	0.159	0.028	0.028	0.03	0.567
50	0.048	0.059	0.158	0.048	0.049	0.019	0.577
51	0.048	0.06	0.153	0.068	0.069	0.012	0.579
52	0.045	0.056	0.154	0.089	0.091	0.005	0.584

Input-8	Input-9	Input-10	Input-11	Input-12	Input-13	Input-14	Target
0.256	0.09	0.047	0.21	0.237	0.217	0.08	0.796
0.251	0.084	0.044	0.217	0.233	0.214	0.077	0.775
0.248	0.081	0.042	0.229	0.224	0.205	0.072	0.758
0.256	0.075	0.04	0.243	0.216	0.203	0.07	0.752
0.266	0.074	0.041	0.261	0.211	0.204	0.067	0.752
0.277	0.073	0.043	0.268	0.207	0.205	0.062	0.745
0.295	0.074	0.046	0.287	0.202	0.206	0.059	0.736
0.312	0.078	0.051	0.297	0.195	0.207	0.056	0.722
0.314	0.082	0.055	0.3	0.195	0.21	0.048	0.708
0.323	0.085	0.056	0.302	0.191	0.21	0.041	0.685
0.327	0.081	0.058	0.287	0.187	0.208	0.035	0.676
0.33	0.065	0.048	0.222	0.192	0.215	0.026	0.67
0.32	0.069	0.058	0.161	0.189	0.211	0.023	0.637
0.302	0.072	0.067	0.106	0.168	0.187	0.049	0.624
0.286	0.079	0.082	0.047	0.154	0.17	0.088	0.628
0.281	0.089	0.093	0.041	0.147	0.163	0.121	0.621
0.271	0.1	0.104	0.062	0.137	0.151	0.16	0.601
0.271	0.091	0.095	0.082	0.133	0.147	0.189	0.622
0.296	0.082	0.086	0.106	0.147	0.168	0.19	0.625
0.321	0.065	0.07	0.128	0.158	0.187	0.178	0.616
0.327	0.061	0.068	0.155	0.158	0.19	0.172	0.641
0.366	0.06	0.067	0.162	0.15	0.182	0.188	0.671
0.404	0.059	0.065	0.167	0.143	0.173	0.208	0.675
0.42	0.062	0.069	0.163	0.129	0.154	0.238	0.663
0.426	0.065	0.071	0.158	0.111	0.129	0.269	0.659
0.44	0.057	0.062	0.13	0.1	0.115	0.287	0.612
0.408	0.051	0.056	0.127	0.094	0.109	0.285	0.554
0.366	0.045	0.05	0.119	0.086	0.101	0.289	0.571
0.372	0.048	0.053	0.117	0.084	0.099	0.293	0.598
0.382	0.051	0.056	0.114	0.082	0.095	0.294	0.618
0.391	0.058	0.064	0.107	0.076	0.088	0.31	0.621
0.398	0.058	0.063	0.102	0.073	0.084	0.306	0.675
0.446	0.062	0.067	0.108	0.075	0.086	0.299	0.714
0.484	0.057	0.061	0.114	0.076	0.086	0.288	0.738
0.506	0.052	0.054	0.123	0.078	0.087	0.28	0.77
0.533	0.046	0.048	0.129	0.083	0.092	0.261	0.824
0.572	0.048	0.049	0.138	0.088	0.098	0.267	0.747
0.515	0.041	0.042	0.121	0.083	0.093	0.241	0.722
0.505	0.038	0.04	0.12	0.083	0.096	0.234	0.704
0.504	0.036	0.039	0.121	0.083	0.099	0.232	0.685
0.516	0.033	0.038	0.119	0.076	0.093	0.222	0.67
0.517	0.033	0.038	0.119	0.067	0.084	0.206	0.756
0.589	0.04	0.046	0.14	0.067	0.086	0.223	0.746
0.587	0.04	0.046	0.143	0.06	0.077	0.218	0.725
0.581	0.04	0.046	0.141	0.043	0.066	0.209	0.712
0.569	0.041	0.047	0.139	0.031	0.066	0.213	0.713
0.569	0.042	0.048	0.132	0.033	0.068	0.212	0.711
0.57	0.043	0.049	0.124	0.033	0.068	0.206	0.716
0.57	0.046	0.053	0.114	0.029	0.063	0.206	0.757
0.584	0.05	0.058	0.106	0.035	0.059	0.207	0.786
0.59	0.05	0.059	0.107	0.041	0.053	0.207	0.8
0.596	0.048	0.057	0.108	0.033	0.043	0.21	0.827

Table 3.20 presents the results from HONN models with their performance measure in terms of MSE, RMSE, and MAPE for different configurations of neurons in the

hidden layer and synaptic operation. In this case study, the best model resulted in MAPE = 3.990%, MSE = 0.001, RMSE = 0.036 by HONN with CSO having three neurons in the hidden layer.

Table 3.20 Performance measure of HONN models for case#2.b.

Synaptic Operation	Number of Hidden Layers	Number of Neurons	MSE		RMSE		MAPE (%)	
			Mean	SD	Mean	SD	Mean	SD
Linear Synaptic Operation	1	1	0.004	0.001	0.065	0.011	7.480	1.104
		2	0.004	0.001	0.060	0.008	6.687	1.008
		3	0.003	0.001	0.052	0.006	6.199	0.631
		4	0.002	0.001	0.048	0.009	5.562	0.748
		5	0.003	0.000	0.054	0.005	6.187	0.435
Quadratic Synaptic Operation	1	1	0.002	0.001	0.046	0.006	5.147	0.734
		2	0.001	0.000	0.038	0.004	4.196	0.434
		3	0.003	0.001	0.054	0.008	6.004	0.964
		4	0.002	0.001	0.048	0.007	5.553	0.396
		5	0.003	0.001	0.054	0.005	6.046	0.855
Cubic Synaptic Operation	1	1	0.003	0.001	0.050	0.007	5.359	0.874
		2	0.002	0.001	0.049	0.006	5.627	0.393
		3	**0.001**	**0.000**	**0.036**	**0.004**	**3.990**	**0.450**
		4	0.003	0.001	0.054	0.008	6.238	1.013
		5	0.002	0.001	0.044	0.010	4.568	0.961

3.3.4 Discussions

From the four case studies reported herein, it is clear that a single well production data are insufficient and the best MAPE that could be achieved was 13 to 15% (case #1.a and b). A major reason for this discrepancy was thought to be insufficient input data particularly with respect to well pressure and presence of other wells in the vicinity. The multiple well modeling discussed above confirmed this as shown by the results of case #2.a and b, where the MAPE has come down to the range of 3 to 4%.

From the case#2.a and b, the performance evaluation criteria indicates that better cumulative oil production forecasting can be achieved from HONN with CSO using oil, gas and water production data or just oil production data for multiple wells. The simulation results from three different lag scenarios also presents that HONN with CSO gives best agreement between simulation results and observed data. In this study, the selection of lag time is an important factor that influences the forecasting results.

In case#2.a, cross-correlation function (CCF) indicates that the most significant lag for oil production forecasting with only oil production data from five producing well is lag1, and HONN with CSO yields the best forecasting cumulative oil production in this case. This can be explained by recalling that five input parameters (oil productions from five wells) generate complex correlation for target parameter (oil production to be predicted). Thus, in this case, nonlinear combination of synaptic operations could result in better prediction. The oil production forecasting from HONN with CSO with single lag1 for next ten months, from month 53 – 63, is compared with measurement production data in Figure 3.13. The figure indicates a good match between the measured production data and forecast results within the overall testing error of 0.025.

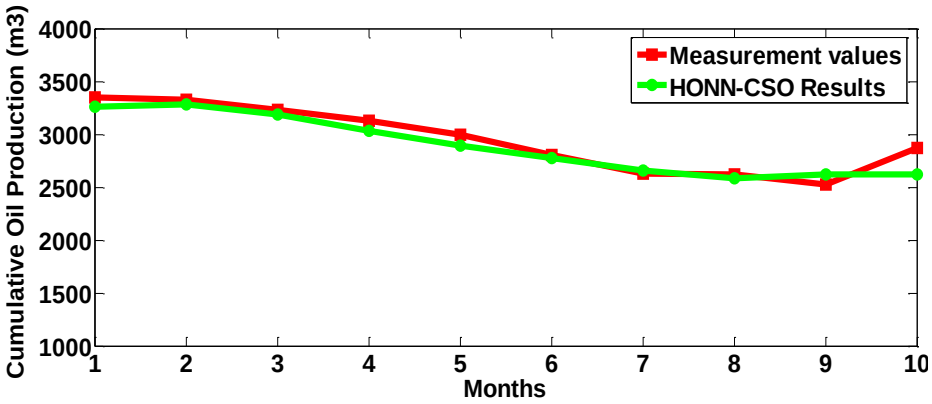

Figure 3.13 Comparison between the measured cumulative oil production and the forecast results from HONN with CSO using single lag-1 for case#2.a.

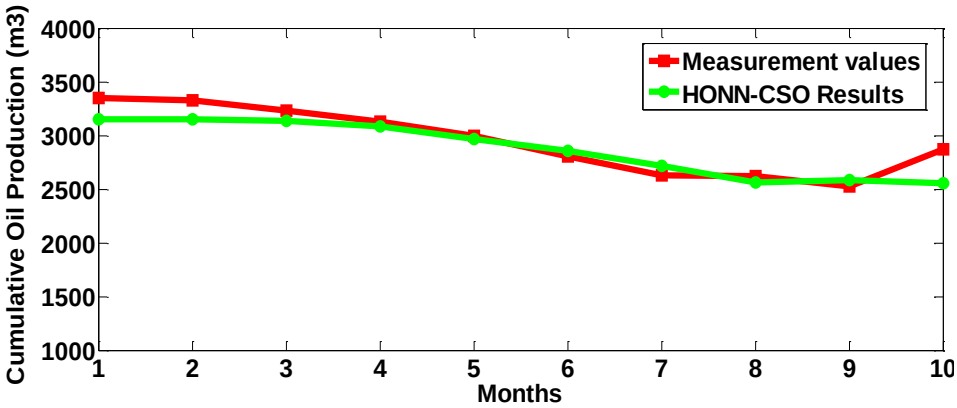

Figure 3.14. Comparison between the measured cumulative oil production and the forecast results from HONN with CSO from case #2.b

Figure 3.14 illustrates the comparison between the measured oil production data and the forecast results from HONN with CSO for ten months from month 53 to 63 within the overall testing error of 0.035. Again the match is reasonably satisfactory.

Through these case studies, it is observed that the performance of HONN with CSO in the case#2.a shows less MAPE (3.46%) than that in the case#2.b (3.99%). The number of input parameters for training HONN in the case#2.b is higher than that in the case#2.a. It should be noted that for the application of HONN for forecasting, the number of input variables is one of the significant factors to determine the order of synaptic operation in the neuron. The results indicate that by increasing the order of combination of neural inputs, the capability of an HONN model increases; however, the uncertainty in input data also gets multiplied resulting in higher MAPE. The performance of HONN with HOSO is very susceptible to higher number of neurons in the hidden layer, which induces longer computational time.

CHAPTER 4

FLOW THROUGH POROUS MEDIA—A SIMULATION APPROACH

Before embarking into the aspects of simulation of multi-phase fluid flow through porous medium, let us glance through components required to construct the geological reservoir model. Reservoir modeling has two major parts; static model and the dynamic model. The static reservoir model provides the framework of structural and geological features of the reservoir obtained during petroleum exploration stage. The geologist maps the sedimentary rock layer outcrops to locate the subsurface structural traps like anticlines and domes. Petroleum geologist uses geological techniques such as 2D, 3D seismic surveys, sparse well log data, satellite images and borehole images for identifying the subsurface structure. The stratigraphy of the reservoir is recognized through wireline well logs (gamma, resistivity, neutron logs etc.,) and seismic surveys to trace the relation between the rock layers such as facies changes. The rock deformations such as faults or folding and tilting are identified from seismic interpretations. The reservoir boundary, sectoring and zonation are included in the geological modeling. The petrophysical rock properties such as porosity and permeability and their distributions at unsampled locations calculated using geostatistical method are defined in the geological model. The reservoir model become dynamic when the rock-fluid properties such as relative permeabilities, fluid saturations, connate water saturations and aquifer properties are included in the reservoir to understand the fluid movement within the system. Once the reservoir is modeled in all such details (some of them tentative such as rock static properties) one proceeds to calculate the movement of the reservoir fluids (oil, gas and water) under available driving force. This is called flow simulation.

Reservoir flow simulation is an essential task for petroleum engineers to carry out performance prediction of the reservoir under study. The reservoir simulator consists of set of nonlinear partial differential equations with appropriate initial and boundary conditions that describe the hydrodynamical fluid flow behavior within the

reservoir over time. In this chapter, we briefly describe the formulation used for black oil reservoir modeling model. The black oil flow models do not consider changes in the composition of hydrocarbon liquid over time because of change in reservoir pressure. On the other hand, compositional flow models account for such change because of inter-phase mass transfer between liquid oil and gas as the pressure in the reservoir declines with time due to production of fluids. The main difference between the black oil flow model and the compositional flow model is that; in case of the former, the fluid properties characterized by the PVT table that comprise of formation volume factors and solution gas-oil ratios vary as a function of pressure. While in compositional flow model, the PVT table additionally includes changes in the fluid compositions (oil and gas mole fractions) as a function of pressure. The formulation of partial differential equations for reservoir modeling presented in this chapter is adapted from the textbooks of (Crichlow, 1977; Ertekin, et al., 2001; Chen, et al., 2006).

4.1 ROCK AND FLUID PROPERTIES

This section provides the definitions of important rock and fluid properties involved in petroleum reservoir context.

Porosity (φ): Rock porosity represents the void space in the porous media, where the fluids get accumulated. Porosity is defined as the ratio of pore volume to the total bulk volume of the rock. It is expressed either in fraction or percentage and is a dimensionless quantity. This property of the rock can be mathematically expressed as:

$$\varphi = \frac{Pore\ volume}{Total\ volume} \tag{4.1}$$

Porosity is dependent on the fluid pressure if the rock is compressible. There are, primarily, two types of porosity, total and effective porosity. The total porosity represents the ratio of total volume of the pore space to the bulk volume, whereas, the effective porosity is the ratio of interconnected pore volume to the bulk volume.

Permeability (k): The ability of a rock to transmit fluid through interconnected pore space is termed as permeability. Mathematically, it is defined by Darcy's law which states

$$q_x = -\frac{k\ \Delta P\ A}{\mu L} \tag{4.2}$$

where, q_x is the flow rate in x direction, $\frac{\Delta P}{L}$ is the pressure gradient causing the flow, A is the flow area and μ is the fluid viscosity. It is expressed in Darcy or millidarcy (mD), though it has the dimension of m^2 in SI- units and is obtained from well test, laboratory analysis, correlations and isoperm maps. When the reservoir rock is 100% saturated with a single phase fluid it is termed as absolute permeability. Effective permeability is the ability of the rock to transmit fluid in presence of other immiscible fluids. Permeability is also a rock property and therefore, varies at different locations and even at the same location with the flow directions. It is strongly correlated to porosity since the interconnections and orientations of pores are vital to fluid flow. Usually, for a reservoir rock the permeability values ranges from 1mD to 1000 mD.

Fluid Saturation (S): Saturation is expressed as that fraction, or percent, of the pore volume occupied by a particular fluid phase (oil, gas, or water) in the void space. Saturation is mathematically defined as:

$$S = \frac{Total\ volume\ of\ the\ fluid}{Pore\ volume} \tag{4.3}$$

All saturation values are based on pore volume and not on the gross reservoir volume. The saturation of each individual phase ranges between 0 to 100%. For a three phase fluid flow of oil, gas and water, the sum of the saturations is 100%, i.e.

$$So + Sg + Sw = 1 \tag{4.4}$$

where, *So*, *Sg* and *Sw* corresponds to fractional saturation of oil, gas and water respectively.

Capillary Pressure (P_c): A discontinuity in pressure exists between the two fluids when two immiscible fluids are in contact, which depends upon the curvature of the interface separating the fluids. This pressure difference is referred as the capillary pressure and mathematically defined as P_c

$$P_c = P_{nw} - P_w \tag{4.5}$$

where P_{nw} is the pressure in nonwetting phase and Pw is the pressure in wetting phase. That is, the pressure excess in the nonwetting fluid is the capillary pressure, and is a function of saturation.

Relative Permeability (k_r): When two or more fluids flow at the same time, at a specific saturation, the ratio of the effective permeability of the corresponding phase to the absolute permeability is termed as relative permeability of the corresponding phase. The relative permeability is affected by the pore geometry, wettability, fluid viscosity and saturation history. Relative permeability is dimensionless and varies between zero and one.

$$k_r = \frac{Effective\ permeability}{Absolute\ permeability} \tag{4.6}$$

When the reservoir displacement process is dominated by gravity, the relative permeabilities are functions of saturations, and its only essential to know the end-point saturations, the irreducible water saturations and residual oil saturations. The residual oil saturation is an important parameter used to determine the overall oil recovery.

Mobility (λ): The mobility of fluid phase is defined as the ratio of the effective phase relative permeability to the phase viscosity. The mobility is expressed as

$$\lambda = \frac{Effective\ \ phase\ permeability}{Phase\ viscosity} \tag{4.7}$$

Phase: Phase is a homogeneous region of a fluid separated from another phase by an interface, e.g., oil, gas or water. Two phases are said to be immiscible if both the phases cannot be mixed in any proportion to form a homogeneous solution.

Component: Component refers to a single chemical entity that may be present in a phase, e.g. aqueous phase contains components like water (H_2O), sodium chloride (NaCl) and dissolved oxygen (O_2).

Compressibility (C_f): The change in volume (V) or density (ρ) of the fluid with respect to the pressure (p) is termed as the compressibility of the fluid and is expressed as

$$C_f = -\frac{1}{V}\left(\frac{\partial V}{\partial p}\right)_T = \frac{1}{\rho}\left(\frac{\partial \rho}{\partial p}\right)_T \tag{4.8}$$

There are three types of basic governing equations that form the mathematical model of the fluid flow behavior in porous media. These equations are; conservation of mass, rate equation and the equations of state which along with appropriate initial and

boundary conditions. A brief description of the three governing equations for a black oil model can be found in the next sections.

4.2 FORMULATION OF FLOW EQUATIONS THROUGH POROUS MEDIUM

This section contains a brief discussion on the fundamental governing equations that describe the flow and transport through porous medium. The explanation of flow equation of single phase is presented in Section 4.2.1 and for three phase black-oil model is depicted in Section 4.2.2.

4.2.1 General Equation for Single Phase Flow

The equation governing single phase flow through porous medium is obtained by combining fundamental equations such as, conservation of mass; rate equation and equation of state. The conservation of mass equation or the continuity equation is a generalized material balance equation, which describes a relationship between the amount of all fluids entering, leaving and remaining in the reservoir. The conservation of mass equation can be generally stated as

$$Mass\ rate\ in - Mass\ rate\ out = Mass\ rate\ of\ accumulation \tag{4.9}$$

For a petroleum reservoir, the principle of conservation of mass state that the amount of fluid (oil, gas, water) accumulated (remaining) in the reservoir after production is equal to the amount of fluid originally present in the reservoir minus the amount of fluid removed (produced), plus the amount of fluid added to the reservoir. Mathematically;

$$\frac{\partial(\rho v)}{\partial x} = -\varphi\frac{\partial \rho}{\partial t} + q \tag{4.10}$$

where φ is the porosity, ρ is the fluid density, v is the superficial Darcy velocity and q denotes either external source or sink. The magnitude of q is positive for sources and negative for sinks. The rate equation or the Darcy's law relates flow velocity to the pressure gradient and is expressed as

$$v = -\frac{k}{\mu}\frac{\partial P}{\partial x} \tag{4.11}$$

where k is the absolute permeability in the direction of flow, μ is the fluid viscosity and $(\partial P/\partial x)$ is the pressure gradient. Substituting Eq 4.11 into Eq 4.0 gives:

$$\frac{\partial(-\frac{k}{\mu}\frac{\partial P}{\partial x}\rho)}{\partial x} = -\varphi\frac{\partial \rho}{\partial t} + q \tag{4.12}$$

The equation of state expresses the fluid density as a function of pressure and can be represented by fluid compressibility c_f as

$$c_f \equiv -\frac{1}{V}\frac{\partial V}{\partial P}\Big|_T = \frac{1}{\rho}\frac{\partial \rho}{\partial P} \tag{4.13}$$

where V is the volume occupied by the fluid at reservoir conditions and T is the reservoir temperature. The Eq 4.12 can be simplified as follows by expanding left-hand side;

$$-\left(\frac{k}{\mu}\frac{\partial^2 P}{\partial x^2}\rho + \frac{k}{\mu}\frac{\partial P}{\partial x}\frac{\partial \rho}{\partial x}\right) = -\varphi\frac{\partial \rho}{\partial t} + q \tag{4.14}$$

Multiplying by (-1) and dividing by ρ on both sides of Eq 4.14 gives;

$$\frac{k}{\mu}\frac{\partial^2 P}{\partial x^2} = \varphi\frac{1}{\rho}\frac{\partial \rho}{\partial P}\frac{\partial P}{\partial t} + q \tag{4.15}$$

Substituting Eq 4.13 into Eq 4.15 gives

$$\frac{k}{\mu}\frac{\partial^2 P}{\partial x^2} = \varphi\, c_f\frac{\partial P}{\partial t} + q \tag{4.16}$$

Thus the equation for the single phase flow through porous media in 1D is

$$\frac{\partial^2 P}{\partial x^2} = \frac{\varphi\,\mu\, c_f}{k}\frac{\partial P}{\partial t} + q \tag{4.17}$$

The above single phase flow equation can be developed in other coordinate systems such as radial, cylindrical and spherical, according to the type of reservoir under study. The detailed descriptions of this can be found in appropriate reservoir simulation books (Mattax and Dalton, 1990; Ertekin, et al., 2001; Chen, et al., 2006). The flow equation (Eq 4.17) can be expanded for 3 dimensional single phase flow through porous medium as

$$\frac{\partial^2 P}{\partial x^2} + \frac{\partial^2 P}{\partial y^2} + \frac{\partial^2 P}{\partial z^2} = \frac{\varphi\, \mu\, c_f}{k} \frac{\partial P}{\partial t} + q \tag{4.18}$$

4.2.2 Basic Flow Equations for a Black Oil Model

A black oil model is used for modeling a petroleum reservoir, whose fluid Pressure-Volume-Temperature (PVT) properties are generated as functions of saturation and pressure. The model comprises of fluid components; oil, gas and water at standard conditions, which are distributed among three distinct fluid phases such as oil, gas and water respectively. In black oil model, oil and water are considered to be immiscible while gas may exist as solution gas or free gas. The black oil model relies on the assumption that the reservoir fluids are in thermodynamic equilibrium throughout the reservoir and maintain constant reservoir temperature (Ertekin, et al., 2001).

Similar to single phase fluid flow, the governing differential flow equations for 3 phase black oil model are developed by combining conservation of mass, Darcy's law and equation of state for each fluid phase. The partial differential equations for 3D, 3-phase black oil flow model are expressed as

$$\begin{aligned} A_x \frac{\partial}{\partial x}\left[\frac{k_{ro}}{\mu_o B_o}\frac{\partial \emptyset_o}{\partial x}\right] + A_y \frac{\partial}{\partial y}\left[\frac{k_{ro}}{\mu_o B_o}\frac{\partial \emptyset_o}{\partial y}\right] + A_z \frac{\partial}{\partial z}\left[\frac{k_{ro}}{\mu_o B_o}\frac{\partial \emptyset_o}{\partial z}\right] \\ = V_b \frac{\partial}{\partial t}\left[\varphi \frac{S_o}{B_o}\right] + q_o \end{aligned} \tag{4.19}$$

$$\begin{aligned} A_x \frac{\partial}{\partial x}\left[\frac{k_{rw}}{\mu_w B_w}\frac{\partial \emptyset_w}{\partial x}\right] + A_y \frac{\partial}{\partial y}\left[\frac{k_{rw}}{\mu_w B_w}\frac{\partial \emptyset_w}{\partial y}\right] + A_z \frac{\partial}{\partial z}\left[\frac{k_{rw}}{\mu_w B_w}\frac{\partial \emptyset_w}{\partial z}\right] \\ = V_b \frac{\partial}{\partial t}\left[\varphi \frac{S_w}{B_w}\right] + q_w \end{aligned} \tag{4.20}$$

$$\begin{aligned} A_x \frac{\partial}{\partial x}\left[\frac{k_{rg}}{\mu_g B_g}\frac{\partial \emptyset_g}{\partial x} + \frac{R_{so} k_{ro}}{\mu_o B_o}\frac{\partial \emptyset_o}{\partial x}\right] + A_y \frac{\partial}{\partial y}\left[\frac{k_{rg}}{\mu_g B_g}\frac{\partial \emptyset_g}{\partial y} + \frac{R_{so} k_{ro}}{\mu_o B_o}\frac{\partial \emptyset_o}{\partial y}\right] \\ + A_z \frac{\partial}{\partial z}\left[\frac{k_{rg}}{\mu_g B_g}\frac{\partial \emptyset_g}{\partial z} + \frac{R_{so} k_{ro}}{\mu_o B_o}\frac{\partial \emptyset_o}{\partial z}\right] \\ = V_b \frac{\partial}{\partial t}\left[\varphi\left(\frac{S_g}{B_g} + \frac{R_{so}\, S_o}{B_o}\right)\right] + q_g \end{aligned} \tag{4.21}$$

where, $x, y\ and\ z$ represents the coordinates of 3D model; $A_x, A_y and\ A_z$ are the cross sectional areas normal to $x, y\ and\ z$ directions respectively; subscripts $o, g, and\ w$ denotes oil phase, gas phase and water phase respectively; k_{ro}, k_{rg} and k_{rw} are the relative permeabilities of the phases, $B_o, B_g and\ B_w$ represent the formation volume factors; $\mu_o, \mu_g and\ \mu_w$ are corresponding phase viscosities; $S_o, S_g\ and\ S_w$ are the phase saturations; $q_o, q_g\ and\ q_w$ are the production rates of the oil, gas and water respectively; φ is the porosity; $R_{so}$is the solution gas oil ratio and V_b is the bulk volume. The fluid potentials $\emptyset_o, \emptyset_g$and $\emptyset_w$ are expressed as

$$\emptyset_o = P_o + \rho_o gh \tag{4.22}$$

$$\emptyset_g = P_g + \rho_g gh \tag{4.23}$$

$$\emptyset_w = P_w + \rho_w gh \tag{4.24}$$

where, $P_o, P_g$and P_w are the phase pressures; ρ_o, ρ_g and ρ_w represents the phase densities of oil, gas and water respectively, g is the acceleration due to gravity and h is the hydraulic pressure head.

The following additional constraint equations are necessary to complete the flow model.

$$S_o + S_g + S_w = 1 \tag{4.25}$$

$$\frac{\partial}{\partial t}[S_o + S_g + S_w] = 0 \tag{4.26}$$

The phase pressure is expressed in terms of capillary pressure as

$$P_{cwo} = P_o - P_w = f(S_w) \tag{4.27}$$

and

$$P_{cgo} = P_g - P_o = f(S_g) \tag{4.28}$$

Eq 4.19 through Eq 4.28 to describe the simultaneous flow of 3 phase fluids in a 3D porous medium using black oil model given the appropriate initial and boundary conditions. The above equations can be appropriately combined to give

$$
\begin{aligned}
&A_x \frac{\partial}{\partial x}\left(\lambda_T \frac{\partial P_o}{\partial x}\right) + A_x \frac{\partial}{\partial x}\left(\lambda_g \frac{\partial P_{cgo}}{\partial x} - \lambda_w \frac{\partial P_{cwo}}{\partial x}\right) \\
&\qquad + A_x \frac{\partial}{\partial x}\left[\lambda_g \frac{\partial(\rho_g g h)}{\partial x} + \lambda_o \frac{\partial(\rho_o g h)}{\partial x} + \lambda_w \frac{\partial(\rho_w g h)}{\partial x}\right] \\
&\qquad = \beta_1 \frac{\partial P_o}{\partial x} + \beta_2 \\
&A_y \frac{\partial}{\partial y}\left(\lambda_T \frac{\partial P_o}{\partial y}\right) + A_y \frac{\partial}{\partial y}\left(\lambda_g \frac{\partial P_{cgo}}{\partial y} - \lambda_w \frac{\partial P_{cwo}}{\partial y}\right) \\
&\qquad + A_y \frac{\partial}{\partial x}\left[\lambda_g \frac{\partial(\rho_g g h)}{\partial y} + \lambda_o \frac{\partial(\rho_o g h)}{\partial y} + \lambda_w \frac{\partial(\rho_w g h)}{\partial y}\right] \\
&\qquad = \beta_1 \frac{\partial P_o}{\partial y} + \beta_2 \\
&A_z \frac{\partial}{\partial z}\left(\lambda_T \frac{\partial P_o}{\partial z}\right) + A_z \frac{\partial}{\partial x}\left(\lambda_g \frac{\partial P_{cgo}}{\partial z} - \lambda_w \frac{\partial P_{cwo}}{\partial z}\right) \\
&\qquad + A_z \frac{\partial}{\partial z}\left[\lambda_g \frac{\partial(\rho_g g h)}{\partial z} + \lambda_o \frac{\partial(\rho_o g h)}{\partial z} + \lambda_w \frac{\partial(\rho_w g h)}{\partial z}\right] \\
&\qquad = \beta_1 \frac{\partial P_o}{\partial z} + \beta_2
\end{aligned}
\tag{4.29}
$$

where, λ is the mobility of the fluid; λ_T is the total mobility of oil, gas and water; $P_{cgo}$is gas/oil capillary pressure; P_{cwo} is oil/water capillary pressure; β_1 are functions of PVT terms; and β_2 are the production terms.

4.2.3 Boundary Conditions

The mathematical model described by the equations in the previous section is complete only if the necessary external boundary conditions and the initial state are specified over the reservoir model domain. Let, Ω denote the entire porous medium domain subjected to external boundary Γ, and let the subscript α represents the corresponding phase (oil, gas and water). Usually there are three kinds of boundary conditions boundary conditions that define the boundaries of the reservoir model and can be specified as:

Dirichlet boundary condition (first kind)*:* The pressure is defined as known function of position and time on Γ, and is expressed as

$$P_\alpha = g_{\alpha,1} \quad \text{on} \quad \Gamma \tag{4.30}$$

Neumann boundary condition (second kind): When the total mass flux is known on Γ, given by

$$\rho_\alpha \boldsymbol{v_\alpha} . \boldsymbol{\Theta} = g_{\alpha,2} \quad \text{on} \quad \Gamma \tag{4.31}$$

where $\boldsymbol{\Theta}$ is the outward unit normal to Γ and $g_{\alpha,2}$. For impervious boundaries $g_{\alpha,2} = 0$.

Robin or Dankwerts boundary conditions (third/ mixed kind): when Γ is a semipervious boundary for the α phase, the mixed kind occurs as

$$g_{\alpha,1} P_\alpha + g_{\alpha,2} \rho_\alpha \boldsymbol{v_\alpha}. \boldsymbol{\Theta} = g_{\alpha,3} \quad \text{on} \quad \Gamma \tag{4.32}$$

where $g_{\alpha,1}$, $g_{\alpha,2}$ and $g_{\alpha,3}$ are given functions. The initial conditions are defined by the pressure over the entire porous medium domain at some initial state, generally at time $t = 0$. In black oil model the choice of primary unknowns depend on the reservoir states. Usually, for saturated reservoir state, the primary unknowns are $P = P_0, S_w and\ S_o$ and for undersaturated reservoir, $P = P_0, S_w and\ P_b$ are the primary unknowns. Hence depending on the initial states of the reservoir, initial conditions can be either

$$P\ (\boldsymbol{X}, 0) = P^0(\boldsymbol{X}),\ \ S_w(\boldsymbol{X}, 0) = S_w^0(\boldsymbol{X}),\quad S_o(\boldsymbol{X}, 0) = S_o^0(\boldsymbol{X});\quad \boldsymbol{X} \in \Omega \tag{4.33}$$

or

$$P\ (\boldsymbol{X}, 0) = P^0(\boldsymbol{X}),\ \ S_w(\boldsymbol{X}, 0) = S_w^0(\boldsymbol{X}),\quad P_b(\boldsymbol{X}, 0) = P_b^0(\boldsymbol{X});\quad \boldsymbol{X} \in \Omega \tag{4.34}$$

where $\boldsymbol{X}$ denotes the spatial variables ($x, y, and\ z$); and P_b is the bubble point pressure.

4.2.4 Solution Procedure

The governing equations that describe flow through porous medium, discussed in the previous text, are highly nonlinear partial differential equations (PDE) which relate the saturation and pressure changes in space and time throughout the medium. Solving these equations analytically is not practical and therefore, numerical solutions are sought. The numerical simulator transforms these continuous partial differential equations into finite difference equations; which provide the solutions at discrete points over space and time for the entire porous domain under consideration. The finite difference form of the partial differential equations is derived using the Taylor

Series expansion of a function at a given point in the neighbourhood and the derivatives are expressed in terms of finite differences given by Eq. 4.35 and Eq. 4.36. Δx and Δt are small in comparison to x and t in order that the linear approximation holds. This means that for solution purposes the entire reservoir is divided into three-dimensional blocks which are small in comparison to the entire reservoir volume. Also integration on time scale is done in small time steps.

$$P'(x) = \frac{\partial P}{\partial x} = \frac{P(x + \Delta x) - P(x)}{\Delta x} \tag{4.35}$$

$$P'(t) = \frac{\partial P}{\partial t} = \frac{P(t + \Delta t) - P(t)}{\Delta t} \tag{4.36}$$

The finite difference transforms the PDE into algebraic equations which are solved by matrix method. The system of equations for the simultaneous flow for all the fluid phases has to be solved for the unknown parameters**;** fluid pressure and saturations. An example of the algebraic equations resulting from finite difference formulation for 3D model are given by Eq. 4.37. The simultaneous equations contain pressure term that has to be solved at different locations over time. The information (pressure value) at time; $t = n$ is used to calculate the new pressure value at future time; $t = n + 1$.

$$aP_{i-1,j,k} + eP_{i,j-1,k} + fP_{i,j,k-1} + bP_{i,j,k} + cP_{i+1,j,k}$$

$$+gP_{i,j+1,k} + mP_{i,j,k+1} = d_{ijk} \tag{4.37}$$

There are different schemes for finite differences to form the approximation of PDE such as Explicit, Implicit, and Crank-Nicholsons schemes. The method of calculating new pressure value one at a time is the explicit scheme as shown in Figure 4.1. Knowing the value of P at n^{th} time step, the value at $n + 1^{th}$ time step, for 1D flow can be calculated using explicit method as

$$\frac{P_i^{n+1} - P_i^n}{\Delta t} = \frac{P_{i+1}^n - 2P_i^n + P_{i-1}^n}{\Delta x^2} \tag{4.38}$$

In Eq 4.38, the time derivative is transformed using forward difference while pressure derivative by 2nd order central differentiation to make the approximation linear.

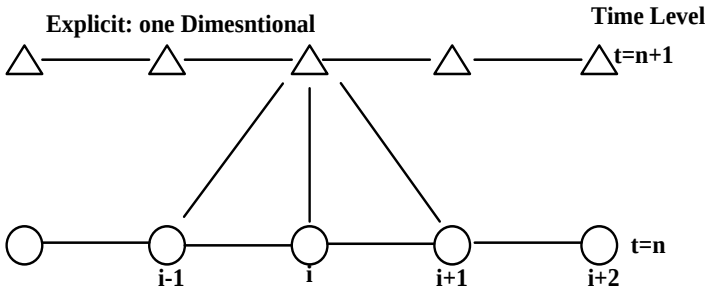

Figure: 4.1 Explicit difference schemes

On the other hand, all the new values are calculated simultaneously for a given time in the implicit scheme as shown in Figure 4.2. The implicit scheme involves the solutions of an $N\,x\,N$ system of simultaneous linear equations. The value of P at $n+1^{th}$ time step and n^{th} time step is solved simultaneously for ID fluid flow equation using implicit method as

$$\frac{P_i^{n+1} - P_i^n}{\Delta t} = \frac{P_{i+1}^{n+1} - 2P_i^{n+1} + P_{i-1}^{n+1}}{\Delta x^2} \tag{4.39}$$

In Eq. 4.39, time derivative is transformed by backward difference and 2^{nd} order central difference transforms the pressure derivative for finite differentiation approximation of PDE.

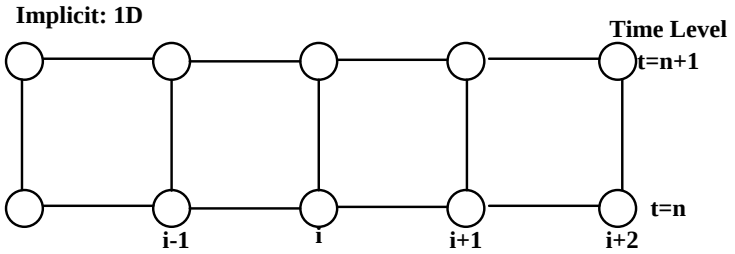

Figure 4.2 Implicit difference schemes

Implicit formulations are unconditionally stable but it may require large computational time while in case of explicit method it may be unstable and are solved for small time step. Some of the other solution procedures to solve the simulator equations of the reservoir model are fully implicit or IMPIS (implicit pressure and implicit saturation method); IMPES (implicit pressure and explicit saturation method) and AIM (adaptive implicit method).The IMPIS method calculates the phase saturations implicitly using capillary pressure relations. IMPIS is very stable and efficient method suited for complex reservoir problems allowing large timestep

simulation studies. IMPES method solves the pressure equations implicitly for the pressure distribution and saturations distributions are calculated explicitly for each point. The IMPES method may become quite unstable for large time step and hence less efficient as compared to the IMPIS procedure and is most suited for less complicated reservoir problems. The IMPES method is simpler and faster than the IMPIS method and is applied for small time step simulations. The AIM combines the advantages of both IMPIS and IMPES methods, to calculate saturation and pressure distribution. In several cases, grid cells in the difficult regions, which are limited in number are solved using IMPIS method, and for simpler region, IMPES method can be used. The execution time required for simulation using AIM is larger than the IMPES and smaller than the IMPIS method, hence one can save the computational times from one third to one half.

The linear equations resulting from finite difference transformation solved using matrix methods. The matrix has a tri-diagonal form: there are three diagonal elements; all other elements are zero. The set of simultaneous equations (Eq 4.37) for single phase can be written in triangular matrix notation as

$$\begin{bmatrix} & c & \\ b & & \\ a & & \end{bmatrix} * \begin{bmatrix} P \end{bmatrix} = \begin{bmatrix} d \end{bmatrix} \qquad (4.40)$$

The system of equations are solved for unknown pressure and saturations over time over the entire reservoir. The finite difference equations are formulated to solve for the dependent parameters over the gridded domain. The spatial domain (area of reservoir) is superimposed by some type of grid which splits the space into number of grids, cells or blocks. These grids are usually block centered or lattice type at which the dependent parameters are calculated. The spatial properties such as porosity, permeability need to be defined for each grid block in the domain. The dynamic properties; relative permeability, transmissibility, water saturations PVT properties are described such that equations can be solved numerically. Additionally, the fault locations, oil-water interface etc., need to be specified to find appropriate solutions.

4.3 RESERVOIR SIMULATOR DESCRIPTION

There are many commercial numerical simulators available for modeling flow behavior of multiple phase fluids in porous medium. The simulation software used in this study is CMG® (Computer Modeling Group Limited, Calgary). The reservoir simulation model was constructed using CMG Builder® module by providing the available rock and fluid data. In the present study, black-oil model is assumed to be applicable and therefore, CMG's black oil simulator called IMEX™ is utilized for simulation studies. Adaptive Implicit Method (AIM) was used for solving the simultaneous flow equations, although IMEX™ provide facility to execute in IMPES and IMPIS also. In CMG® IMEX™, AIM is set as the default mode.

In this study, two distinct reservoirs were used for history matching. The first reservoir (Case#3) is a two phase (oil and gas), two dimensional synthetic reservoir, taken from 10th SPE Comparative Solution Project. The second reservoir (Case#4) is a real 3D reservoir with all the three phases (oil, gas and water) flowing simultaneously. For both cases it was assumed that porosity distribution was fairly well established and known throughout the reservoirs. The relative permeability parameters were also taken to be known to keep the dimensions of the problem within manageable limits. The only parameter to be calculated for each grid block was the permeability which was focused in the least square sense by minimizing the sum of square of the error between field measured flow and the model calculated flow. Genetic algorithm was used for solving the optimization problem**.**

CHAPTER- 5

HISTORY MATCHING USING GENETIC ALGORITHM:

2D SYNTHETIC RESERVOIR

5.1 INTRODUCTION

History matching seeks to generate the geological models that are reasonably customized to available static (e.g., permeability; porosity etc) and dynamic (e.g., reservoir pressure; fluid production; injection data etc) parameters of the reservoir. Estimating the reservoir rock properties that provide a realistic history matched model is really an exhaustive work for reservoir engineers. The non-linear nature of the parameters and high dimensionality of the reservoir model makes this task complex. Generally, reservoir history matching is considered to be an inverse problem, where one seeks to back calculate system parameters from given system output. In the normal modeling exercise, the system parameters are known and our aim is to develop appropriate relationships so as to be able to predict system performance. In history matching, the reservoir production data are available but the reservoir static parameters (permeabilities and porosities) are unknown which need to be estimated. The spatial variation of these properties due to rock heterogeneity makes it an ill-posed problem since a very large number of permeability maps may lead to the same output, where most of these may be unrealistic. There are many stochastic soft computing techniques available to solve this inverse problem. In this thesis, an evolutionary optimization technique, called the genetic algorithm (GA) has been employed to solve the history matching problem. This optimization technique usually involves minimizing the objective function that describes the mismatch between the available field historical data and reservoir simulator response. The simulator used was the CMG® - IMEX™ algorithm from Computer Modeling Group LTD (Calgary, Canada) in the present work. Black-oil model was used which assumes the oil composition to remain constant with time. A simple GA (SGA) and an adaptive genetic algorithm (AGA) have been employed in this work under Case#3.a and

Case#3.b. The methodology was tested and validated by solving the history matching problem of a synthetic 2D reservoir (Chitralekha, et al., 2010). This algorithm was applied to a small real 3D, reservoir. The history matched model was, then, used for reservoir production forecasting. A comparison between the results from simple genetic algorithm (SGA) and adaptive genetic algorithm (AGA) in terms of their computational efficiency has been illustrated in this chapter.

5.2 GENETIC ALGORITHM

Genetic algorithm is one of the most popular and robust, stochastic search technique available for solving optimization problems. The technique resides on the Darwin's principles of evolution theory. The following sections in the text describe the theoretical aspects of a simple genetic algorithm and an adaptive genetic algorithm used for reservoir history matching problem solution.

5.2.1 Theoretical Aspects of GA/ SGA

The GA or simple genetic algorithm (SGA) utilizes the computer logic to mimic the mechanism of natural selection and natural genetics. The concept of GA was envisaged by Professor John Holland of University of Michigan in 1975 (Holland, (1975). The procedure starts with a set of several initial solutions called the initial population within the problem constraints. Each solution of the population is called chromosome. These chromosomes evolve through consecutive iterations called generations based on the principles of natural selection, inheritance, crossover and mutation operations to generate new chromosomes, which have better fitness values as compared to the previous population. During each iteration, the chromosomes are evaluated based on their fitness to survive to next generation. The fitness of the chromosomes are analyzed through an objective function called the fitness function that characterizes the performance of individual chromosomes in the search space. The superior the fitness value of a chromosome, greater the chances of it being selected to the next generation. Some parents and the offspring chromosomes may get rejected to maintain a fixed population size during generations. The algorithm converges to the best set of chromosomes after numerous iterations, which is considered as the potential set of solutions to the problem.

As mentioned earlier, the SGA method utilizes mainly three operators; selection, crossover (recombination) and mutation. The chromosomes which are selected from the population according to their fitness value, given by the objective function, are recombined through crossover and mutation operators to produce the next generation chromosomes. The performance of genetic algorithm is mainly powered by crossover and mutation operators. The crossover operator induces a randomized exchange of genetic material between a pair of chromosomes with an assumption that the good chromosomes produce better ones that are fitter closer to optimal solution. It is not essential that all the chromosomes in the population undergo crossover, few of them remain unchanged. The crossover operation is carried out with a probability, called crossover probability or crossover rate (P_c) on the chromosomes selected for recombination. The optimal values for P_c reported in literature ranges between 0.5 ~ 1.00 for SGA, which is usually predefined by the user. Some of the established crossover operators are; single point, two point, k-point crossover, uniform crossover operation etc. Further, the chromosomes are subjected to mutation operation with a probability, called the mutation probability or mutation rate (P_m). Usually, the P_m ranges between 0.001 ~ 0.05 for SGA. During mutation, the genetic material of chromosomes get modified to maintain genetic diversity. The mutation operation helps to recall the lost or uncharted genetic materials into the population, in order to avoid early convergence to local optimum solutions. Swap mutation, arithmetic mutation, jump mutation, uniform mutation and creep mutation are some of the well-known mutation operators. There are several publications available in the literature that describe various recombination operators used for GA process (Goldberg, 1989, Eiben and Smith, 2003; Schmitt, 2004; Sivanandam and Deepa, 2007; Picek, et al., 2012). This process of GA continues with the newly generated offsprings until a termination criterion is satisfied. More detailed description and mathematics of genetic algorithm can be found in the books of Goldberg, (1989); Deb, (1998) and from other GA literatures. The pseudo- code representation of simple genetic algorithm is presented in Figure 5.1.

```
Start
{
Initialize the population that has randomized solutions represented by chromosomes;
Evaluate population for its fitness;
While conditions not satisfied Do
        {
        Select chromosomes from population;
        Execute crossover and mutation operation;
        Evaluate population;
        Select chromosomes for next population;
        }
}
```

Figure 5.1 Pseudo-code for simple genetic algorithm

The foremost parameters that control the performance and progress of SGA are P_c and $P_{m.}$. Determining the values of P_c and P_m is a crucial step, and there are no definite rules for choosing suitable values. In fact, the choice of optimal values for P_c and P_m depend on the problem under consideration (Srinivas and Patnaik, 1994). Various studies detailing the effect of P_c and P_m on the performance of GA have been attempted (De Jong, 1988; Grefenstette, 1986; Schaffer and Morishma, 1987; Goldberg, 1989; Eiben, et al., 1999); Herrera and Lozano, (2003); Fernandez-Prieto, et al., 2010), and can serve as guide for choosing optimal values for P_c and $P_{m.}$.

The choice of inappropriate values for P_c and P_m provoke imbalance in GA's exploration and exploitation process. This discrepancy may lead to premature convergence that has major effect on GA performance. Since there exists a complex relationship between the GA performance and the control parameters, selecting robust control parameter values is a nontrivial task (Herrera and Lozano, 2003). For instance, a higher value of P_c rapidly introduces new solutions into population, which may disrupt the optimal solutions. Increased value of P_m completely transforms GA into purely randomized search algorithm. At the same time, a small mutation is necessary to prevent premature convergence of GA. Moreover, different sets of control parameters are required during evolutionary process of GA to maintain balanced

exploration and exploitation process, as different control parameters sets might be optimal at different phases of the GA process (Fernandez-Prieto, et al., 2010).

The simple genetic algorithm employed in this work utilizes tournament selection operator for selecting the fittest solutions from the population to the mating pool. The uniform crossover operation and uniform mutation operations were utilized for the present study. Two chromosomes are combined to form two new chromosomes during recombination.

In order to improve the performance of simple genetic algorithm and to lessen the burden of specifying the parameters values, adaptive operators were introduced. The adaptation of the values of genetic operators during the course of optimization has been investigated by Schaffer and Morishma, (1987); Whitley and Starkweather, (1990); Srinivas and Patnaik, (1994), and named as adaptive genetic algorithm (AGA). AGA has the ability to adjust the selected control parameters or the genetic operators dynamically during the evolution process so as to reach the optimal solutions in fewer iterations.

5.2.2 Adaptive Genetic Algorithm (AGA)

The adaptive genetic algorithm is an improved form of simple genetic algorithm in the sense that for AGA, the crossover and mutation probabilities are adjusted by the algorithm at each generation. The main difference between SGA and AGA is that, while the values of control parameters; P_c and P_m are predefined and remain constant for entire generations for SGA, in case of AGA, the initially assigned values of P_c and P_m are allowed to change adaptively according to the fitness function response of the solution generated in the subsequent generations. The design of AGA proposed by Srinivas and Patnaik, (1994), adaptively tune the crossover and mutation probabilities between the maximum fitness and the average fitness value of the population to the fitness of the individual solution. In their design, the individual solutions with sub-average fitness are completely removed while retaining the high fitness solutions. This leads the algorithm to get stuck at local optimum solutions. Moreover, tuning P_c and P_m based on individual fitness solutions require large computation time (Wang and Shen, 2001). Several researchers Wang and Shen, (2001); Fernandez-Prieto, et al., (2010); Wang and Tang, (2011); Tang, (2012) have

subsequently improvised the adaptation mechanism leading in more efficient AGA algorithms.

In the present work, an adaptive genetic algorithm was employed for history matching of petroleum reservoir by tuning the P_c and P_m according to the fitness of whole population during evolution rather than of individual solution fitness (Wang and Tang, 2011). The following section describes the AGA methodology employed in this work.

5.2.3 Details of Adaptive Genetic Algorithm

This section describes the structure and design of a real coded GA algorithm that incorporates adaptivity in the genetic operators. The objective function, selection mechanism, formulation of adaptive operators used in the study are detailed here.

5.2.3.1 Objective Function: The objective of history matching is to find those static parameters of the reservoir which minimizes the error between field observations and simulator predictions. In reservoir history matching, the objective function (Q) represents the minimization problem that minimizes the square of difference between the field historic production data with simulator response. As history matching is a minimization problem, the most fit model has the lowest numerical value associated with the objective function. Since the GA code is written for minimization as fitness function, in the present case, objective function is same as fitness function. In general, the formulation of objective function used to find the optimal history matched models expressed as

$$Q = \sum_{i}^{n_p} \sum_{j}^{n_w} \sum_{k}^{n_t} \left(\frac{d_{ijk}^{O} - d_{ijk}^{S}}{d_{ijk}^{O}} \right)^2 \tag{5.1}$$

where, Q denotes the objective function, d^O is the observed data such as fluid production and injection rates; bottom hole flowing pressure etc; d^S is the corresponding simulator (CMG®)- IMEX™ reservoir simulator) output. The summation indices $i, j, and\ k$ run over the production data types, number of wells and reported time steps with $n_p, n_w,$ and n_t being the corresponding number of samples. The optimization is carried over the static parameters (permeability and porosity) of the reservoir.

The objective function has been formulated based on the objectives of the case studies. For the 2D synthetic reservoir history matching problem (see section 5.4 for details), the objective function includes the quarterly oil and gas production data from one producing well. Hence, $n_p = 2$; $n_w = 1$; and $n_t = 32$ quarters over which data are available.

5.2.3.2 Selection Mechanism: Selection or the reproduction operator selects the solutions from the population based on their fitness. A popular selection operator called the tournament selection has been applied in this work. The fitness of the solution represented by the objective function is calculated using Eq. 5.1. The string with a lower fitness value has greater chance of being copied in the mating pool compared to the string with a higher fitness value. Strings with low fitness values may be copied more than once, whereas strings with high values may be left out thus leading to a pool of strings (chromosomes) with improved overall fitness but of the same size of population.

5.2.3.3 Adaptive Crossover Operator (P_c): Crossover operation facilitates the transferring of genetic material between the individuals in the population. In this work, adaptive crossover operation has been designed to deal with the initial realizations of the reservoir. The breeding of two chromosomes from the population based on the crossover rate and chromosome length have been utilized to generate new chromosomes. The newly generated population inherits the properties of their parent population.

The rate at which the solutions are subjected to crossover operations is controlled by crossover probability P_c. The formulation of P_c is mathematically expressed as

$$P_c = P_c^0 \left[1 + \xi \quad \frac{\left(f_{avg}\right)^{\eta}}{(f_{max} - f_{min})^{\eta} + \left(f_{avg}\right)^{\eta}} \right] \tag{5.2}$$

where, ξ and η are the coefficient factors; P_c^0 and P_c are the initial crossover probability and adaptive crossover probability. f_{avg} ; f_{min}; and f_{max} denote the average fitness, minimum fitness, and maximum fitness of the population in each generation respectively. The adaptive crossover operation implemented in this work is described in the following text.

Let, R be a randomly generated positive number (0 ~ 1), L_c be the length of the chromosome, and P_c be the crossover probability for i^{th} generation, K_c is the number of locations in the chromosome that undergoes crossover. K_c is computed by multiplying length of the chromosome; L_c, by the crossover probability; P_c for the corresponding i^{th} generation. This is mathematically represented as

$$K_c = L_c \times P_c \tag{5.3}$$

Another random number between (0, $L_c - 1$) is generated K_c times to find cross-site randomly. Crossover is performed at any K^{th} location, if R_1 and $R_2 > R$, where R_1 and R_2 are two more random numbers (0~ 1) corresponding to the K^{th} location. For example, if $L_c = 100$; $P_c = 0.5$; then the corresponding number of crossover locations; $K_c = 50$. Figure. 5.2 illustrates an example of crossover operation implemented in this study. Let R be 0.4 and R_1 and R_2 as given in the figure corresponding to the locations of crossover for the two strings C_1 and C_2 participating in this operations. Figure 5.2 shows gene values of only crossover sites. Now check each of these locations, one at a time and affect a crossover of gene values if both R_1 and R_2 are greater than R (=0.4). The first crossover site (from the right) has $R_1 = 0.78$ and $R_2 = 0.41$. Since both are greater than 0.4, the crossover takes place and 72 and 8 from C_1 and C_2 are crossed in the new strings N_1 and N_2. This process is continued for the remaining 49 locations to complete the operation between C_1 and C_2. For the adaptive crossover operation presented here, the number of locations for crossover is controlled by the adaptive crossover probability (P_c) generated at each generation. As the value of P_c increases the number of locations (K_c) for crossover also increases.

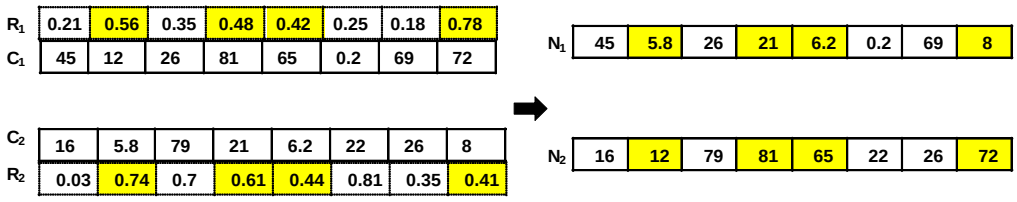

Figure 5.2 Example of adaptive crossover operation

Generation of new chromosomes because of the crossover operation increases the pool size and hence the population is doubled. One simple way to keep the population fixed is to discard all the parents and use only children in the new pool. However, a

preferred way is what is known as "elitism" in which the chromosome with lower fitness values are retained, be they from parents or from children and the rest are discarded keeping the population size constant.

5.2.3.4 Adaptive Mutation Operator (P_m): The function of mutation operator is to maintain genetic diversity by introducing new genes randomly in the chromosomes. The rate at which the chromosomes are subjected to the mutation operation is controlled by the mutation probability (P_m). Mathematically, the calculation of P_m at each iteration, is done according to,

$$P_m = P_m^0 \left[1 + \omega \quad \frac{(f_{max} - f_{min})^{\eta} - \left(f_{avg}\right)^{\eta}}{\psi\,(f_{max} - f_{min})^{\eta} + \left(f_{avg}\right)^{\eta}} \right] \tag{5.4}$$

where

$$\psi = \left(\frac{f_{max} - f_{min}}{f_{avg}} \right)^{\eta} \tag{5.5}$$

where, ω and η are the coefficient factors, P_m and P_m^0 represent the adaptive mutation probability and initial mutation probability respectively, f_{avg}; f_{min}; and f_{max} denote the average, minimum and maximum fitness of the population in each generation.

If L_c is the length of the chromosome, P_m is the mutation probability at the ith generation and K_m is the number of locations in the chromosome that undergo mutation, then K_m is calculated as,

$$K_m = L_c \times P_m \tag{5.6}$$

A random number $(0,\ L_c - 1)$ is generated K_m times to locate the mutation sites. Then the mutation operator adds a randomly generated number $(0,\ 1)$ to gene value at the mutation site of the chromosome. The number of location in the chromosome for mutation increases with the increase in adaptive mutation probability.

The genetic algorithm is terminated at a specified number of generations. Then the quality of population is checked against the problem definition else the process continues until achieving a satisfactory solution.

5.3 WORKFLOW OF GENETIC ALGORITHM

Figure 5.3 shows the workflow of the methodology adopted for history matching. SGA and AGA codes were developed in MATLAB® environment for minimization. The code is available in Appendix-B. The GA code was interfaced with the CMG®- IMEX™ reservoir simulator for forward simulations. The program initializes with a set of initial realizations of reservoir generated from geostatistical software (see next section for details). The fitness values of the initial chromosomes (set of initial solutions) are calculated using the CMG® simulator along with Eq. 5.1. The initial population passes through the GA operators (selection, crossover and mutation). The selection operator selects the chromosomes to mating pool based on their fitness. The fitness of the realization is represented by objective function and is calculated by Eq.5.1. In fact, the objective function provides how good each realization is and honors the field historical data. The calculation of objective function of a realization comprises of one forward simulation by reservoir simulator. Hence, the number of forward simulations increase with number of realizations and the iterations. The selected realizations undergo crossover operations based on crossover probability given by Eq. 5.2 and followed by mutation operations based on mutation probability given by Eq. 5.4 and 5.5, to generate new reservoir realizations.

While carrying out GA operations, it is necessary to recognize that the static parameters at well locations are observed values and hence cannot be allowed to change. This means that the permeabilities and porosities of the grid blocks which coincide with well locations should not take part in crossover and mutation operations. The value of chromosomes at well locations remain constant throughout the procedure. This completes one generation by the algorithm, and the process continues until satisfactory realizations are generated that represents the good history matched models.

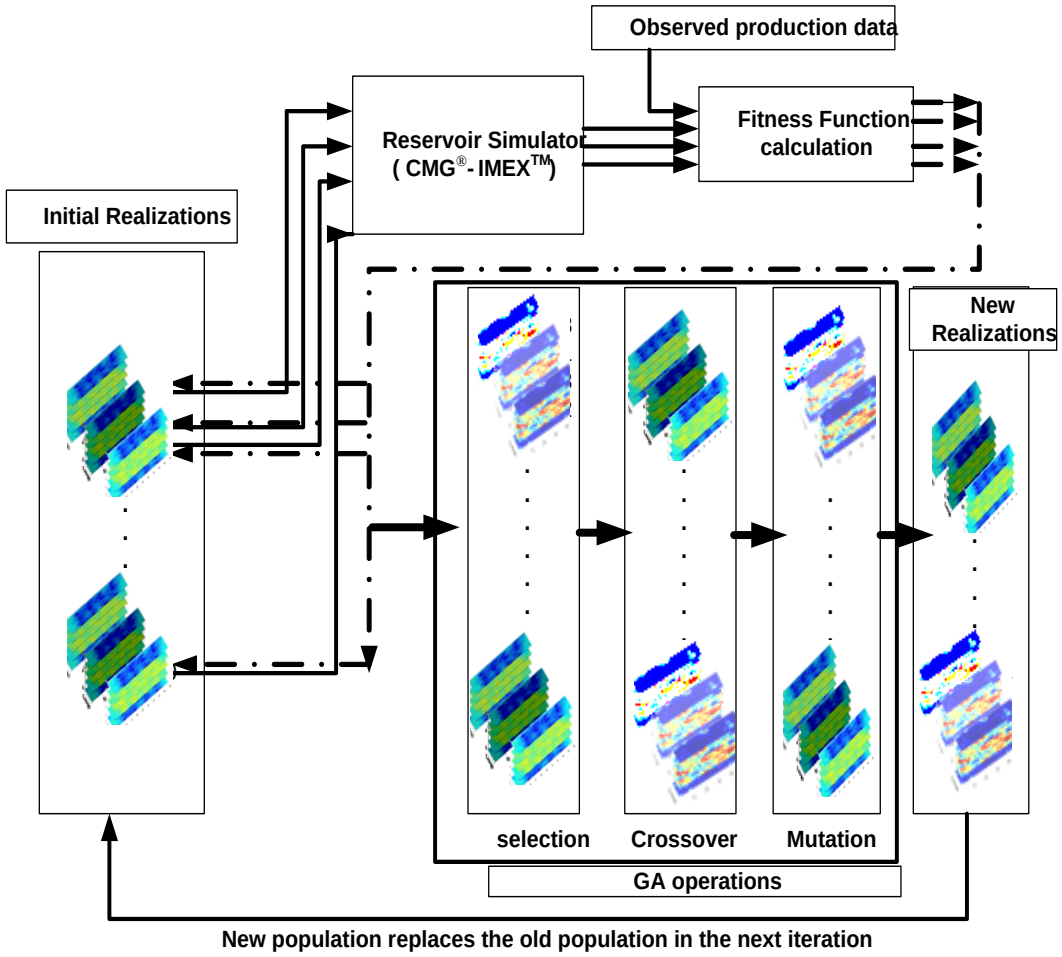

Figure 5.3 Workflow of genetic algorithm

5.3.1 Initial Population Generation

An approximate set of solutions, called the initial population are utilized to initialize the genetic algorithm. In history matching context, the populations represent the reservoir realizations or the ensembles, which contains the reservoir rock properties such as permeability and porosity etc. In order to generate initial population or the initial ensembles, geostatistical methods (Deutsch and Journel, 1998; Deutsch, 2002) are used. Several authors have reported the use of geostatistical methods in generating the initial ensembles that represent the prior knowledge of the distribution of static variables (permeability and porosity). These realizations are conditioned to honor the spatial correlation and variogram of the reservoir properties. A geostatistical method called, stochastic conditional simulation is used to generate the multiple equiprobable descriptions of reservoir parameters. The method is stochastic and conditional as the reservoir properties are generated by hybrid method which is

partially deterministic and partially random. The generated reservoir realizations honor the observations at the well locations (Romero and Carter, 2001).

The initial realizations that are conditioned to available measurements from the well locations are generated by employing the algorithms presented in the geostatistical toolbox of MATLAB®, 'mGstat'. In the present case study the initial realizations were generated using GSLIB's VSIM and SGeMS geostatistical software packages using the 'mGstat' interface of MATLAB®.

5.3.2 Inputs to the CMG® Simulator

Reservoir simulation model is build by integrating; geological model which describes the structure of the reservoir, area, shaliness, gross- thickness, reservoir rock properties (geostatistical properties) such as porosity and permeability distribution maps etc., description of simulation grid, fluid model (PVT properties), rock fluid model (relative permeability, saturation), fluid contact, faulting, aquifer modeling, production and completion history.

5.3.2.1. Geological Model: A proper geological framework should be planned before building a reservoir simulation model. The framework consists of sandstone gross-thickness map which establishes the reservoir bulk volume, structure maps that provides the orientation and extension of sedimentary bodies, net-pay thicknesses depth of fluid contacts, values of porosity and permeability obtained from core analysis, pressure-transient testing etc. The distributions of porosity and permeability map prepared by geostatistical software package that incorporates core log and 3D seismic data in a consistent and realistic manner.

5.3.2.2 Grid Selection: The reservoir under investigation is divided into grid blocks for ease of computations using numerical integration of flow equations embedded in the CMG® software. These grid blocks can be two or three-dimensional and grid type can be variable depth and thickness Cartesian, radial or cylindrical, orthogonal corner point, and non-orthogonal corner point grids depending on the reservoir. The size of each grid block depends on the size of the reservoir. A larger number of grid blocks (or smaller size of each grid block) makes the algorithm slower by increasing computational load. On the other hand, if the physical size of each grid block is too

large, then the results become less accurate since it is assumed that throughout a single grid block, permeability and porosity (static parameters) are uniform. Grid selection is, therefore, problem dependent, and will, therefore, be discussed separately for the case studies investigated.

5.3.2.3 Faulting: An important factor influencing the reservoir behavior is the distribution of faults within the reservoir. The fault affects the petrophysical properties of the fault rock and modify the connectivity in sedimentological flow units. The location of the fault in the reservoir is obtained from geological analysis. The effect of fault transmissibility such as sealing or non-sealing fault, must be inferred from special pressure testing (pulse and interference testing), analysis of production data, field pressure survey.

5.4 HISTORY MATCHING OF A 2D SYNTHETIC RESERVOIR (CASE#3)

Before embarking on a meaningful real field problem, it is important to validate the GA code, the problem formulation for history matching and the proposed scheme and, methodology of history matching. For this purpose, a 2D synthetic reservoir problem was chosen (Chitralekha, et al., 2010). The authors used Ensemble Kalman Filter for 2D synthetic history matching problem. Since the synthetic reservoir construction started with known permeability distribution, the problem suited our purpose well. The true permeability map is shown in Figure 5.4.

5.4.1 The 2D Synthetic Reservoir under Study

The synthetic reservoir presented here was taken from Chitralekha, et al., 2010), which is a modified model of 10th SPE Comparative Solution project (Christie and Blunt, 2001). The synthetic black oil reservoir is a simple 2-phase, 2D model consisting of 20 layers discretized in a Cartesian coordinate system. The reservoir model is discretized into 100 x 1 x 20 grid blocks, in which each grid block measures 25ft x 25ft. The phases present in the reservoir are oil and gas. The reservoir model is considered to be fully saturated by oil initially (no connate water). There is no fault presence in the reservoir. There are 2 producers (Well-1 and Well-2) that are placed symmetrically on either side of 1 injector (I-1), which is located at the center of the reservoir (grid block, (50,1,1)). Wells, Well-1; Well-2 and I-1 are perforated through

all the 20 layers of the model reservoir. Figure 5.4, shows the aerial view of the 2D, 2-phase, heterogeneous black oil reservoir model. The reservoir has a constant porosity of 0.2 throughout all the layers with varying permeabilities in i direction (see Figure 5.5). The permeabilities in j and k directions are set equal to permeability values in i direction. In addition, two core holes are considered to be drilled vertically through all layers and are located at grid block locations (25, 1) and (75, 1). The permeability values at the wells and core hole locations are assumed to be known. The problem is to find the permeability in reminder of the 2000 grid blocks so as to match the known fluid production history.

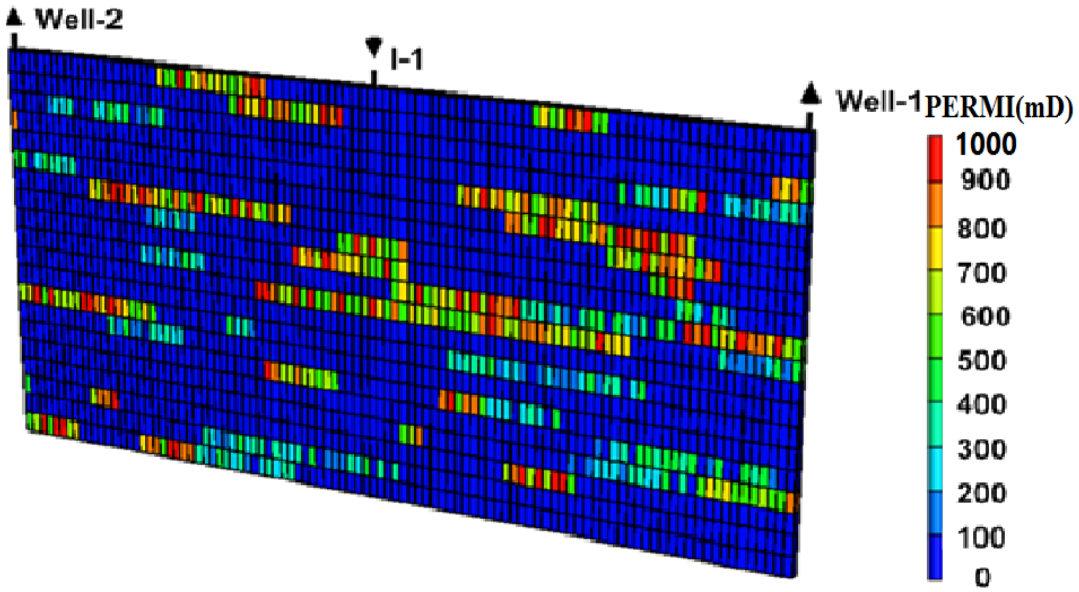

Figure 5.4. 2D heterogeneous black oil reservoir model with 2 producing wells and 1 injector well

5.4.2 Selection of GA Parameters

A 2D synthetic black-oil reservoir model history matching problem has been used for initial testing of the simple genetic algorithm (SGA) and adaptive genetic algorithm (AGA). The standard genetic operators such as reproduction, recombination and mutation operators were employed in this study.

The genetic operators for SGA are; the tournament selection as the selection or reproduction operator for selecting the fittest member from the population to the mating pool. The crossover operation in the chromosomes are carried out by uniform k-point crossover. The mutation process in the chromosomes are induced by uniform

mutation operator to generate new population. The probabilities of control parameters for testing the SGA algorithm was assigned with crossover probability; $P_c = 0.5$ and mutation probability; P_m= 0.001 and 0.005, to produce optimal solutions for 2D synthetic history matching problem.

The AGA methodology used the same three operators as used with SGA. However, the crossover and mutation probabilities were updated in every generation. The AGA for synthetic case study was assigned with initial crossover probability $P_c^0 = 0.5$ and initial mutation probability $P_m^0 = 0.001$ and 0.005 after several investigations. For calculating the adaptive crossover (P_c) and adaptive mutation probability (P_m) according to Eq. 5.2 and 5.4, and 5.5, the coefficient factors were preferred as; ξ = 0.02, ω = 0.02 and η = 0.05.

5.4.3 Input to CMG® Simulator for Case#3

Reservoir model properties

Initial reservoir Pressure	100 psia
Datum Depth	0.0 ft
Porosity	0.2

PVT properties

The pressure-volume-temperature data for the synthetic reservoir are given below. The fluids are assumed to be incompressible and immiscible.

Initial Reservoir Pressure	100 psia
Oil density	43.68 lb/ft^3
Gas density	0.0624 lb/ft^3
Oil Viscosity	1 cp
Gas Viscosity	0.01 cp

5.4.4 Grid Selection for 2D Reservoir

A two dimensional grid, 100 x 20 was imposed on the reservoir which divided it in 2000 grid blocks measure of 25ft x 25ft. The porosity was constant throughout the reservoir. This meant that history matching exercise required to estimate only

permeability for each of the grid blocks given oil and gas production history. Clearly, GA formulation will lead to chromosomes of string length 2000, each element representing unknown permeability of each grid block with the exception that at the well location, the permeability is known and must not be allowed to change during GA operations. A population size of 40 was chosen and hence 40 initial realizations were generated using conditional direct simulation in VISIM geostatistical software. Figure 5.6 shows the initial realization generated using VISIM.

5.4.5 Generation of Initial Population

Conditional direct sequential simulation of VISIM geostatistical software was utilized to generate a population size of 40 initial realizations for 2D synthetic reservoir. The simulation of these realizations are conditioned to the well location and core hole data. The plausible variogram for generating realization is anisotropic variogram with a maximum correlation range of 75 grid blocks in x direction. The grid blocks of the reservoir were populated using known permeability values, which are assumed to be the true. The production data obtained from simulating the true reservoir is considered as the field historic data for history matching. The grid blocks permeability distribution of 2D heterogeneous reservoir in x direction, which is assumed to be true is shown in Figure 5.5. Figure 5.6 shows the initial realizations of permeability for 2D reservoir generated using VSIM.

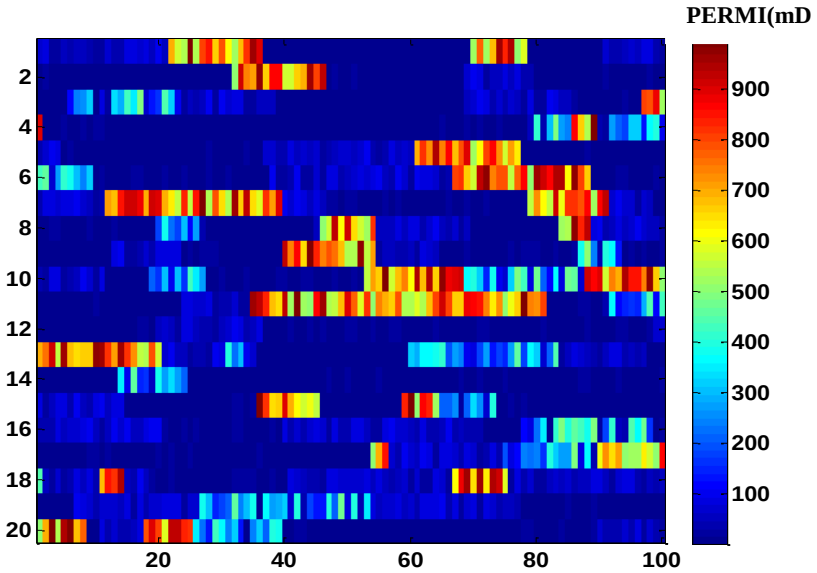

Figure 5.5 True grid block permeability distribution of 2D heterogeneous reservoir

The objective of this case study is to estimate the permeability values at each of the 2000 grid blocks of the reservoir that honours the geological description and production history of the field.

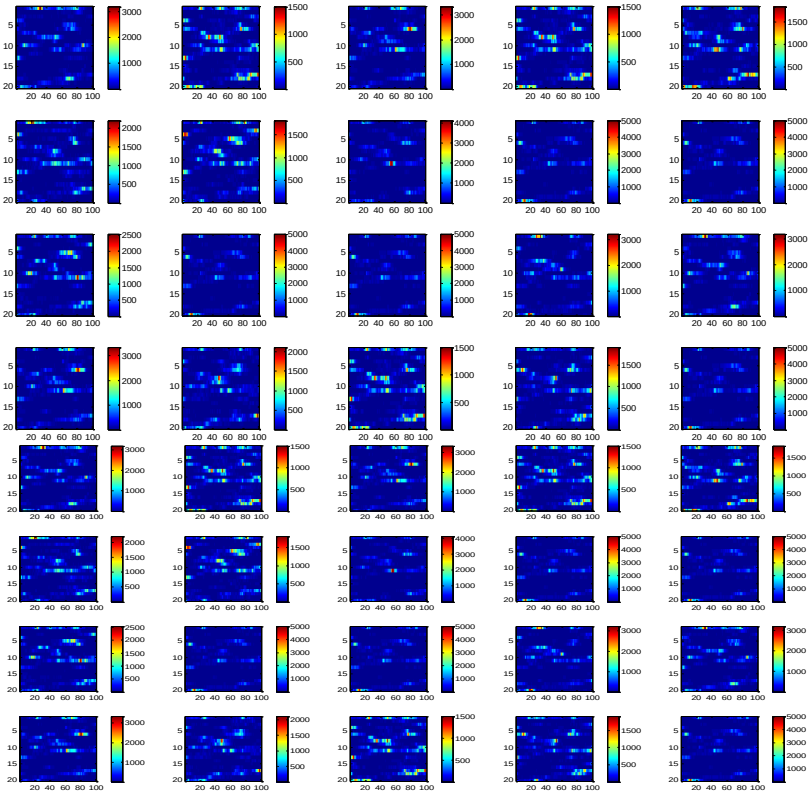

Figure 5.6 Initial permeability realizations (40 Nos.) of the model reservoir

5.4.6 Objective Function

The objective of the study is to produce valid history matched permeability map that is conditioned to the field observations and to prove the efficiency and robustness of the method towards history matching of petroleum reservoir. The results presented show a comparison between adaptive genetic algorithm (AGA) with the SGA for history matching of the 2D synthetic heterogeneous reservoir.

The formulation of objective function for history matching of synthetic reservoir aims to minimize the mismatch between the quarterly oil production (bbl/day) and gas production (ft^3/day) from Well-1and the simulator output. The objective function for the case study of 2D synthetic reservoir becomes;

$$Q = \sum_{k=1}^{32} \left(\frac{d_{k,oil}^{O} - d_{k,oil}^{S}}{d_{k,oil}^{O}} \right)_{Well-1}^{2} + \sum_{k=1}^{32} \left(\frac{d_{k,gas}^{O} - d_{k,gas}^{S}}{d_{k,gas}^{O}} \right)_{Well-1}^{2} \quad (5.7)$$

where, the $d_{k,oil}^{O}$ and $d_{k,gas}^{O}$ are the quarterly observed oil and gas production data; $d_{k,oil}^{S}$ and $d_{k,gas}^{S}$ denote the corresponding simulator predictions and k is the time period, that represents 8 years (or 32 quarters) production history. The best matched reservoir model is validated by checking the mismatch between the model predicted quarterly oil and gas production and the corresponding field data.

5.5 RESULTS AND DISCUSSION

Table 5.1 shows the objective function values of the initial realizations of the reservoir calculated using Eq. 5.7. The quarterly oil and gas productions from Well-1 from 40 initial realizations of the reservoir (before history matching) are shown in Figure 5.7.

Table 5.1 The value of objective function (Q) for the initial realizations of the reservoir

No: of Initial Realizations	Objective function	No: of Initial Realizations	Objective function
1	1.769	21	7.274
2	1.801	22	8.188
3	1.830	23	8.313
4	1.903	24	8.537
5	2.322	25	8.600
6	2.510	26	8.637
7	2.879	27	9.130
8	2.985	28	9.221
9	3.546	29	9.358
10	4.039	30	9.541
11	4.260	31	10.127
12	4.627	32	11.869
13	4.899	33	14.679
14	5.164	34	14.312
15	5.419	35	18.610
16	5.640	36	20.420
17	6.250	37	30.870
18	6.278	38	56.246
19	6.380	39	65.237
20	6.423	40	68.127

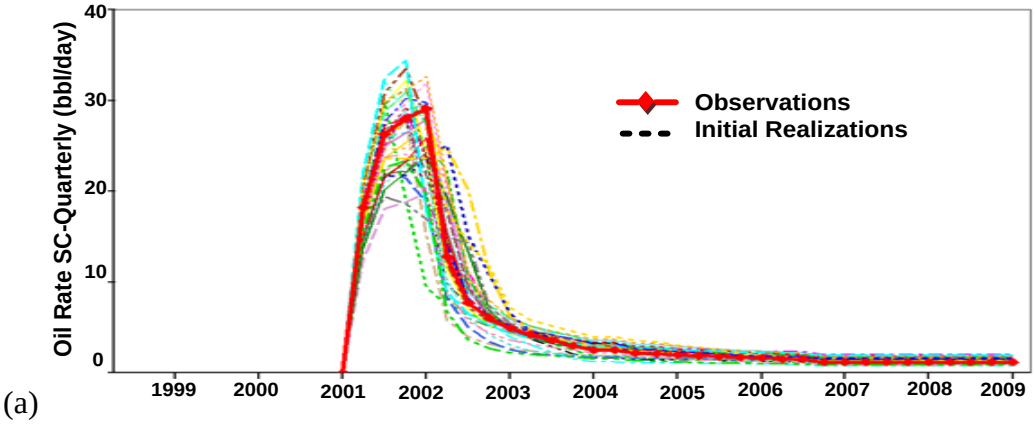

(a)

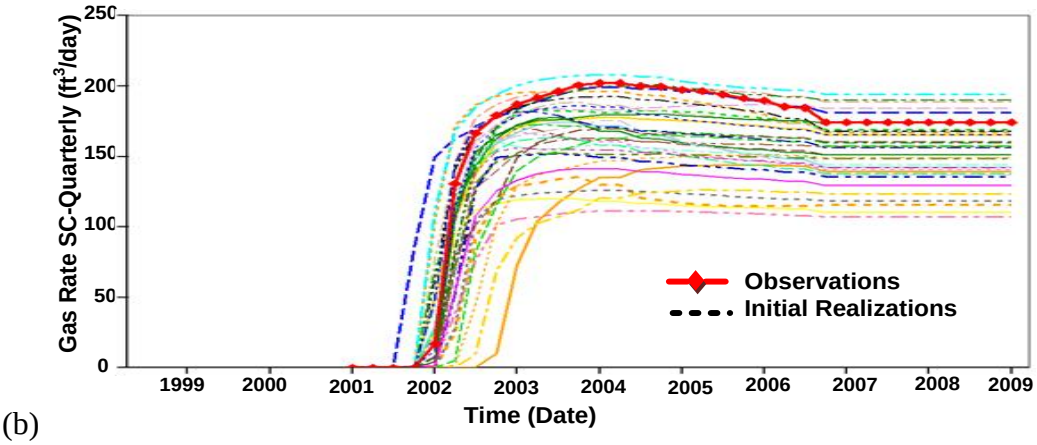

(b)

Figure 5.7 Quarterly production data from Well-1 for 40 initial realizations (a) oil production data (b) gas production data

5.5.1 Results from SGA for 2D synthetic reservoir (Case#3.a)

The algorithm has been tested for history matching using crossover probability of 0.5 and mutation probability of 0.001 and 0.005. Tables 5.2 and 5.3 show the results obtained from SGA for the two cases. From the tables, it is clear that the initial permeability realizations of the reservoir are moving towards the real map as number of iterations increases. The better history matched models have lower objective function values. It is assumed that all the realizations will converge to optimal solutions eventually with larger number of iterations. Figure 5.8 shows how average fitness of the population decreased with increasing number of iterations. Since the aim of the method is to acquire better history matched models, the best 10 realizations at 400^{th} iteration are plotted in Figure 5.9. The best history matched model from SGA is compared with the measured values of oil and gas production in Figure 5.10.

Table 5.2 The objective function (Q) evaluation of 40 reservoir realizations resulting from SGA with $P_c = 0.5$ and $P_m = 0.001$ after every 50 iterations

No: of Realizations	Iterations							
	Q_{50}	Q_{100}	Q_{150}	Q_{200}	Q_{250}	Q_{300}	Q_{350}	Q_{400}
1	1.723	1.638	1.636	1.477	1.347	1.126	0.877	0.832
2	2.138	2.015	2.001	1.928	1.576	1.738	1.306	1.127
3	2.357	2.312	2.385	2.220	1.905	1.890	1.883	1.145
4	2.510	2.793	2.638	2.511	2.510	2.985	2.510	2.430
5	2.977	2.985	3.520	2.985	2.985	3.203	2.746	2.821
6	2.985	3.112	4.174	3.314	3.788	4.031	2.985	2.960
7	3.081	3.924	4.224	3.440	4.123	4.053	4.244	2.985
8	3.949	4.056	4.341	3.508	4.467	4.265	4.378	3.541
9	4.024	4.208	4.627	3.652	4.499	4.627	4.412	3.875
10	4.468	4.212	4.783	4.260	4.627	4.742	4.627	3.904
11	4.627	4.627	5.024	4.627	4.672	5.365	5.061	4.236
12	5.069	4.833	5.043	4.845	4.971	5.599	5.239	4.627
13	5.126	4.886	5.365	5.049	5.193	5.640	5.365	4.734
14	5.365	5.365	5.599	5.163	5.269	5.641	5.599	4.993
15	5.469	5.405	5.640	5.365	5.365	5.859	5.618	5.204
16	5.599	5.599	5.647	5.599	5.493	6.134	5.640	5.365
17	5.614	5.640	6.134	5.640	5.599	6.460	5.903	5.599
18	5.640	6.134	6.478	6.066	5.640	6.478	6.134	5.640
19	6.134	6.314	6.488	6.134	6.134	6.842	6.478	5.648
20	6.459	6.478	6.842	6.149	6.478	7.039	6.842	6.083
21	6.478	6.724	8.091	6.478	6.842	7.050	6.860	6.134
22	7.644	6.842	8.327	6.609	7.526	7.319	6.928	6.478
23	7.842	7.300	8.475	6.842	8.537	7.971	7.771	6.842
24	8.321	8.088	8.537	6.842	8.874	8.436	8.010	7.403
25	8.535	8.537	8.719	8.537	8.958	8.537	8.122	7.645
26	8.537	8.958	8.958	8.646	8.965	8.697	8.238	7.856
27	9.730	9.221	9.221	8.958	9.066	8.958	8.537	8.537
28	9.958	10.068	9.435	9.221	9.221	9.221	8.734	8.958
29	10.127	10.127	9.832	10.127	10.127	10.127	8.958	9.221
30	10.869	10.869	10.127	10.869	10.869	10.869	9.221	9.336
31	10.954	11.468	10.852	10.870	12.206	11.596	10.127	9.675
32	11.366	12.225	10.869	11.717	12.225	12.225	10.827	10.127
33	13.225	12.789	11.884	12.225	12.789	12.776	10.869	10.869
34	14.752	12.976	12.225	12.789	12.976	12.789	11.015	12.225
35	14.789	13.246	12.789	12.976	13.246	12.976	12.225	12.789
36	18.976	13.959	12.976	13.246	13.959	13.179	12.323	12.976
37	23.246	15.703	13.246	13.959	14.089	13.246	12.789	13.246
38	30.959	17.773	13.959	15.160	14.464	13.959	12.976	13.959
39	62.156	64.124	50.655	15.616	15.867	19.818	13.246	19.818
40	68.013	66.148	60.517	56.166	46.680	23.355	23.355	23.355

Table 5.3 The objective function (Q) evaluation of 40 reservoir realizations resulting from SGA with $P_c = 0.5$ and $P_m = 0.005$ after every 50 iterations

No: of Realizations	Iterations							
	Q_{50}	Q_{100}	Q_{150}	Q_{200}	Q_{250}	Q_{300}	Q_{350}	Q_{400}
1	1.501	1.501	1.501	1.244	1.233	1.209	0.856	0.691
2	1.830	1.597	1.696	1.268	1.501	1.501	0.865	0.756
3	2.087	1.623	1.830	1.501	1.830	1.789	1.501	0.876
4	2.388	1.830	1.967	1.905	1.975	1.830	1.830	1.481
5	2.510	2.510	2.510	1.830	2.510	2.378	2.056	2.055
6	2.544	2.879	2.803	2.714	2.106	2.435	2.510	2.127
7	2.804	2.985	2.879	2.879	2.510	2.510	2.659	2.751
8	2.879	3.195	2.985	2.985	2.723	2.839	2.879	2.886
9	2.985	4.227	3.290	3.536	2.879	2.879	2.969	2.985
10	3.393	4.408	3.321	3.872	2.985	2.985	2.982	3.268
11	3.782	4.627	4.426	4.026	3.015	3.050	2.985	3.510
12	4.192	5.340	4.627	4.627	3.374	4.027	3.032	3.567
13	4.261	5.640	4.654	5.486	3.578	4.627	3.896	3.571
14	4.428	5.843	5.199	5.640	4.126	4.727	4.253	4.203
15	4.627	5.962	5.640	5.679	4.513	4.814	4.267	4.227
16	4.986	5.978	6.115	5.733	4.627	4.996	4.269	4.247
17	5.306	6.382	6.423	6.423	4.741	5.111	4.627	4.515
18	5.322	6.423	6.478	6.478	5.462	5.538	5.054	4.627
19	5.640	6.478	6.842	6.524	5.474	5.583	5.451	5.184
20	5.652	6.763	7.036	6.842	5.640	5.640	5.498	5.640
21	6.423	6.842	7.194	7.091	6.079	5.731	5.640	5.898
22	6.478	7.028	7.307	7.399	6.423	5.656	5.979	6.423
23	6.842	7.077	7.456	7.715	6.478	6.445	6.423	6.478
24	7.212	8.034	8.160	7.789	6.842	6.478	6.478	6.669
25	8.188	8.159	8.188	8.188	7.624	6.692	6.842	6.804
26	8.537	8.176	8.537	8.537	7.548	6.842	7.346	6.842
27	8.566	8.188	8.563	8.637	7.665	7.647	8.188	6.909
28	8.637	8.403	8.637	8.887	8.306	7.165	8.418	7.411
29	8.641	8.537	9.032	9.032	8.325	8.637	8.434	8.139
30	8.992	8.637	9.221	9.074	8.537	8.856	8.537	8.188
31	9.032	9.032	9.349	9.221	8.637	8.917	8.637	8.537
32	9.221	9.115	9.732	9.241	9.032	8.930	9.032	8.637
33	10.127	9.221	10.127	9.523	9.221	9.032	9.221	9.032
34	10.610	9.525	10.869	9.732	9.732	9.221	9.937	9.221
35	10.869	10.127	10.918	10.127	9.466	9.466	10.127	10.127
36	11.775	10.869	11.225	10.200	10.869	10.149	10.869	10.869
37	13.469	11.225	12.442	10.869	10.826	11.155	11.565	11.430
38	18.984	18.440	14.685	12.443	11.585	11.912	11.885	11.714
39	21.420	19.420	17.420	16.167	15.929	15.279	15.279	15.056
40	32.786	23.309	18.432	18.432	17.420	17.420	17.420	17.420

The objective function value of initial realizations reported in Table 5.1 are $Q_{min} = 1.77$, $Q_{max} = 68.12$ and $Q_{avg} = 12.01$. The SGA with crossover probability; $P_c = 0.5$ and mutation probability $P_m = 0.001$ produced the objective function values; $Q_{min} = 0.83$, $Q_{max} = 23.36$ and $Q_{avg} = 7.38$ at 400th iteration. The SGA with $P_c = 0.5\ and\ P_m = 0.005$, resulted $Q_{min} = 0.69$, $Q_{max} = 17.42$ and $Q_{avg} = 6.13$ after 400 iterations.

The average objective function values after every 50 iteration for SGA with $P_c = 0.5\ and\ P_m = 0.001$ and $P_c = 0.5\ and\ P_m = 0.005$ are presented in Figure 5.8 (a) and (b). The average objective function value for initial realization $Q_{avg} = 12.01$ have converged to $Q_{avg} = 7.38$ for SGA with $P_c = 0.5\ and\ P_m = 0.001$ at 400 iterations and $Q_{avg} = 6.13$ for SGA with $P_c = 0.5\ and\ P_m = 0.005$ at 400 iterations

(a)

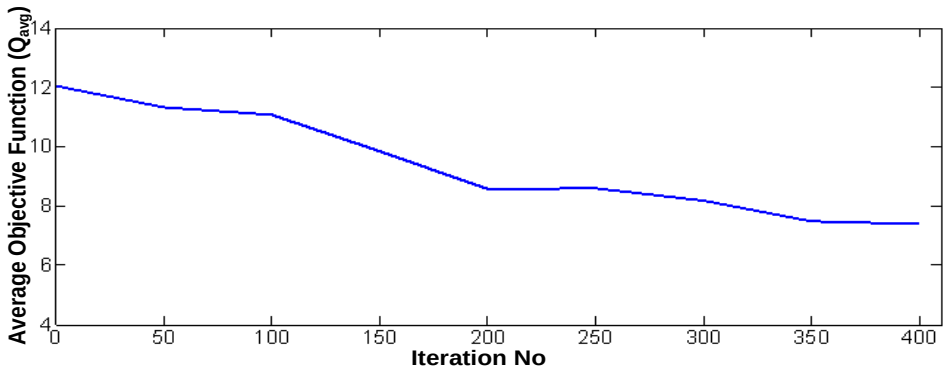

(b)

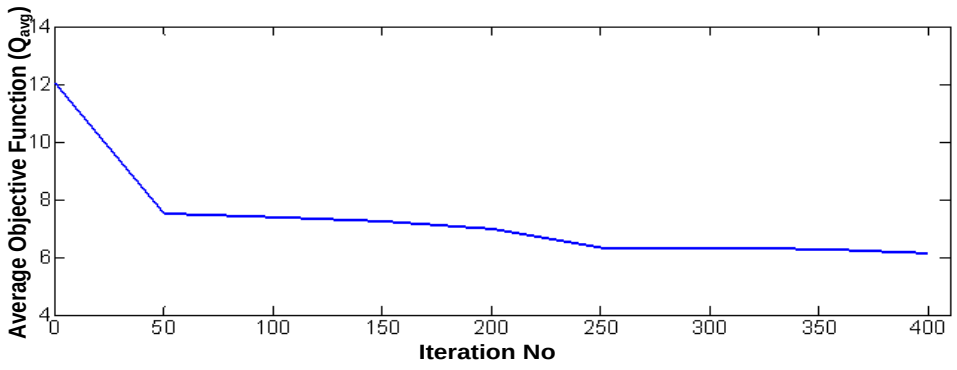

Figure 5.8 Average objective function value versus iteration number (every 50 iterations) (a) $P_c = 0.5\ and\ P_m = 0.001$ (b) $P_c = 0.5\ and\ P_m = 0.005$

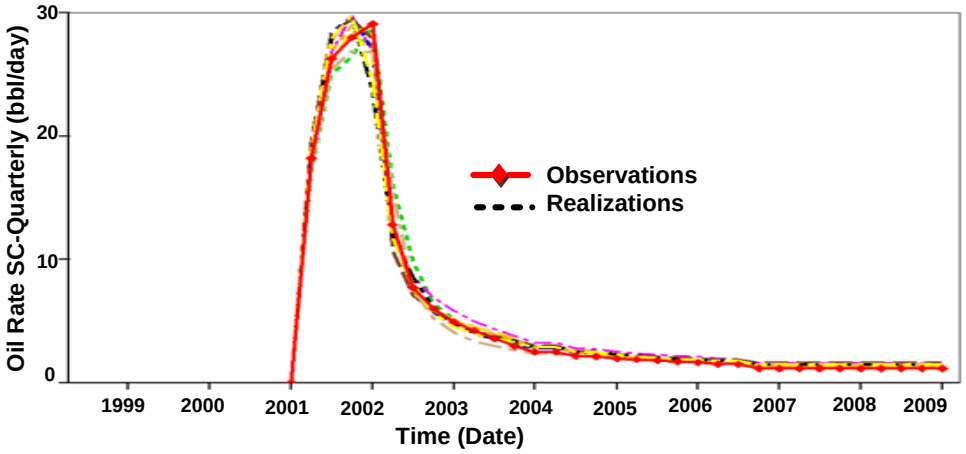

(a)

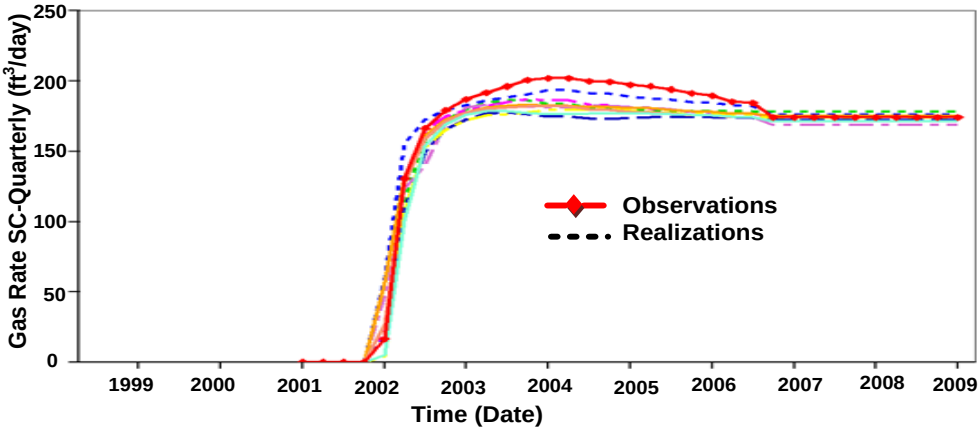

(b)

Figure 5.9. History match for 10 best realizations resulting from SGA with $P_c = 0.5$ *and* $P_m = 0.005$ (a) quarterly oil production rate (bbl/day) (b) quarterly gas production rate (ft^3/day).

As seen in Figure 5.9 the oil production history matches quite well with the actual (true) values. The match in gas production is also reasonable.

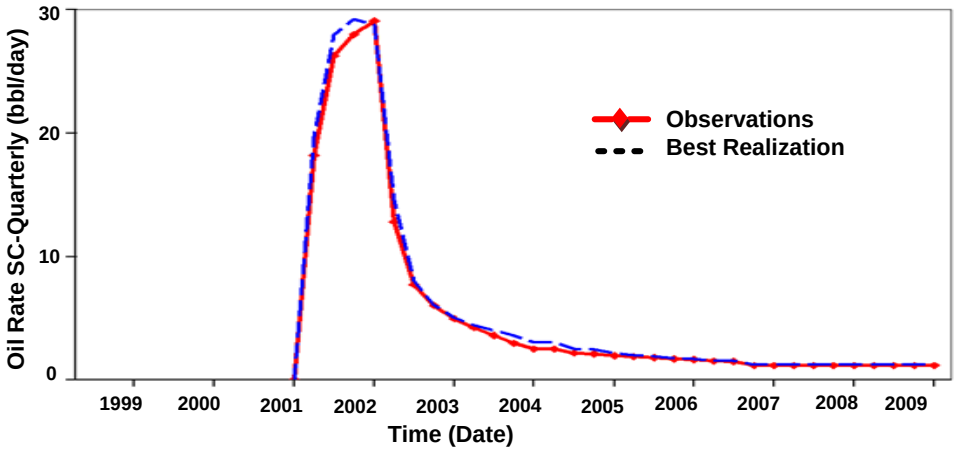

(a)

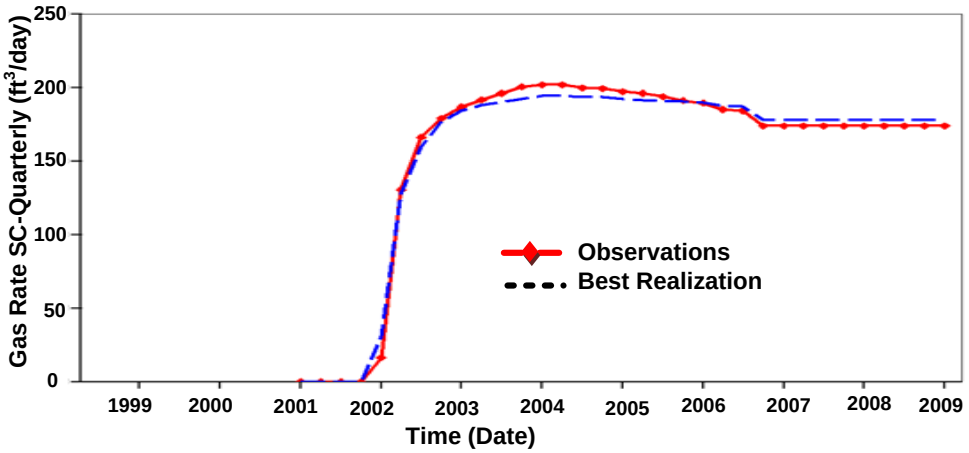

(b)

Figure 5.10. History match for the best realization resulting from SGA. (a) quarterly oil production (bbl/day), (b) quarterly gas production (ft^3/day).

5.5.2 Results from AGA for the 2D Synthetic Reservoir (Case#3.b)

The adaptive genetic algorithm was subsequently used for the history matching of 2D synthetic reservoir. For AGA, the values of genetic operators are according to the value of objective function of the solution. The AGA method was tested by setting the parameters as,

(1) Population size 40, initial crossover probability, $P_c^0 = 0.5$ and initial mutation probability, $P_m^0 = 0.001$; the coefficient factors ξ = 0.02, ω = 0.02 and $\eta = 0.05$ (refer to Eq. 5.2, 5.4 and 5.5)

(2) Population size 40, initial crossover probability $P_c^0 = 0.5$ and initial mutation probability, $P_m^0 = 0.005$; the coefficient factors $\xi = 0.02, \omega = 0.02$ and $\eta = 0.05$

The values of coefficient factors ξ, ω and η can be chosen either through experiments or by ad-hoc method. In the present case, a few preliminary computations were carried to fix the above values. Tables 5.4 and 5.5, present the results obtained from AGA with $P_c^o = 0.5\ and\ P_m^0 = 0.001$; and $P_c^0 = 0.5\ and\ P_m^0 = 0.005$ as the initial probability values respectively. Since the genetic operators are adaptive, the values of crossover probability and the mutation probability vary from the initially defined values according to the fitness of the realizations in subsequent generations.

For AGA with genetic parameters having initial values; $P_m^0 = 0.001$ and $P_c^0 = 0.5$, the variation of P_c and P_m in subsequent iterations are shown in Figure 5.11 (a). The figure shows that the initial value of P_c have reached 0.75 and $P_m = 0.0018$ at 174th iteration. In case of AGA with the initial probability values $P_m^0 = 0.005$ and $P_c^0 = 0.5$, the value of probabilities have reached, $P_c = 0.78$ and $P_m = 0.0077$ at 172th iteration as shown in Figure 5.11 (b). The genetic operators of AGA with initial probabilities; $P_m^0 = 0.005$ and $P_c^0 = 0.5$, generated the best permeability realizations at 172th iterations with minimum objective function value, $Q = 0.502$.

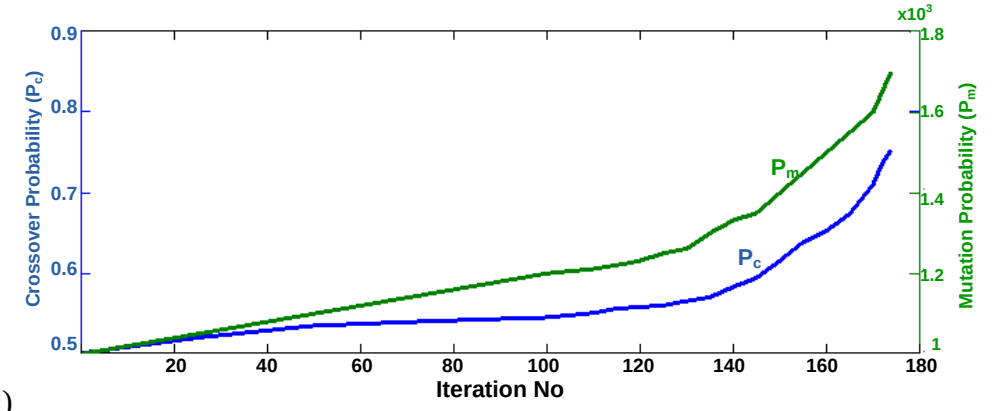

(a)

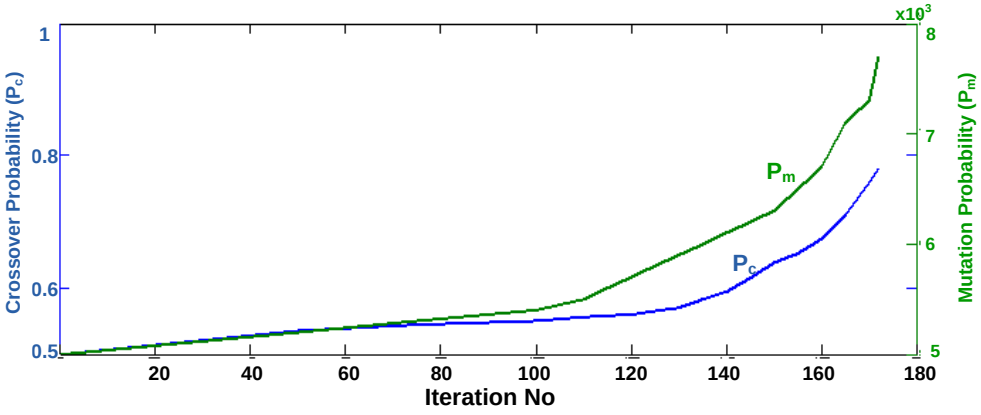

(b)

Figure 5.11 Adaptive crossover and adaptive mutation probability versus iteration for (a) $P_c^0 = 0.5$ and $P_m^0 = 0.001$ (b) $P_c^0 = 0.5$ and $P_m^0 = 0.005$

Table 5.4. The objective function evaluation (Q) of 40 realizations of reservoir resulting from AGA with $P_c^0 = 0.5\ and\ P_m^0 = 0.001$ as the initial values.

No: of Realizations	Iterations								
	Q_{50}	Q_{100}	Q_{150}	Q_{155}	Q_{160}	Q_{165}	Q_{170}	Q_{172}	Q_{174}
1	1.501	1.501	1.501	1.387	1.292	0.950	0.856	0.681	0.616
2	1.830	1.728	1.797	1.797	1.501	1.501	1.501	0.846	0.753
3	2.060	1.830	1.830	1.830	1.830	1.830	1.662	1.501	0.943
4	2.510	2.282	2.281	2.073	2.004	2.004	1.830	1.830	1.402
5	2.510	2.429	2.351	2.282	2.221	2.067	2.055	1.963	1.652
6	2.866	2.510	2.510	2.510	2.510	2.185	2.123	2.055	1.754
7	2.879	2.770	2.530	2.752	2.644	2.237	2.281	2.055	1.830
8	2.985	2.855	2.707	2.879	2.879	2.360	2.510	2.533	2.510
9	3.243	2.866	2.879	2.919	2.985	2.510	2.738	2.617	2.562
10	3.530	2.879	2.985	2.985	3.155	2.879	2.879	2.879	2.644
11	3.701	2.985	3.243	3.365	3.333	2.976	2.985	2.985	2.685
12	4.002	3.701	4.025	3.936	3.383	2.985	3.021	3.156	2.879
13	4.119	4.002	4.166	3.975	3.519	3.150	3.156	3.166	2.985
14	4.166	4.107	4.188	4.149	3.645	3.166	3.166	3.485	3.025
15	4.204	4.119	4.202	4.205	3.895	3.466	3.530	3.654	3.519
16	4.627	4.247	4.251	4.244	3.947	3.487	3.639	3.660	3.645
17	4.899	4.533	4.260	4.627	4.045	4.120	4.154	3.697	3.895
18	5.078	4.627	4.627	4.722	4.627	4.165	4.899	3.784	3.941
19	5.128	4.899	4.782	4.781	4.685	4.628	4.949	3.877	4.056
20	5.553	5.049	4.899	4.897	4.899	4.704	5.456	5.340	4.156
21	5.640	5.128	5.122	4.899	5.156	5.390	5.640	5.640	4.685
22	5.987	5.553	5.640	4.899	5.612	5.620	5.849	5.689	5.057
23	6.395	5.640	5.704	4.943	5.640	5.640	6.103	5.878	5.458
24	6.423	5.979	5.987	5.640	5.658	5.656	6.395	5.986	5.612
25	6.478	6.228	6.224	5.987	6.478	6.073	6.423	6.125	6.423
26	6.842	6.423	6.423	6.141	6.627	6.389	6.431	6.307	6.478
27	7.264	6.478	6.478	6.423	6.680	6.423	6.478	6.423	6.680
28	7.429	6.842	6.842	6.478	6.842	6.478	6.842	6.478	6.842
29	7.760	7.596	7.181	6.842	7.021	6.495	7.165	6.811	6.865
30	8.188	8.188	8.188	8.161	7.702	6.842	7.264	6.842	7.165
31	8.537	8.537	8.383	8.188	7.973	7.767	7.429	8.188	7.973
32	8.637	8.637	8.537	8.537	8.181	8.188	7.760	8.212	8.181
33	8.831	8.831	8.637	8.637	8.188	8.537	8.166	8.537	8.188
34	10.072	9.072	9.221	9.221	8.537	8.637	8.537	8.637	8.537
35	10.127	9.221	9.510	10.127	9.221	9.166	8.637	9.221	8.637
36	10.221	10.127	10.127	10.127	9.352	9.221	9.487	10.127	9.221
37	10.869	10.818	10.380	10.869	10.127	10.135	10.146	10.380	10.127
38	12.225	12.462	11.255	11.886	10.898	12.225	10.869	10.546	10.456
39	14.780	13.565	12.656	12.225	12.225	17.420	12.225	12.225	12.225
40	18.420	18.420	18.475	17.420	17.420	17.420	17.420	17.420	17.420

Table 5.5. The objective function evaluation (Q) of 40 realizations of reservoir resulting from AGA with $P_c^0 = 0.5\ and\ P_m^0 = 0.005$ as the initial values.

No: of Realizations	Iterations							
	Q_{50}	Q_{100}	Q_{150}	Q_{155}	Q_{160}	Q_{165}	Q_{170}	Q_{172}
1	1.414	1.392	1.381	1.288	1.220	0.823	0.742	0.503
2	1.481	1.433	1.501	1.243	1.288	0.931	0.946	0.691
3	1.501	1.501	1.549	1.485	1.397	1.381	0.799	1.381
4	2.486	1.549	1.691	1.501	1.501	1.501	1.055	1.501
5	2.453	2.054	1.793	1.549	1.549	1.549	1.759	1.549
6	2.174	2.076	1.802	1.895	1.631	1.802	1.945	1.948
7	2.174	2.174	2.216	1.782	1.126	1.001	1.182	0.981
8	2.330	2.417	2.257	2.417	1.054	1.122	1.269	0.781
9	2.417	2.510	2.291	2.510	2.058	2.005	1.456	1.456
10	2.510	2.628	2.307	2.724	2.510	2.106	2.830	1.015
11	2.774	2.985	2.417	2.956	2.657	2.510	2.985	1.264
12	2.945	3.004	2.510	2.985	2.745	2.740	2.045	2.008
13	2.985	3.248	2.753	2.045	2.860	2.985	2.006	2.780
14	3.737	3.307	2.985	3.402	2.951	2.105	3.007	2.895
15	4.896	3.364	2.992	3.771	2.985	3.322	3.715	2.985
16	4.165	4.009	3.671	3.751	3.263	3.595	3.913	3.036
17	4.016	4.020	4.035	3.973	3.476	3.752	4.018	3.126
18	4.022	4.218	4.212	4.240	3.005	3.005	4.129	3.290
19	4.627	4.322	4.244	4.231	4.163	3.468	4.264	3.839
20	5.061	4.563	4.355	4.285	4.627	4.411	4.459	3.867
21	5.233	4.627	4.458	4.627	4.828	4.479	4.627	3.015
22	5.302	4.699	4.627	4.740	4.007	4.627	4.695	4.627
23	5.398	4.897	4.921	4.002	5.398	4.035	3.784	4.687
24	5.640	5.398	5.398	5.254	5.636	5.054	4.213	4.741
25	5.754	5.631	5.640	5.320	5.640	5.398	5.398	4.054
26	5.796	5.640	5.868	5.398	5.868	5.640	5.640	5.640
27	5.868	5.868	6.160	5.640	5.008	5.727	5.796	5.766
28	6.895	6.033	6.478	5.868	6.478	5.868	5.809	5.868
29	6.214	6.045	6.598	5.872	6.502	6.478	5.868	5.001
30	6.416	7.798	6.842	6.478	6.584	6.590	5.002	6.478
31	7.917	7.165	7.250	6.758	6.819	6.842	6.776	6.578
32	7.490	7.057	7.612	6.842	6.842	6.872	6.817	6.783
33	8.985	8.462	7.642	7.374	6.008	6.911	6.842	6.842
34	8.013	8.013	8.013	8.013	8.013	7.183	7.465	7.887
35	9.789	8.537	8.013	8.013	8.537	8.206	7.168	8.206
36	9.654	9.221	8.537	8.537	8.588	8.537	8.537	8.537
37	10.186	9.221	9.221	9.221	9.221	9.802	8.165	9.221
38	10.127	10.127	10.127	10.127	10.127	9.513	9.155	9.044
39	11.893	11.796	10.981	10.874	10.645	10.542	10.315	10.315
40	13.921	12.416	12.225	12.225	12.225	12.225	12.225	12.225

The AGA with $P_c^0 = 0.5$ and $P_m^0 = 0.005$ have generated better reservoir realizations than the AGA with $P_c^0 = 0.5$ and $P_m^0 = 0.001$ as shown in Tables 5.4 and 5.5. The objective function values ($Q_{min} = 1.77$, $Q_{max} = 68.13$ and $Q_{avg} = 12.01$) of initial realizations generated using geostatistical models, converged to $Q_{min} = 0.616$, $Q_{max} = 17.42$ and $Q_{avg} = 5.34$ at 174th iteration for $P_m^0 = 0.001$ and to $Q_{min} = 0.502$, $Q_{max} = 12.22$ and $Q_{avg} = 4.41$ at 172th iteration for $P_m^0 = 0.005$ respectively. An increase in the initial adaptive mutation probability ($P_m^0 = 0.005$) enhanced the convergence rate and produced better results in fewer iterations compared to AGA with initial mutation probability; $P_m^0 = 0.001$.

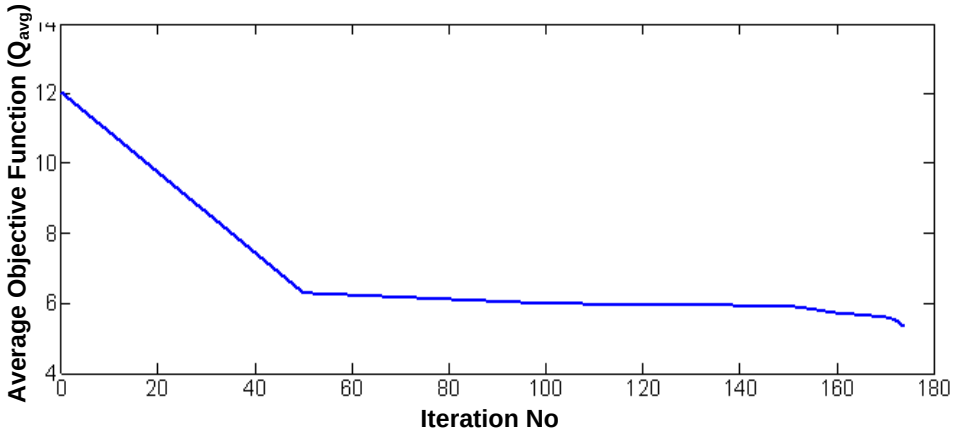

(a)

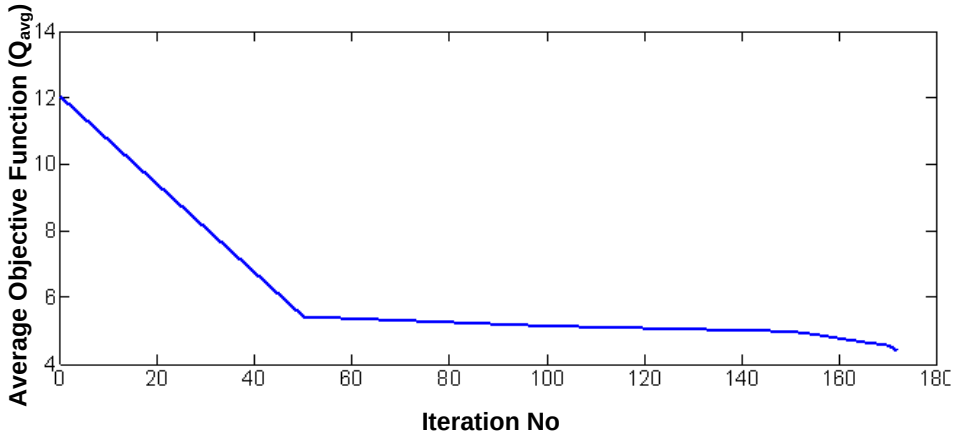

(b)

Figure 5.12. Average objective function values versus iteration number (every 20 iterations) (a) $P_c^0 = 0.5$ and $P_m^0 = 0.001$ (b) $P_c^0 = 0.5$ and $P_m^0 = 0.005$.

The average objective function values after every 20 iteration for AGA with $P_c^0 = 0.5$ *and* $P_m^0 = 0.001$ and $P_c^0 = 0.5$ *and* $P_m^0 = 0.005$ are presented in Figure 5.12 (a) and (b).

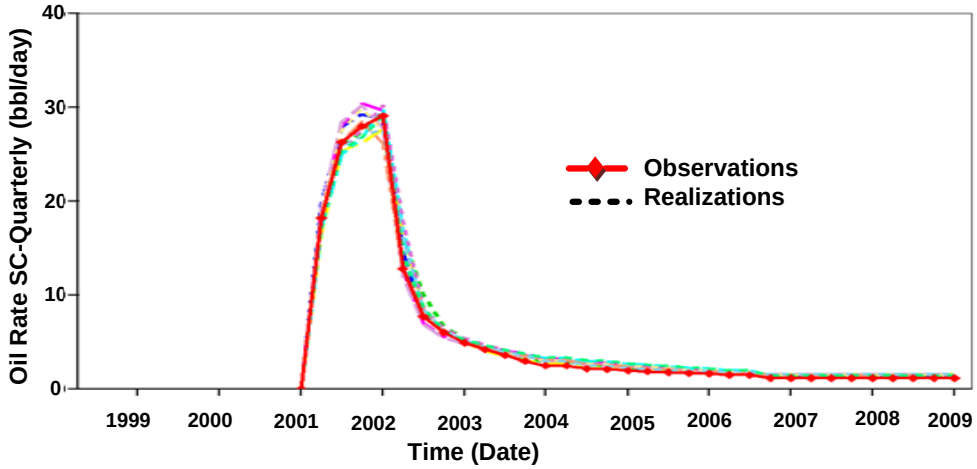

(a)

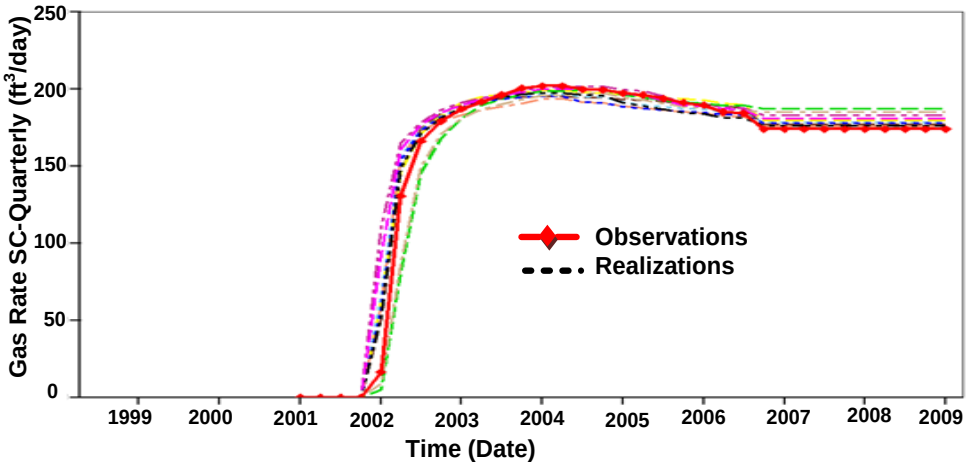

(b)

Figure 5.13 History match for 10 best reservoir realizations resulting from AGA with $P_c^0 = 0.5$ and *and* $P_m^0 = 0.005$ (a) quarterly oil production rate (bbl/day) (b) quarterly gas production rate (ft^3/day).

The history match of the best 10 realizations of the reservoir resulting from AGA with $P_c^0 = 0.5$ and $P_m^0 = 0.005$ are shown in Figure 5.13 (a) and (b). It is observed from these figures that the AGA was able to achieve a satisfactory history match for quarterly oil production data and a reasonable match of quarterly gas production for Well-1. Figure 5.14 (a) and (b) presents the history match of the best realization produced from AGA with $P_c^0 = 0.5$ and $P_m^0 = 0.005$, which confirm a reasonable history match for quarterly oil and gas productions rates from Well-1.

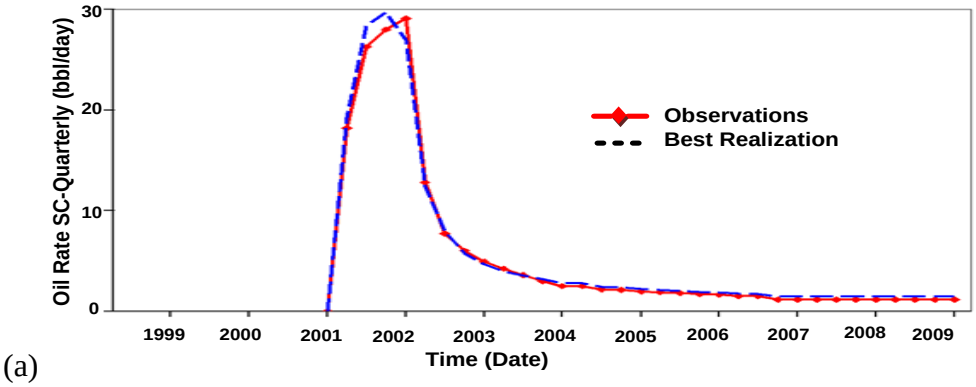

(a)

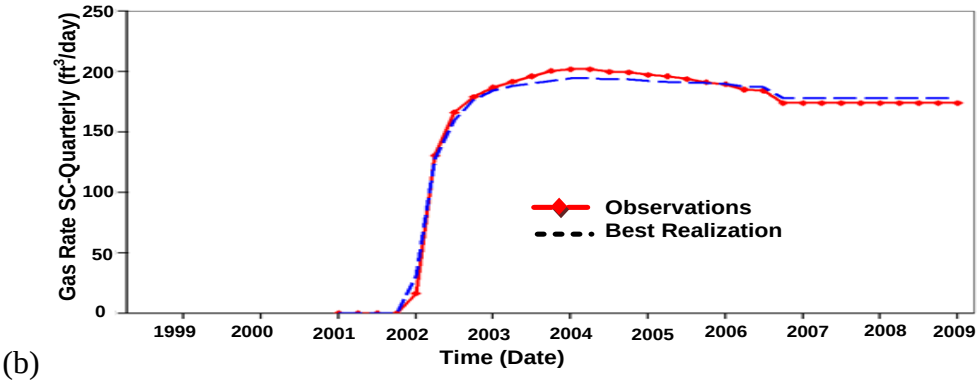

(b)

Figure 5.14. History match for the best reservoir realization resulting from AGA with $P_c^0 = 0.5$ and $P_m^0 = 0.005$(a) quarterly oil production (bbl/day), (b) quarterly gas production (ft^3/day).

The permeability distribution of 2D heterogeneous reservoir obtained from the history matched model which is conditioned to quarterly oil and gas production data acquired from the AGA with $P_c^0 = 0.5$ and $P_m^0 = 0.005$ is shown in Figure 5.15 (b). Figure 5.15 (a) shows the true permeability map and has been juxtaposed for comparison. The permeability colour code is same as Figure 5.5.

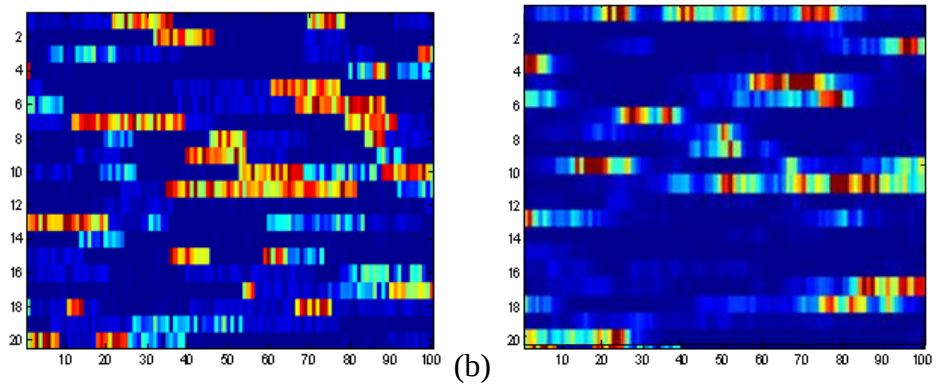

(a) (b)

Figure 5.15. Permeability distribution of 2D synthetic reservoir (a) True reservoir map (10^{th} SPE comparative project) (b) Realization of best history matched reservoir from AGA

5.6 Comparison between SGA and AGA

A comparison between the results from SGA and AGA shows that AGA was able to converge to optimal reservoir realizations much faster than the SGA. Table 5.6 demonstrates a comparison between the results obtained from SGA and AGA and in terms of minimum objective function value at different iterations.

Table 5.6 Comparison of results from SGA and AGA

SGA		**AGA**	
Iterations	Minimum Objective Function (Q_{min})	Iterations	Minimum Objective Function Q_{min})
50	1.5014	50	1.4139
100	1.5014	100	1.3924
150	1.5014	150	1.3812
200	1.2439	155	1.2877
250	1.2325	160	1.22
300	1.2093	165	0.8226
350	0.8562	170	0.7418
400	0.6912	172	0.5027

It is observed from the table (Table 5.6) that the AGA evolved to optimum solution in fewer number of iterations when compared to SGA. This is due to the fact that the adaptive capability of the genetic operators adjusts the crossover and mutation probability according the objective function value of the realization generated at each iteration. However, SGA may also result in equally good realization, if the algorithm evolves for more number of iterations or optimized values of crossover and mutation probability are used.

5.7 CONCLUDING REMARKS

History matching using GA methodology has been successfully validated for 2D synthetic model reservoir. The GA technique showed its capability in producing history match for oil and gas production which are conditioned to observations from Well-1. The history match for oil and gas production from Well-1 obtained through the GA technique shows equally good match as presented by Chitralekha, et al., (2010) using Ensemble Kalman Filter for history matching of the same reservoir. The permeability map generated by AGA showed similarity to true permeability map

hidden from algorithm. The permeability distribution map would have perhaps replicated the same if the history match for Well-2 was included in the objective function calculation. Since the objective of the synthetic case study was to validate the GA code and methodology developed for history matching, the study was restricted to match the history for productions from Well-1 only.

The time taken for history match for the synthetic reservoir using AGA was 30 to 40 minutes. Although the actual computation time was much less but since the marriage between CMG program and the GA was not perfect and permeability data file from MATLAB to CMG had to be moved manually after every generation, the total time increased. The time taken for the real reservoirs, to be discussed in the next chapter, was of the order of 60 to 90 minutes since the number of grid blocks for that problem were about four times that of the above case.

CHAPTER- 6
HISTORY MATCHING USING GENETIC ALGORITHM: A REAL 3D RESERVOIR

6.1 INTRODUCTION

This chapter describes the application of SGA and AGA to history matching of a real field reservoir situated in the Cambay Basin in Gujarat. The details of the structure and parameters of the reservoir are described in the next section. The total pressure drop over its entire production history (2000~ 2009) is less than 10% of the initial pressure, it was sufficient to use the "black-oil" model for flow simulation. Two case studies; Case#4.a and Case#4.b present the application of SGA and AGA to automate the real field history matching problem. The history matching model was then used to predict the performance of the reservoir for next three years and also predict productions from two new wells drilled in the same field.

6.2 THE REAL FIELD RESERVOIR UNDER STUDY

The oil field is located in the south-western part of Cambay Basin and to the west of Cambay Gas Field in Gujarat, India. The field was discovered in July 1999. The field consists of a total of 8 oil producing wells. The oil producing sandstone has varying thickness up to 25 m and the sandstone is divided into three layers; Layer-1, Layer-2 and Layer-3.The sandstone layers are separated by thin shales that vary 1 to 2 m in thickness. The structure of the field trends NNW-SSE in direction and is bounded by a fault on either side, which separates the structure from the adjoining lows. The reservoir structure is controlled by East-West trending normal fault in the north, and it narrows down towards south. The fault surrounding the reservoir is non-communicating and hence it is assumed that there is no hydrodynamical flow between the reservoir and the remaining area.

The initial reservoir pressure was recorded as 144 kg/cm^2 at 1397m. The quantity of reserved oil inplace was 2.47MMt, and the cumulative oil production until September 2009 was 0.72MMt which is 29.1% of the inplace reserve and 64.5% of ultimate reserve. The marginal drop in reservoir pressure against cumulative oil production of

0.72MMt indicates that the reservoir is operating under active water drive. The presence of two aquifers towards the N-W side and towards the narrow region of the reservoir in Layer-3 has been reported. Most of the wells are producing gas to oil ratio (GOR) in the range of 30-35 v/v as producing wells are flowing above the bubble point pressure. Hence the model shows constant producing GOR. The grid bottom structure 3D real reservoir is shown in Figure 6.1.

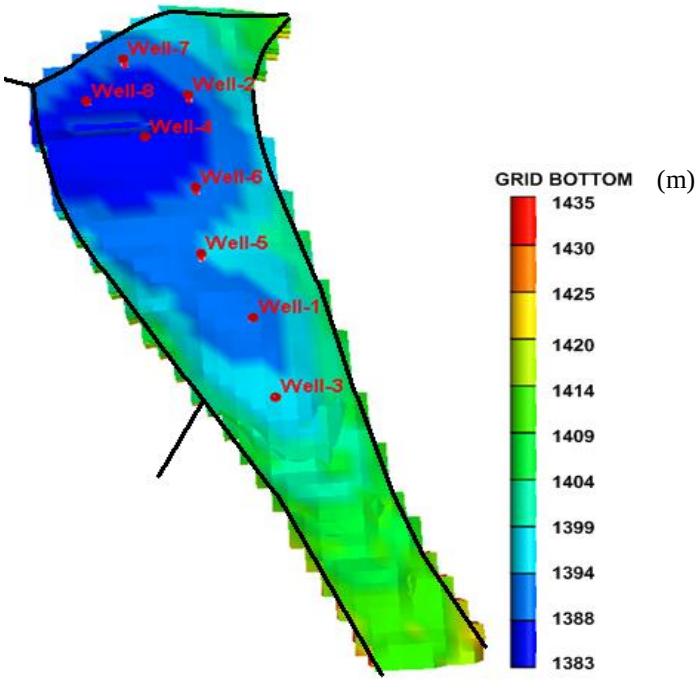

Fig 6.1. 3D view of grid bottom structure of real reservoir

The field started producing through the wells Well-1, and Well-2 from February, 2000 and December, 2000 respectively. The initial reservoir pressure recorded at Well-1 was 144.6 kg/cm^2 at 1385m. The cumulative productions of oil, gas and water from Well-1 till September 2009 are 0.156MMt, 8.1MMm^3, and 7.2 MMm^3, respectively. Subsequently, the other wells (Well-3 - Well-8) were drilled and put on production in different years until 2009. The producing wells; Well- 3 and Well- 5 are perforated in Layer- 1 and Layer- 2; while Well- 1; Well-2; Well- 4; and Well- 6 are perforated through Layer-2 and Layer-3.

The case studies carried out here consider six oil producing wells (Well-1 – Well-6) from the total of 8 oil producing wells. The historical production is available for a period of 9 years. For the case studies, 70 months' historical productions for the period of 2000 – 2005 were used for history matching using GA methodology and remaining

data till 2009 were used for validating the model and the technique. Well-7 and Well-8 were put on production in January 2009.

6.2.1 Inputs to CMG®- Builder™ suit

The reservoir model is constructed by amalgamating many parameters such as petrophysical data, geological structure (structural contour map, pay-sand thickness map etc.,), grid definition (size and type), PVT properties, reservoir fluid properties, well completion data, initial conditions etc.,. The reservoir rock, fluid, PVT parameters and initial conditions used to built a reservoir model through CMG®-Builder™ are produced in Tables 6.1 and 6.2.

Table 6.1 Reservoir Model Parameters

Initial reservoir Pressure		144 kg/cm^2
Datum Depth		1400 m
Porosity	Layer-1	0.21
	Layer-2	0.22
	Layer-3	0.23
Depth of Water Oil Contact	Layer-1	1397 m
	Layer-2	1401 m
	Layer-3	1402 m

The relative permeability data have been generated using Corey's correlation. The measured permeability values at the well locations are given in Table 6.3. The other data required for model building are included in Appendix-C.

Table 6.2 Reservoir PVT Properties

Initial Reservoir Pressure	144 kg/cm^2
Bubble Point Pressure	82 kg/cm^2
Reservoir Temperature	96.8 C
Oil density	0.85 gm/cc
Gas gravity	0.95
Oil Viscosity	0.98 cp
Initial solution GOR	32 v/v
Oil formation volume factor*	1.2

*Reservoir barrels/ stock tank barrel

Table 6.3 Permeability (k) values at well locations

Layer 1			
Well Name	**X Cord (m)**	**Y Cord (m)**	**k (mD)**
Well-3	2921.478	2608.444	300.000
Well-5	2469.090	3727.096	300.000
Layer 2			
Well-8	2020.866	5101.895	533.200
Well-2	2516.858	4935.464	732.700
Well-4	2181.874	4702.655	412.700
Well-7	1764.404	4607.200	394.100
Well-6	2569.139	4357.980	329.700
Well-5	2468.298	3735.591	420.000
Well-1	2793.034	3191.109	446.800
Well-3	2915.995	2620.678	446.700
Layer 3			
Well-8	2025.845	5091.209	533.200
Well-2	2511.532	4924.293	732.700
Well-4	2181.381	4692.627	412.700
Well-7	1767.349	4603.087	394.100
Well-6	2564.105	4350.277	329.700
Well-1	2790.579	3187.187	446.800

The reservoir model consists of 3 layers and 6 producing wells. The three layers have different porosities but remain constant within each layer. Layer-1 of the reservoir has a homogeneous permeability of 300mD whereas Layer-2 and Layer-3 have heterogeneous permeability distributions. The production wells; Well-1, Well-2, Well-4, and Well-6 have penetrated through Layer-2 -3 while Well-3, Well-5 have penetrated through Layer-1-2.

6.2.2 Grid Selection

For the numerical integration of flow equations using finite difference method, the CMG® simulator uses a 50m x 50m size block grid on the reservoir which for the present case will result in 100 x 120x 3 grid blocks. However, in the present study, a coarse scale grid was used to limit the dimensionality of the GA variables and hence a 100m x 100m size was used for each block resulting in 50 x 60 x 3 grid blocks.

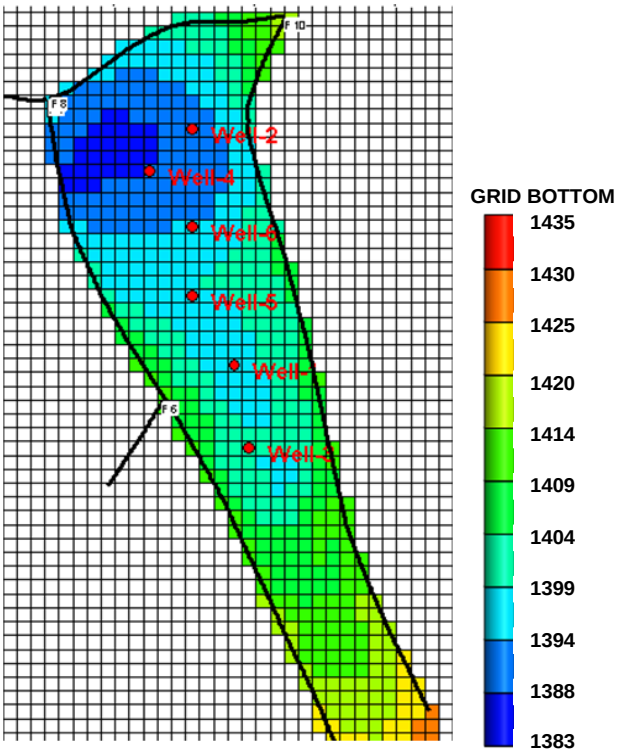

Figure 6.2. Layer-2 grid bottom structure of coarse scaled reservoir in 2D view

6.3 WORKFLOW OF GENETIC ALGORITHM FOR HISTORY MATCHING

The workflow of history matching of real field reservoir follows the same methodology as described in Chapter-5. The algorithm starts with a set of initial population of feasible solutions (realizations) which undergo genetic operations such as; selection, recombination and mutation, through generations to evolve to the optimal solution. The genetic operations such as crossover and mutation are applied on the active grid blocks of the reservoir, except for the grid blocks that represents the well locations, from where the measured data are available. The rock permeabilities (gene value) at the well location remain unchanged throughout the genetic evolutions so as to ensure the newly generated realizations honor the field measurements. For the real reservoir shown in Figure 6.3, region highlighted in yellow shade represents the active grid blocks, while region highlighted in green shade denotes the inactive grid blocks. In the figure, the grid blocks highlighted in red represents the well locations. The genetic operators are programmed such that it operators on the region highlighted in yellow shade.

(a) 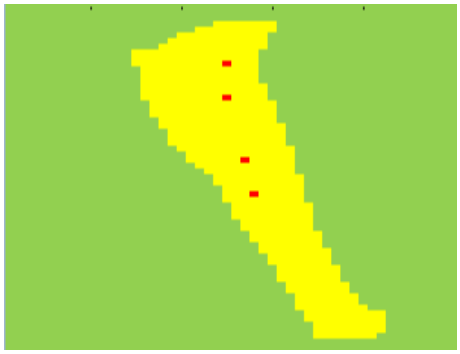 (b) 

Figure 6.3 Graphical view of active (yellow shade) and inactive grid blocks (green shade) of real reservoir for (a) Layer-2 (b) Layer-3

The Layer-1 of the reservoir has homogeneous permeability distribution of 300mD for all the grid blocks. The objective of the present study is to estimate the active grid block permeability distributions in Layer-2 and Layer-3, since both the layers are highly heterogeneous.

6.3.1 Generation of Initial Population

The initial population was generated using geostatistical toolbox of MATLAB®, mGstat, which is interfaced to the SGeMS (geostatistical modeling software by GSLIB). The sequential gaussian simulation (SGSIM) method has been employed for generating initial realizations which honor the spatial variations and histogram of the real reservoir. The sequential gaussian simulation determines each distribution of petrophysical properties under the multivariate gaussian model.

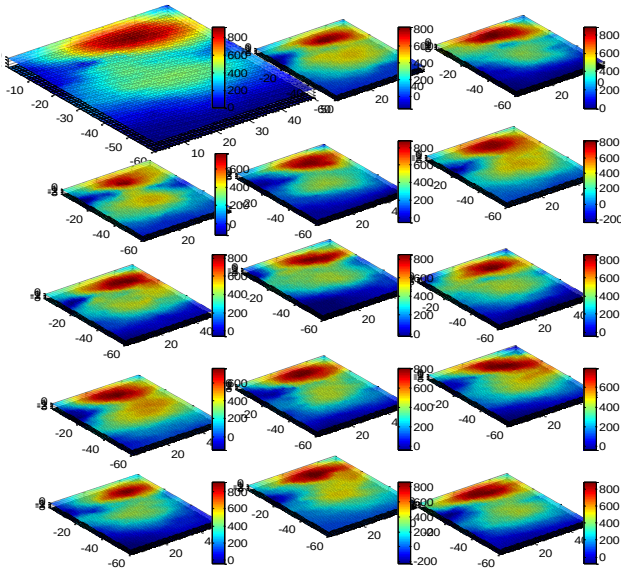

Figure 6.4 3D view of few initial realizations generated using SGeMS for Layer-2 and Layer-3 of the reservoir

A Gaussian variogram model having correlation range of 20 grid blocks and with a sill value of 1 were used to estimate the permeability of each grid block in the realizations. The population size of 30 was chosen and hence a set of 30 initial realizations representing the permeability distributions were generated using Gaussian simulations that honor the permeability values at the well locations in the reservoir. Figure 6.4 shows some of the initial permeability distributions generated by SGSIM.

6.3.2 Selection of GA parameters

The history matching of real field reservoir using reservoir parameterization was tested using simple genetic algorithm (SGA) and adaptive genetic algorithm (AGA). For SGA and AGA, the tournament selection operator was employed for selecting the fittest members from the population to the mating pool. In case of SGA, a uniform k-point crossover and uniform mutation operator were used as the other genetic operators with crossover probability; P_c= 0.5 and mutation probability; P_m= 0.005. In case of AGA, the same operators were used except with initial crossover probability, P_c^0 = 0.5 and initial mutation probability P_m^0= 0.005. The coefficient factors; ξ = 0.02, ω = 0.02 and η = 0.05 were chosen for calculating adaptive crossover and mutation probabilities during evolutions according to the fitness of the population (see Eqs 5.2, 5.4 and 5.5 in Chapter-5).

6.4 HISTORY MATCHING

The present study intends to accomplish the automatic history match of the real reservoir by applying GA methodology. The GA procedure updates the initial solutions of permeability distributions called the initial realizations through generations to achieve a match between the field observations and the simulator output in terms of oil production rates, gas-oil ratio (GOR), water cut (WC) and bottom hole flowing pressure (BHP). In this study, the most sensitive parameter, the field permeability distribution that has significant impact on field performance (production rates and flowing bottom hole pressure) was the only control variable. There are other uncertain parameters such as transmissibility, connate water saturation, depth of water-oil contact (DWOC) and aquifer properties which are sensitive to field observations. These uncertain parameters were not included in the objective function

for estimation because of the computational constraints. However, some these are adjusted manually as required.

6.4.1 Objective Function

The objective of this study to find the optimal field permeability distribution in Layer-2 and 3 that minimizes the difference between the field observations and the simulator output. The objective function is formulated based on Eq. 5.1 taking into account the type of field observations, number of wells, and time period etc. In this case study the field data comprises oil production rate, GOR, water cut and BHP from all 6 producing wells over a period of 6 years (70 months) of production history (Mar, 2000 ~ Dec, 2005). Hence the objective function Q, is expressed as

$$Q = \sum_{w=1}^{6}\sum_{k=1}^{70}\left(\frac{d^{O}_{ijk\ oil} - d^{S}_{ijk\ oil}}{d^{O}_{ijk\ oil}}\right)^{2} + \left(\frac{d^{O}_{ijk\ GOR} - d^{S}_{ijk\ GOR}}{d^{O}_{ijk\ GOR}}\right)^{2} + \left(\frac{d^{O}_{ijk\ WC} - d^{S}_{ijk\ WC}}{d^{O}_{ijk\ WC}}\right)^{2} + \left(\frac{d^{O}_{ijk\ BHP} - d^{S}_{ijk\ BHP}}{d^{O}_{ijk\ BHP}}\right)^{2} \quad (6.1)$$

where subscripts w, k denote the number of wells and time period respectively; d^{O}_{ijk} and d^{S}_{ijk} are the field observations and corresponding CMG® simulator outputs in terms of monthly oil production rate, GOR, WC and BHP. Q was minimized using GA and search was terminated when successive iterations produced essentially same values of the objective function.

6.5 RESULTS AND DISCUSSION

The objective function values of the initial realizations representing the field permeability distributions are presented in Table 6.4. The minimum and maximum objective function value ranges between 24.58 ~ 68.19 with the average value for Q_{avg} being 35.096. The oil production rates (m^3/day), water cut -%, GOR (m^3/m^3) and BHP (kg/cm^2) for the entire field resulted from the initial realizations is shown in Figure 6.5. Also included in this figure are field observations for comparison.

Table 6.4 Objective function (Q) values of 30 initial realizations of the real reservoir

No: of Initial Realizations	Objective Function (Q)	No: of Initial Realizations	Objective Function (Q)
1	24.578	16	28.543
2	24.603	17	28.621
3	24.734	18	28.991
4	25.529	19	29.485
5	25.832	20	30.12
6	26.27	21	30.942
7	26.631	22	31.081
8	26.932	23	31.095
9	27.129	24	35.561
10	27.523	25	55.467
11	27.604	26	59.874
12	27.91	27	63.634
13	28.173	28	64.381
14	28.413	29	66.596
15	28.428	30	68.193

As seen in figures 6.5 (a) and (c) the oil production rate and GOR appear to match well for all the 30 initial guesses of the permeability distributions but water cut and bottom hole pressures show significant variations. This is due to the fact that the reservoir is producing under strong water drive mechanism provided by the two aquifers, which maintains near constant reservoir pressure for oil and gas productions, and there is no free gas cap.

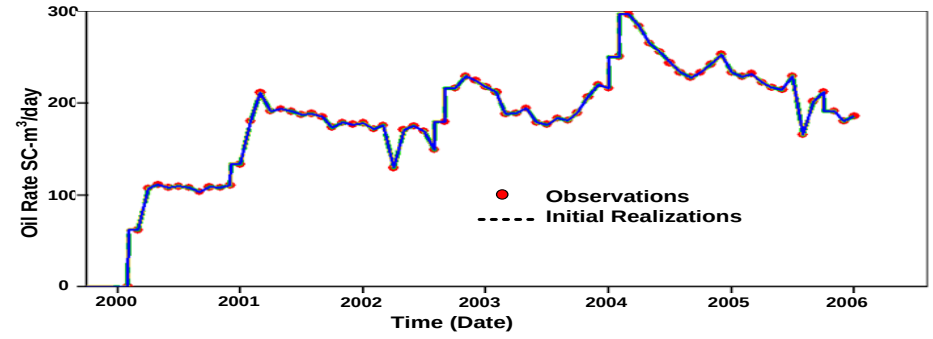

(a)

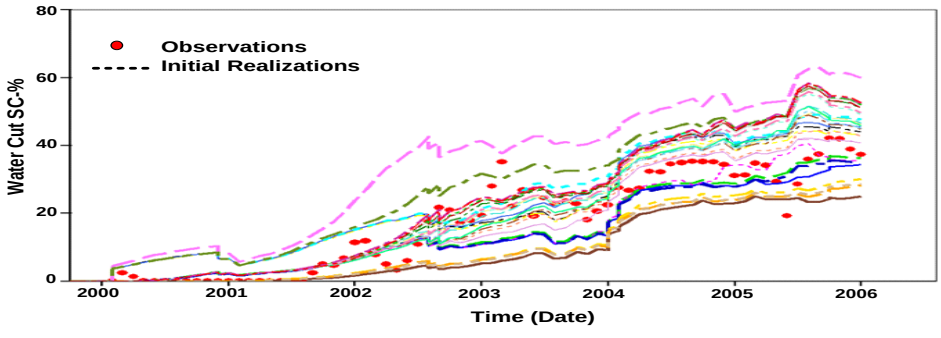

(b)

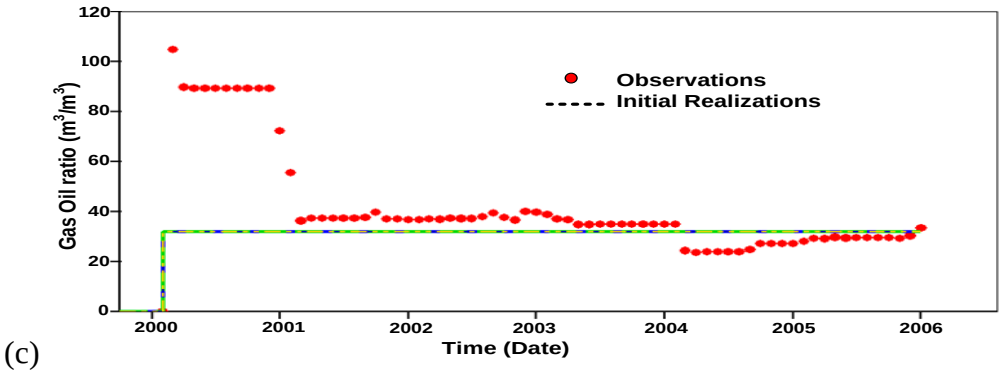

(c)

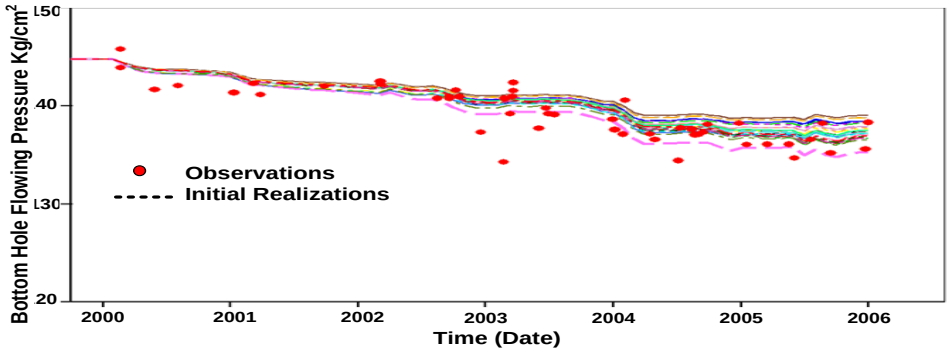

(d)

Figure 6.5. Comparison between the field observations and the simulator output generated from 30 initial realizations (a) Oil production rate SC (m3/day) (b) GOR (m3/m3) (c) Water cut SC- % (d) BHP (kg/cm2)

6.5.1 Results from SGA (Case#4.a)

The objective function values of the realizations resulting from SGA for the real reservoir after every 40 iterations are presented in Table 6.5. The SGA search was terminated after 240 iterations which resulted in an average value for $Q_{avg} = 25.673$ minimum value of Q_{min} = 19.98 (range 19.98 ~ 54.34). The objective function values resulting from SGA do not appear to be very small when compared to the initial realizations Q values. However, the water cut and BHP showed better match with the field data. The variation of Q_{avg} with iterations numbers is shown in Figure 6.6. The comparison between the observed and simulator output from the 30 realizations resulted from SGA in terms of WC and BHP is shown in Figure 6.7.

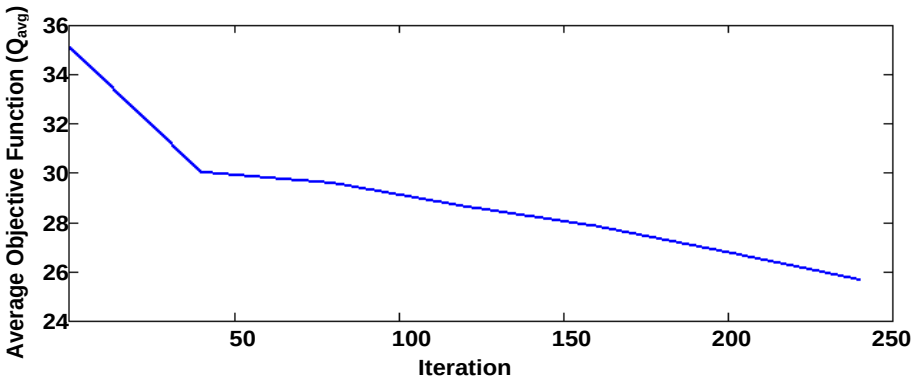

Figure 6.6. Average value for objective functions versus number of iterations from SGA.

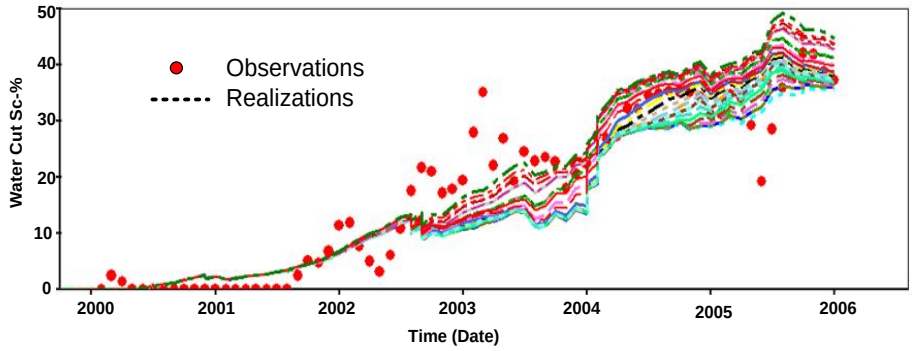

(a)

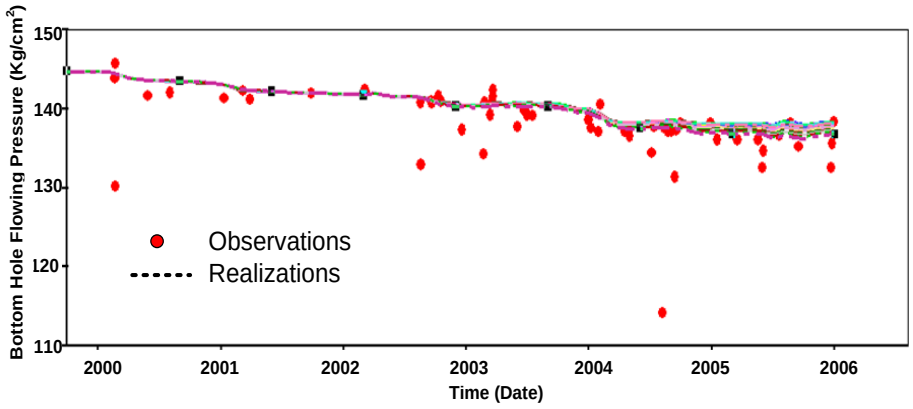

(b)

Figure 6.7. Comparison between the field observations and the simulator output generated from 30 realizations resulted from SGA (a) Water cut SC- % (b) BHP (kg/cm2)

Table 6.5. Objective function (Q) values of 30 reservoir realizations resulting from SGA after every 40 iterations

No: of Realizations	Iterations					
	Q_{40}	Q_{80}	Q_{120}	Q_{160}	Q_{200}	Q_{240}
1	24.553	23.545	22.351	21.351	20.447	19.984
2	24.573	23.598	23.355	22.406	21.198	20.159
3	24.607	24.502	24.459	22.459	21.859	20.473
4	25.511	24.565	24.522	22.521	21.945	20.498
5	25.702	25.693	24.912	22.855	22.351	20.907
6	25.702	25.693	25.458	23.35	22.476	21.351
7	25.897	25.889	25.61	24.358	23.54	21.736
8	25.965	25.955	25.65	24.38	23.543	21.942
9	26.36	25.983	25.65	25.409	23.58	21.958
10	26.612	26.352	25.689	25.65	23.65	22.118
11	26.663	26.602	25.846	25.688	24.008	22.349
12	26.993	26.654	25.94	25.845	24.354	23.357
13	27.193	26.732	26.308	25.869	24.658	23.366
14	27.742	26.982	26.761	25.927	24.727	23.426
15	27.799	27.184	26.846	26.308	24.909	23.542
16	27.814	27.789	26.869	26.398	25.358	24.352
17	27.816	27.804	26.898	26.461	25.396	24.637
18	27.877	27.809	26.927	26.545	25.459	24.666
19	27.899	27.867	26.939	26.745	25.741	24.715
20	27.922	27.889	27.141	26.824	25.969	24.781
21	27.991	27.912	27.351	26.939	26.093	24.851
22	28.951	27.941	27.745	27.141	26.778	24.869
23	28.953	27.971	27.765	27.35	26.885	25.47
24	28.98	28.945	27.824	27.485	27.157	25.867
25	29.537	29.528	28.485	28.765	28.565	27.098
26	33.839	33.831	32.788	31.691	29.395	28.348
27	38.314	36.306	34.263	33.263	30.763	30.742
28	44.503	41.495	36.452	34.452	34.344	34.043
29	49.24	49.233	46.189	45.389	44.317	44.229
30	59.399	59.391	56.348	55.524	54.444	54.343

6.5.2 Results from AGA (Case#4.b)

Table 6.6 presents the objective function values of the 30 realizations resulting from the application of AGA after every 20 iterations. The minimum and maximum objective function values after 120 iteration are $Q_{min} = 19.606$ and $Q_{max} = 40.018$ with the average value, $Q_{avg} = 21.515$. As mentioned earlier, the high values of the objective function is due to large error in predictions of water cut.

The average objective function values (Q_{avg}) of the realizations resulting from AGA after every 20 iterations are shown in Figure 6.8. As seen in this figure, Q_{avg} decreased rapidly up to 20 iterations and then gradually to the final value. The figure

also shows that $Q_{avg} = 35.096$ for initial realizations have converged to $Q_{avg} = 21.515$ after 120 iterations.

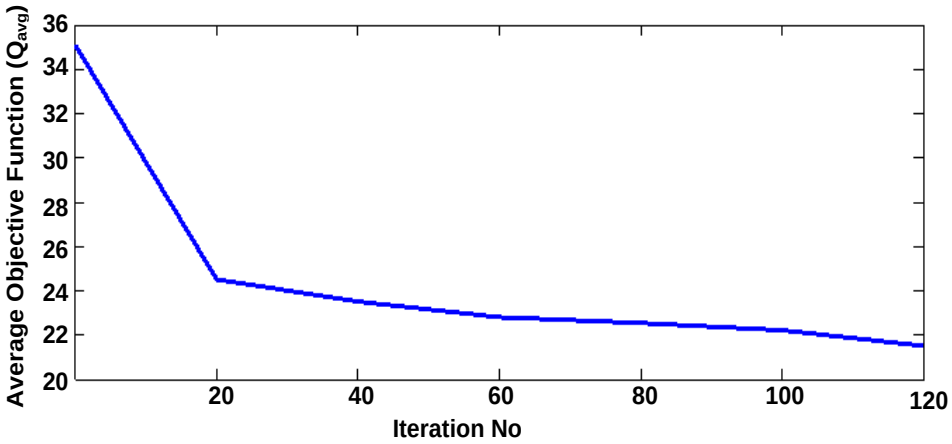

Figure 6.8 Average value of objective functions versus iteration number from AGA.

Figure 6.9 shows the variation of crossover probability and adaptive mutation probability with every 20 iterations. After 120 iterations, the values of the probabilities were $P_c = 0.767$ and $P_m = 0.0077$. A comparison of AGA results with those of SGA clearly establishes the superiority of AGA over SGA. The converged range and average values of the objective functions in case of AGA are lower than the corresponding numbers for SGA, achieved in half the number of iterations.

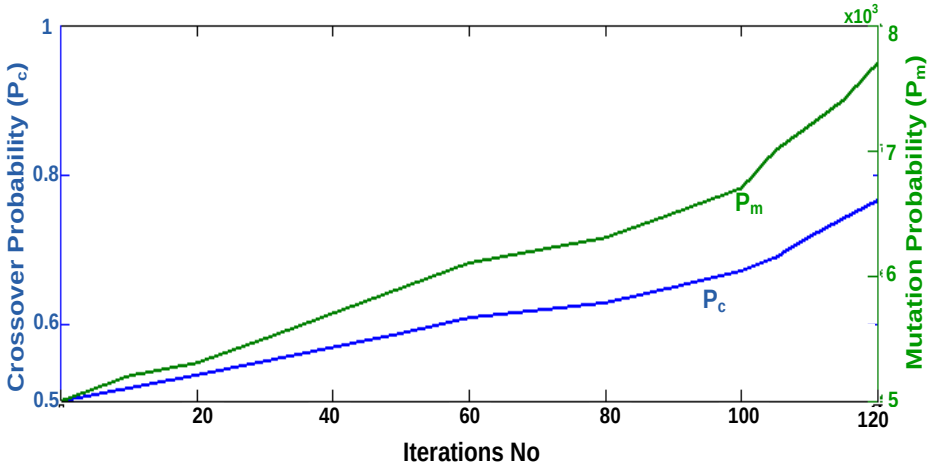

Figure 6.9 Adaptive crossover and mutation probabilities versus iteration number for $P_c^0 = 0.5$ and $P_m^0 = 0.005$.

Table 6.6 Objective function (Q) values of 30 reservoir realizations resulting from AGA after every 20 iterations

No: of Realizations	Iterations					
	Q_{20}	Q_{40}	Q_{60}	Q_{80}	Q_{100}	Q_{120}
1	20.135	20.102	19.867	19.86	19.618	19.606
2	20.193	20.143	19.871	19.868	19.64	19.613
3	20.274	20.151	19.927	19.889	19.644	19.624
4	20.332	20.199	19.939	19.913	19.722	19.629
5	20.413	20.212	19.939	19.939	19.722	19.64
6	20.446	20.221	20.04	19.939	19.772	19.652
7	20.478	20.285	20.096	19.9	19.819	19.66
8	20.514	20.293	20.141	20.068	19.827	19.7
9	20.52	20.316	20.148	20.125	19.889	19.81
10	21.471	20.355	20.17	20.141	19.931	19.816
11	21.505	20.377	20.225	20.206	19.947	19.817
12	21.516	20.43	20.289	20.273	20.018	19.867
13	21.52	20.44	20.325	20.312	20.053	19.921
14	21.521	21.001	20.353	20.342	20.07	19.935
15	21.547	21.05	20.353	20.35	20.101	19.985
16	22.103	21.104	20.357	20.351	20.137	20.014
17	22.552	21.12	20.358	20.351	20.14	20.018
18	22.565	21.12	20.358	20.353	20.14	20.026
19	23.574	21.33	20.362	20.354	20.141	20.03
20	23.574	22.476	20.415	20.379	20.143	20.107
21	23.716	22.602	21.799	20.747	20.382	20.141
22	24.136	22.974	21.305	21.235	20.831	20.143
23	24.62	23.098	22.943	21.852	21.371	20.382
24	25.269	24.969	22.804	22.691	22.148	20.831
25	26.364	25.148	23.967	23.828	23.202	21.002
26	28.136	27.858	25.642	25.472	24.726	22.226
27	29.807	28.451	28.158	27.095	27.038	24.018
28	36.972	33.371	32.026	31.012	30.575	27.075
29	38.869	37.215	36.98	35.486	35.248	33.148
30	49.827	46.843	45.202	43.805	42.385	40.018

The history match resulting from best 10 permeability maps are shown in Figure 6.10. Included in this figure are the field observation data for comparison. GA methodology appears to be working satisfactory in finding a reasonable match. The simulator predictions using the best permeability map obtained from application of AGA are compared with the field data in Figure 6.11. As seen in this figure, the oil production and GOR continue to show good match. The initial high values of GOR in the first year cannot be predicted from the model for reasons not well understand. It is, however, possible that the calculations of PVT properties may be in error which was fixed at a later date. The water cut match also reasonable barring some period around 2003. The reason for the mismatch during this period is not clear and must perhaps be

related to some unusual event. Also a course grid of 100m x 100m was used in the present case but one can expect better match if a finer grid say 25m x 25m or a normal grid, 50 m x 50m was used. This was not attempted since that would have increased GA variables to 16 or 4 times making simulation calculation very lengthy. Usually it is difficult to match everything over the entire time period owing to inhomogeneities and structural complexities of actual reservoirs, no matter which history matching technique is used. The bottom hole pressure, however, shows a much better match in the entire range, validating the history matching procedure developed in this study.

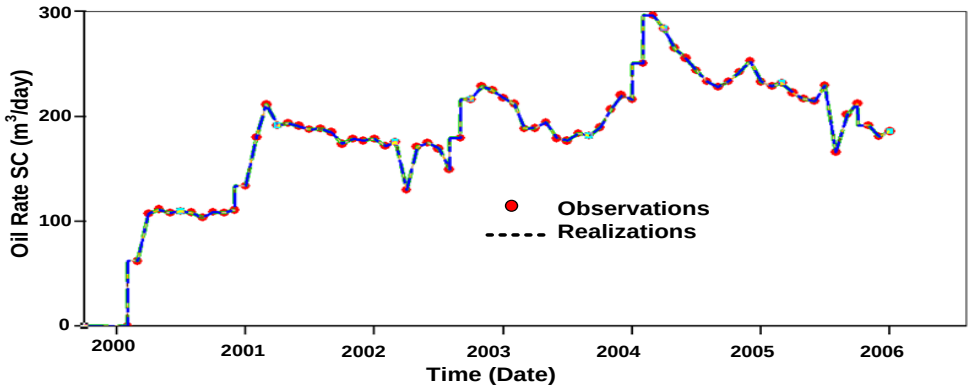

(a)

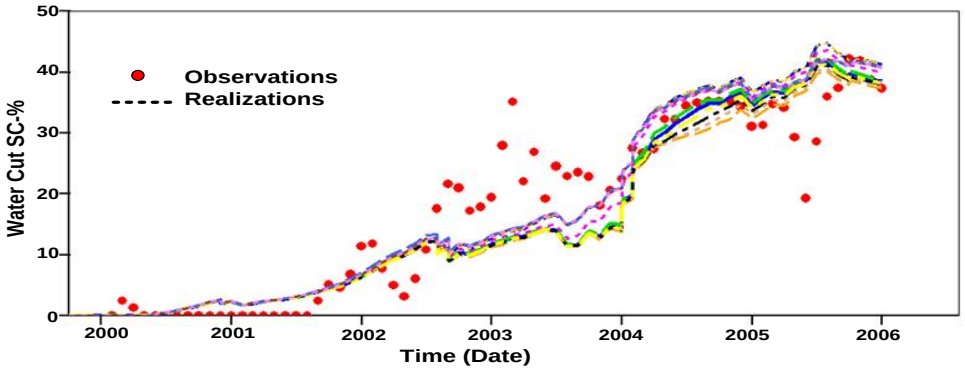

(b)

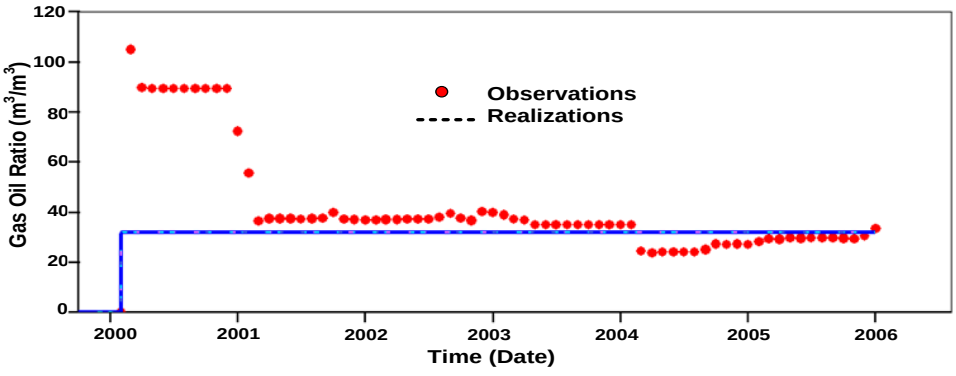

(c)

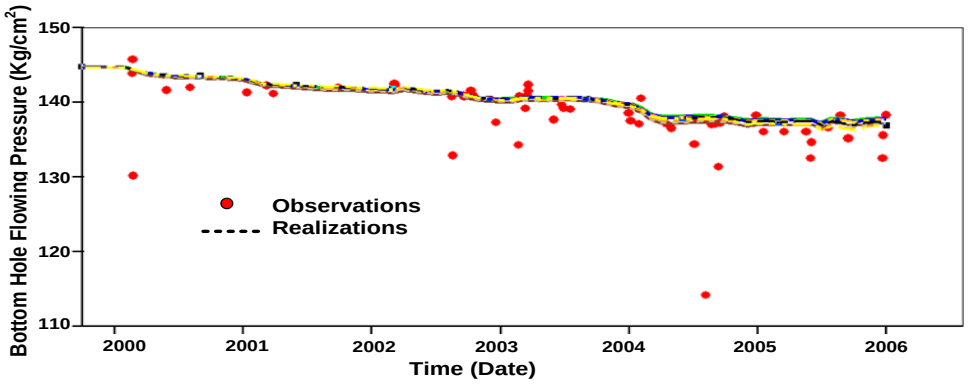

(d)

Figure 6.10. History match for entire field from best 10 permeability realizations resulting from AGA (a) oil production rate (m3/day) (b) Water cut -% (c) GOR (m3/m3) (d) BHP (kg/cm2)

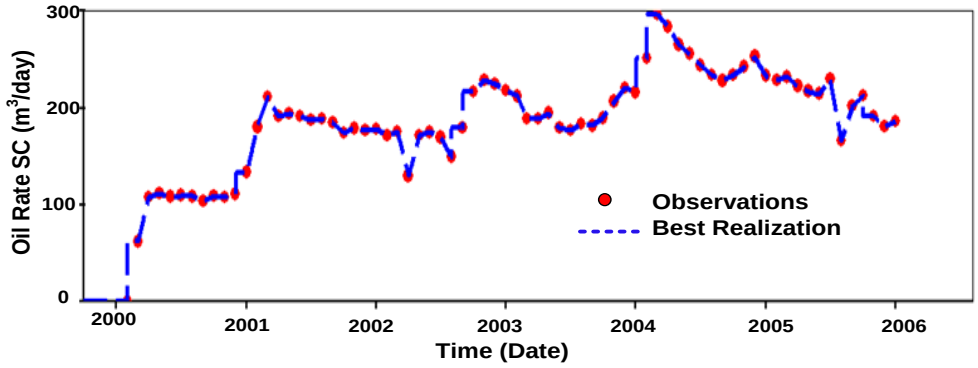

(a)

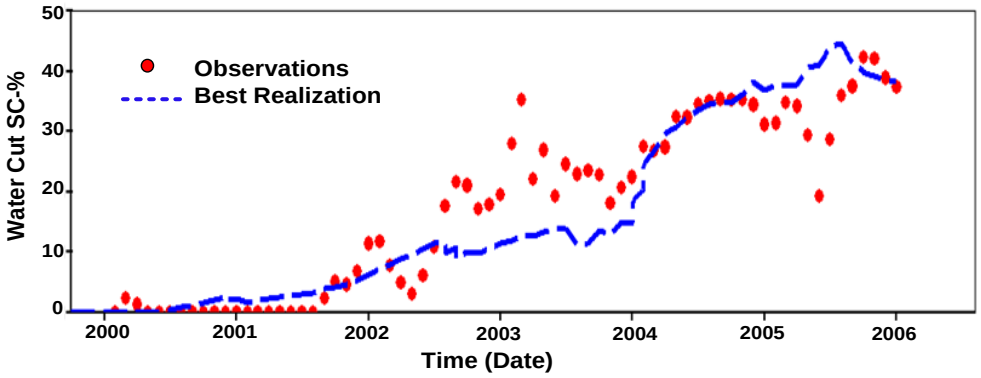

(b)

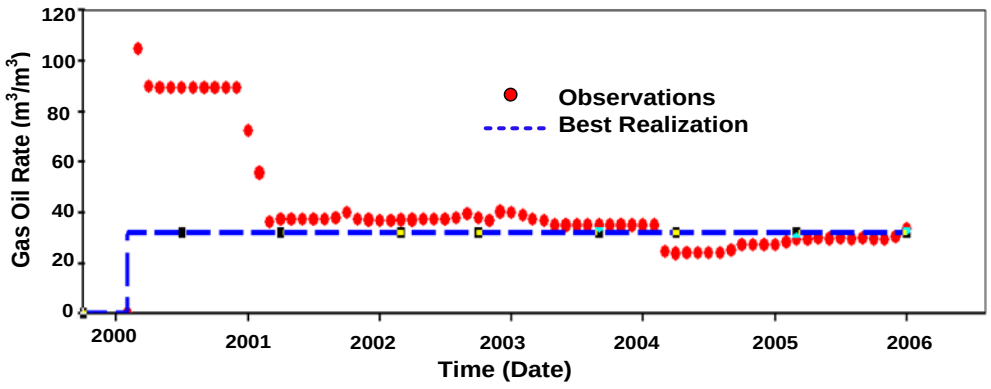

(c)

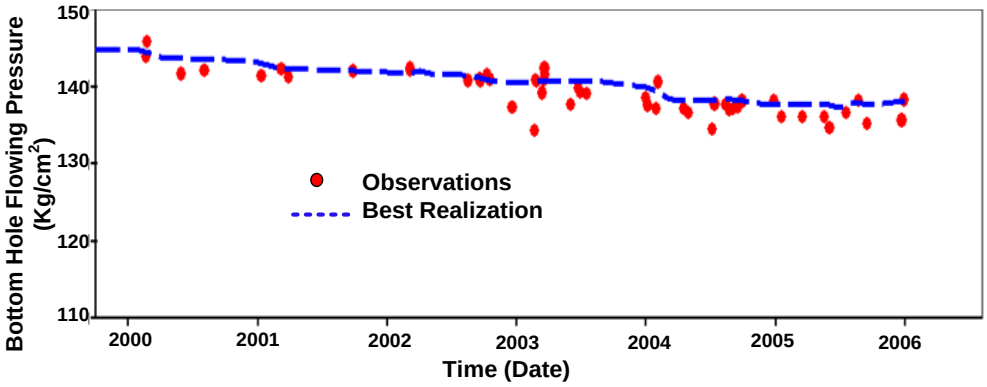

(d)

Figure 6.11. History match for entire field from the best permeability realization generated by AGA (a) oil production rate (m3/day) (b) Water cut -% (c) GOR (m3/m3) (d) BHP (kg/cm2).

6.5.3 Validation of the Reservoir Model

The history matched reservoir permeability map based on data from 6 wells for a period March, 2000 ~ December, 2005, with CMG® - IMEX™ simulator was used to predict the reservoir performance over the next three years (January, 2006 ~ December, 2008). The model predicted values were compared with field data available for this period but not used for model development (history matching). These comparisons are shown in Figure 6.12 which also includes the data for the period; March, 2000 ~ December, 2005 which were used in GA methodology. A very good match, during 2006 ~ 2008, between simulator results and field data lends support to the technique of extracting reservoir properties using GA optimization.

Two new wells (Well-7 and Well-8) were drilled in 2009, their locations are marked in Figure 6.1. The production from these wells was included in the cumulative production data (from all the 8 wells) for the period January ~ September, 2009. For this period, the validated model was used to predict the productions profile and Figure 6.12 includes these comparisons for the said period. This further confirms the GA calculated permeability map is indeed realistic and capable of future predictions as well as field development by way of drilling new wells.

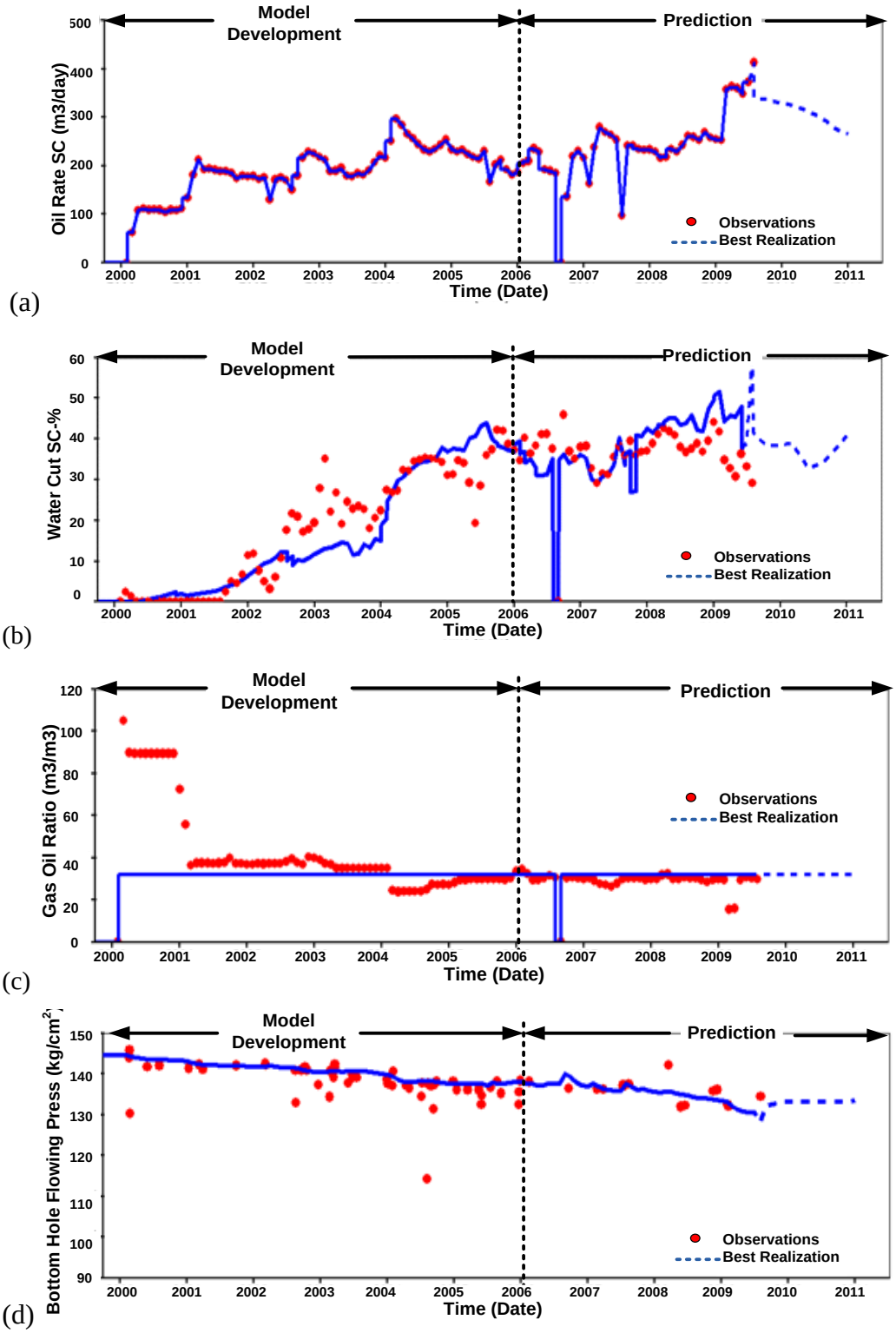

Figure 6.12. Production forecast of using history matched model from 6 wells (2006 ~ 2008) and 8 wells (2009) (a) oil production rate (m3/day) (b) Water cut -% (c) GOR (m3/m3) (d) BHP (kg/cm2).

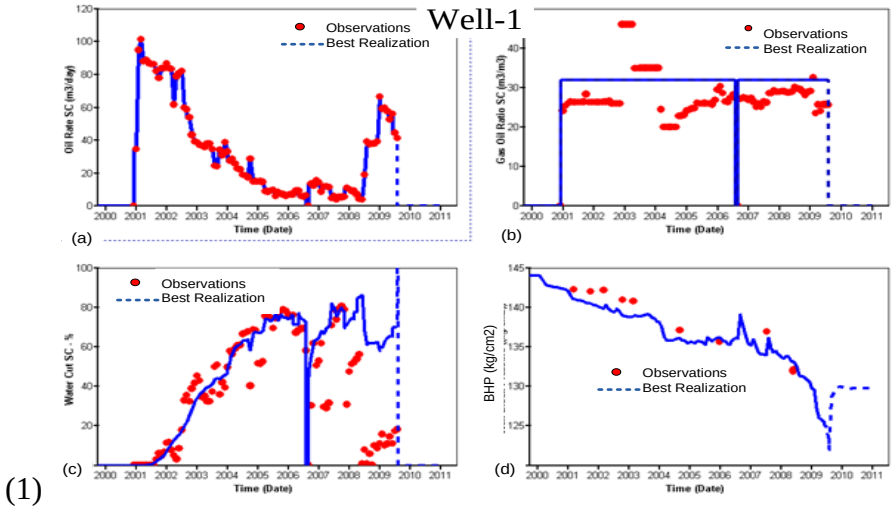
Well-1
Observations
Best Realization
Oil Rate SC (m3/day)
Gas Oil Ratio SC (m3/m3)
Water Cut SC - %
BHP (kg/cm2)
Time (Date)
(a)
(b)
(c)
(d)

(1)

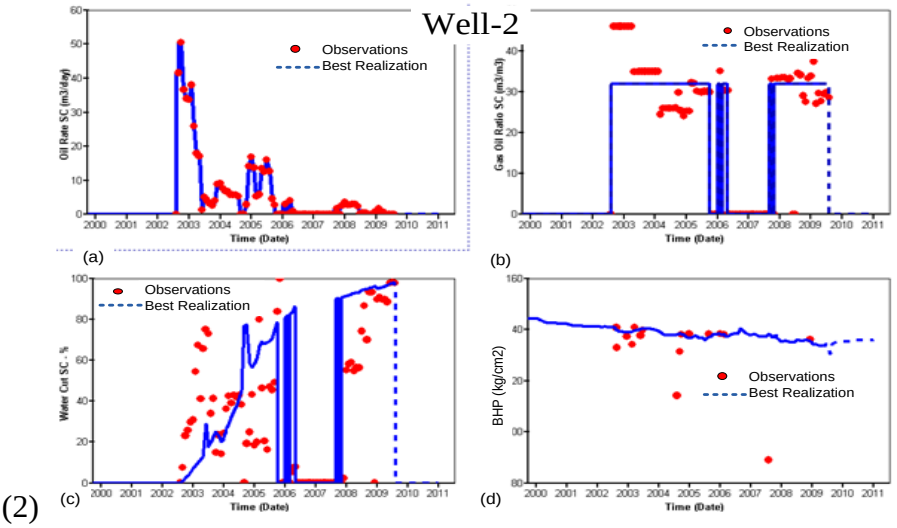
Well-2
Observations
Best Realization
Oil Rate SC (m3/day)
Gas Oil Ratio SC (m3/m3)
Water Cut SC - %
BHP (kg/cm2)
Time (Date)
(a)
(b)
(c)
(d)

(2)

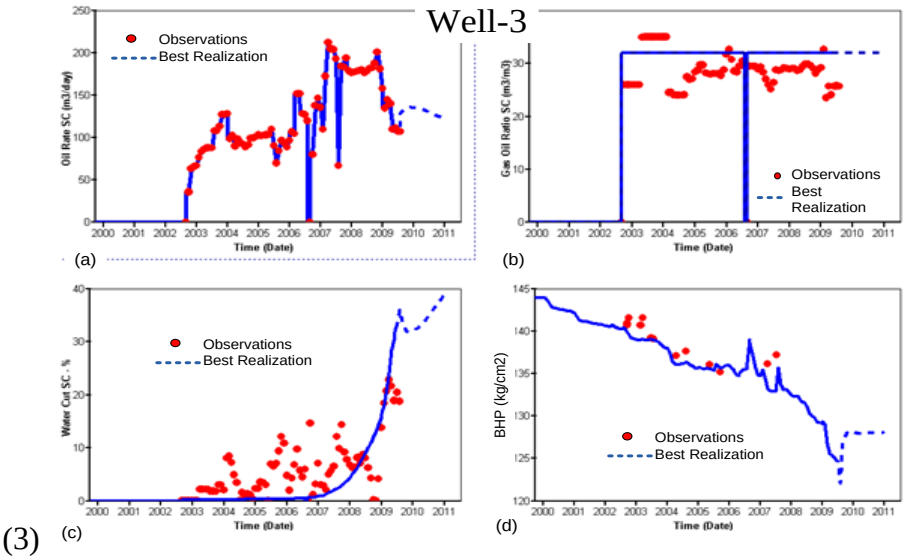
Well-3
Observations
Best Realization
Oil Rate SC (m3/day)
Gas Oil Ratio SC (m3/m3)
Water Cut SC - %
BHP (kg/cm2)
Time (Date)
(a)
(b)
(c)
(d)

(3)

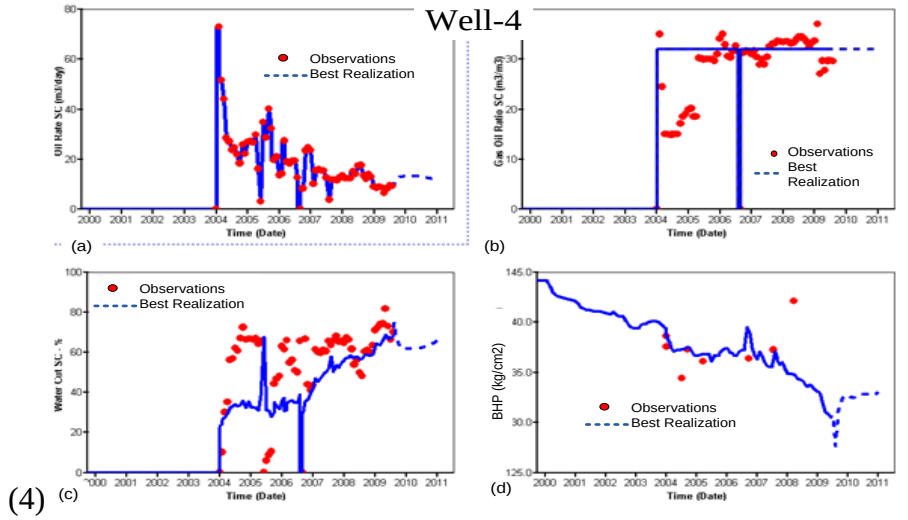
Well-4
Observations
Best Realization
Oil Rate SC (m3/day)
Gas Oil Ratio SC (m3/m3)
Water Cut SC - %
BHP (kg/cm2)
Time (Date)
(a)
(b)
(c)
(d)

(4)

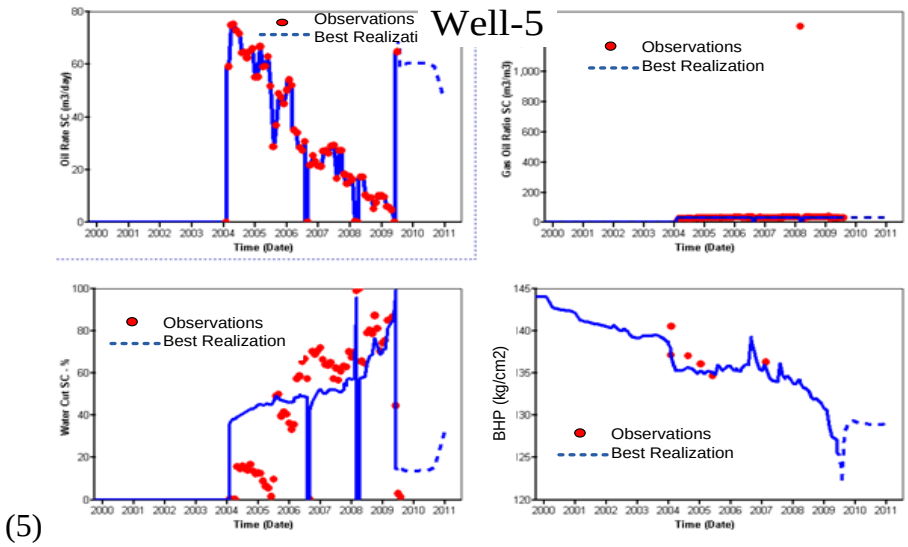
Well-5
Observations
Best Realizati
Best Realization
Oil Rate SC (m3/day)
Gas Oil Ratio SC (m3/m3)
Water Cut SC - %
BHP (kg/cm2)
Time (Date)

(5)

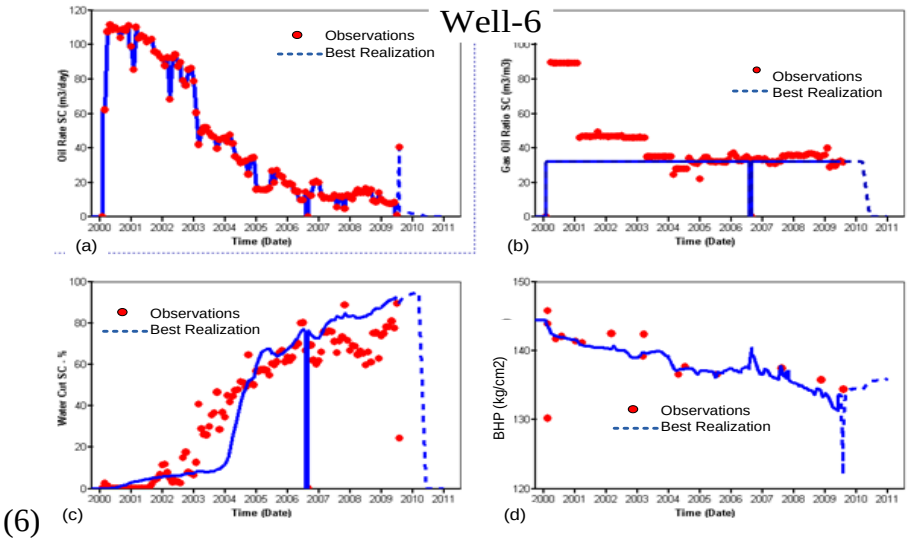
Well-6
Observations
Best Realization
Oil Rate SC (m3/day)
Gas Oil Ratio SC (m3/m3)
Water Cut SC - %
BHP (kg/cm2)
Time (Date)
(a)
(b)
(c)
(d)

(6)

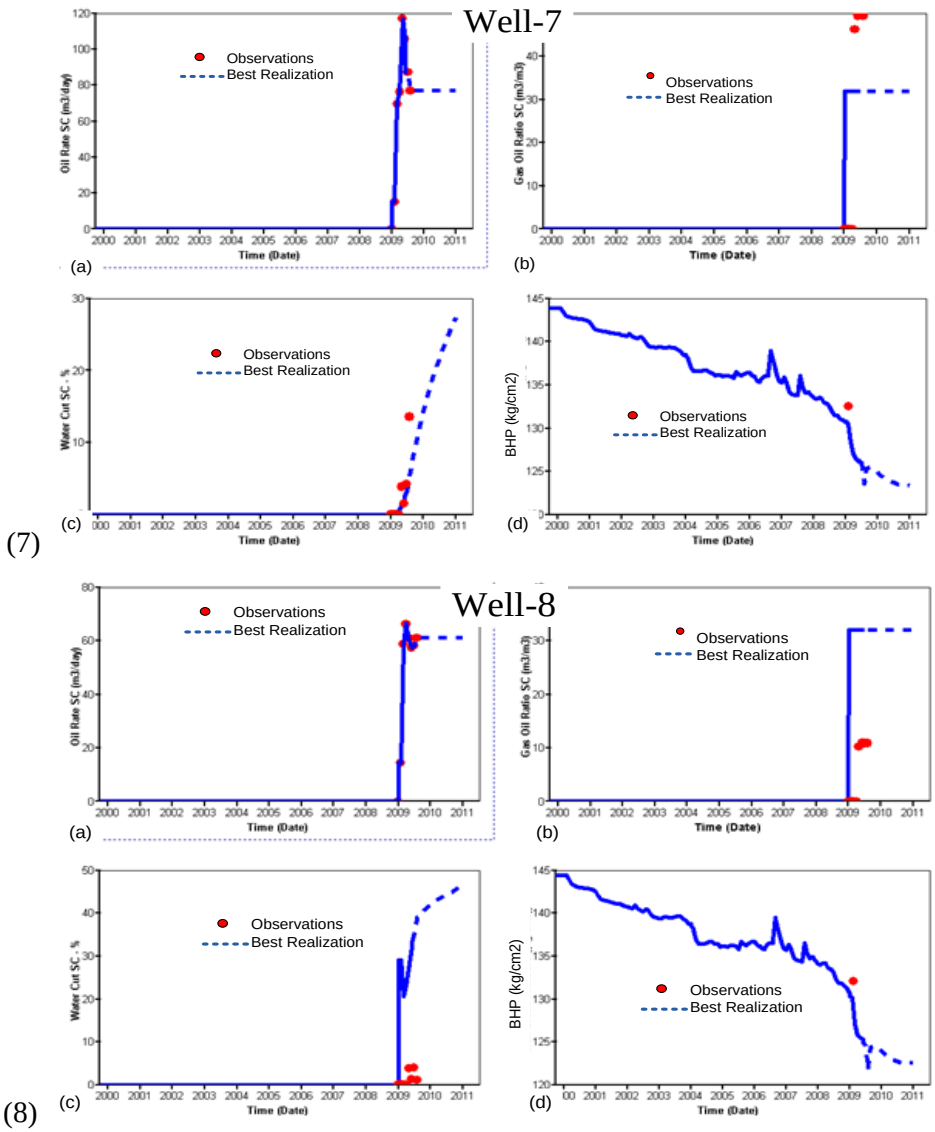

Figure 6.13. History match and production forecast of individual wells in terms of (a) oil production rate (b) GOR (c) WC and (d) BHP. (1) Well-1 (2) Well-2 (3) Well-3 (4) Well-4 (5) Well-5 (6) Well-6 (7) Well-7 (8) Well-8.

Figure 6.13 shows a match between model predictions and field production data including bottom hole flowing pressure for individual wells (Well-1 to Well-8), for the entire period from 2000 to 2009. For Well-7 and Well-8, the field data are available for a few months only. For these wells the bottom hole pressure (BHP) predictions have been made for the entire duration which for the period between 2000 ~ 2008, simply means what the pressure profile would have been if these wells existed at these locations.

CHAPTER-7

CONCLUSIONS AND RECOMMENDATIONS

This chapter discusses the contributions from the present work, the extent of success achieved from the developed methodologies for forecasting oil production and history matching. Few recommendations for further research directions have also been included in this chapter.

7.1 CONCLUSIONS

The developed higher order neural network (HONN) model has proved to be an effective and successful tool for petroleum reservoir production forecasting. The prediction of cumulative oil production, using higher order neural network was successfully accomplished with mean absolute error of less than 5% when used on a real reservoir. Second and third order networks required fewer neurons in the hidden layer and converged faster with smaller prediction error compared to linear or first order networks (ANN). Production forecasting for a single well using HONN showed a much larger error because of interference from the presence of other producing wells in the vicinity. Preprocessing the input data, which included production from individual wells, was found to be important in reducing noise and thereby improving network learning rate. A simple low pass moving average filter was found to be effective in reducing measurement noise. Another important factor was the selection of input parameters. Autocorrelation function (ACF) and cross-correlation function (CCF) provided valuable information regarding time lags which helped in the choice of input variables optimally.

The successful application of genetic algorithm in extracting a realistic permeability map of a 2D synthetic reservoir showed the technique as a promising optimization tool towards automatic history matching. The history matched model when used with CMG flow simulator was able to predict production of oil and gas which was in good agreement with actual productions. The results were comparable to

those reported by Chitralekha, et al., (2010) for the same 2D reservoir using Ensemble Kalman Filtering technique. Adaptive genetic algorithm (AGA), in which crossover and mutation probabilities are dynamically adjusted according to the population fitness through generations outperformed simple GA (SGA). AGA required less than half the iterations and resulted in smaller fitness function values as compared to SGA. This validated history matching methodology using GA as optimization tool was then applied to a real 3D petroleum reservoir. The results showed good match for oil production rate, gas-oil ratio (GOR), bottom hole flowing pressure (BHP) and reasonable match for water cut (WC). The WC mismatch during the period around 2003 and initial high value for GOR production may be due to unusual events and perhaps error in the PVT calculations. The coarse grid size, with each block measures 100m x 100m, used in the present investigation may have contributed to higher error in certain wells. AGA was found to be more efficient and accurate as compared to SGA for the real 3D reservoir also. Successful match of historic production of oil, water and gas and satisfactory future predictions from existing and new wells drilled at later date in the reservoir established the power and efficacy of the technique.

7.2 RECOMMENDATIONS

The following aspects based on the discussion through the chapters of this thesis can be considered for further extension of this research work.

- It may be possible to extend the HONN methodology into making a tool for reservoir characterization (finding porosity and permeability distribution maps), which can correlate the rock properties with the seismic and well log data as inputs.
- In the present study, history matching using GA was attempted only with permeability distribution map characterization. The GA technique can be further extended to include other parameters such as porosity, transmissibility, aquifer properties, initial depth of water-oil contact and connate water saturation in the search vector to improve the efficacy of history match.
- The current study is based on history matching of simple 3D black-oil reservoir having 8 wells only. GA code can be extended further to handle more complex and large reservoirs having large number of wells.

- The coarse grid block size used in the present study may have introduced some error by not properly accounting for spatial variations in rock properties. The GA code could be extended to use smaller grid block size for greater accuracy.

REFERENCE

Abdassah, D., Mucharam, L., Soengkowo, I., Trikoranto, H., and Sumantri, R., 1996. "Coupling Seismic Data With Simulated Annealing Method Improves Reservoir Characterization," in *SPE Asia Pacific Oil and Gas Conference*, 28-31 October 1996, Adelaide, Australia.

Agbalaka, C. and Oliver, D., 2008. "Application of the EnKF and Localization to Automatic History Matching of Facies Distribution and Production Data," *Mathematical Geosciences*, vol. 40, pp. 353-374.

Al-Fattah, S.M. and Startzman, R.A., 2001. "Predicting Natural Gas Production Using Artificial Neural Network," in *SPE Hydrocarbon Economics and Evaluation Symposium*, 2-3 April 2001, Dallas, Texas.

Ali Ahmadi, M., Zendehboudi, S., Lohi, A., Elkamel, A., and Chatzis, I., 2012. "Reservoir Permeability Prediction by Neural Networks Combined With Hybrid Genetic Algorithm and Particle Swarm Optimization," *Geophysical Prospecting*, vol. 61, pp. 582-598.

Alkaabi, A.U. and Lee, W.J., 1993. "Using Artificial Neural Nets to Identify the Well-Test Interpretation Model," *SPE Formation Evaluation* vol. 8, pp. 233-240.

Aminzadeh, F., Barhen, J., Glover, C.W., and Toomarian, N.B., 2000. "Reservoir Parameter Estimation Using a Hybrid Neural Network," *Computational Geosciences*, vol. 26, pp. 869-875.

Amir, H., Rasul, R., and Mohammad, H.S., 2013. "Improving Performance of a Neural Network Model by Artificial Ant Colony Optimization for Predicting Permeability of Petroleum Reservoir Rocks," *Middle-East Journal of Scientific Research*, vol. 13, pp. 1217-1223.

Anterion, F., Eymard, R., and Karcher, B., 1989. "Use of Parameter Gradients for Reservoir History Matching," in *SPE Symposium on Reservoir Simulation*, 6-8 February,Houston, Texas.

Arroyo-Negrete, E., Devegowda, D., Datta-Gupta, A., and Choe, J., 2008. "Streamline-Assisted Ensemble Kalman Filter for Rapid and Continuous Reservoir Model Updating," *SPE Reservoir Evaluation and Engineering*, vol. 11, pp. 1046-1060.

Awotunde, A.A., 2012. "Reservoir Parameter Estimation With Improved Particle Swarm Optimization," in *SPE Annual Technical Conference and Exhibition*, 8-10 October, San Antonio, Texas, USA.

Azadeh, A., Ghaderi, S.F., and Sohrabkhani, S., 2007. "Forecasting Electrical Consumption by Integration of Neural Network, Time Series and ANOVA," *Applied Mathematics and Computation,* vol. 186, pp. 1753-1761.

Aziz, K. and Settari, A., 1979. *Petroleum Reservoir Simulation*. London: Applied Science Publishers.

Ballester, P.J. and Carter, J.N., 2004. "An Effective Real-parameter Genetic Algorithm With Parent Centric Normal Crossover for Multimodal Optimization," in *Lecture Notes in Computer Science, 3102*, Deb, K., Ed.: Springer, pp. 901-913.

Ballester, P.J. and Carter, J.N., 2007. "A Parallel Real-coded Genetic Algorithm for History Matching and its Application to a Real Petroleum Reservoir," *Journal of Petroleum Science and Engineering,* vol. 59, pp. 157-168.

Bi, Z., Oliver, D.S., and Reynolds, A.C., 2000. "Conditioning 3D Stochastic Channels to Pressure Data," *Society of Petroleum Engineers Journal,* vol. 5, pp. 474-484.

Birk, A., Demiris, J., Lee, W.-P., Hallam, J., and Lund, H., 1998. "Learning Complex Robot Behaviours by Evolutionary Computing With Task Decomposition," in *Learning Robots*. vol. 1545: Springer Berlin Heidelberg, pp. 155-172.

Bissell, R., 1994. "Calculating Optimal Parameters for History Matching," in *4th European Conference on theMathematics of Oil Recovery*.

Bissell, R., Dubrule, O., Lamy, P., Swaby, P., and Lepine, O., 1997. "Combining Goestatistical Modelling With Gradient Information for History Matching: The Pilot Point Method," in *SPE Annual Technical Conference and Exhibition,* San Antonio, Texas, pp. 139–154.

Box, G.E.P. and Jenkins, G.M., 1976. *Time Series Analysis : Forecasting and Control*. San Francisco: Holden-Day.

Bush, M.D. and Carter, J.N., 1996. "Application of a Modified Genetic Algorithm to Parameter Estimation in the Petroleum Industry," in *Intelligent Engineering Systems Through Artificial Neural Networks 6,* New York,: ASME Press, pp. 397-402.

Caers, J., 2003. "Efficient Gradual Deformation Using a Streamline-Based Proxy Method," *Journal of Petroleum Science and Engineering,* vol. 39, pp. 57-83.

Carter, R.D., L.F, K., Pierce, A.C., and Williams, D.L., 1974. "Performance Matching With Constraints," *SPE Journal,* vol. 14, pp. 187-196.

Castellano-Mendez, M., Gonzalez-Manteiga, W., Febrero-Bande, M., Prada-Sanchez, J.M., and Lozano-Calderon, R., 2004. "Modelling of the Monthly and Daily Behaviour of the Runoff of the Xallas River Using Box-Jenkins and Neural Networks Methods," *Journal of Hydrology,* vol. 296, pp. 38-58.

Cerný, V., 1985. "Thermodynamical Approach to the Traveling Salesman Problem: An Efficient Simulation Algorithm," *Journal of Optimization Theory and Applications,* vol. 45, pp. 41-51.

Chakra, N.C., Song, K.-Y., Gupta, M.M., and Saraf, D.N., 2013.a. "An Innovative Neural Forecast of Cumulative Oil Production from a Petroleum Reservoir Employing Higher-order Neural Networks (HONNs)," *Journal of Petroleum Science and Engineering,* vol. 106, pp. 18-33.

Chakra, N.C.C., Song, K.-Y., Saraf, D.N., and Gupta, M.M., 2013.b. "Production Forecasting of Petroleum Reservoir applying Higher-Order Neural Networks (HONN) with Limited Reservoir Data," *International Journal of Computer Applications,* vol. 72, pp. 23-35.

Chavent, G., Dupuy, M., and Lemonnier, P., 1975. "History Matching by Use of Optimal Theory," *SPE Journal,* vol. 15, pp. 74-86.

Chen, W.H., Gavalas, G.R., Seinfeld, J.H., and Wasserman, M.L., 1974. "A New Algorithm for Automatic History Matching," *SPE Journal,* vol. 14, pp. 593-608.

Chen, Y., Oliver, D.S., and Zhang, D., 2008. "Efficient Ensemble-Based Closed-Loop Production Optimization," *SPE Symposium on Improved Oil Recovery,* vol. 1, pp. 205-223.

Chen, Z., 2007. *Reservoir Simulation Mathematical Techniques in Oil Recovery*. Philadelphia, PA: Society for Industrial and Applied Mathematics.

Chen, Z., Huan, G., and Ma, Y., 2006. "Computational Methods for Multiphase Flows in Porous Media," in *Computational Science and Engineering.* Philadelphia: Society for Industrial and Applied Mathematics.

Chidambaram, P. and Ertekin, T., 2009. "Development and Testing of an Artificial Neural Network Based History Matching Protocol to Characterize Reservoir Properties," in *Department of Energy and Mineral Engineering* PhD Thesis: The Pennsylvania State University

Chitralekha, S.B., Trivedi, J.J., and Shah, S.L., 2010. "Application of the Ensemble Kalman Filter for Characterization and History Matching of Unconventional Oil Reservoirs," in *Canadian Unconventional Resources and International Petroleum Conference,* 19-21 October, Calgary, Alberta, Canada.

Choudhary, M.K., Yoon, S., and Ludvigsen, B.E., 2007. "Application of Global Optimization Methods for History Matching and Probabilistic Forecasting - Case Studies," in *SPE Middle East Oil and Gas Show and Conference,* 11-14 March, Kingdom of Bahrain.

Christie, M., Demyanov, V., and Erbas, D., 2006. "Uncertainty Quantification for Porous Media Flows," *Journal of Computational Physics,* vol. 217, pp. 143-158.

Christie, M.A. and Blunt, M.J., 2001. "Tenth SPE Comparative Solution Project: A Comparison of Upscaling Techniques,," *SPE Reservoir Evaluation and Engineering* vol. 4, pp. 308-317.

Chu, L., Reynolds, A.C., and Oliver, D.S., 1995. "Computation of Sensitivity Coefficients for Conditioning the Permeability Feild to Well-Test Pressure Data," *In Situ,* vol. 19, pp. 179-223.

CMG®. http://www.cmgl.ca/soft-imex.

Coats, K.H., Dempsey, J.R., and Henderson, J.H., 1970. "A New Technique for Determining Reservoir Description from Field Performance Data," *SPE Journal,* vol. 10, pp. 66-74.

Cominelli, A., Ferdinandi, F., de Montleau, P.C., and Rossi, R., 2007. "Using Gradients To Refine Parameterization in Field-Case History-Matching Projects," *SPE Reservoir Evaluation and Engineering,* vol. 10, pp. 233-240.

Contreras-Moreira, B., Fitzjohn, P.W., Marc, O., Smith, G.R., and Bates, P.A., 2003. "Novel Use of a Genetic Algorithm for Protein Structure Prediction: Searching Template and Sequence Alignment Space," *Proteins,* p. 424.

Cosentino, L., 2001. *Integrated Reservoir Studies*. Paris: Editions Technip.

Crichlow, H.B., 1977. *Modern Reservoir Engineering - A Simulation Approach*. Englewood Cliffs, N.J: Prentice-Hall.

Cuypers, M., Dubrule, O., Lamy, P., and Bissell, R., 1998. "Optimal Choice of Inversion Parameters for History-Matching with the Pilot Method," in *6th European Conference on the Mathematics of Oil Recovery,* 08 September, Peebles.

Dadashpour, M., 2009. "Reservoir Characterization Using Production Data and Time-Lapse Seismic Data," Thesis, *Dep. of Petroleum Engineering and Applied Geophysics*: Norwegian University of Science and Technology.

Dam, M. and Saraf, D.N., 2006. "Design of Neural Networks Using Genetic Algorithm for On-Line Property Estimation of Crude Fractionator Products," *Computers & Chemical Engineering*, vol. 30, pp. 722-729.

De Jong, K.A., 1988. "An Analysis of the Behavior of a Class of Genetic Adaptive Systems," PhD Thesis, University of Michigan.

de Marsily, G., Lavedan, G., Boucher, M., and Fasanino, G., 1984. "Interpretation of Interference Tests in a Well Field Using Geostatistical Techniques to Fit the Permeability Distribution in a Reservoir Model," in *Geostatistics for Natural Resources Characterization*, Part 2 ed: D. Reidel Pub. Co, pp. 831-849.

Deb, K., 1998. *Optimization for Engineering Design : Algorithms and Examples*. New Delhi Prentice-Hall of India.

Deschamps, T., Grussaute, T., Mayers, D., and Bissell, R., 1998. "The Results of Testing Six Different Gradient Optimisers on Two History Matching Problems," in *6th European Conference on the Mathematics of Oil Recovery*, 08 September, Peebles, Scotland.

Deutsch, C.V., 2002. *Geostatistical Reservoir Modeling*: Oxford University Press.

Deutsch, C.V. and Journel, A.G., 1994. "The Application of Simulated Annealing to Stochastic Reservoir Modeling," *SPE Advanced Technology Series*, vol. 2, pp. 222-227.

Deutsch, C.V. and Journel, A.G., 1998. *GSLIB: Geostatistical Software Library and User's Guide*, Second Edition ed.: Oxford University Press.

Donaldson, R.G., Kamstra, M., and Kim, H.Y., 1993. *Evaluating Alternative Models for Conditional Stock Volatility : Evidence from International Data*. Thesis, Burnaby, B.C.: Simon Fraser University, Dep. of Economics.

Dong, Y. and Oliver, S., 2005. "Quantitative Use of 4D Seismic Data for Reservoir Description," *SPE Journal*, vol. 10, pp. 91-99.

Dorigo, M., Maniezzo, V., and Colorni, A., 1996. "Ant System: Optimization by a Colony of Cooperating Agents," *IEEE Transactions on Systems, Man, and Cybernetics - Part B*, vol. 26, pp. 29-41.

Eiben, A.E., Hinterding, R., and Michalewicz, Z., 1999. "Parameter Control in Evolutionary Algorithms," *IEEE Transaction on Evolutionary Computation*, vol. 3, pp. 124-141.

Eiben, A.E. and Smith, J.E., 2003. *Introduction to Evolutionary Computing*. New York: Springer.

Emerick, A.A. and Reynolds, A.C., 2011. "History Matching a Field Case Using the Ensemble Kalman Filter With Covariance Localization," *SPE Reservoir Evaluation and Engineering*, vol. 14, pp. 443-452.

Emerick, A.A. and Reynolds, A.C., 2013. "Investigation of the Sampling Performance of Ensemble-Based Methods With a Simple Reservoir Model," *Computational Geosciences*, vol. 17, pp. 325-350.

Erbaş, D. and Christie, M.A., 2007. "Effect of Sampling Strategies on Prediction Uncertainty Estimation," in *SPE Reservoir Simulation Symposium*, 26-28 February, Houston, Texas, U.S.A.

Ertekin, T., Abou-Kassem, J.H., and King, G.R., 2001. *Basic Applied Reservoir Simulation*. Richardson, Tex.: Society of Petroleum Engineers.

Evensen, G., 1994. "Sequential Data Assimilation with a Nonlinear Quasi-Geostrophic Model Using Monte Carlo Methods to Forecast Error Statistics," *Journal of Geophysical Research: Oceans*, vol. 99, pp. 10143-10162.

Eydinov, D., Gao, G., Li, G., and Reynolds, A.C., 2009. "Simultaneous Estimation of Relative Permeability and Porosity/ Permeability Fields by History Matching Production Data," *Journal of Canadian Petroleum Technology*, vol. 48, pp. 13-25.

Fanchi, J.R., 2001. *Principles of Applied Reservoir Simulation*, , Second ed. Boston, USA: Gulf Professional Publ.

Farmer, C.L., 1989. "The Mathematical Generation of Reservoir Geology," in *Joint IMA/SPE Eur. Conf. on the Mathematics of Oil Recovery*, July 25-27,Cambridge University, UK. .

Fasanino, G., Molinard, J.E., de Marsily, G., Pelce, V., and Gaz de, F., 1986. "Inverse Modeling in Gas Reservoirs," in *SPE Annual Technical Conference and Exhibition*, 5-8 October,New Orleans, Louisiana,United States: Society of Petroleum Engineers,Richardson, TX.

Fatemeh, R. and Farhang, J.-F., 2008. "Oil Production Optimization in Petroleum Reservoirs by Ant Algorithm," *Chemical Product and Process Modeling*, vol. 3, pp. 1934-2659.

Fernandez-Prieto, J.A., Canada-Bago, J., Gadeo-Martos, M.A., and Velasco, J.R., 2010. "A Case Study of Parameter Control in a Genetic Algorithm: Computer Network Performance," in *Mobile Lightweight Wireless Systems*. vol. 45: Springer Berlin Heidelberg, pp. 650-661.

Fernández Martïnez, J., Mukerji, T., Echeverría Ciaurri, D., and García Gonzalo, E., 2009. "Application of Particle Swarm Optimization for Enhanced Reservoir

Characterization and Inversion of Production and Seismic Data," in *American Geophysical Union - Fall Meeting Abstracts*.

Floris, F.J.T., 1996. "Direct Conditioning of Gaussian Random Fields to Dynamic Production Data," in *5th European Conference on the Mathematics of Oil Recovery* , 3-6 Spetember, Leoben, Austria.

Foss, B. and Jensen, J.P., 2011. "Performance Analysis for Closed-Loop Reservoir Management," *SPE Journal*, vol. 16, pp. 183-190.

Gao, G. and Reynolds, A.C., 2006. "An Improved Implementation of the LBFGS Algorithm for Automatic History Matching," *SPE Journal*, vol. 11, pp. 5-18.

Gao, G., Zafari, M., and Reynolds, A.C., 2006. "Quantifying Uncertainty for the PUNQ-S3 Problem in a Bayesian Setting With RML and EnKF," *SPE Journal*, vol. 11, pp. 506-515.

Gavalas, G.R., Shah, P.C., and Seinfeld, J.H., 1976. "Reservoir History Matching by Bayesian Estimation," *SPE Journal*, vol. 16, pp. 337-350.

Gervais, V., Gautier, Y., Le Ravalec, M., and Roggero, F., 2007. "History Matching Using Local Gradual Deformation," in *EUROPEC/EAGE Conference and Exhibition*, 11-14 June, London, U.K.

Giles, C.L. and Maxwell, T., 1987. "Learning, Invariance, and Generalization in High-order Neural Networks," *Applied Optics*, vol. 26, pp. 4972-4978.

Goldberg, D.E., 1987. "Computer-Aided Pipeline Operation Using Genetic Algorithms and Rule Learning. PART I: Genetic Algorithms in Pipeline Optimization," *Engineering With Computers*, vol. 3, pp. 35-45.

Goldberg, D.E., 1989. *Genetic Algorithms in Search, Optimization, and Machine Learning*. Reading, Mass.: Addison-Wesley Pub. Co.

Gosh, J. and Shin, Y., 1992. "Effcient Higher-Order Neural Networks For Classification And Function Approximation," *International Journal of Neural Systems*, vol. 3, pp. 323-350.

Grefenstette, J., 1986. "Optimization of Control Parameters for Genetic Algorithms," *IEEE Transactions on Systems, Man, and Cybernetics*, vol. 16, pp. 122-128.

Gu, Y. and Oliver, D.S., 2005. "History Matching of the PUNQ-S3 Reservoir Model Using the Ensemble Kalman Filter," *SPE Journal*, vol. 10, pp. 217-224.

Guerreiro, J.N.C., Barbosa, H.J.C., Garcia, E.L.M., Loula, A.F.D., and Malta, S.M.C., 1998. "Identification of Reservoir Heterogeneities Using Tracer Breakthrough Profiles and Genetic Algorithms," *SPE Reservoir Evaluation & Engineering*, vol. 1, pp. 218-223.

Gul, A., 2011. "Applications of Ensemble Kalman Filter for Characterization and History Matching of SAGD Reservoirs," Thesis, *Dep. of Petroluem Engineering*, University of Alberta, Edmonton, Alberta.

Guojian, C., Yao, A., Zhe, W., and Kai, Z., 2012. "Oil Well Placement Optimization Using Niche Particle Swarm Optimization," in *Eighth International Conference on- Computational Intelligence and Security (CIS),*, Guangzhou, 17-18 Nov., pp. 61-64.

Gupta, M.M., 2008. "Correlative Type Higher-Order Neural Units With Applications," in *IEEE International Conference on Automation and Logistics*, 1-3 Sept., pp. 715-718.

Gupta, M.M., Homma, N., Hou, Z.-G., Solo, A.M.G., and Bukovsky, I., 2010. "Higher Order Neural Networks: Fundamentals Theroy and Appplications," in *Artificial Higher-Order Neural Networks for Computer Science and Engineeing: Trends for emerging Applications*, Zhang, M., Ed.: Information Science Reference, pp. 397-422.

Gupta, M.M., Jin, L., and Homma, N., 2003. "Static and Dynamic Neural Networks from Fundamentals to Advanced Theory," New York: Wiley.

Gupta, M.M. and Rao, D.H., 1994. "Neuro-Control Systems : Theory and Applications," in *IEEE Neural Networks Council* New York: IEEE Press.

Habiballah, W.A., Startzman, R.A., and Barrufet, M.A., 1996. "Use of Neural Networks for Prediction of Vapor/Liquid Equilibrium K Values for Light-Hydrocarbon Mixtures," *SPE Reservoir Engineering*, vol. 11, pp. 121-126.

Hajizadeh, Y., 2011. "Population-Based Algorithms for Improved History Matching and Uncertainty Quantification of Petroleum Reservoirs," *Thesis*, Heriot-Watt University Petroleum Engineering.

Hajizadeh, Y., Christie, M., and Demyanov, V., 2011. "Ant Colony Optimization for History Matching and Uncertainty Quantification of Reservoir Models," *Journal of Petroleum Science and Engineering*, vol. 77, pp. 78-92.

Han, Y., Park, C., and Kang, J.M., 2011. "Prediction of Nonlinear Production Performance in Waterflooding Project Using a Multi-Objective Evolutionary Algorithm," *Energy Exploration and Exploitation*, vol. 29, pp. 129-142.

Haugen, V., Naevdal, G., Natvik, L.J., Evensen, G., Berg, A.M., and Flornes, K.M., 2008. "History Matching Using the Ensemble Kalman Filter on a North Sea Field Case," *SPE Journal*, vol. 13, pp. 382-391.

He, N., Reynolds, A., and Oliver, D., 1997. "Three-Dimensional Reservoir Description From Multiwell Pressure Data and Prior Information," *SPE Journal*, vol. 2, pp. 312-327.

Heidari, L., Gervais, R., Ravalec, M.L., and Wackernagel, H., 2013. "History Matching of Petroleum Reservoir Models by the Ensemble Kalman Filter and Parameterization Methods," *Computational Geosciences*, vol. 55, pp. 84-95.

Herrera, F. and Lozano, M., 2003. "Fuzzy Adaptive Genetic Algorithms: Design, Taxonomy, and Future Directions," *Soft Computing*, vol. 7, pp. 545-562.

Hill, T., Marquez, L., O'Connor, M., and Remus, W., 1994. "Artificial Neural Network Models for Forecasting and Decision Making," *International Journal of Forecasting*, vol. 10, p. 5.

Hirasaki, G., 1975. "Sensitivity Coefficients for History Matching Oil Displacement Processes," *SPE Journal*, vol. 15, pp. 39-49.

Hoffman, B.T., 2005. "Geologically Consistent History Matching While Perturbing Facies," in *Dept. of Petroleum Engineering*: Stanford University.

Holland, J.H., 1975. *Adaptation in Natural and Artificial Systems : An Introductory Analysis With Applications to Biology, Control, and Artificial Intelligence*. Ann Arbor: University of Michigan Press.

Homma, N. and Gupta, M.M., 2002. "Superimposing Learning for Backpropagation Neural Networks," in *Bulletin of College of Medical Sciences*. vol. 11: Tohoku University, pp. 253-259.

Hou, Z.-G., Song, K.-Y., Gupta, M., and Tan, M., 2007. "Neural Units with Higher-Order Synaptic Operations for Robotic Image Processing Applications," *Soft Computing*, vol. 11, pp. 221-228.

Hu, L.Y., 2000. "Gradual Deformation and Iterative Calibration of Gaussian-Related Stochastic Models," *Mathematical Geology*, vol. 32, pp. 87-108.

Hu, L.Y., Blanc, G., and Nœtinger, B., 2001. "Gradual Deformation and Iterative Calibration of Sequential Stochastic Simulations," *Mathematical Geology*, vol. 33, pp. 475-489.

Hu, L.Y. and Jenni, S., 2005. "History Matching of Object-Based Stochastic Reservoir Models," *SPE Journal*, vol. 10, pp. 312-323.

Huang, Y., Wong, P.M., and Gedeon, T.D., 1998. "Prediction of Reservoir Permeability Using Genetic Algorithms," *AI Applications*, vol. 12, pp. 67-75.

Huang, Y., Wong, P.M., and Gedeon, T.D., 2000. "Permeability Prediction in Petroleum Reservoir Using a Hybrid System," in *Soft Computing in Industrial*

Applications, Suzuki, Roy, Ovaska, Furuhashi, and Dote, Eds. London: Springer-Verlag.

Irani, R. and Nasimi, R., 2012. "An Evolving Neural Network Using an Ant Colony Algorithm for a Permeability Estimation of the Reservoir," *Petroleum Science and Technology*, vol. 30, pp. 375-384.

Jacquard, P. and Jains, C., 1965. "Permeability Distribution From Field Pressure Data," *SPE Journal,* vol. 5, pp. 281-294.

Jafarpour, B. and McLaughlin, D., 2008. "History Matching With an Ensemble Kalman Filter and Discrete Cosine Parameterization," *Computational Geosciences,* vol. 12, pp. 227-244.

Jahns, H., 1966. "A Rapid Method for Obtaining a Two-Dimensional Reservoir Description From Well Pressure Response Data," *SPE Journal,* vol. 6, pp. 315 - 327.

Jutila, H.A. and Goodwin, N.H., 2006. "Schedule Optimisation to Complement Assisted History Matching And Prediction Under Uncertainty," in *SPE Europec/EAGE Annual Conference and Exhibition,* 12-15 June, Vienna, Austria.

Kathrada, M., 2009. "Uncertainty Evaluation of Reservoir Simulation Models Using Particle Swarms and Hierarchical Clustering," PhD Thesis, Heriot-Watt University.

Kennedy, J. and Eberhart, R., 1995. "Particle Swarm Optimization " in *Proceedings of IEEE International Conference on Neural Networks, .* vol. 4, pp. 1942-1948

Killough, J.E., Sharma, Y., Dupuy, A., Bissell, R., and Wallis, J., 1995. "A Multiple Right Hand Side Iterative Solver for History Matching," in *SPE Reservoir Simulation Symposium, 12-15 February* San Antonio, Texas.

Kirkpatrick, S., Gelatt, C.D., and Vecchi, M.P., 1983. *Optimization by Simulated Annealing*. New York: IMB Thomas J. Watson Research Center.

Kovalenko, A., Mannseth, T., and Nævdal, G., 2012. "Sampling Error Distribution for the Ensemble Kalman Filter Update Step," *Computational Geosciences,* vol. 16, pp. 455-466.

Kromah, M.J., Liou, J., and MacDonald, D.G., 2005. "Step Change in Reservoir Simulation Breathes Life Into a Mature Oil Field," in *SPE Latin American and Caribbean Petroleum Engineering Conference,* 20-23 June, Rio de Janeiro, Brazil.

Kruger, W.D., 1961. "Determining Areal Permeability Distribution by Calculations," *Journal of Petroleum Technology*, vol. 13, pp. 691-696.

Landa, J.L., 1997. "Reservoir Parameter Estimation Constrained to Pressure Transients, Performance History and Distributed Saturation Data," PhD Thesis, *Deptartment of Petroleum Engineering*, Stanford University.

Landa, J.L. and Horne, R.N., 1997. "A Procedure to Integrate Well Test Data, Reservoir Performance History and 4-D Seismic Information into a Reservoir Description," in *SPE Annual Technical Conference and Exhibition*, San Antonio, Texas: Society of Petroleum Engineers, Inc.

Landa, J.L., Kalia, R.K., Nakano, A., Nomura, K., and Vashishta, P., 2005. "History Match and Associated Forecast Uncertainty Analysis - Practical Approaches Using Cluster Computing," in *International Petroleum Technology Conference* Doha, Qatar.

Lange, A.G., 2009. "Assisted History Matching for the Characterization of Fractured Reservoirs," in *AAPG Bulletin*. vol. 93, pp. 1609-1619.

Lee, Y.C., Doolen, G., Chen, H.H., Sun, G.Z., Maxwell, T., Lee, H.Y., and Giles, C.L., 1986. "Machine Learning Using a Higher Order Correlation Network," *Phys. D*, vol. 2, pp. 276-306.

Li, R., Reynolds, A.C., and Oliver, D.S., 2003. "History Matching of Three-Phase Flow Production Data," *SPE Journal*, vol. 8, pp. 328-340.

Li, X., 2008. "Continuous Reservoir Model Updating by Ensemble Kalman Filter on Grid Computing Architectures," PhD Thesis, Louisiana State University, Baton Rouge.

Li, Y.-x., Yuan, K.-h., Tong, X.-a., Zhu, K.-j., and Wei, W., 2010 "A Dynamic Clustering Based on Hybrid PS-ACO for Recognizing Oil-Bearing Reservoir," in *International Conference on Computational and Information Sciences (ICCIS)*, , 17-19 Dec, Chengdu, 17-19 Dec. 2010, pp. 1204-1207.

Li, Y., Ang, K., Chong, G., Feng, W., Tan, K., and Kashiwagi, H., 2004. "CAutoCSD-Evolutionary Search and Optimisation Enabled Computer Automated Control System Design," *International Journal of Automation and Computing*, vol. 1, pp. 76-88.

Liang, B., 2007. "An Ensemble Kalman Filter Module for Automatic History Matching," PhD Thesis, University of Texas, Austin.

Liang, B., Alpak, F.O., Sepehrnoori, K., and Delshad, M., 2007. "A Singular Evolutive Interpolated Kalman Filter for Rapid Uncertainty Quantification," in

SPE Reservoir Simulation Symposium, 26-28 February, Houston, Texas, U.S.A.

Litvak, M.L. and Angert, P.F., 2009. "Field Development Optimization Applied to Giant Oil Fields," in *SPE Reservoir Simulation Symposium*, 2-4 February, The Woodlands, Texas.

Liu, N. and Oliver, D.S., 2005. "Critical Evaluation of the Ensemble Kalman Filter on History Matching of Geologic Facies," *SPE Reservoir Evaluation And Engineering,* vol. 8, pp. 470-477.

Liu, N. and Oliver, S., 2004. "Automatic History Matching of Geologic Facies," *SPE Journal* vol. 9, pp. 429-436.

Lodoen, O.P. and Omre, H., 2008. "Scale-Corrected Ensemble Kalman Filtering Applied to Production-History Conditioning in Reservoir Evaluation," *SPE Journal,* vol. 13, pp. 177-194.

Lorentzen, R.J., Nævdal , G., and Lage, A.C.V.M., 2003. "Tuning of Parameters in a Two-Phase Flow Model Using an Ensemble Kalman Filter," *International Journal of Multiphase Flow*, vol. 29, pp. 1283-1309.

Makhlouf, E.M., Chen, W.H., Wasserman, M.L., and Seinfeld, J.H., 1993. "A General History Matching Algorithm for Three-Phase, Three-Dimensional Petroleum Reservoirs. ," *SPE Advanced Technology Series,* vol. 1, pp. 83-91.

Maschio, C., de Carvalho, C.P.V., and Schiozer, D.J., 2010. "A New Methodology to Reduce Uncertainties in Reservoir Simulation Models Using Observed Data and Sampling Techniques," *Journal of Petroleum Science and Engineering,* vol. 72, pp. 110-119.

Mattax, C.C. and Dalton, R.L., 1990. *Reservoir simulation*. Richardson, TX: Henry L. Doherty Memorial Fund of AIME, Society of Petroleum Engineers.

Mayer, A.S. and Huang, C., 1999. "Development and Application of a Coupled-Process Parameter Inversion Model Based on the Maximum Likelihood Estimation Method," *Advances in Water Resources,* vol. 22, pp. 841-853.

Milliken, W.J., Emanuel, A.S., and Chakravarty, A., 2001. "Applications of 3D Streamline Simulation To Assist History Matching," *SPE Reservoir Evaluation And Engineering,* vol. 4, pp. 502-508.

Mohaghegh, S., Richardson, M., and Ameri, S., 2001. "Use of Intelligent Systems in Reservoir Characterization Via Synthetic Magnetic Resonance Logs," *Journal of Petroleum Science and Engineering,* vol. 29, pp. 189-204.

Mohamed, L., Christie, M., and Demyanov, V., 2010. "Comparison of Stochastic Sampling Algorithms for Uncertainty Quantification," *SPE Journal*, vol. 15, pp. 31-38.

Monfared, A.D., Helalizadeh, A., and Parvizi, H., 2012. "Automatic History Matching Using the Integration of Response Surface Modeling With a Genetic Algorithm," *Petroleum Science and Technology*, vol. 30, pp. 360-374.

Montoya-O, S.J., Jovel-T, W.A., Hernandez-R, J.A., and Gonzalez-R, C., 2000. "Genetic Algorithms Applied to the Optimum Design of Gas Transmission Networks," in *SPE International Petroleum Conference and Exhibition*, 1-3 February, Villahermosa, Mexico.

Murgante, B., Gervasi, O., Misra, S., Nedjah, N., Rocha, A.M.A.C., Taniar, D., Apduhan, B.O., Santos Amorim, E.P., Xavier, C.R., Campos, R.S., and Santos, R.W., 2012. "Comparison between Genetic Algorithms and Differential Evolution for Solving the History Matching Problem," in *Computational Science and Its Applications*. vol. 7333: Springer Berlin Heidelberg, pp. 635-648.

Nævdal, G., Mannseth, T., and Vefring, E.H., 2002. "Near-Well Reservoir Monitoring Through Ensemble Kalman Filter," in *SPE/DOE Improved Oil Recovery Symposium*, 13-17 April, Tulsa, Oklahoma.

Nayak, P.C., Sudheer, K.P., Rangan, D.M., and Ramasastri, K.S., 2004. "A Neuro-Fuzzy Computing Technique for Modeling Hydrological Time Series," *Journal of Hydrology*, vol. 291, pp. 52-66.

Nwankwor, E., Nagar, A.K., and Reid, D.C., 2013. "Hybrid Differential Evolution and Particle Swarm Optimization for Optimal Well Placement," *Computational Geosciences*, vol. 17, pp. 249-268.

Odinukwe, J. and Correia, C., 2010. "History Matching and Uncertainty Assessment of the Norne Field E-Segment Using Petrel RE," Thesis, *Dept of Petroleum Engineering and Applied Geophysics*: Norwegian University of Science and Technology.

Oliver, D.S. and Chen, Y., 2011. "Recent Progress on Reservoir History Matching: A Review," *Computational Geosciences*, vol. 15, pp. 185-221.

Oliver, D.S., Liu, N., and Reynolds, A.C., 2008. "Inverse Theory for Petroleum Reservoir Characterization and History Matching," Cambridge; New York: Cambridge University Press.

Onwunalu, J.E. and Durlofsky, L.J., 2010. "Application of a Particle Swarm Optimization Algorithm for Determining Optimum Well Location and Type," *Computational Geosciences*, vol. 14, pp. 183-198.

Ouenes, A., 1992. "Application of Simulated Annealing to Reservoir Characterization and Petrophysics Inverse Problems ". PhD Thesis, New Mexico Institute of Mining and Technology.

Ouenes, A., Fasanino, G., France;, G.d., and Lee, R.L., 1992. "Simulated Annealing for Interpreting Gas/Water Laboratory Corefloods," in *SPE Annual Technical Conference and Exhibition*, 4-7 October 1992, Washington, D.C.

Ouenes, A. and Saad, N., 1993. "A New, Fast Parallel Simulated Annealing Algorithm for Reservoir Characterization," in *SPE Annual Technical Conference and Exhibition*, 3-6 October 1993, Houston, Texas.

Ouenes, A., Weiss, W.W., Sultan, A.J., Gum, T., and Brooks, L.C., 1994. "A New Method To Characterize Fractured Reservoirs: Applications to Infill Drilling," in *SPE/DOE Improved Oil Recovery Symposium*, 17-20 April, Tulsa, Oklahoma.

Panda, M.N. and Lake, L.W., 1993. "Parallel Simulated Annealing for Stochastic Reservoir Modeling," in *SPE Annual Technical Conference and Exhibition*, 3-6 October 1993, Houston, Texas.

Parish, R., Calderbank, V., Watkins, A., Muggeridge, A., Goode, A., and Robinson, P., 1993. "Effective History Matching: The Application of Advanced Software Techniques to the History-Matching Process," in *SPE Symposium on Reservoir Simulation*, 28 February-3 March, New Orleans, Louisiana.

Phale, H.A. and Oliver, D.S., 2011. "Data Assimilation Using the Constrained Ensemble Kalman Filter," *SPE Journal*, vol. 16, pp. 331-342.

Picek, S., Golub, M., and Jakobovic, D., 2012. "Evaluation of Crossover Operator Performance in Genetic Algorithms with Binary Representation," *Lecture notes in computer science.*, pp. 223-230.

Popa, A.S., Sivakumar, K., and Cassidy, S., 2012. "Associative Data Modeling and Ant Colony Optimizaton Approach for Waterflood Analysis," in *SPE Western Regional Meeting*, 21-23 March, Bakersfield, California, USA: SPE.

Portella, R.C.M. and Frais, E., 1999. "Use of Automatic History Matching and Geostatistical Simulation to Improve Production Forecast " in *SPE Latin American and Caribbean Petroleum Eng. Conf.*, April 21-23,Caracas, Venezuela.

Ravalec-Dupin, M.L. and Nœtinger, B., 2002. "Optimization With the Gradual Deformation Method," *Mathematical Geology*, vol. 34, pp. 125-142.

Redlapalli, S.K., 2004. "Development of Neural Units with Higher-order Synaptic Operations and Their Applications to Logic Circuits and Control Poblems," PhD Thesis, *Department of Mechanical Engineering*, Canada: University of Saskatchewan.

Reynolds, A.C., He, N., Chu, L., and Oliver, D.S., 1996. "Reparameterization Techniques for Generating Reservoir Descriptions Conditioned to Variograms and Well-Test Pressure Data," *SPE Journal*, vol. 1, pp. 413-426.

Rodrigues, J.R.P., 2006. "Calculating Derivatives for Automatic History Matching," *Computational Geosciences*, vol. 10, pp. 119-136.

Roggero, F. and Hu, L.Y., 1998. "Gradual Deformation of Continuous Geostatistical Models for History Matching," in *SPE Annual Technical Conference and Exhibition*, 27-30 September, New Orleans, Louisiana.

Romero, C.E. and Carter, J.N., 2001. "Using Genetic Algorithms for Reservoir Characterisation," *Journal of Petroleum Science and Engineering*, vol. 31, pp. 113-123.

Rotondi, M., Nicotra, G., Godi, A., Contento, F.M., Blunt, M.J., and Christie, M.A., 2006. "Hydrocarbon Production Forecast and Uncertainty Quantification: A Field Application," in *SPE Annual Technical Conference and Exhibition*, 24-27 September, San Antonio, Texas, USA.

Rumelhart, D.E. and McClelland, J.L., 1986. *Parallel Distributed Processing : Explorations in the Microstructure of Cognition*. Cambridge, Mass.: MIT Press.

Rutkowski, L., Tadeusiewicz, R., Zadeh, L., Zurada, J., Razavi, F., and Jalali-Farahani, F., 2008. "Ant Colony Optimization: A Leading Algorithm in Future Optimization of Petroleum Engineering Processes," in *Artificial Intelligence and Soft Computing- ICAISC 2008*. vol. 5097: Springer Berlin Heidelberg, pp. 469-478.

Sagar, R.K., Kelkar, M.G., and Thompson, L.G., 1995. "Reservoir Description by Integrating Well-Test Data and Spatial Statistics," *SPE Formation Evaluation*, vol. 10, pp. 267-274.

Saleri, N.G. and Toronyi, R.M., 1998. "Engineering Control in Reservoir Simulation: Part I," in *Annual Technical Conference and Exhibition,2-5 October 1988*, Houston, Texas: Society of Petroleum Engineers.

Sambridge, M., 1999. "Geophysical Inversion With a Neighbourhood Algorithm-II. Appraising the Ensemble," *Geophysical Journal International,* vol. 138, pp. 727-746.

Schaffer, J.D. and Morishma, A., 1987. "An Adaptive Crossover Mechanism for Genetic Algorithms," in *Proc. Second Int. Conf Genetic Algorithms*, pp. 36-40.

Schmitt, L.M., 2004. "Theory of Genetic Algorithms II: Models for Genetic Operators Over the String-Tensor Representation of Populations and Convergence to Global Optima for Arbitrary Fitness Function under Scaling," *Theoretical Computer Science*, vol. 310, pp. 181-231.

Sen, M.K., Datta-Gupta, A., Stoffa, P.L., Lake, L.W., and Pope, G.A., 1995. "Stochastic Reservoir Modeling Using Simulated Annealing and Genetic Algorithms," *SPE Formation Evaluation,* vol. 10, pp. 49-56.

Shah, S., Gavalas, G.R., and Seinfeld, J.H., 1978. "Error Analysis in History Matching: The Optimum Level of Parameterization," *SPE Journal,* vol. 18, pp. 219-228.

Shahkarami, A., 2012. "Artificial Intelligence Assisted History Matching -- Proof of Concept," *Thesis,*West Virginia University- United States, p. 120.

Sivanandam, S.N. and Deepa, S.N., 2007. "Introduction to Genetic Algorithms," Berlin; New York: Springer.

Skjervheim, J.A., Evensen, G., Aanonsen, S.I., Ruud, B.O., and Johansen, T.A., 2007. "Incorporating 4D Seismic Data in Reservoir Simulation Models Using Ensemble Kalman Filter," *SPE Journal*, vol. 12, pp. 282-292.

Slater, G.E. and Durrer, E.J., 1971. "Adjustment of Reservoir Simulation Models to Match Field Performance," *SPE Journal*, vol. 11, pp. 295-305.

Smith, S.W., 1997. *The Scientist and Engineer's Guide to Digital Signal Processing*. San Diego, California: California Technical Pub.

Soleng, H.H., 1999. "Oil Reservoir Production Forecasting With Uncertainty Estimation Using Genetic Algorithms," in *Proceedings of the 1999 Congress on Evolutionary Computing*, Washington, DC.

Song, K.-Y., Gupta, M.M., and Jena, D., 2009. "Design of an Error-Based Robust Adaptive Controller," in *IEEE International Conference on Systems, Man and Cybernetics*, pp. 2386-2390.

Sousa, S.H.G., Maschio, C., and Schiozer, D.J., 2006. "Scatter Search Metaheuristic Applied to the History-Matching Problem," in *SPE Annual Technical Conference and Exhibition*, 24-27 September, San Antonio, Texas, USA.

Srinivas, M. and Patnaik, L.M., 1994. "Adaptive Probabilities of Crossover and Mutation in Genetic Algorithms," *IEEE Transactions on Systems, Man and Cybernetics,* vol. 24, pp. 656-667.

Subbey, S., Christie, M., and Sambridge, M., 2004. "Prediction Under Uncertainty in Reservoir Modeling," *Journal of Petroleum Science and Engineering,* vol. 44, pp. 143-153.

Sultan, A.J., Ouenes, A., and Weiss, W.W., 1993. "Reservoir Description by Inverse Modeling: Application to EVGSAU Field," in *SPE Annual Technical Conference and Exhibition*, 3-6 October, Houston, Texas.

Suzuki, S., Caumon, G., and Caers, J., 2008. "Dynamic Data Integration for Structural Modeling: Model Screening Approach Using a Distance-Based Model Parameterization," *Computational Geosciences,* vol. 12, pp. 105-119.

Tamhane, D., Wong, P.M., Aminzadeh, F., and Nikravesh, M., 2000. "Soft Computing for Intelligent Reservoir Characterization," in *SPE Asia Pacific Conference on Integrated Modelling for Asset Management*, 25-26 April, Yokohama, Japan.

Tan, T. and Kalogerakis, N., 1992. "A Three - Dimensional Three - Phase Automatic History Matching Model: Reliability of Parameter Estimates," *Journal of Canadian Petroleum Technology,* vol. 31, pp. 34-41.

Tanaka, Y., Ishiguro, A., and Uchikawa, Y., 1994. "An Analytical Method for Inverse Problems in Electromagnetics Using Genetic Algorithms," *IEEJ Transactions on Industry Applications,* vol. 114, pp. 689-696.

Tang, H., 2012. "An Improved Adaptive Genetic Algorithm," in *Knowledge Discovery and Data Mining*. vol. 135: Springer Berlin Heidelberg, pp. 717-723.

Tavakoli, R., Pencheva, G., Wheeler, M., and Ganis, B., 2013. "A Parallel Ensemble-Based Framework for Reservoir History Matching and Uncertainty Characterization," *Computational Geosciences,* vol. 17, pp. 83-97.

Thomas, L., Hellums, L.J., and Reheis, G.M., 1972. "A Nonlinear Automatic History Matching Technique for Reservoir Simulation Models," *SPE Journal,* vol. 12, pp. 508-514.

Tiwari, M.K., Chatterjee, C., Song, K.-Y., and Gupta, M.M., 2012. "River-Flow Forecasting Using Higher-Order Neural Networks," *Journal of Hydrologic Engineering,* vol. 17, pp. 655-666.

Tokar, A.S. and Johnson, P.A., 1999. "Rainfall-Runoff Modeling Using Artificial Neural Networks," *Journal of Hydrologic Engineering,* vol. 4, pp. 232-239.

Vefring, E.H., Nygaard, G., Lorentzen, R.J., Naevdal, G., and Fjelde, K.K., 2006. "Reservoir Characterization During Underbalanced Drilling (UBD): Methodology and Active Tests," *SPE Journal,* vol. 11, pp. 181-192.

Velez-Langs, O., 2005. "Genetic Algorithms in Oil Industry: An Overview," *Journal of Petroleum Science and Engineering,* vol. 47, pp. 15-22.

Walker, G.J., Kromah, M., Pham, H., Adeyeye, D., and Winchester, A., 2008. "Assisted History Matching as a Useful Business Tool: An Example from Trinidad," in *SPE Indian Oil and Gas Technical Conference and Exhibition,* 4-6 March, Mumbai, India.

Wang, L. and Shen, T., 2001. "Improved Adaptive Genetic Algorithm and Its Application to Image Segmentation," in *Proc. SPIE 4550, Image Extraction, Segmentation, and Recognition*, pp. 115-120.

Wang, L. and Tang, D.-b., 2011. "An Improved Adaptive Genetic Algorithm Based on Hormone Modulation Mechanism for Job-Shop Scheduling Problem," *Expert Systems With Applications,* vol. 38, pp. 7243-7250.

Watson, A.T., Seinfeld, J.H., Gavalas, G.R., and Woo, P.T., 1980. "History Matching in Two-Phase Petroleum Reservoirs," *SPE Journal,* vol. 20, pp. 521-532.

Weiss, W.W., Balch, R.S., and Stubbs, B.A., 2002. "How Artificial Intelligence Methods Can Forecast Oil Production," in *SPE/DOE Improved Oil Recovery Symposium,* 13-17 April 2002, Tulsa, Oklahoma.

Wen, X.H. and Chen, W.H., 2005. "Real-Time Reservoir Model Updating Using Ensemble Kalman Filter," in *SPE Reservoir Simulation Symposium,* 31 January -2 Feburary , The Woodlands, Texas.

Wen, X.H., Deutsch, C.V., and Cullick, A.S., 1998. "High-Resolution Reservoir Models Integrating Multiple-Well Production Data," *SPE Journal* vol. 3, pp. 344-355.

Whitley, D. and Starkweather, T., 1990. "GENITOR II: A Distributed Genetic Algorithm," *Journal of Experimental & Theoretical Artificial Intelligence,* vol. 2, pp. 189-214.

Williams, G.J.J., Mansfield, M., MacDonald, D.G., and Bush, M.D., 2004. "Top-Down Reservoir Modelling," in *SPE Annual Technical Conference and Exhibition,* 26-29 September, Houston, Texas.

Williams, M.A., Keating, J.F., and Barghouty, M.F., 1998. "The Stratigraphic Method: A Structured Approach to History-Matching Complex Simulation Models," *SPE Reservoir Evaluation & Engineering,* vol. 1, pp. 169-176.

Wu, Z. and Datta-Gupta, A., 2002. "Rapid History Matching Using a Generalized Travel-Time Inversion Method," *SPE Journal*, vol. 7, pp. 113-122.

Wu, Z., Reynolds, A.C., and Oliver, D.S., 1999. "Conditioning Geostatistical Models to Two-Phase Production Data," *SPE Journal*, vol. 4, pp. 142-155.

Xue, G., Datta-Gupta, A., Valko, P., and Blasingame, T., 1997. "Optimal Transformations for Multiple Regression: Application to Permeability Estimation From Well Logs," *SPE formation evaluation*, vol. 12, pp. 85-94.

Yang, P.H. and Watson, A.T., 1988. "Automatic History Matching With Variable-Metric Methods," *SPE Reservoir Engineering*, vol. 3, pp. 995-1001.

Zafari, M. and Reynolds, A.C., 2007. "Assessing the Uncertainty in Reservoir Description and Performance Predictions With the Ensemble Kalman Filter," *SPE Journal*, vol. 12, pp. 382-391.

Zhang, F. and Reynolds, A.C., 2002. "Optimization Algorithms for Automatic History Matching of Production Data " in *8th European Conference on the Mathematics of Oil Recovery*, 3-6 September, Freiberg, Germany.

Zhang, F., Reynolds, A.C., and Oliver, D.S., 2003. "An Initial Guess for the Levenberg-Marquardt Algorithm for Conditioning a Stochastic Channel to Pressure Data," *Mathematical Geology*, vol. 35, pp. 67-88.

Zhang, Y. and Oliver, D.S., 2011. "History Matching Using the Ensemble Kalman Filter With Multiscale Parameterization: A Field Case Study," *SPE Journal*, vol. 16, pp. 307-317.

APPENDICES

APPENDIX—A: Source Code of HONN for reservoir production forecasting that has inbuilt smoother, ACF, CCF for choosing optimal neural inputs

Available with the authors

APPENDIX—B: Source Code of GA for History Matching

Available with the authors

APPENDIX—C: Data Used for Modeling of Real Reservoir

This section presents the relative permeability data used for real field modeling and the field historic data such as fluid production rate and bottom hole flowing pressure (BHP) used to compare the reservoir simulator response.

1. Relative Permeability Data

Layer-1			**Layer-2**			**Layer-3**		
Total Water Saturation (SWT)			**Total Water Saturation (SWT)**			**Total Water Saturation (SWT)**		
Sw	0.39		Sw	0.47		Sw	0.45	
Soirw	0.24		Soirw	0.21		Soirw	0.22	
Kro	0.984		Kro	0.984		Kro	0.984	
Krw	0.084		Krw	0.051		Krw	0.061	
Total Liquid Saturation (SLT)			**Total Liquid Saturation (SLT)**			**Total Liquid Saturation (SLT)**		
Sgc	0.01		Sgc	0.03		Sgc	0.05	
Krog	0.984		Krog	0.984		Krog	0.984	
Krg	0.776	at Swc+Soir	Krg	0.669	at Swc+Soir	Krg	0.698	at Swc+Soir

2. Production Field History of Entire Reservoir

Date	Oil (m^3/day)	Gas (m^3/day)	Water (m^3/day)	Date	Oil (m^3/day)	Gas (m^3/day)	Water (m^3/day)
2/1/2000	0	0	0	7/1/2003	183.814	6433.49	54.5738
3/1/2000	62.1497	6517.52	1.56897	8/1/2003	181.586	6355.48	55.9333
4/1/2000	107.442	9645.42	1.46774	9/1/2003	189.578	6635.13	56.066
5/1/2000	111.597	9966.93	0	10/1/2003	206.843	7239.54	45.6506
6/1/2000	108.435	9684.74	0	11/1/2003	220.352	7712.53	57.2029
7/1/2000	109.557	9782.03	0	12/1/2003	216.12	7564.32	62.541
8/1/2000	108.506	9690.06	0	1/1/2004	250.824	8778.88	95.2039
9/1/2000	103.887	9275.94	0	2/1/2004	296.624	7267.27	108.429
10/1/2000	108.773	9711.83	0	3/1/2004	283.882	6728.68	106.816
11/1/2000	108.149	9655.9	0	4/1/2004	265.315	6359.96	126.685
12/1/2000	110.889	9899.4	0	5/1/2004	255.698	6132.48	121.604
1/1/2001	133.642	9669.61	0	6/1/2004	243.967	5879.24	128.468
2/1/2001	180.365	10043.7	0	7/1/2004	233.499	5603.97	125.461
3/1/2001	191.274	7146.52	0	8/1/2004	228.186	5702.04	124.525
4/1/2001	193.902	7250.77	0	9/1/2004	233.58	6381.66	126.972
5/1/2001	191.05	7153.51	0	10/1/2004	242.384	6589.96	131.526
6/1/2001	187.749	7008.74	0	11/1/2004	253.107	6915.03	132.418
7/1/2001	188.678	7053.61	0	12/1/2004	233.179	6344.1	105.199
8/1/2001	185.097	6973.93	4.63645	1/1/2005	229.004	6467.09	104.346
9/1/2001	173.889	6933.1	9.29734	2/1/2005	232.116	6820.24	123.619
10/1/2001	178.851	6646.36	8.70581	3/1/2005	222.603	6505.29	115.333
11/1/2001	176.982	6556.4	12.841	4/1/2005	217.207	6471.31	90.0152
12/1/2001	178.487	6572.58	23.0107	5/1/2005	214.53	6342.84	51.2416
1/1/2002	171.804	6312.74	23.0594	6/1/2005	229.553	6812.2	91.8411
2/1/2002	175.783	6511.82	14.6479	7/1/2005	165.925	4919.58	93.1678
3/1/2002	129.809	4806.06	6.85033	8/1/2005	201.852	5990.94	120.797
4/1/2002	171.152	6387.83	5.598	9/1/2005	212.351	6285.24	154.727
5/1/2002	174.97	6525.48	11.3071	10/1/2005	191.695	5615.46	138.519
6/1/2002	169.451	6316.63	20.6673	11/1/2005	180.717	5498.93	114.775
7/1/2002	149.668	5685.32	31.9361	12/1/2005	185.979	6230.58	110.793
8/1/2002	179.549	7082.78	49.6548	1/1/2006	204.587	7043.97	108.779
9/1/2002	216.43	8163.57	57.4403	2/1/2006	209.229	6782.32	140.979
10/1/2002	229.096	8401.83	47.5858	3/1/2006	234.787	6933.28	134.35
11/1/2002	225.021	9037.6	49.0133	4/1/2006	228.956	6711.37	142.127
12/1/2002	217.92	8687.33	52.5122	5/1/2006	191.814	5838.32	134.106
1/1/2003	212.093	8240.19	82.2704	6/1/2006	189.096	5947.5	132.649
2/1/2003	188.402	6996.47	102.113	7/1/2006	184.06	5621.8	110.957
3/1/2003	188.965	6969	53.5991	8/1/2006	0	0	0
4/1/2003	194.626	6789	71.4166	9/1/2006	135.953	4126.07	115.48
5/1/2003	179.186	6260.74	42.5709	10/1/2006	218.896	6670.16	128.454
6/1/2003	176.9	6191.5	57.6167	11/1/2006	230.89	6989.07	124.959

Date	Oil (m^3/day)	Gas (m^3/day)	Water (m^3/day)
12/1/2006	215.21	6410.45	131.966
1/1/2007	162.644	4923.68	100.823
2/1/2007	237.712	6913.25	115.706
3/1/2007	278.696	7684.38	114.911
4/1/2007	268.754	7282.33	123.534
5/1/2007	263.666	6938.74	119.886
6/1/2007	253.401	7027.77	139.545
7/1/2007	97.2281	2908	60.2178
8/1/2007	240.976	7242.03	135.956
9/1/2007	241.322	7280.04	157.591
10/1/2007	233.87	7057.17	131.802
11/1/2007	232.301	7008.53	130.749
12/1/2007	232.836	7018.49	130.377
1/1/2008	228.755	6920.19	132.445
2/1/2008	215.96	6947.18	140.806
3/1/2008	217.336	7030.61	130.861
4/1/2008	233.52	7033.43	121.515
5/1/2008	228.714	6943.23	116.645
6/1/2008	242.173	7516.13	118.878
7/1/2008	261.729	8069.48	116.208
8/1/2008	259.151	7905.29	111.054
9/1/2008	252.88	7506.84	105.908
10/1/2008	269.16	7752.16	105.669
11/1/2008	257.732	7665.13	102.308
12/1/2008	254.287	7600.1	140.242
1/1/2009	252.638	7454.74	156.956
2/1/2009	356.793	5486.72	158.804
3/1/2009	363.142	5794.17	159.431
4/1/2009	359.788	10509.1	161.253
5/1/2009	347.608	10673	119.22
6/1/2009	372.242	11277.9	100.284
7/1/2009	412.729	12316.5	83.1067

Pressure Field History of Entire Reservoir

Date	BHP kg/cm^2	Date	BHP kg/cm^2
2/21/2000	143.871	9/21/2006	136.375
5/29/2000	141.658	2/22/2007	136.275
8/3/2000	142.045	3/28/2007	136.175
1/11/2001	141.344	7/30/2007	88.975
3/8/2001	142.283	8/14/2007	137.450
9/27/2001	142.002	3/20/2008	142.125
3/6/2002	142.485	5/24/2008	132.095
8/17/2002	140.768	6/18/2008	132.200
9/19/2002	140.960	11/19/2008	135.765
10/9/2002	141.583	12/10/2008	136.100
12/19/2002	137.307	2/6/2009	132.520
2/21/2003	134.288	2/11/2009	132.080
3/13/2003	139.194	8/6/2009	134.410
6/2/2003	137.688		
7/18/2003	139.113		
12/31/2003	138.607		
1/6/2004	137.557		
2/4/2004	140.553		
4/16/2004	137.130		
7/5/2004	134.410		
8/6/2004	114.189		
9/2/2004	137.117		
9/2/2004	138.233		
1/17/2005	136.056		
3/17/2005	136.079		
5/18/2005	136.079		
6/2/2005	134.657		
7/19/2005	136.574		
8/23/2005	138.233		
9/15/2005	135.185		
12/21/2005	132.526		
2/16/2006	138.050		

LIST OF PUBLICATIONS

Chakra, N.C., Song, K.-Y., Gupta, M.M., and Saraf, D.N., 2013.a. "An Innovative Neural Forecast of Cumulative Oil Production from a Petroleum Reservoir Employing Higher-order Neural Networks (HONNs)," *Journal of Petroleum Science and Engineering*, vol. 106, pp. 18-33.

Chakra, N.C.C., Song, K.-Y., Saraf, D.N., and Gupta, M.M., 2013.b. "Production Forecasting of Petroleum Reservoir applying Higher-Order Neural Networks (HONN) with Limited Reservoir Data," *International Journal of Computer Applications*, vol. 72, pp. 23-35

Chakra, N.C.C, and Saraf, D.N., "History Matching of an Actual Petroleum Reservoir Using Adaptive Genetic Algorithm," Manuscript under preparation.